World Journal of

Gastroenterology

World Journal of Gastroenterology

Contents

Contents

Contents

ABOUT COVER

Editorial board member of *World Journal of Gastroenterology*, Maria Gazouli, PhD, Associate Professor, Department of Basic Medical Sciences, Laboratory of Biology, Medical School, National and Kapodistrian University of Athens, Athens 11527, Greece

AIMS AND SCOPE

World Journal of Gastroenterology (*World J Gastroenterol*, *WJG*, print ISSN 1007-9327, online ISSN 2219-2840, DOI: 10.3748) is a peer-reviewed open access journal. The *WJG* Editorial Board consists of 642 experts in gastroenterology and hepatology from 59 countries.

The primary task of *WJG* is to rapidly publish high-quality original articles, reviews, and commentaries in the fields of gastroenterology, hepatology, gastrointestinal endoscopy, gastrointestinal surgery, hepatobiliary surgery, gastrointestinal oncology, gastrointestinal radiation oncology, *etc*. *WJG* is dedicated to become an influential and prestigious journal in gastroenterology and hepatology, to promote the development of above disciplines, and to improve the diagnostic and therapeutic skill and expertise of clinicians.

INDEXING/ABSTRACTING

World Journal of Gastroenterology (*WJG*) is now indexed in Current Contents®/Clinical Medicine, Science Citation Index Expanded (also known as SciSearch®), Journal Citation Reports®, Index Medicus, MEDLINE, PubMed, PubMed Central and Directory of Open Access Journals. The 2018 edition of Journal Citation Report® cites the 2017 impact factor for *WJG* as 3.300 (5-year impact factor: 3.387), ranking *WJG* as 35th among 80 journals in gastroenterology and hepatology (quartile in category Q2).

RESPONSIBLE EDITORS FOR THIS ISSUE

Chronic hepatitis B and metabolic risk factors: A call for rigorous longitudinal studies

Wai-Kay Seto

Wai-Kay Seto, Department of Medicine, the University of Hong Kong, Queen Mary Hospital, Hong Kong, China

Wai-Kay Seto, Department of Medicine, the University of Hong Kong-Shenzhen Hospital, Shenzhen 518053, Guangdong Province, China

Wai-Kay Seto, State Key Laboratory for Liver Research, the University of Hong Kong, Hong Kong, China

Corresponding author: Wai-Kay Seto, FRCP (C), MBBS, MD, Associate Professor, Doctor, Department of Medicine, the University of Hong Kong Queen Mary Hospital, 102 Pokfulam Road, Hong Kong, China. wkseto@hku.hk
Telephone: +86-852-22553994
Fax: +86-852-28162863

Abstract

Long-term nucleos(t)ide analogue therapy in chronic hepatitis B virus (HBV) infection is effective in suppressing viral replication and reducing liver-related complications. However, HBV-related liver events can still occur in different patient sub-groups. There is emerging evidence that, similar to chronic hepatitis C virus infection, metabolic risk factors may play a role in the disease process of chronic HBV. While the mechanistic nature of metabolic-HBV interactions remains uncertain, studies in different HBV-infected populations have demonstrated that hepatic steatosis, increased body-mass index, diabetes, or a combination of different metabolic risk factors are associated with an increased risk of hepatocellular carcinoma and cirrhosis. The impact of metabolic risk factors is especially prominent in patients with quiescent virological activity, including on-treatment patients with effective viral suppression. As the proportion of on-treatment chronic HBV patients increases worldwide, longitudinal studies determining the relative risks of different metabolic parameters with respect to clinical outcomes are needed. Future studies should also determine if metabolic-directed interventions can improve disease outcomes in chronic HBV.

Key words: Hepatitis B virus; Diabetes; Obesity; Steatosis; Non-alcoholic fatty liver disease; Body-mass index

Core tip: Metabolic risk factors, including hepatic steatosis, increased body-mass index

and diabetes, may be associated with worsened disease outcomes and reduced treatment response in chronic hepatitis B. Their effect may be most pronounced in patients with quiescent viral activity, including patients on long-term nucleos(t)ide analogue therapy.

INTRODUCTION

Affecting 248 million individuals worldwide, chronic hepatitis B virus (HBV) infection is a leading cause of liver-related morbidity and mortality[1]. Current nucleos(t)ide analogues, when taken long-term, can effectively suppress viral replication, improve liver histology, and reduce liver-related complications[2]. Yet nucleos(t)ide analogue therapy is never a "magic bullet" that can eliminate and prevent all HBV-related complications, with the benefit of therapy mitigated in certain patient sub-groups. For example, in an Asian population-based study, nucleoside analogue failed to significantly reduce liver cancer incidence in elderly chronic HBV patients[3].

Metabolic parameters have been demonstrated to play a prominent role in the disease course of chronic hepatitis C virus infection[4]. The interaction of metabolic factors with chronic HBV has been less extensively studied. Now, there is emerging evidence on how metabolic risk factors may influence the natural history and treatment response of chronic HBV (Figure 1), and these will be described in detail in this editorial.

HEPATIC STEATOSIS

The impact of liver fat on the disease course of HBV is controversial. There are studies indicating that steatosis may actually be protective. A cohort study from Taiwan involving 83339 participants showed hepatitis B surface antigen (HBsAg)-positive patients to have a lower risk of non-alcoholic fatty liver disease (NAFLD) development compared to HBsAg-negative individuals[5]. Another study demonstrated that a treatment-naïve chronic HBV patient with co-existing NAFLD had significantly lower serum HBV DNA levels compared to chronic HBV without steatosis, after adjusting for potential confounders[6].

Paradoxically, there is evidence that co-existing hepatic steatosis may contribute to the chronic HBV disease process. A study employed the noninvasive quantification of steatosis using controlled attenuation parameter (commonly known as CAP) measurements, with standardized cut-off values used to categorize steatosis severity[7]. Severe steatosis (CAP ≥ 280 dB/m) was found to be independently associated with increased liver fibrosis in both treatment-naïve patients and on-treatment patients achieving long-term virological suppression. The results suggest that even during quiescent viral activity, fibrogenesis can still develop in the presence of hepatic steatosis[8].

The above findings will require longitudinal validation in the clinical setting, as well as mechanistic studies for any HBV-steatosis interaction. Nonetheless, the management implications can be potentially huge, since both chronic HBV and NAFLD are common diseases. In Asia, the prevalence of NAFLD is greater than 30%[9], while more than a quarter of chronic HBV patients have concomitant NAFLD[10].

OBESITY

An increased body-mass index (BMI) has been demonstrated to worsen the disease outcome of chronic HBV. In a population-based study involving 2903 HBsAg-positive men after a mean follow-up of 14.7 years, obesity (BMI ≥ 30 kg/m²) was associated with increased risk of both hepatocellular carcinoma (HCC) and liver-related
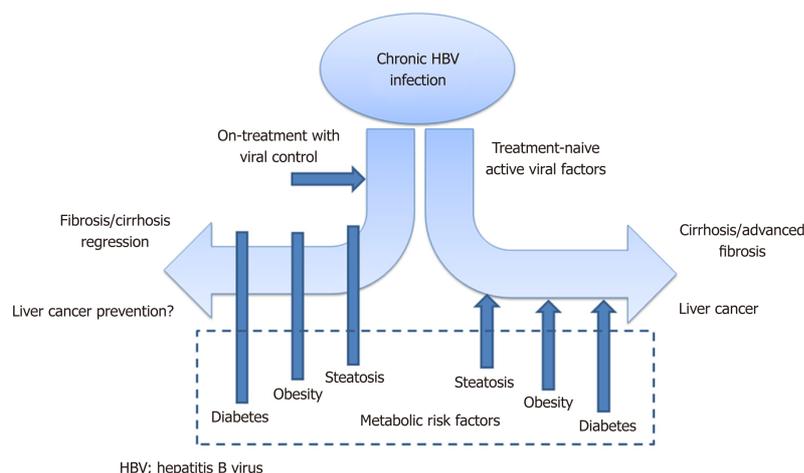
Figure 1 Potential association of metabolic risk factors with the natural history and treatment response of chronic hepatitis B virus infection. HBV: Hepatitis B virus.

mortality[11]. Obesity also diminishes treatment response by lessening fibrosis regression during long-term nucleos(t)ide analogue therapy. In a study with paired liver biopsies over a course of five years, increased BMI (≥ 25 kg/m^2) in HBV-infected patients of majority European descent was associated with persistent severe fibrosis or cirrhosis during treatment when compared to patients with normal BMI[2]. Results were also similar in another study involving Asian on-treatment patients with paired transient elastography over a median duration of 87.5 mo[12].

Obesity is associated with adipokine dysregulation, including reduced adiponectin and increased leptin production, which leads to enhanced liver fibrogenesis[13]. However, it remains unclear whether this adipokine dysfunction has any mechanistic interaction with HBV. With the prevalence of obesity in HBV-endemic regions increasing[14], studies specifically concentrating on the obese HBV population will be needed.

DIABETES MELLITUS

Diabetes has a synergistic impact on the disease course of chronic HBV. While the exact mechanism remains unclear, hyperglycemia activates oxidative stress[15], which can be linked with the severity of liver disease in chronic HBV infection[16]. Diabetic chronic HBV patients have an increased chance of alanine aminotransferase elevation and liver damage compared to non-diabetic patients[17]. Diabetes also increases the risk of HBV-related cirrhotic decompensation[18] and liver-related mortality[19].

Large-population cohort studies have further established the association of diabetes with liver-related clinical outcomes. A cohort study involving 23,820 Taiwan residents and a mean follow-up duration of 14 years found that diabetes independently increased the risk of HCC in HBsAg-positive individuals[20]. In addition, in a recent study involving 512,891 Chinese adults (both HBsAg-positive and -negative) with a median follow-up duration of 10.1 years, the presence of diabetes significantly increased the risk of HCC and cirrhosis (adjusted hazards ratios of 1.49 and 1.87, respectively). In addition, in patients without previously diagnosed diabetes, an increase of plasma glucose levels by 1 mmol/L, even in the non-diabetic range, significantly increased the probability of HCC and cirrhosis (adjusted hazards ratios of 1.04 and 1.07, respectively)[21].

METABOLIC RISK FACTORS IN COMBINATION

The combination of different metabolic risk factors in HBV-infected patients can increase the risk of liver-related events. Metabolic syndrome, which is a combination of increased waist circumference or obesity with the presence of different metabolic risk factors (hyperglycemia, hyperlipidemia, hypertriglyceridemia or hypertension) is a known risk factor for the development of HBV-related fibrosis progression[22]. More recently, a Taiwanese study followed up with 1690 men with chronic HBV infection for a median duration of 19 years. Having three or more metabolic risk factors

(including diabetes, obesity, hypertriglyceridemia, hypercholesterolemia or hypertension) increased the risk of HCC and liver-related death (hazards ratios of 2.32 and 2.72, respectively). Notably, in patients with available virological data, the risk of HCC among patients with three or more metabolic risk factors was especially accentuated when serum HBV DNA was less than 2000 IU/mL (hazards ratio of 14.38)[23].

CONCLUSION

HBV and metabolic risk factors: Partners in crime?

Despite the emerging evidence of metabolic risk factors being associated with HBV-related outcomes, one fundamental question remains unanswered: are HBV and metabolic-related liver injury synergistic, or simply two unrelated and different disease processes? Mechanistic studies to investigate their interaction are technically difficult, mainly due to the limitations of current HBV animal models which are unable to support the full HBV life cycle, restricting the study of host-viral interactions[24].

Nonetheless, the more important clinical question will be the magnitude of impact of different metabolic risk factors on HBV-related clinical outcomes. From available evidence, this impact is especially prominent in quiescent HBV disease[8,12,23], either in treatment-naïve patients with intrinsically low HBV DNA levels or in nucleos(t)ide analogue-treated patients with effective virological suppression. The proportion of patients receiving long-term treatment is increasing worldwide[25], while at the same time, the HBV patient cohort is ageing, suggesting that the concomitant presence of metabolic risk factors will increase. Taken together, these data suggest that the metabolic impact on the disease course of HBV will become more and more predominant. Finally, well-designed longitudinal studies will be needed to determine whether interventions directed at metabolic risk factors *e.g.*, glycemic control in diabetes or weight loss, can improve HBV-related outcomes. Clinical data on this metabolic-HBV interaction will prove useful if we are to meet the World Health Organization's objective in removing HBV as a public health threat by 2030.

REFERENCES

1   **Schweitzer A**, Horn J, Mikolajczyk RT, Krause G, Ott JJ. Estimations of worldwide prevalence of chronic hepatitis B virus infection: a systematic review of data published between 1965 and 2013. *Lancet* 2015; **386**: 1546-1555 [PMID: 26231459 DOI: 10.1016/S0140-6736(15)61412-X]

2   **Marcellin P**, Gane E, Buti M, Afdhal N, Sievert W, Jacobson IM, Washington MK, Germanidis G, Flaherty JF, Aguilar Schall R, Bornstein JD, Kitrinos KM, Subramanian GM, McHutchison JG, Heathcote EJ. Regression of cirrhosis during treatment with tenofovir disoproxil fumarate for chronic hepatitis B: a 5-year open-label follow-up study. *Lancet* 2013; **381**: 468-475 [PMID: 23234725 DOI: 10.1016/S0140-6736(12)61425-1]

3   **Seto WK**, Lau EH, Wu JT, Hung IF, Leung WK, Cheung KS, Fung J, Lai CL, Yuen MF. Effects of nucleoside analogue prescription for hepatitis B on the incidence of liver cancer in Hong Kong: a territory-wide ecological study. *Aliment Pharmacol Ther* 2017; **45**: 501-509 [PMID: 27976416 DOI: 10.1111/apt.13895]

4   **Serfaty L**. Metabolic Manifestations of Hepatitis C Virus: Diabetes Mellitus, Dyslipidemia. *Clin Liver Dis* 2017; **21**: 475-486 [PMID: 28689587 DOI: 10.1016/j.cld.2017.03.004]

5   **Joo EJ**, Chang Y, Yeom JS, Ryu S. Hepatitis B virus infection and decreased risk of nonalcoholic fatty liver disease: A cohort study. *Hepatology* 2017; **65**: 828-835 [PMID: 28035771 DOI: 10.1002/hep.28917]

6   **Hui RWH**, Seto WK, Cheung KS, Mak LY, Liu KSH, Fung J, Wong DK, Lai CL, Yuen MF. Inverse relationship between hepatic steatosis and hepatitis B viremia: Results of a large case-control study. *J Viral Hepat* 2018; **25**: 97-104 [PMID: 28772340 DOI: 10.1111/jvh.12766]

7   **Karlas T**, Petroff D, Sasso M, Fan JG, Mi YQ, de Lédinghen V, Kumar M, Lupsor-Platon M, Han KH, Cardoso AC, Ferraioli G, Chan WK, Wong VW, Myers RP, Chayama K, Friedrich-Rust M, Beaugrand M, Shen F, Hiriart JB, Sarin SK, Badea R, Jung KS, Marcellin P, Filice C, Mahadeva S, Wong GL, Crotty P, Masaki K, Bojunga J, Bedossa P, Keim V, Wiegand J. Individual patient data meta-analysis of controlled attenuation parameter (CAP) technology for assessing steatosis. *J Hepatol* 2017; **66**: 1022-1030 [PMID: 28039099 DOI: 10.1016/j.jhep.2016.12.022]

8   **Seto WK**, Hui RWH, Mak LY, Fung J, Cheung KS, Liu KSH, Wong DK, Lai CL, Yuen MF. Association Between Hepatic Steatosis, Measured by Controlled Attenuation Parameter, and Fibrosis Burden in Chronic Hepatitis B. *Clin Gastroenterol Hepatol* 2018; **16**: 575-583.e2 [PMID: 28970146 DOI: 10.1016/j.cgh.2017.09.044]

9   **Seto WK**, Yuen MF. Nonalcoholic fatty liver disease in Asia: emerging perspectives. *J Gastroenterol* 2017; **52**: 164-174 [PMID: 27637587 DOI: 10.1007/s00535-016-1264-3]

10   **Machado MV**, Oliveira AG, Cortez-Pinto H. Hepatic steatosis in hepatitis B virus infected patients: meta-analysis of risk factors and comparison with hepatitis C infected patients. *J Gastroenterol Hepatol* 2011; **26**: 1361-1367 [PMID: 21649726 DOI: 10.1111/j.1440-1746.2011.06801.x]

11   **Yu MW**, Shih WL, Lin CL, Liu CJ, Jian JW, Tsai KS, Chen CJ. Body-mass index and progression of hepatitis B: a population-based cohort study in men. *J Clin Oncol* 2008; **26**: 5576-5582 [PMID:

18955457 DOI: 10.1200/JCO.2008.16.1075]

12   **Seto WK**, Fung J, Cheung KS, Mak LY, Hui RW, Liu KS, Lai CL, Yuen MF. Body-mass index is associated with fibrosis regression during long-term nucleoside analogue therapy in chronic hepatitis B. *Aliment Pharmacol Ther* 2016; **44**: 1071-1079 [PMID: 27659292 DOI: 10.1111/apt.13804]

13   **Saxena NK**, Anania FA. Adipocytokines and hepatic fibrosis. *Trends Endocrinol Metab* 2015; **26**: 153-161 [PMID: 25656826 DOI: 10.1016/j.tem.2015.01.002]

14   **Ng M**, Fleming T, Robinson M, Thomson B, Graetz N, Margono C, Mullany EC, Biryukov S, Abbafati C, Abera SF, Abraham JP, Abu-Rmeileh NM, Achoki T, AlBuhairan FS, Alemu ZA, Alfonso R, Ali MK, Ali R, Guzman NA, Ammar W, Anwari P, Banerjee A, Barquera S, Basu S, Bennett DA, Bhutta Z, Blore J, Cabral N, Nonato IC, Chang JC, Chowdhury R, Courville KJ, Criqui MH, Cundiff DK, Dabhadkar KC, Dandona L, Davis A, Dayama A, Dharmaratne SD, Ding EL, Durrani AM, Esteghamati A, Farzadfar F, Fay DF, Feigin VL, Flaxman A, Forouzanfar MH, Goto A, Green MA, Gupta R, Hafezi-Nejad N, Hankey GJ, Harewood HC, Havmoeller R, Hay S, Hernandez L, Husseini A, Idrisov BT, Ikeda N, Islami F, Jahangir E, Jassal SK, Jee SH, Jeffreys M, Jonas JB, Kabagambe EK, Khalifa SE, Kengne AP, Khader YS, Khang YH, Kim D, Kimokoti RW, Kinge JM, Kokubo Y, Kosen S, Kwan G, Lai T, Leinsalu M, Li Y, Liang X, Liu S, Logroscino G, Lotufo PA, Lu Y, Ma J, Mainoo NK, Mensah GA, Merriman TR, Mokdad AH, Moschandreas J, Naghavi M, Naheed A, Nand D, Narayan KM, Nelson EL, Neuhouser ML, Nisar MI, Ohkubo T, Oti SO, Pedroza A. Global, regional, and national prevalence of overweight and obesity in children and adults during 1980-2013: a systematic analysis for the Global Burden of Disease Study 2013. *Lancet* 2014; **384**: 766-781 [PMID: 24880830 DOI: 10.1016/S0140-6736(14)60460-8]

15   **Monnier L**, Mas E, Ginet C, Michel F, Villon L, Cristol JP, Colette C. Activation of oxidative stress by acute glucose fluctuations compared with sustained chronic hyperglycemia in patients with type 2 diabetes. *JAMA* 2006; **295**: 1681-1687 [PMID: 16609090 DOI: 10.1001/jama.295.14.1681]

16   **Bolukbas C**, Bolukbas FF, Horoz M, Aslan M, Celik H, Erel O. Increased oxidative stress associated with the severity of the liver disease in various forms of hepatitis B virus infection. *BMC Infect Dis* 2005; **5**: 95 [PMID: 16262897 DOI: 10.1186/1471-2334-5-95]

17   **Khalili M**, Lombardero M, Chung RT, Terrault NA, Ghany MG, Kim WR, Lau D, Lisker-Melman M, Sanyal A, Lok AS; HBRN. Diabetes and prediabetes in patients with hepatitis B residing in North America. *Hepatology* 2015; **62**: 1364-1374 [PMID: 26390278 DOI: 10.1002/hep.28110]

18   **Huang YW**, Wang TC, Lin SC, Chang HY, Chen DS, Hu JT, Yang SS, Kao JH. Increased risk of cirrhosis and its decompensation in chronic hepatitis B patients with newly diagnosed diabetes: a nationwide cohort study. *Clin Infect Dis* 2013; **57**: 1695-1702 [PMID: 24051864 DOI: 10.1093/cid/cit603]

19   **Hsiang JC**, Gane EJ, Bai WW, Gerred SJ. Type 2 diabetes: a risk factor for liver mortality and complications in hepatitis B cirrhosis patients. *J Gastroenterol Hepatol* 2015; **30**: 591-599 [PMID: 25250942 DOI: 10.1111/jgh.12790]

20   **Chen CL**, Yang HI, Yang WS, Liu CJ, Chen PJ, You SL, Wang LY, Sun CA, Lu SN, Chen DS, Chen CJ. Metabolic factors and risk of hepatocellular carcinoma by chronic hepatitis B/C infection: a follow-up study in Taiwan. *Gastroenterology* 2008; **135**: 111-121 [PMID: 18505690 DOI: 10.1053/j.gastro.2008.03.073]

21   **Pang Y**, Kartsonaki C, Turnbull I, Guo Y, Clarke R, Chen Y, Bragg F, Yang L, Bian Z, Millwood IY, Hao J, Han X, Zang Y, Chen J, Li L, Holmes MV, Chen Z. Diabetes, Plasma Glucose, and Incidence of Fatty Liver, Cirrhosis, and Liver Cancer: A Prospective Study of 0.5 Million People. *Hepatology* 2018; **68**: 1308-1318 [PMID: 29734463 DOI: 10.1002/hep.30083]

22   **Wong GL**, Chan HL, Yu Z, Chan AW, Choi PC, Chim AM, Chan HY, Tse CH, Wong VW. Coincidental metabolic syndrome increases the risk of liver fibrosis progression in patients with chronic hepatitis B--a prospective cohort study with paired transient elastography examinations. *Aliment Pharmacol Ther* 2014; **39**: 883-893 [PMID: 24612251 DOI: 10.1111/apt.12658]

23   **Yu MW**, Lin CL, Liu CJ, Yang SH, Tseng YL, Wu CF. Influence of Metabolic Risk Factors on Risk of Hepatocellular Carcinoma and Liver-Related Death in Men With Chronic Hepatitis B: A Large Cohort Study. *Gastroenterology* 2017; **153**: 1006-1017.e5 [PMID: 28711626 DOI: 10.1053/j.gastro.2017.07.001]

24   **Protzer U**. Viral hepatitis: The bumpy road to animal models for HBV infection. *Nat Rev Gastroenterol Hepatol* 2017; **14**: 327-328 [PMID: 28400622 DOI: 10.1038/nrgastro.2017.44]

25   **Spradling PR**, Xing J, Rupp LB, Moorman AC, Gordon SC, Teshale ET, Lu M, Boscarino JA, Schmidt MA, Trinacty CM, Holmberg SD; Chronic Hepatitis Cohort Study Investigators. Distribution of disease phase, treatment prescription and severe liver disease among 1598 patients with chronic hepatitis B in the Chronic Hepatitis Cohort Study, 2006-2013. *Aliment Pharmacol Ther* 2016; **44**: 1080-1089 [PMID: 27640985 DOI: 10.1111/apt.13802]

Roles of Na+/Ca2+ exchanger 1 in digestive system physiology and pathophysiology

Qiu-Shi Liao, Qian Du, Jun Lou, Jing-Yu Xu, Rui Xie

Qiu-Shi Liao, Qian Du, Jun Lou, Jing-Yu Xu, Rui Xie, Department of Gastroenterology, Affiliated Hospital to Zunyi Medical College, Zunyi 563000, Guizhou Province, China

Corresponding author: Rui Xie, MD, PhD, Professor, Department of Gastroenterology, Affiliated Hospital to Zunyi Medical College, No. 149, Dalian Road, Huichuan District, Zunyi 563000, Guizhou Province, China. xr19841029@aliyun.com
Telephone: +86-15120390646
Fax: +86-851-28609205

Abstract

The Na+/Ca2+ exchanger (NCX) protein family is a part of the cation/Ca2+ exchanger superfamily and participates in the regulation of cellular Ca2+ homeostasis. NCX1, the most important subtype in the NCX family, is expressed widely in various organs and tissues in mammals and plays an especially important role in the physiological and pathological processes of nerves and the cardiovascular system. In the past few years, the function of NCX1 in the digestive system has received increasing attention; NCX1 not only participates in the healing process of gastric ulcer and gastric mucosal injury but also mediates the development of digestive cancer, acute pancreatitis, and intestinal absorption. This review aims to explore the roles of NCX1 in digestive system physiology and pathophysiology in order to guide clinical treatments.

Key words: Na+/Ca2+ exchanger; Digestive system diseases; Ion channel; Sodium; Calcium

Core tip: The Na+/Ca2+ exchange 1 protein (NCX1) is a membrane transporter and participates in the regulation of cellular Ca2+ homeostasis. As we known,NCX1 is expressed widely in various organs and tissues and plays an especially important role in the physiological and pathological processes of nerves and the cardiovascular system. This review aims to explore the roles of NCX1 in digestive system physiology and pathophysiology in order to guide clinical treatments.

INTRODUCTION

Ca^{2+} is an important cellular signal. Changes in intracellular Ca^{2+} control various cellular processes that are relevant to the regulation of normal function and to the development of diseases. These processes include muscle contraction, blood coagulation, nerve excitation, angiogenesis, cell apoptosis[1-3], and the development of cancer[4,5]. The homeostasis of intracellular calcium is controlled by a variety of proteins and ion channels, including the plasma membrane Na^+/Ca^{2+} exchanger (NCX). Members of the NCX family can exchange Na^+ and Ca^{2+} in either direction depending on the transmembrane electrochemical gradients and membrane potential[6], and these exchangers have a two-way transport mode such that under physiological conditions, one Ca^{2+} ion exits and three Na^+ ions enter the cell but the reverse transport occurs under special conditions (such as cancer or inflammation), that is, three Na^+ ions exit and one Ca^{2+} ion enters[7]. The NCX family contains three separate gene products exhibiting differential expression: NCX1, NCX2, and NCX3. NCX1 is widely expressed in mammalian organs and tissues[8], and NCX2 and NCX3 are expressed mainly in nerves and skeletal muscle[9]. Numerous studies have shown that NCX1 is involved in a variety of physiological and pathophysiological processes. For example, in the cardiovascular system, NCX1 can control the contraction and relaxation of vascular smooth muscle[10], while NCX1 can regulate heart rhythm, which is related to arrhythmia[11,12], and participate in the regulation of myocardial ischemia-reperfusion injury[13]. In the nervous system, NCX1 regulates neurotransmitter release[14] and microglia-related functions[15], which is associated with cerebral ischemia-reperfusion and Alzheimer's disease[16,17]. In the urinary system, NCX1 is involved in renal Ca^{2+} reabsorption and associated with renal ischemia-reperfusion[18,19]. In the endocrine system, NCX1 can regulate insulin secretion[20]. In the immune system, NCX1 is associated with the development of systemic lupus erythematosus[21]. In recent years, NCX1 has been found to be expressed in all of the organs of the digestive system and play important roles in the physiological processes and digestive diseases (such as pancreatitis, gastric ulcer, and gastrointestinal cancers)[22-24], However, the mechanism and function of NCX1 in the gastrointestinal tract have not yet been completely elucidated, particularly relating to certain digestive diseases and tumors. This review intends to explore the roles of NCX1 in digestive system physiology and pathophysiology as well as current treatments utilizing NCX1-based therapeutics.

STRUCTURAL FEATURES OF NCX1

NCX1 is a transmembrane bidirectional transporter with a molecular weight of 110 kDa and consists of 970 amino acids. NCX1 has 9 transmembrane segments, forming a large central cytoplasmic loop between the 5th and 6th transmembrane segments[25,26]. In addition, the NCX1 transmembrane segment has two internal repeat regions, the α1 and α2 repeat regions [27]. The first half of the transmembrane segment, including the α-repeat region, may be involved in ion transport[28-30]. In contrast, the second half, which contains the central cytoplasmic ring, has an inhibitory effect on the entire sodium-calcium exchanger[31,32]. In addition, there are two binding sites that can regulate Na^+ and Ca^{2+}[33,34], and there is a secondary Ca^{2+} adapter site[35] (Figure 1).

NCX1 AND THE ESOPHAGUS

The esophagus is a muscular portion of the digestive tract that transports food from the pharynx to the stomach depending on the contraction of muscle. In normal conditions, the tension of the lower esophageal smooth muscle (LES) depends mainly on the intracellular Ca^{2+} concentration. A high concentration of intracellular Ca^{2+} can cause smooth muscle contraction, and a low concentration of Ca^{2+} causes smooth muscle relaxation[36]. However, the contraction of the esophageal body is mainly dependent on the gradient of extracellular calcium. The occurrence of esophagitis is also closely related to the regulation of Ca^{2+} in pathological conditions. Calcium channel blockers (CCBs) have been used in the treatment of esophageal-related diseases, such as achalasia[36,37]. Achalasia is a kind of neuropathy where the smooth muscle fiber is not relaxed or cannot relax completely, a partial loss of esophageal body peristalsis occurs, and the motility is not coordinated. Gelfond *et al*[38] first reported that use of the L-type CCB nifedipine can relax the esophageal smooth muscle to reduce the pressure of the lower esophageal sphincter by blocking the flow of calcium ions into the cells and intracellular calcium release, thereby achieving the
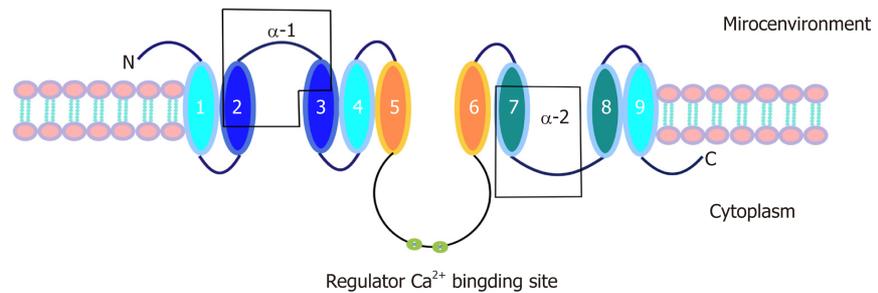
Figure 1 Structural features of NCX1.

purpose of treating achalasia. However, taking CCBs for a long time will cause the LES to become too relaxed and will lead to reflux esophagitis (RE)[39]. There is no definitive evidence as to whether NCX1 plays a regulatory role in RE. However, Kim *et al*[40] found that NCX1 is widely expressed in the esophageal muscle layer. Furthermore, the estrogen E2-induced inhibition of smooth muscle contraction in the esophagus and the mucus secretion in the esophageal mucosa are mainly achieved by downregulating the expression of calcium-related genes such as NCX1, CaBP-9k, and PMCA1 and decreasing the intracellular calcium level. It is suggested that NCX1 may play an important role in the regulation of contraction and relaxation in the LES. In addition, at present, our research group also confirmed that NCX1 expression was significantly increased along with the expression of TRPC6, TRPV4, and other acid-sensitive calcium channels that have a regulatory role in Barrett's esophagus or reflux esophagitis caused by acid reflux or bile reflux. Interfering with NCX1 can significantly inhibit the release of inflammatory mediators and the expression of intestinal metaplasia genes caused by the aforementioned pathogenic factors. Therefore, NCX1 is likely to be an important treatment target for esophageal functional diseases.

NCX1 also plays an important role in the correlation between smoking and the pathogenesis of esophageal squamous cell carcinoma (ESCC)[41]. Clinical evidence showed that the expression of NCX1 in ESCC tissue was significantly higher than that in esophageal noncancerous tissue and demonstrated a positive correlation between the NCX1 expression level and the smoking status of ESCC patients. The tobacco-derived carcinogen 4-(methylnitrosamino)-1-(3-pyridyl)-1-butanone (NNK) can significantly enhance NCX1 expression in normal esophageal cells and human ESCC cells. NNK mediates an increase in the intracellular Ca^{2+} concentration through NCX1 activation and promotes the proliferation and migration of human ESCC cells[41]. These findings indicate that tobacco smoking could cause Ca^{2+} entry through enhanced expression and function of NCX1, finally resulting in the pathogenesis of ESCC. Furthermore, NCX1 is also involved in the proliferation and migration of ESCC cells. To elucidate the mechanism of NCX1 in ESCC, it is necessary to study the function of NCX1 in ESCC in the future.

EXPRESSION AND FUNCTION OF NCX1 IN THE STOMACH

The stomach, the main digestive organ of the human body, is connected to the esophagus and the duodenum. It is known that the plasma membrane Ca^{2+}-ATPase (PMCA), NCX, and the endoplasmic reticulum (ER) Ca^{2+}-ATPase are the main mechanisms for the transport of intracellular Ca^{2+} to the extracellular space of gastric smooth muscle cells[42,43]. Studies have shown that NCX1 is widely expressed in the antrum of guinea pigs, while NCX2 has higher expression in the fundus[44]. Researchers believe that different NCX subtypes, which have different physiological functions, are expressed in different parts of the stomach and regulate each other. NCX1 is mainly involved in gastric antral motility, while NCX2 mainly changes the intracellular Ca^{2+} homeostasis in fundus smooth muscle cells to control the contraction and relaxation of the fundus smooth muscle[44]. This information suggests that the NCX family may control the movement of the whole stomach by controlling the movement of the gastric antrum and fundus smooth muscle.

In a study of gastrointestinal motility diseases, Hagi *et al*[45] found that NO and PACAP act as important mediators of the transient and sustained relaxation in the mouse gastric fundus. A change in functional coupling and/or collaborative functions between NO signaling and PACAP signaling may cause intracellular Ca^{2+} concentration changes, thereby controlling gastric fundus relaxation in mice. The

overexpression of NCX1 in smooth muscle may result in increased functional coupling and/or collaborative functions between NO signaling and PACAP signaling, resulting in the occurrence of functional gastrointestinal disorders[46]. Interestingly, studies on experimental gastric ulcer (GU) indicate that nitric oxide synthase (NOS) activity may be an important marker of neutrophil infiltration[47,48]. NO also contributes to ethanol-induced gastric ulceration and inflammatory bowel diseases (IBD) due to its role in the stimulation of cell proliferation in the gastric mucosa[49-51]. However, the overexpression of NCX1 in gastrointestinal smooth muscle may affect the function of the NO signaling pathway, and whether this change will promote GU and IBD process through the NO signaling pathway needs further study. It has also been reported that electric field stimulation (EFS) can induce sustained relaxation of the stomach fundus, but not other intestinal regions[52-54]. The study suggested that this sustained status may be closely related to the regulatory functions of NCX1 and NCX2. In the past few years, studies have shown that NCX1 and NCX2 are expressed in smooth muscles and neurons to regulate the relaxation and motility of the gastric fundus. Upon NCX1 or NCX2 heterozygosity deletion, the fundus relaxation and the gastric peristalsis can be enhanced by EFS[55]. Therefore, the NCX family may be an important treatment target for functional gastrointestinal diseases. In addition, Lajos V also found that NCX family members (NCX1, NCX2, and NCX3) are expressed extensively in human gastric myofibroblasts and participate in the regulation of intracellular calcium oscillations. Knockdown of NCX1 significantly inhibited the migration and proliferation of gastric myofibroblasts induced by insulin-like growth factor II (IGF-II)[22]. Gastric myofibroblasts are a kind of contractile, nonexcitatory cell induced by inflammatory factors such as transforming growth factor (TGF-β), and these cells are localized to the subepithelium throughout the whole gastrointestinal tract[56,57]. It is known that gastric myofibroblasts can not only regulate the secretion of extracellular matrix proteins and the formation of new blood vessels, promoting the healing process of ulcers[58,59], but also participate in the development of chronic gastritis and gastric cancer cell invasion and metastasis[60,61]. Further study on the role of NCX in gastrointestinal smooth muscle may elucidate the regulatory mechanisms of ulcer healing and tumor invasion and metastasis.

NCX1 AND THE INTESTINE

NCX1 and the small intestine

The expression of NCX1 protein has been detected in the small intestine, colon, and rectum[62,63], and it participates in the physiological regulation mechanism of intestinal calcium absorption, bicarbonate secretion, ileal smooth muscle movement and so on. The small intestine absorbs 90% of calcium[3,64,65]. Additionally, NCX1 mainly participates in the process of extracellular discharge of calcium ions from the basal membrane of intestinal epithelial cells. NCX1 can transport three Na^+ ions into the cell and transport one Ca^{2+} ion out of the cell; this transport is regulated by vitamin D and $1,25-(OH)_2D_3$[66], which can enhance the expression and activity of NCX on the basal membrane and promote the transport of Ca^{2+} from the cell to the outside[66]. Moreover, Wongdee *et al* found that vitamin D can upregulate the expression of the Ca^{2+} transporter gene NCX1, thus enhancing the Ca^{2+} transmembrane transport[67].

It is well known that the gastric acid defense barrier involves bicarbonate, and the hyposecretion of bicarbonate is one of the key mechanisms for the pathogenesis of duodenal ulcers. It has been reported that intracellular calcium signals can promote HCO_3^- secretion depending on the activation of the HCO_3^- secreting channel cystic fibrosis transmembrane conductance regulator (CFTR) or on the activation of the intermediate-conductance Ca^{2+} activated K^+ channel ($IKCa^{2+}$), which provide a driving force for HCO_3^- secretion[68]. However, NCX1 may be the key to the regulation of intracellular calcium changes. Dong *et al* found that the NCX1 protein is functionally expressed in the mouse duodenal mucosal epithelium, and a dynamic calcium ion experiment determined that the reverse regulation mode of NCX1 occurs, causing Na^+ efflux and Ca^{2+} entry to regulate HCO_3^- secretion[69]. Subsequent research confirmed that the muscarinic receptor agonists carbachol and 5-hydroxytryptamine (5-HT) can increase the intracellular calcium concentration and promote duodenal bicarbonate secretion after stimulating mouse duodenal mucosal or epithelial cells and confirmed that disturbing or inhibiting the function of NCX1 can obviously block the intracellular calcium change and promote bicarbonate secretion[70]. These results suggest that NCX1 and its mediated Ca^{2+} influx play a critical and extensive role in regulating the secretion of HCO_3^- in the duodenal mucosa. Other studies have shown that NCX1 and NCX2 are also involved in ileal smooth muscle contraction and ileal motility regulation[71]. Nishiyama *et al* found that NCX2 regulates ileal motility

primarily by controlling the sensitivity of acetylcholine (AchE) and substance P (SP) in smooth muscle[71]. Compared with that in the wild-type model, the contraction amplitude induced by AchE and SP after NCX2 knockout was significantly reduced; although NCX1 also plays a role in the regulation of ileal contraction, this decline was not evident in the NCX1 knockout model[71]. This finding suggests that NCX2 plays a more important role than NCX1 in ileal movement.

NCX1 and the colon
NCXs (NCX1 and NCX2) are also widely expressed in colonic smooth muscle and the myenteric plexus layers[72]. Nishiyama *et al* showed that NCX1 overexpression in the mouse distal colon enhanced the relaxation amplitude induced by EFS, suggesting that NCX1 can affect the distal colonic smooth muscle movement in mice[71]. Furthermore, it was found that the secretion of the mucin MUC5AC induced by ATP depends on the influx of Ca^{2+} into colonic goblet cells and that ATP requires the activation of TRPM5 channels to increase intracellular Na^+, which activates the NCX reverse transport mode and increases intracellular Ca^{2+} uptake; thus, inhibiting NCX can significantly reduce the MUC5AC secretion in goblet cells[73]. There is also evidence that the NCX family may also be involved in the pathogenesis of diarrhea. Although NCX1 and NCX2 were found to be expressed in the myenteric nerve plexus of the proximal colon and the colon transversum as well as longitudinal and annular muscular layers, the function of NCX1 and NCX2 in intermuscular neurons may be different from that in smooth muscle[74]. Kazuhiro *et al* have found that in a diarrhea model induced with magnesium sulfate or 5-HT, the diarrhea in NCX2 heterozygous knockout mice (NCX2 HET) was more serious than that in wild-type mice (WT), but the diarrhea in NCX1 heterozygous knockout mice (NCX1 HET) showed no significant changes from that of WT[75]. Magnesium sulfate-induced diarrhea was exacerbated in NCX2 HET by decreasing normal and soft fecal materials and increasing watery fecal materials, however, PGE2-induced diarrhea in NCX1 HET and NCX2 HET was similar to that in the WT[75]. The researchers believe that this finding may be due to the mechanism of 5-HT-induced diarrhea involving stimulation of the 5-HT3 receptor in myenteric plexus neurons and its downstream cholinergic and tachykinin excitatory pathways[76,77]. However, PGE2 acts directly on smooth muscle and stimulates fluid accumulation to induce diarrhea[78,79]. Therefore, NCX2 rather than NCX1 in the myenteric plexus may play a critical role in the occurrence and development of diarrhea. Further study of NCX may provide new targets for the diarrhea caused by gastrointestinal dysfunction.

NCX1 AND THE PANCREAS

Expression and distribution of NCX in the pancreas
NCX1 is functionally expressed in the β-cells, acinar cells, and ductal cells of the rat pancreas and has a distinct pattern of distribution in pancreatic ducts depending on their size and proximity to acini[80]. Two splicing variants of NCX1, NCX1.3 and NCX1.7, are mainly expressed in rat pancreatic cells[81-84]; however, three other variants, NCX1.2, NCX1.9, and NCX1.13, were also found in guinea pigs, hamsters and mice. In the past few years, studies have proved that different types of NCX1 have different expression levels between different species.

Role of NCX1 in pancreatic physiological processes
The physiological functions of the pancreas include secreting various digestive enzymes and insulin. Normally, the intracellular ATP/ADP ratio increases after pancreatic β-cells uptake glucose, *via* the closure of K^+-ATP channels, causing β-cell depolarization and inducing extracellular calcium influx through calcium channels in the membrane; the intracellular calcium increase causes fusion of the vesicular membrane containing insulin with the cytoplasmic membrane and the subsequent secretion of insulin from cells *via* vesicular exocytosis[85]. It has been found that both the voltage-dependent calcium channel (CaV) and the intracellular IP3-sensitive calcium pool are important in insulin secretion regulation in the past few years[86], but the role of the NCX family in this process is just beginning to be evaluated.

In normal pancreatic islet β-cells, NCX1 is mainly responsible for Ca^{2+} efflux from cells. The aim is to control the Ca^{2+} concentration within the normal physiological range in order to accurately control the insulin release level[83,87]. In native pancreatic ducts, the NCX1 expression level is downregulated by acetylcholine and secretin but upregulated by insulin[80]; as the main physiological stimulant of insulin release, glucose has the reverse regulatory effect on the transcription, expression, and activity of NCX[88].

NCX1 and pancreatic diseases

Pathologically, NCX also has a regulatory mechanism affecting the insulin secretion from the β-cells of diabetic patients. In the past few years, research has shown that NCX overexpression can lead to ER stress and Ca^{2+} release from the ER, thus promoting β-cell apoptosis, reducing β-cell proliferation, and decreasing insulin secretion[88]. Herchuelz *et al*[89] found that heterozygous inactivation of NCX1 (Ncx1+/-) leads to an increase in β-cell function and a 5-fold increase in both β-cell mass and proliferation. The mutation also increases the β-cell resistance to hypoxia, and Ncx1+/- islets show a 2-4 times higher rate of curing diabetes than Ncx1+/+ islets when transplanted into diabetic animals. However, in some cases, NCX may change into the reverse regulation mode to promote Ca^{2+} entry, prolonging the duration of the peak electrical activity associated with glucose and increasing insulin release[90]. In summary, the different NCX1 expression and transport modes can regulate insulin secretion, so selective inhibition of NCX1 may improve insulin secretion, which provides more theoretical evidence for novel glucose-sensitive insulinotropic drugs for type 2 diabetes that target NCX1.

In addition to regulating physiological insulin secretion, the Ca^{2+} homeostasis is also a key factor leading to pancreatitis, hypercalcemia, pancreatic cancer, and other diseases. Pancreatitis is one of the most common acute abdomen problems, and the pathogenesis is the abnormal accumulation of intracellular Ca^{2+} (calcium overload) to promote excessive activation of trypsinogen, resulting in pancreatic autodigestive injury[91]. Previous studies have reported that the calcium overload in acute pancreatitis may be related to calcium channels such as CRAC/TRPV1/TRPV3[92,93]; however, it has recently been found that the NCX1 reverse regulation mode may also be involved in this overload. Yu *et al* confirmed that the mRNA and protein expression of NCX1 in tissues of acute pancreatitis induced by cerulein was significantly increased in cell experiments and animal experiments[94]. The authors found that the expression of inflammatory mediators such as TNF-α and interleukin-6 (IL-6) caused by cerulein was decreased significantly after treatment with KB-R7943 (a specific inhibitor of NCX1)[94]. This finding suggests that NCX1 may play a critical role in the occurrence and development of acute pancreatitis. In addition, pancreatic cancer is a kind of cancer with high malignancy and poor prognosis, and duct cell carcinoma is the main pathological type of pancreatic cancer[95,96]. However, it is generally accepted that alterations in TGF-β signaling and its downstream SMAD pathway play an important role in pancreatic cancer development[97]. The study by Chow *et al* found that TRPC1 and NCX1 are expressed and functional in pancreatic cancer cells. TGF-β activates TRPC1 and NCX1 channels to mediate a cytoplasmic Ca^{2+} concentration increase in pancreatic cancer cells, which activates the downstream PKC/SMAD4 pathway to regulate pancreatic cancer cell motility[98]. These results suggest that NCX1 may be involved in the malignant biological behavior regulation of pancreatic cancer (Figure 2).

NCX1 AND THE LIVER

NCX1 and hepatic ischemia-reperfusion

Although NCX1 is expressed in normal livers, liver fibrosis, and liver cancer, the transcription levels and regulation modes are different under these three conditions, suggesting that NCX may have different functions and effects in the development of hepatitis, liver fibrosis, and liver cancer[99]. In the study of liver ischemia-reperfusion injury, intracellular calcium accumulation is a critical mechanism of cell apoptosis and injury[100]. NCX mainly adopts the forward control mode in ischemic-reperfusion injury. Trisulfated disaccharide (TD) can transport excess intracellular calcium out of the cell by activating NCX1, thus reducing the serum levels of inflammation markers (TNF-α, IL-6, and IL-10) and the lipid peroxidation after liver injury[101].

NCX1 and liver fibrosis

Hepatic fibrosis is a necessary process in the progression from chronic hepatitis to cirrhosis. The activation and proliferation of hepatic stellate cells (HSCs) are the central link of hepatic fibrosis. Nakamura *et al* found that the NCX mRNA and protein expression levels were significantly upregulated in response to the activation of rat HSCs induced by CCl4[102]. It was also reported that NCX expression is upregulated in cirrhotic tissue, although the specific mechanism is not clear; NCX may be a new target in liver fibrosis or cirrhosis research[93].

NCX1 and liver cancer

Finally, in hepatocellular carcinoma (HCC) research, our research group has
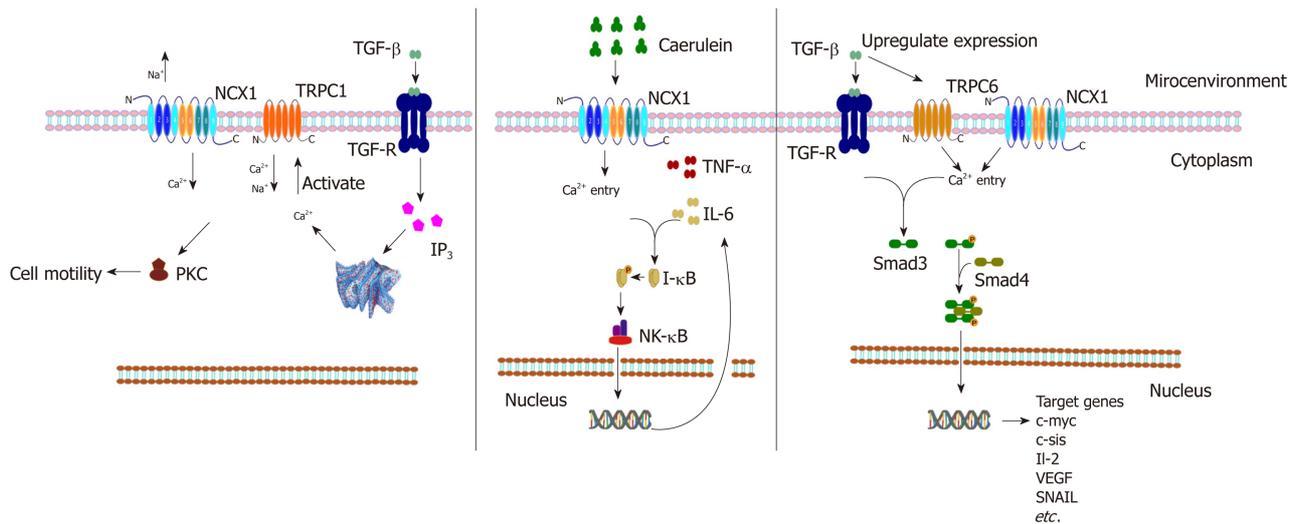
Figure 2 The regulated signal pathways and transcription factors of NCX1 in digestive diseases. Transforming growth factor-β (TGF-β) stimulates the activation of PLC-IP3 and Ca²⁺ release from the endoplasmic reticulum, which activates TRPC1 and the reverse mode of NCX1 resulting in Ca²⁺ influx, and the increase of Ca²⁺ mediates cell motility directly or indirectly *via* activation of Ca²⁺-dependent PKC in pancreatic cancer. Cerulein activates NCX1 and induces activation of inflammatory factors TNF-α and IL-6 and the downstream NK-κB pathway in pancreatic cells. TGF-β can upregulate the expression of NCX1 and TRPC6 and activate the downstream SMAD pathway to regulate the migration and invasion of hepatocellular carcinoma cells.

published articles confirming that the expression of NCX1 is obviously upregulated in hepatoma cells and tissues and that NCX1 can affect the intracellular calcium level to affect the cytokines TGF-β or IL-6 in the malignant behavior of hepatoma cells. A study found that TGF-β can upregulate the expression of NCX1 and the transient receptor potential channel TRPC6 in hepatoma cells and further induce intracellular calcium activation in HCC to promote the formation of a complex between NCX1 and TRPC6, thus activating the downstream SMAD pathway, which can regulate HCC malignant biological behaviors such as migration and invasion[103]. Not only was the phosphorylation of Smad proteins dependent on TRPC6 and NCX1, but also the Smad signaling, especially the phosphorylation of Smad2, augmented the expression of TRPC6 and NCX1. At the same time the upregulated expression of TRPC6 and NCX1 can be strongly correlated with the stage and pathologic grade of HCC, which may become useful biomarkers for monitoring disease progression of liver cancer patients[103,104]. In a related study of IL-6 and liver cancer, it was also confirmed that an intracellular pH regulator (NHE1), NCX1, and calmodulin (CaM) coexisted in the same lipid-crossing structure of the cell membrane and that their expression levels were upregulated in liver cancer tissues[105] (Figure 2). Moreover, IL-6 activated NHE1 to promote H⁺ excretion and an NCX1-induced external Ca²⁺ influx, and NHE1 pumped H⁺ in exchange for Na⁺ influx to promote NCX1 activation, which enhanced the interaction between NCX1 and CaM, thus promoting the occurrence and development of liver cancer[106]. The above findings provide the basis for the important role of NCX in hepatic carcinogenesis and also provide a new possibility for drug development for early intervention in inflammation-associated tumors.

CONCLUSION

In summary, the NCX1 channel protein regulates the Ca²⁺ signaling pathway *via* its forward/reverse modes in the digestive system and regulates the cell function, thus participating in the occurrence and development of digestive system diseases (Figures 3 and 4). The functions of NCX1 in inflammation-associated digestive diseases (such as inflammatory bowel disease and hepatitis) will become a new research hotspot. NCX1 could be a new molecular marker for the digestive system disease diagnosis and treatment, and drug development targeting NCX1 will represent a new direction of the treatment of digestive system diseases.
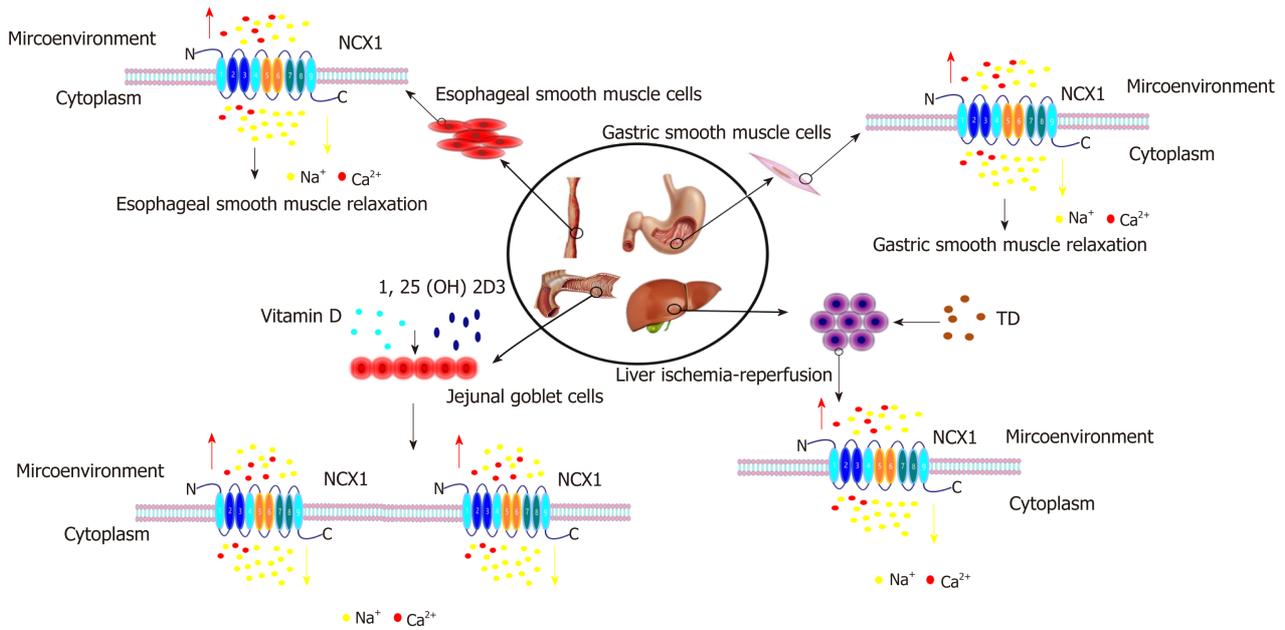
Figure 3 The effects of NCX1 positive mode in the digestive system. Under normal circumstances, NCX1 adopts the positive mode in esophageal smooth muscle and gastric smooth muscle, excreting Ca^{2+} from the cells, reducing intracalcium concentration and inducing smooth muscle relaxation. In the jejunum, vitamin D and 1,25-$(OH)_2D_3$ can enhance the expression and activity of NCX1 to increase the excretion of Ca^{2+}. NCX1 mainly adopts the forward control mode in ischemic-reperfusion injury. Trisulfated disaccharide (TD) can transport excess intracellular Ca^{2+} out of the cell by activating NCX1.
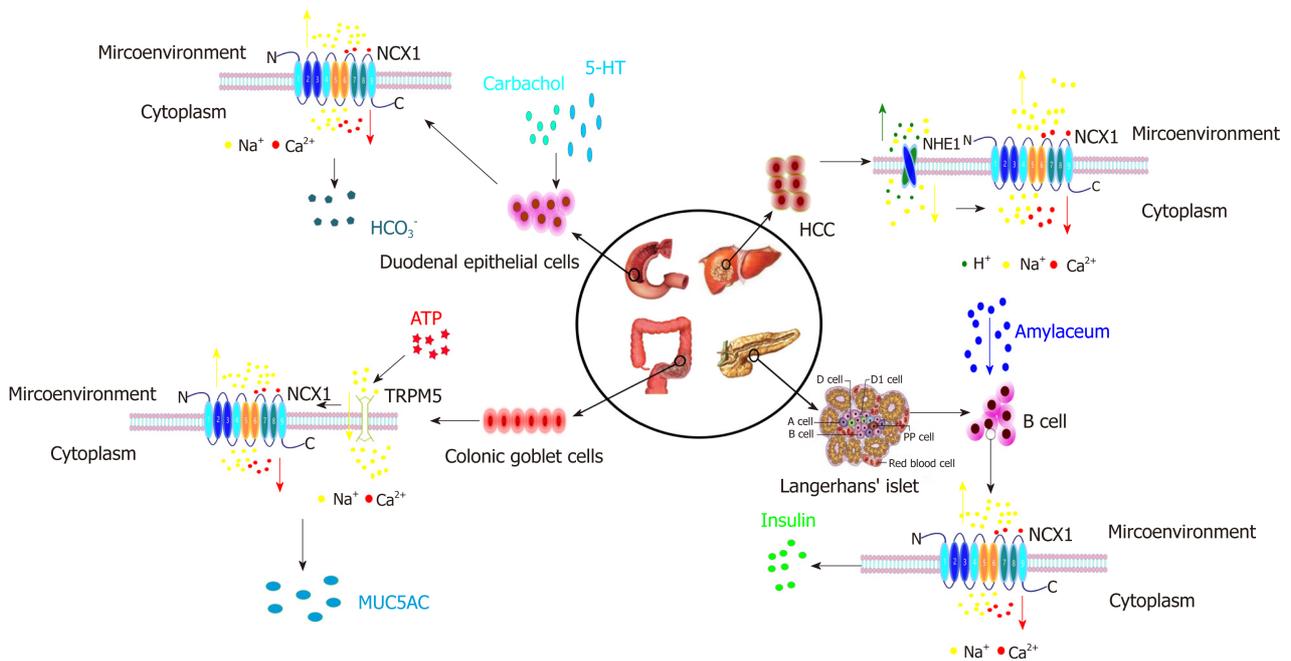
Figure 4 The roles of NCX1 reverse mode in the digestive system. In duodenal epithelial cells, carbachol and 5-HT can activate the reverse mode of NCX1, enhancing Ca^{2+} influx to release HCO_3^-. In hepatoma cells, NHE1 can promote H^+ excretion and Na^+ influx and activate the reverse mode of NCX1 to induce Ca^{2+} influx. In colon goblet cells, ATP activates the TRPM5 channel to induce Na^+ influx, and an increase of Na^+ concentration starts the NCX1 reverse mode and increases Ca^{2+} influx and MUC5AC expression. In pancreatic islet β cells, under glucose stimulation, NCX1 can be converted to a reverse mode to promote Ca^{2+} influx to increase insulin secretion.

REFERENCES

1 **Berridge MJ**, Lipp P, Bootman MD. The versatility and universality of calcium signalling. *Nat Rev Mol Cell Biol* 2000; **1**: 11-21 [PMID: 11413485 DOI: 10.1038/35036035]

2 **Clapham DE**. Calcium signaling. *Cell* 2007; **131**: 1047-1058 [PMID: 18083096 DOI: 10.1016/j.cell.2007.11.028]

3 **Hoenderop JG**, Nilius B, Bindels RJ. Calcium absorption across epithelia. *Physiol Rev* 2005; **85**: 373-422 [PMID: 15618484 DOI: 10.1152/physrev.00003.2004]

4 **Rachow S**, Zorn-Kruppa M, Ohnemus U, Kirschner N, Vidal-y-Sy S, von den Driesch P, Börnchen C, Eberle J, Mildner M, Vettorazzi E, Rosenthal R, Moll I, Brandner JM. Occludin is involved in adhesion, apoptosis, differentiation and Ca2+-homeostasis of human keratinocytes: implications for tumorigenesis. *PLoS One* 2013; **8**: e55116 [PMID: 23390516 DOI: 10.1371/journal.pone.0055116]

5 **Zeng F**, Chen X, Cui W, Wen W, Lu F, Sun X, Ma D, Yuan Y, Li Z, Hou N, Zhao H, Bi X, Zhao J, Zhou J, Zhang Y, Xiao RP, Cai J, Zhang X. RIPK1 Binds MCU to Mediate Induction of Mitochondrial Ca^{2+} Uptake and Promotes Colorectal Oncogenesis. *Cancer Res* 2018; **78**: 2876-2885 [PMID: 29531160 DOI: 10.1158/0008-5472.can-17-3082]

6 **Khananshvili D**. Sodium-calcium exchangers (NCX): molecular hallmarks underlying the tissue-specific and systemic functions. *Pflugers Arch* 2014; **466**: 43-60 [PMID: 24281864 DOI: 10.1007/s00424-013-1405-y]

7 **Khananshvili D**. The SLC8 gene family of sodium-calcium exchangers (NCX) - structure, function, and regulation in health and disease. *Mol Aspects Med* 2013; **34**: 220-235 [PMID: 23506867 DOI: 10.1016/j.mam.2012.07.003]

8 **Liao J**, Li H, Zeng W, Sauer DB, Belmares R, Jiang Y. Structural insight into the ion-exchange mechanism of the sodium/calcium exchanger. *Science* 2012; **335**: 686-690 [PMID: 22323814 DOI: 10.1126/science.1215759]

9 **Papa M**, Canitano A, Boscia F, Castaldo P, Sellitti S, Porzig H, Taglialatela M, Annunziato L. Differential expression of the Na+-Ca2+ exchanger transcripts and proteins in rat brain regions. *J Comp Neurol* 2003; **461**: 31-48 [PMID: 12722103 DOI: 10.1002/cne.10665]

10 **Blaustein MP**, Leenen FH, Chen L, Golovina VA, Hamlyn JM, Pallone TL, Van Huysse JW, Zhang J, Wier WG. How NaCl raises blood pressure: a new paradigm for the pathogenesis of salt-dependent hypertension. *Am J Physiol Heart Circ Physiol* 2012; **302**: H1031-H1049 [PMID: 22058154 DOI: 10.1152/ajpheart.00899.2011]

11 **Antoons G**, Willems R, Sipido KR. Alternative strategies in arrhythmia therapy: evaluation of Na/Ca exchange as an anti-arrhythmic target. *Pharmacol Ther* 2012; **134**: 26-42 [PMID: 22197992 DOI: 10.1016/j.pharmthera.2011.12.001]

12 **Herrmann S**, Lipp P, Wiesen K, Stieber J, Nguyen H, Kaiser E, Ludwig A. The cardiac sodium-calcium exchanger NCX1 is a key player in the initiation and maintenance of a stable heart rhythm. *Cardiovasc Res* 2013; **99**: 780-788 [PMID: 23761399 DOI: 10.1093/cvr/cvt154]

13 **Ohtsuka M**, Takano H, Suzuki M, Zou Y, Akazawa H, Tamagawa M, Wakimoto K, Nakaya H, Komuro I. Role of Na+-Ca2+ exchanger in myocardial ischemia/reperfusion injury: evaluation using a heterozygous Na+-Ca2+ exchanger knockout mouse model. *Biochem Biophys Res Commun* 2004; **314**: 849-853 [PMID: 14741714]

14 **Roome CJ**, Power EM, Empson RM. Transient reversal of the sodium/calcium exchanger boosts presynaptic calcium and synaptic transmission at a cerebellar synapse. *J Neurophysiol* 2013; **109**: 1669-1680 [PMID: 23255722 DOI: 10.1152/jn.00854.2012]

15 **Noda M**, Ifuku M, Mori Y, Verkhratsky A. Calcium influx through reversed NCX controls migration of microglia. *Adv Exp Med Biol* 2013; **961**: 289-294 [PMID: 23224888 DOI: 10.1007/978-1-4614-4756-6_24]

16 **Morimoto N**, Kita S, Shimazawa M, Namimatsu H, Tsuruma K, Hayakawa K, Mishima K, Egashira N, Iyoda T, Horie I, Gotoh Y, Iwasaki K, Fujiwara M, Matsuda T, Baba A, Komuro I, Horie K, Takeda J, Iwamoto T, Hara H. Preferential involvement of Na/Ca² exchanger type-1 in the brain damage caused by transient focal cerebral ischemia in mice. *Biochem Biophys Res Commun* 2012; **429**: 186-190 [PMID: 23137542 DOI: 10.1016/j.bbrc.2012.10.114]

17 **Annunziato L**, Pignataro G, Di Renzo GF. Pharmacology of brain Na+/Ca2+ exchanger: from molecular biology to therapeutic perspectives. *Pharmacol Rev* 2004; **56**: 633-654 [PMID: 15602012 DOI: 10.1124/pr.56.4.5]

18 **Moor MB**, Haenzi B, Legrand F, Koesters R, Hynes NE, Bonny O. Renal Memo1 Differentially Regulates the Expression of Vitamin D-Dependent Distal Renal Tubular Calcium Transporters. *Front Physiol* 2018; **9**: 874 [PMID: 30038585 DOI: 10.3389/fphys.2018.00874]

19 **Yamashita J**, Kita S, Iwamoto T, Ogata M, Takaoka M, Tazawa N, Nishikawa M, Wakimoto K, Shigekawa M, Komuro I, Matsumura Y. Attenuation of ischemia/reperfusion-induced renal injury in mice deficient in Na+/Ca2+ exchanger. *J Pharmacol Exp Ther* 2003; **304**: 284-293 [PMID: 12490603 DOI: 10.1124/jpet.102.039024]

20 **Hamming KS**, Soliman D, Webster NJ, Searle GJ, Matemisz LC, Liknes DA, Dai XQ, Pulinilkunnil T, Riedel MJ, Dyck JR, Macdonald PE, Light PE. Inhibition of beta-cell sodium-calcium exchange enhances glucose-dependent elevations in cytoplasmic calcium and insulin secretion. *Diabetes* 2010; **59**: 1686-1693 [PMID: 20413506 DOI: 10.2337/db09-0630]

21 **Vasques ER**, Cunha JEM, Kubrusly MS, Coelho AM, Sanpietri SN, Nader HB, Tersariol ILS, Lima MA, Chaib E, D'Albuquerque LAC. The M-RNA, expression of SERCA2 and NCX1 in the process of pharmacological cell protection in experimental acute pancreatitis induced by taurocholate. *Arq Bras Cir Dig* 2018; **31**: e1352 [PMID: 29947686 DOI: 10.1590/0102-672020180001e1352]

22 **Kemény LV**, Schnúr A, Czepán M, Rakonczay Z Jr, Gál E, Lonovics J, Lázár G, Simonka Z, Venglovecz V, Maléth J, Judák L, Németh IB, Szabó K, Almássy J, Virág L, Geisz A, Tiszlavicz L, Yule DI, Wittmann T, Varró A, Hegyi P. Na+/Ca2+ exchangers regulate the migration and proliferation of human gastric myofibroblasts. *Am J Physiol Gastrointest Liver Physiol* 2013; **305**: G552-G563 [PMID: 23907822 DOI: 10.1152/ajpgi.00394.2012]

23 **Xu J**, Jiang Y, Xie R, Wen G, Dong H, Tuo B. Su1578 Expression and Functional Role of Ncx1 in Human Hepatocellular Carcinoma. *Gastroenterology* 2012; **142**: S-970-S-970

24 **Tang B**, Chow JY, Dong TX, Yang SM, Lu DS, Carethers JM, Dong H. Calcium sensing receptor

suppresses human pancreatic tumorigenesis through a novel NCX1/Ca(2+)/β-catenin signaling pathway. *Cancer Lett* 2016; **377**: 44-54 [PMID: 27108064 DOI: 10.1016/j.canlet.2016.04.027]

25   **Plain F**, Turnbull D, Fraser NJ, Fuller W. Understanding the rules governing NCX1 palmitoylation. *Channels (Austin)* 2017; **11**: 377-379 [PMID: 28617626 DOI: 10.1080/19336950.2017.1342501]

26   **Reilly L**, Howie J, Wypijewski K, Ashford ML, Hilgemann DW, Fuller W. Palmitoylation of the Na/Ca exchanger cytoplasmic loop controls its inactivation and internalization during stress signaling. *FASEB J* 2015; **29**: 4532-4543 [PMID: 26174834 DOI: 10.1096/fj.15-276493]

27   **Nicoll DA**, Ren X, Ottolia M, Phillips M, Paredes AR, Abramson J, Philipson KD. What we know about the structure of NCX1 and how it relates to its function. *Ann N Y Acad Sci* 2007; **1099**: 1-6 [PMID: 17303833 DOI: 10.1196/annals.1387.014]

28   **Nicoll DA**, Hryshko LV, Matsuoka S, Frank JS, Philipson KD. Mutation of amino acid residues in the putative transmembrane segments of the cardiac sarcolemmal Na+-Ca2+ exchanger. *J Biol Chem* 1996; **271**: 13385-13391 [PMID: 8662775]

29   **Doering AE**, Nicoll DA, Lu Y, Lu L, Weiss JN, Philipson KD. Topology of a functionally important region of the cardiac Na+/Ca2+ exchanger. *J Biol Chem* 1998; **273**: 778-783 [PMID: 9422731]

30   **Iwamoto T**, Uehara A, Imanaga I, Shigekawa M. The Na+/Ca2+ exchanger NCX1 has oppositely oriented reentrant loop domains that contain conserved aspartic acids whose mutation alters its apparent Ca2+ affinity. *J Biol Chem* 2000; **275**: 38571-38580 [PMID: 10967097 DOI: 10.1074/jbc.M003788200]

31   **Li Z**, Nicoll DA, Collins A, Hilgemann DW, Filoteo AG, Penniston JT, Weiss JN, Tomich JM, Philipson KD. Identification of a peptide inhibitor of the cardiac sarcolemmal Na(+)-Ca2+ exchanger. *J Biol Chem* 1991; **266**: 1014-1020 [PMID: 1985930]

32   **Matsuoka S**, Nicoll DA, He Z, Philipson KD. Regulation of cardiac Na(+)-Ca2+ exchanger by the endogenous XIP region. *J Gen Physiol* 1997; **109**: 273-286 [PMID: 9041455]

33   **Levitsky DO**, Nicoll DA, Philipson KD. Identification of the high affinity Ca(2+)-binding domain of the cardiac Na(+)-Ca2+ exchanger. *J Biol Chem* 1994; **269**: 22847-22852 [PMID: 8077237]

34   **Matsuoka S**, Nicoll DA, Hryshko LV, Levitsky DO, Weiss JN, Philipson KD. Regulation of the cardiac Na(+)-Ca2+ exchanger by Ca2+. Mutational analysis of the Ca(2+)-binding domain. *J Gen Physiol* 1995; **105**: 403-420 [PMID: 7769381]

35   **Reyes RC**, Verkhratsky A, Parpura V. Plasmalemmal Na+/Ca2+ exchanger modulates Ca2+-dependent exocytotic release of glutamate from rat cortical astrocytes. *ASN Neuro* 2012; **4**: pii: e00075 [PMID: 22268447 DOI: 10.1042/an20110059]

36   **Liu JF**, Lu HL, Wen SW, Wu RF. Effects of acetylcholine on sling and clasp fibers of the human lower esophageal sphincter. *J Gastroenterol Hepatol* 2011; **26**: 1309-1317 [PMID: 21443668 DOI: 10.1111/j.1440-1746.2011.06731.x]

37   **Hoogerwerf WA**, Pasricha PJ. Pharmacologic therapy in treating achalasia. *Gastrointest Endosc Clin N Am* 2001; **11**: 311-324, vii [PMID: 11319064]

38   **Gelfond M**, Rozen P, Keren S, Gilat T. Effect of nitrates on LOS pressure in achalasia: a potential therapeutic aid. *Gut* 1981; **22**: 312-318 [PMID: 7239323]

39   **Kellerman R**, Kintanar T. Gastroesophageal Reflux Disease. *Prim Care* 2017; **44**: 561-573 [PMID: 29132520 DOI: 10.1016/j.pop.2017.07.001]

40   **Kim K**, Lee D, Ahn C, Kang HY, An BS, Seong YH, Jeung EB. Effects of estrogen on esophageal function through regulation of Ca^{2+}-related proteins. *J Gastroenterol* 2017; **52**: 929-939 [PMID: 28078471 DOI: 10.1007/s00535-016-1305-y]

41   **Wen J**, Pang Y, Zhou T, Qi X, Zhao M, Xuan B, Meng X, Guo Y, Liu Q, Liang H, Li Y, Dong H, Wang Y. Essential role of Na+/Ca2+ exchanger 1 in smoking-induced growth and migration of esophageal squamous cell carcinoma. *Oncotarget* 2016; **7**: 63816-63828 [PMID: 27588478 DOI: 10.18632/oncotarget.11695]

42   **Wray S**, Burdyga T. Sarcoplasmic reticulum function in smooth muscle. *Physiol Rev* 2010; **90**: 113-178 [PMID: 20086075 DOI: 10.1152/physrev.00018.2008]

43   **Webb RC**. Smooth muscle contraction and relaxation. *Adv Physiol Educ* 2003; **27**: 201-206 [PMID: 14627618 DOI: 10.1152/advan.00025.2003]

44   **Sakai Y**, Kinoshita H, Saitou K, Homma I, Nobe K, Iwamoto T. Functional differences of Na+/Ca2+ exchanger expression in Ca2+ transport system of smooth muscle of guinea pig stomach. *Can J Physiol Pharmacol* 2005; **83**: 791-797 [PMID: 16333381 DOI: 10.1139/y05-079]

45   **Hagi K**, Azuma YT, Nakajima H, Shintani N, Hashimoto H, Baba A, Takeuchi T. Involvements of PHI-nitric oxide and PACAP-BK channel in the sustained relaxation of mouse gastric fundus. *Eur J Pharmacol* 2008; **590**: 80-86 [PMID: 18602629 DOI: 10.1016/j.ejphar.2008.05.045]

46   **Fujimoto Y**, Hayashi S, Azuma YT, Mukai K, Nishiyama K, Kita S, Morioka A, Nakajima H, Iwamoto T, Takeuchi T. Overexpression of Na$^+$/Ca^{2+} exchanger 1 display enhanced relaxation in the gastric fundus. *J Pharmacol Sci* 2016; **132**: 181-186 [PMID: 27816547 DOI: 10.1016/j.jphs.2016.10.003]

47   **Coskun T**, Yeğen BC, Alican I, Peker O, Kurtel H. Cold restraint stress-induced gastric mucosal dysfunction. Role of nitric oxide. *Dig Dis Sci* 1996; **41**: 956-963 [PMID: 8625769]

48   **Neurath MF**. Cytokines in inflammatory bowel disease. *Nat Rev Immunol* 2014; **14**: 329-342 [PMID: 24751956 DOI: 10.1038/nri3661]

49   **Li Y**, Wang WP, Wang HY, Cho CH. Intragastric administration of heparin enhances gastric ulcer healing through a nitric oxide-dependent mechanism in rats. *Eur J Pharmacol* 2000; **399**: 205-214

50   **Soufli I**, Toumi R, Rafa H, Touil-Boukoffa C. Overview of cytokines and nitric oxide involvement in immuno-pathogenesis of inflammatory bowel diseases. *World J Gastrointest Pharmacol Ther* 2016; **7**: 353-360 [PMID: 27602236 DOI: 10.4292/wjgpt.v7.i3.353]

51   **Boutemine IM**, Amri M, Amir ZC, Fitting C, Mecherara-Idjeri S, Layaida K, Sennoun N, Berkane S, Cavaillon JM, Touil-Boukoffa C. Gastro-protective, therapeutic and anti-inflammatory activities of Pistacia lentiscus L. fatty oil against ethanol-induced gastric ulcers in rats. *J Ethnopharmacol* 2018; **224**: 273-282 [PMID: 29859303 DOI: 10.1016/j.jep.2018.05.040]

52   **Mukai K**, Takeuchi T, Toyoshima M, Satoh Y, Fujita A, Shintani N, Hashimoto H, Baba A, Hata F. PACAP- and PHI-mediated sustained relaxation in circular muscle of gastric fundus: findings obtained in PACAP knockout mice. *Regul Pept* 2006; **133**: 54-61 [PMID: 16229904 DOI:

10.1016/j.regpep.2005.09.019]

53   **Mulè F**, Serio R. NANC inhibitory neurotransmission in mouse isolated stomach: involvement of nitric oxide, ATP and vasoactive intestinal polypeptide. *Br J Pharmacol* 2003; **140**: 431-437 [PMID: 12970100 DOI: 10.1038/sj.bjp.0705431]

54   **Baccari MC**, Calamai F. Modulation of nitrergic relaxant responses by peptides in the mouse gastric fundus. *Regul Pept* 2001; **98**: 27-32 [PMID: 11179775]

55   **Azuma YT**, Hayashi S, Nishiyama K, Kita S, Mukai K, Nakajima H, Iwamoto T, Takeuchi T. Na(+) /Ca(2+) exchanger-heterozygote knockout mice display increased relaxation in gastric fundus and accelerated gastric transit in vivo. *Neurogastroenterol Motil* 2016; **28**: 827-836 [PMID: 26787195 DOI: 10.1111/nmo.12779]

56   **Hinz B**, Phan SH, Thannickal VJ, Galli A, Bochaton-Piallat ML, Gabbiani G. The myofibroblast: one function, multiple origins. *Am J Pathol* 2007; **170**: 1807-1816 [PMID: 17525249 DOI: 10.2353/ajpath.2007.070112]

57   **Desmoulière A**, Chaponnier C, Gabbiani G. Tissue repair, contraction, and the myofibroblast. *Wound Repair Regen* 2005; **13**: 7-12 [PMID: 15659031 DOI: 10.1111/j.1067-1927.2005.130102.x]

58   **Nishida T**, Tsuji S, Kimura A, Tsujii M, Ishii S, Yoshio T, Shinzaki S, Egawa S, Irie T, Yasumaru M, Iijima H, Murata H, Kawano S, Hayashi N. Endothelin-1, an ulcer inducer, promotes gastric ulcer healing via mobilizing gastric myofibroblasts and stimulates production of stroma-derived factors. *Am J Physiol Gastrointest Liver Physiol* 2006; **290**: G1041-G1050 [PMID: 16384872 DOI: 10.1152/ajpgi.00462.2005]

59   **Chai J**, Norng M, Tarnawski AS, Chow J. A critical role of serum response factor in myofibroblast differentiation during experimental oesophageal ulcer healing in rats. *Gut* 2007; **56**: 621-630 [PMID: 17068115 DOI: 10.1136/gut.2006.106674]

60   **Guo X**, Oshima H, Kitamura T, Taketo MM, Oshima M. Stromal fibroblasts activated by tumor cells promote angiogenesis in mouse gastric cancer. *J Biol Chem* 2008; **283**: 19864-19871 [PMID: 18495668 DOI: 10.1074/jbc.M800798200]

61   **McCaig C**, Duval C, Hemers E, Steele I, Pritchard DM, Przemeck S, Dimaline R, Ahmed S, Bodger K, Kerrigan DD, Wang TC, Dockray GJ, Varro A. The role of matrix metalloproteinase-7 in redefining the gastric microenvironment in response to Helicobacter pylori. *Gastroenterology* 2006; **130**: 1754-1763 [PMID: 16697739 DOI: 10.1053/j.gastro.2006.02.031]

62   **Kim JA**, Yang H, Hwang I, Jung EM, Choi KC, Jeung EB. Expression patterns and potential action of the calcium transport genes Trpv5, Trpv6, Ncx1 and Pmca1b in the canine duodenum, kidney and uterus. *In Vivo* 2011; **25**: 773-780 [PMID: 21753133]

63   **Hwang I**, Jung EM, Yang H, Choi KC, Jeung EB. Tissue-specific expression of the calcium transporter genes TRPV5, TRPV6, NCX1, and PMCA1b in the duodenum, kidney and heart of Equus caballus. *J Vet Med Sci* 2011; **73**: 1437-1444 [PMID: 21737966]

64   **Wasserman RH**. Vitamin D and the dual processes of intestinal calcium absorption. *J Nutr* 2004; **134**: 3137-3139 [PMID: 15514288 DOI: 10.1093/jn/134.11.3137]

65   **Bronner F**. Recent developments in intestinal calcium absorption. *Nutr Rev* 2009; **67**: 109-113 [PMID: 19178653 DOI: 10.1111/j.1753-4887.2008.00147.x]

66   **Khuituan P**, Wongdee K, Jantarajit W, Suntornsaratoon P, Krishnamra N, Charoenphandhu N. Fibroblast growth factor-23 negates 1,25(OH)2D3-induced intestinal calcium transport by reducing the transcellular and paracellular calcium fluxes. *Arch Biochem Biophys* 2013; **536**: 46-52 [PMID: 23747333 DOI: 10.1016/j.abb.2013.05.009]

67   **Wongdee K**, Charoenphandhu N. Vitamin D-enhanced duodenal calcium transport. *Vitam Horm* 2015; **98**: 407-440 [PMID: 25817876 DOI: 10.1016/bs.vh.2014.12.010]

68   **Xie R**, Dong X, Wong C, Vallon V, Tang B, Sun J, Yang S, Dong H. Molecular mechanisms of calcium-sensing receptor-mediated calcium signaling in the modulation of epithelial ion transport and bicarbonate secretion. *J Biol Chem* 2014; **289**: 34642-34653 [PMID: 25331955 DOI: 10.1074/jbc.M114.592774]

69   **Dong H**, Sellers ZM, Smith A, Chow JY, Barrett KE. Na(+)/Ca(2+) exchange regulates Ca(2+)-dependent duodenal mucosal ion transport and HCO3(-) secretion in mice. *Am J Physiol Gastrointest Liver Physiol* 2005; **288**: G457-G465 [PMID: 15499079 DOI: 10.1152/ajpgi.00381.2004]

70   **Smith AJ**, Chappell AE, Buret AG, Barrett KE, Dong H. 5-Hydroxytryptamine contributes significantly to a reflex pathway by which the duodenal mucosa protects itself from gastric acid injury. *FASEB J* 2006; **20**: 2486-2495 [PMID: 17142798 DOI: 10.1096/fj.06-6391com]

71   **Nishiyama K**, Azuma YT, Morioka A, Yoshida N, Teramoto M, Tanioka K, Kita S, Hayashi S, Nakajima H, Iwamoto T, Takeuchi T. Roles of Na(+)/Ca(2+) exchanger isoforms NCX1 and NCX2 in motility in mouse ileum. *Naunyn Schmiedebergs Arch Pharmacol* 2016; **389**: 1081-1090 [PMID: 27411318 DOI: 10.1007/s00210-016-1271-1]

72   **Nishiyama K**, Morioka A, Kita S, Nakajima H, Iwamoto T, Azuma YT, Takeuchi T. Na/Ca(2+) exchanger 1 transgenic mice display increased relaxation in the distal colon. *Pharmacology* 2014; **94**: 230-238 [PMID: 25427675 DOI: 10.1159/000363246]

73   **Mitrovic S**, Nogueira C, Cantero-Recasens G, Kiefer K, Fernández-Fernández JM, Popoff JF, Casano L, Bard FA, Gomez R, Valverde MA, Malhotra V. TRPM5-mediated calcium uptake regulates mucin secretion from human colon goblet cells. *Elife* 2013; **2**: e00658 [PMID: 23741618 DOI: 10.7554/eLife.00658]

74   **Nishiyama K**, Azuma YT, Kita S, Azuma N, Hayashi S, Nakajima H, Iwamoto T, Takeuchi T. Na/Ca² exchanger 1/2 double-heterozygote knockout mice display increased nitric oxide component and altered colonic motility. *J Pharmacol Sci* 2013; **123**: 235-245 [PMID: 24162024]

75   **Nishiyama K**, Tanioka K, Azuma YT, Hayashi S, Fujimoto Y, Yoshida N, Kita S, Suzuki S, Nakajima H, Iwamoto T, Takeuchi T. Na$^+$/Ca^{2+} exchanger contributes to stool transport in mice with experimental diarrhea. *J Vet Med Sci* 2017; **79**: 403-411 [PMID: 27928109 DOI: 10.1292/jvms.16-0475]

76   **Briejer MR**, Schuurkes JA. 5-HT3 and 5-HT4 receptors and cholinergic and tachykininergic neurotransmission in the guinea-pig proximal colon. *Eur J Pharmacol* 1996; **308**: 173-180 [PMID: 8840129]

77   **Tuladhar BR**, Costall B, Naylor RJ. 5-HT3 and 5-HT4 receptor-mediated facilitation of the emptying phase of the peristaltic reflex in the marmoset isolated ileum. *Br J Pharmacol* 1996; **117**: 1679-1684 [PMID: 8732276]

78   **Rivière PJ**, Farmer SC, Burks TF, Porreca F. Prostaglandin E2-induced diarrhea in mice:

importance of colonic secretion. *J Pharmacol Exp Ther* 1991; **256**: 547-552 [PMID: 1993994]

79   **Wardle TD**, Hall L, Turnberg LA. Inter-relationships between inflammatory mediators released from colonic mucosa in ulcerative colitis and their effects on colonic secretion. *Gut* 1993; **34**: 503-508 [PMID: 8491398]

80   **Ankorina-Stark I**, Amstrup J, Novak I. Regulation of the Na+/Ca2+ exchanger in rat pancreatic ducts. *J Membr Biol* 2002; **186**: 43-53 [PMID: 11891588 DOI: 10.1007/s00232-001-0134-x]

81   **Quednau BD**, Nicoll DA, Philipson KD. Tissue specificity and alternative splicing of the Na+/Ca2+ exchanger isoforms NCX1, NCX2, and NCX3 in rat. *Am J Physiol* 1997; **272**: C1250-C1261 [PMID: 9142850 DOI: 10.1152/ajpcell.1997.272.4.C1250]

82   **Hamming KS**, Riedel MJ, Soliman D, Matemisz LC, Webster NJ, Searle GJ, MacDonald PE, Light PE. Splice variant-dependent regulation of beta-cell sodium-calcium exchange by acyl-coenzyme As. *Mol Endocrinol* 2008; **22**: 2293-2306 [PMID: 18635667 DOI: 10.1210/me.2008-0053]

83   **Herchuelz A**, Diaz-Horta O, van Eylen F. Na/Ca exchange and Ca2+ homeostasis in the pancreatic beta-cell. *Diabetes Metab* 2002; **28**: 3S54-60; discussion 3S108-12 [PMID: 12688634]

84   **Van Eylen F**, Bollen A, Herchuelz A. NCX1 Na/Ca exchanger splice variants in pancreatic islet cells. *J Endocrinol* 2001; **168**: 517-526 [PMID: 11241183]

85   **Rorsman P**, Renström E. Insulin granule dynamics in pancreatic beta cells. *Diabetologia* 2003; **46**: 1029-1045 [PMID: 12879249 DOI: 10.1007/s00125-003-1153-1]

86   **Bruce JI**, Yang X, Ferguson CJ, Elliott AC, Steward MC, Case RM, Riccardi D. Molecular and functional identification of a Ca2+ (polyvalent cation)-sensing receptor in rat pancreas. *J Biol Chem* 1999; **274**: 20561-20568 [PMID: 10400686]

87   **Herchuelz A**, Diaz-Horta O, Van Eylen F. Na/Ca exchange in function, growth, and demise of beta-cells. *Ann N Y Acad Sci* 2002; **976**: 315-324 [PMID: 12502574]

88   **Herchuelz A**, Kamagate A, Ximenes H, Van Eylen F. Role of Na/Ca exchange and the plasma membrane Ca2+-ATPase in beta cell function and death. *Ann N Y Acad Sci* 2007; **1099**: 456-467 [PMID: 17446486 DOI: 10.1196/annals.1387.048]

89   **Herchuelz A**, Pachera N. The Na^+/Ca^{2+} exchanger and the Plasma Membrane Ca^{2+}-ATPase in β-cell function and diabetes. *Neurosci Lett* 2018; **663**: 72-78 [PMID: 28780165 DOI: 10.1016/j.neulet.2017.08.009]

90   **Van Eylen F**, Horta OD, Barez A, Kamagate A, Flatt PR, Macianskiene R, Mubagwa K, Herchuelz A. Overexpression of the Na/Ca exchanger shapes stimulus-induced cytosolic Ca(2+) oscillations in insulin-producing BRIN-BD11 cells. *Diabetes* 2002; **51**: 366-375 [PMID: 11812743]

91   **Petersen OH**, Tepikin AV, Gerasimenko JV, Gerasimenko OV, Sutton R, Criddle DN. Fatty acids, alcohol and fatty acid ethyl esters: toxic Ca2+ signal generation and pancreatitis. *Cell Calcium* 2009; **45**: 634-642 [PMID: 19327825 DOI: 10.1016/j.ceca.2009.02.005]

92   **Gerasimenko JV**, Gryshchenko O, Ferdek PE, Stapleton E, Hébert TO, Bychkova S, Peng S, Begg M, Gerasimenko OV, Petersen OH. Ca2+ release-activated Ca2+ channel blockade as a potential tool in antipancreatitis therapy. *Proc Natl Acad Sci U S A* 2013; **110**: 13186-13191 [PMID: 23878235 DOI: 10.1073/pnas.1300910110]

93   **Vigna SR**, Shahid RA, Liddle RA. Ethanol contributes to neurogenic pancreatitis by activation of TRPV1. *FASEB J* 2014; **28**: 891-896 [PMID: 24221085 DOI: 10.1096/fj.13-236208]

94   **Yu SY**, Xie R, Chen YY, Yang SM, Zhu B. Role of sodium-calcium exchanger-1 in development of rat acute pancreatitis. *Di-San Junyi Daxue Xuebao* 2015; **37**: 1325-1330 [DOI: 10.16016/j.1000-5404.201501236]

95   **Jemal A**, Siegel R, Ward E, Hao Y, Xu J, Murray T, Thun MJ. Cancer statistics, 2008. *CA Cancer J Clin* 2008; **58**: 71-96 [PMID: 18287387 DOI: 10.3322/ca.2007.0010]

96   **Schmidt CM**, Powell ES, Yiannoutsos CT, Howard TJ, Wiebke EA, Wiesenauer CA, Baumgardner JA, Cummings OW, Jacobson LE, Broadie TA, Canal DF, Goulet RJ Jr, Curie EA, Cardenes H, Watkins JM, Loehrer PJ, Lillemoe KD, Madura JA. Pancreaticoduodenectomy: a 20-year experience in 516 patients. *Arch Surg* 2004; **139**: 718-25; discussion 725-7 [PMID: 15249403 DOI: 10.1001/archsurg.139.7.718]

97   **Truty MJ**, Urrutia R. Basics of TGF-beta and pancreatic cancer. *Pancreatology* 2007; **7**: 423-435 [PMID: 17898532 DOI: 10.1159/000108959]

98   **Dong H**, Shim KN, Li JM, Estrema C, Ornelas TA, Nguyen F, Liu S, Ramamoorthy SL, Ho S, Carethers JM, Chow JY. Molecular mechanisms underlying Ca2+-mediated motility of human pancreatic duct cells. *Am J Physiol Cell Physiol* 2010; **299**: C1493-C1503 [PMID: 20861471 DOI: 10.1152/ajpcell.00242.2010]

99   **Xu JY**, Jiang YX, Xie R, Jin H, Wen GR, Tuo BG. The expression of NCX1 and its effect on proliferation and migration of hepatocellular carcinoma cells through regulation of intracellular Ca2+. *Zhongguo Aizheng Zazhi* 2016; **26**: 735-742 [DOI: 10.19401/j.cnki.1007-3639.2016.09.003]

100   **Guan LY**, Fu PY, Li PD, Li ZN, Liu HY, Xin MG, Li W. Mechanisms of hepatic ischemia-reperfusion injury and protective effects of nitric oxide. *World J Gastrointest Surg* 2014; **6**: 122-128 [PMID: 25068009 DOI: 10.4240/wjgs.v6.i7.122]

101   **Vasques ER**, Cunha JE, Coelho AM, Sampietre SN, Patzina RA, Abdo EE, Nader HB, Tersariol IL, Lima MA, Godoy CM, Rodrigues T, Chaib E, D'Albuquerque LA. Trisulfate Disaccharide Decreases Calcium Overload and Protects Liver Injury Secondary to Liver Ischemia/Reperfusion. *PLoS One* 2016; **11**: e0149630 [PMID: 26901764 DOI: 10.1371/journal.pone.0149630]

102   **Nakamura T**, Arii S, Monden K, Furutani M, Takeda Y, Imamura M, Tominaga M, Okada Y. Expression of the Na+/Ca2+ exchanger emerges in hepatic stellate cells after activation in association with liver fibrosis. *Proc Natl Acad Sci U S A* 1998; **95**: 5389-5394 [PMID: 9560286]

103   **Xu J**, Yang Y, Xie R, Liu J, Nie X, An J, Wen G, Liu X, Jin H, Tuo B. The NCX1/TRPC6 Complex Mediates TGFβ-Driven Migration and Invasion of Human Hepatocellular Carcinoma Cells. *Cancer Res* 2018; **78**: 2564-2576 [PMID: 29500176 DOI: 10.1158/0008-5472.can-17-2061]

104   **Tian Y**, Zhu MX. A novel TRPC6-dependent mechanism of TGF-β-induced migration and invasion of human hepatocellular carcinoma cells. *Sci China Life Sci* 2018; **61**: 1120-1122 [PMID: 30136057 DOI: 10.1007/s11427-018-9365-7]

105   **Rusolo F**, Pucci B, Colonna G, Capone F, Guerriero E, Milone MR, Nazzaro M, Volpe MG, Di Bernardo G, Castello G, Costantini S. Evaluation of selenite effects on selenoproteins and cytokinome in human hepatoma cell lines. *Molecules* 2013; **18**: 2549-2562 [PMID: 23442931 DOI: 10.3390/molecules18032549]

106 **Xu J**, Ji B, Wen G, Yang Y, Jin H, Liu X, Xie R, Song W, Song P, Dong H, Tuo B. Na+/H+ exchanger 1, Na+/Ca2+ exchanger 1 and calmodulin complex regulates interleukin 6-mediated cellular behavior of human hepatocellular carcinoma. *Carcinogenesis* 2016; **37**: 290-300 [PMID: 26775040 DOI: 10.1093/carcin/bgw004]

Endoscopic resection techniques for colorectal neoplasia: Current developments

Franz Ludwig Dumoulin, Ralf Hildenbrand

ORCID number: Franz Ludwig Dumoulin (0000-0002-1058-7867); Ralf Hildenbrand (0000-0002-8708-2023).

Franz Ludwig Dumoulin, Department of Medicine and Gastroenterology, Gemeinschaftskrankenhaus Bonn, Bonn 53113, Germany

Ralf Hildenbrand, Institute for Pathology, Bonn Duisdorf, Bonn 53123, Germany

Corresponding author: Franz Ludwig Dumoulin, MD, PhD, Associate Professor, Department of Medicine and Gastroenterology, Gemeinschaftskrankenhaus Bonn, Bonner Talweg 4-6, Bonn 53113, Germany. f.dumoulin@gk-bonn.de
Telephone: +49-228-5081561
Fax: +49-228-5081562

Abstract

Endoscopic polypectomy and endoscopic mucosal resection (EMR) are the established treatment standards for colorectal polyps. Current research aims at the reduction of both complication and recurrence rates as well as on shortening procedure times. Cold snare resection is the emerging standard for the treatment of smaller (< 5mm) polyps and is possibly also suitable for the removal of non-cancerous polyps up to 9 mm. The method avoids thermal damage, has reduced procedure times and probably also a lower risk for delayed bleeding. On the other end of the treatment spectrum, endoscopic submucosal dissection (ESD) offers *en bloc* resection of larger flat or sessile lesions. The technique has obvious advantages in the treatment of high-grade dysplasia and early cancer. Due to its minimal recurrence rate, it may also be an alternative to fractionated EMR of larger flat or sessile lesions. However, ESD is technically demanding and burdened by longer procedure times and higher costs. It should therefore be restricted to lesions suspicious for high-grade dysplasia or early invasive cancer. The latest addition to endoscopic resection techniques is endoscopic full-thickness resection with specifically developed devices for flexible endoscopy. This method is very useful for the treatment of smaller difficult-to-resect lesions, *e.g.*, recurrence with scar formation after previous endoscopic resections.

Key words: Colorectal neoplasia; Colorectal cancer screening; Cold snare resection; Endoscopic polypectomy; Endoscopic mucosal resection; Endoscopic submucosal dissection; Endoscopic full-thickness resection; Adenoma recurrence rate

Core tip: Endoscopic polypectomy and endoscopic mucosal resection are the standard treatment options for colorectal neoplasia. Current research is evaluating cold snare

resection for the treatment of smaller non-cancerous polyps, aiming to reduce procedure times and complication rates. Endoscopic submucosal dissection has great potential for the *en bloc* resection of larger flat or sessile lesions. However, it is technically demanding and time consuming and should be reserved for histologically advanced lesions. Endoscopic full-thickness resection is a welcome addition to the armamentarium of endoscopic resection techniques and is very useful for the treatment of smaller difficult-to-resect lesions.

INTRODUCTION

Colorectal cancer screening and endoscopic polyp resection can reduce mortality from colorectal cancer[1] and are now recommended by many national guidelines[2]. Snare polypectomy and endoscopic mucosal resection (EMR) are the established treatment standards for polyp removal[3-6]. The advantages of these methods are relatively short procedure times and an accepted complication rate, with delayed bleeding in 0.9% and a risk of perforation between 0.4% and 1.3% depending on the size and location of the resected lesion[5]. A recent modification is underwater EMR. A limited number of studies suggest that larger lesions can be removed *en bloc* with low complication rates and short procedure times[7]. However, despite being widely practiced, the standard EMR techniques are not perfect. Thus, there still is a considerable rate of adverse events, particularly perforation and bleeding. Moreover, larger lesions cannot reliably be removed, which results in incomplete resections. Finally, dense fibrosis results in nonlifting, difficult-to-treat lesions. This minireview will focus on current advances in endoscopic resection techniques attempting to overcome these problems, particularly cold snare resection to reduce complication rates, endoscopic submucosal dissection (ESD) to increase the *en bloc* resection rate for larger flat or sessile lesions, and endoscopic full-thickness resection (EFTR) for difficult-to-resect (nonlifting) lesions.

REMOVING POLYPS MORE QUICKLY AND SAFELY: COLD SNARE RESECTION

The disadvantages of conventional hot snare resection are caused by thermal injury. Possible complications are delayed bleeding and thermal injury resulting in postpolypectomy syndrome and delayed perforation. Recently, cold snare resection has been introduced as a possible alternative. The method involves snaring - mostly with dedicated devices - without the use of additional electrocautery (Figure 1). It has mainly been applied to small (up to 5 mm) polyps but has recently been extended to larger lesions. This method offers possible advantages of reducing procedure time and postinterventional complications while maintaining the same efficacy as conventional hot snare resection.

Several studies have been published on this subject. A recent meta-analysis included eight randomized controlled studies with 3195 interventions[8]. Compared to conventional techniques, cold snare resection showed similar efficacy but significantly shortened procedure times and a trend towards reduced rates of delayed bleeding. On the other hand, possible disadvantages of cold snare resection techniques were highlighted in a histopathology study on 184 polyps[9]. In this study, cold snare resection was associated with increased rates of specimen damage, increased rates of positive margins and a decreased resection depth. Incomplete resections were observed predominantly for serrated/hyperplastic lesions[9]. Therefore, cold snare resection does not seem to be suitable for malignant lesions where one-piece EMR or ESD are recommended[6]. In addition, cold snare resection has also been applied to slightly larger lesions. Along these lines, piecemeal cold snare resection was reported for 94 lesions > 10 mm with no adverse events and a short-term recurrence rate of 9.7%[10]. A similar series of 41 lesions with a median size of 15 mm showed no
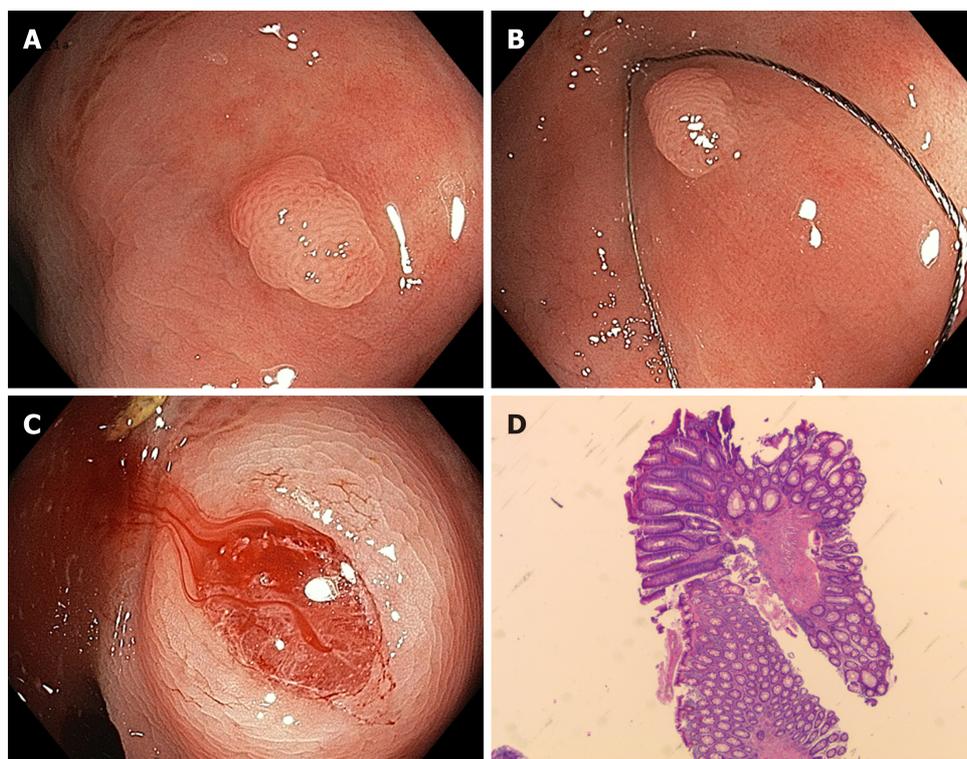
Figure 1 Cold snare resection. A: Endoscopic appearance of a small polyp in the sigmoid colon. B: Positioning of a specifically dedicated snare for cold snare resection. C: Appearance of the resection field with mild bleeding. D: Histopathology showing tubular adenoma (hematoxylin/eosine, magnification: 80-fold).

evidence of complications or recurrence after a follow-up period of 6 mo[11]. The current European guideline recommends cold snare resection as the preferred technique for removal of diminutive polyps (size ≤ 5 mm). In addition, the guideline recommends this technique also for sessile polyps of 6-9 mm size, although formal evidence comparing efficacy with conventional hot snare polypectomy is still lacking[6]. With regard to technical issues, the use of dedicated snares seems to be beneficial[12].

In summary, cold snare resection is becoming the standard of treatment for diminutive (up to 5 mm) and also to small sessile non-cancerous polyps (up to 9 mm). Larger studies will need to define the exact role of cold snare resection in polyp removal.

EXPANDING THE BORDER FOR THE RESECTION OF LARGER LESIONS: ESD

The major advantages of EMR are the relatively short procedure times (ca. 35 min for larger lesions[13]) and an acceptable complication rate, with delayed bleeding in 0.9%[5] and a perforation rate between 0.4% and 1.3%[5,14]. It should be emphasized that the complication rates depend on the size and location of the resected lesion. Thus, a delayed bleeding rate of 6.7% was reported in a recent multicenter study including > 2000 EMRs[15]. Risk factors for bleeding included the size lesion, polyp location in the right colon and patient comorbidity[15]. The frequency of perforation after EMR is between 0.4% and 1.3% and depends on the size and location of the resected lesion[5,14].

The disadvantage of EMR is its size limitation of approximately 20 mm. Larger lesions cannot be resected *en bloc* and instead must be removed in fragments (piecemeal EMR technique). This fragmentation implies that a complete resection cannot be confirmed by histopathology and piecemeal EMR is associated with recurrence rates of approximately 15%-20% in retrospective series[16,17] and more than 30% in a recent prospective study on endoscopic piecemeal resection of 252 adenomas > 20 mm in size[18]. Many risk factors for recurrences have been identified, including lesion size, number of resected fragments, and more advanced histology (tubulovillous adenoma or high-grade intraepithelial neoplasia)[17,19]. Moreover, multiple recurrences are not a rare event (ca. 20%-40%), although most of them are amenable to further endoscopic treatment[14]. Notably, incomplete endoscopic

resection of adenomas is thought to be responsible for 20%-25% of interval cancers[20]. The recurrence rate implies the necessity of endoscopic controls and compliance with follow-up endoscopy[16,17].

Whereas EMR of larger flat or sessile lesions will result in fragmented resection, ESD - developed in Japan for the treatment of early gastric cancer - offers the possibility of *en bloc* resection for larger lesions. The method consists of incision of the mucosa followed by submucosal dissection underneath the lesion to yield an *en bloc* specimen with no size restriction (Figure 2). ESD is much more technically demanding than EMR and requires longer procedure times, with a median procedure time of ca. 70 min in a recent meta-analysis[21,22]. The procedure time and level of complexity depend primarily on endoscopic access to the lesion and access to the submucosal compartment[23]. The method is not considered standard in Europe[6], but it has been included in the Japanese guidelines as the standard technique for larger neoplastic lesions for which *en bloc* resection is desirable[4]. Most clinical data on colorectal ESD are from Asia. Larger (> 500 patients) retrospective or prospective observational studies report *en bloc* and R0 resection rates of 84% to 94.5%, with very few recurrences[4,24]. In contrast, experience with colorectal ESD is very limited in the Western world. This is mainly due to the lack of training opportunities, the high level of skills necessary to perform colorectal ESD and the fact that this method has longer procedure times and probably also higher complication rates than piecemeal EMR. However, it is possible to achieve competence in colorectal ESD without prior expertise in gastric ESD, particularly if training is performed under the supervision of (Eastern) ESD experts[25-27]. Consequently, data from Western endoscopists are rare, with smaller case series and only two publications on larger (*n* > 150) series, mainly including lesions localized in the rectum[28,29]. Both *en bloc* and R0 resection rates are lower in those publications than in studies from Asian populations, which is particularly true for larger lesions in the proximal colon[28]. Adverse events are more common for ESD than for EMR, with published perforation rates of approximately 4.8% (2%-14%) for the former[4,30,31]. However, most perforations are minor and can be closed with standard clips during or at the end of the procedure, and the rate of emergency surgery is relatively low (ca. 0.5%). Delayed bleeding is observed after 1.5%-2.8% of interventions. Strictures are observed only occasionally, *e.g.*, after circumferential resections in the rectum[30].

A recent meta-analysis highlighted the differences between EMR and ESD[22], with the latter having higher *en bloc* resection rates that come at the cost of higher complication rates (although most complications can be treated conservatively) and longer procedure times. Finally, while the concept of *en bloc* resection of neoplasia is appealing, ESD also has higher costs than EMR. A recent cost-effectiveness analysis of wide-field EMR *vs* ESD concluded that selective ESD for high-risk lesions is the most cost-effective application of colorectal ESD[32]. Compared with laparoscopic surgery, ESD has major advantages, although a formal head-to-head comparison is still lacking[33-36].

TREATMENT OPTION FOR DIFFICULT-TO-RESECT NEOPLASIA: EFTR

Conventional endoscopic resection may not be technically feasible in cases of severe fibrosis, *e.g.*, due to scar formation in adenoma recurrences after previous resection or in cases of adenomas in specific anatomical locations, *e.g.*, close to a diverticulum or at the appendiceal orifice. In these situations, EFTR may be a useful alternative. This method involves a full-thickness plication of the bowel wall, which is secured by an over-the-scope clip followed by resection of the bowel wall above the clip. The full thickness resection device (FTRD®) System (Ovesco, Tübingen, Germany) is a single-step full-thickness resection device combining a modified over-the-scope clip with an integrated snare[37]. After the lesion is marked, the colonoscope is retracted, and the FTRD is mounted and advanced to the target. The lesion is then pulled into the resection cap, and after deployment of the clip, the snare is closed and the tissue is cut (Figure 3). Alternatively, a flat over-the-scope clip (Padlock clip, US Endoscopy, Mentor, Ohio, United States) is used to create a plication, and the tissue above is then resected with a snare.

EFTR is particularly useful for the resection of smaller (up to 15-20 mm) nonlifting lesions. To date, there are only limited data on the efficacy of the method, usually performed with the FTRD device[38-41]. Procedure time depends mainly on the location of the lesion (sometimes passage to proximal locations can be difficult or even impossible). It is more time consuming than EMR, and the size of the lesions is limited by the size of the cap. In the largest prospective study published so far, the R0
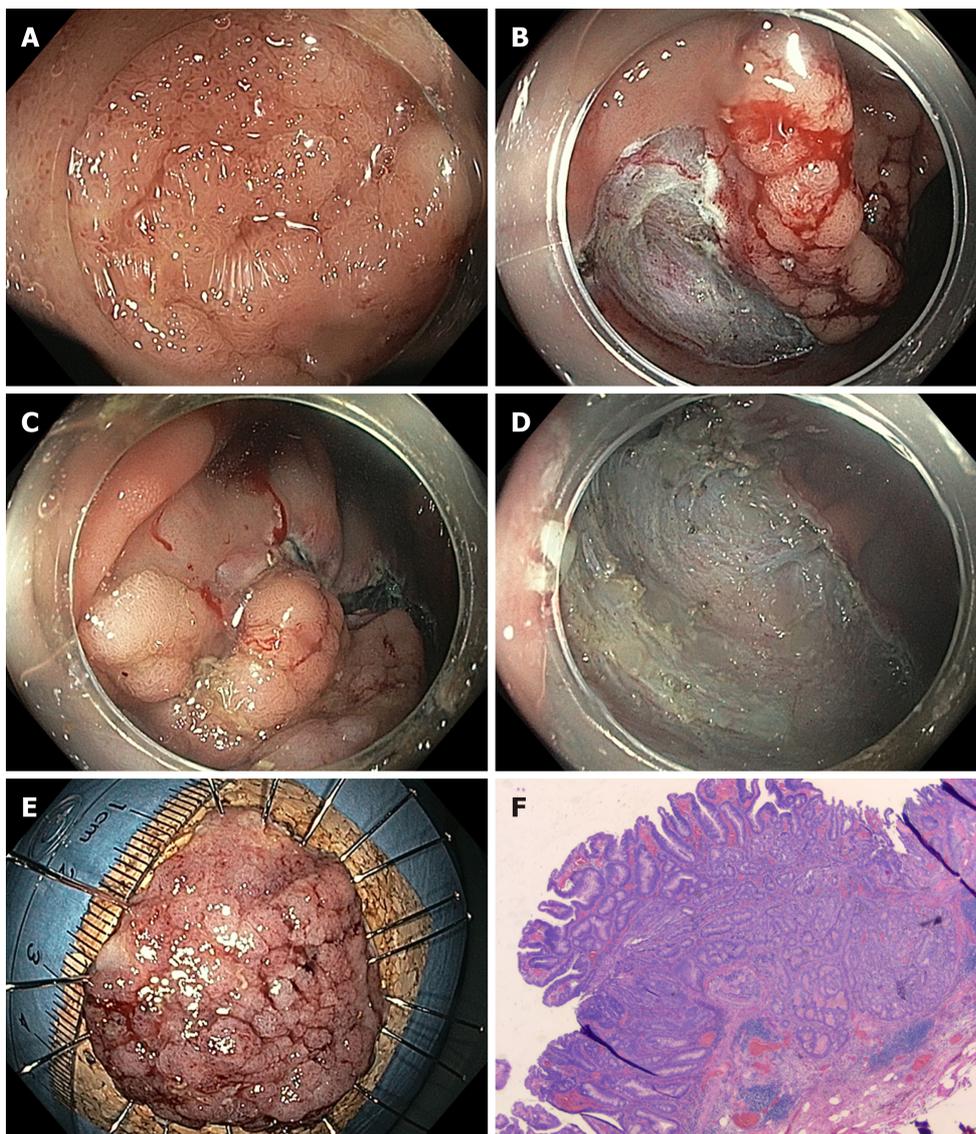
Figure 2 Endoscopic submucosal dissection. A: Endoscopic aspect of a large sessile lesion (Paris 0-Is/0-IIa; lateral spreading tumor, granular type) in the cecum. B: Start of endoscopic submucosal dissection at the proximal site. C: Mucosal incision at the distal margin. D: Completed resection with resection bed in the cecum. E: Resected specimen on corkboard. F: Histopathology: tubulovillous adenoma with focal high-grade intraepithelial neoplasia (hematoxylin/eosine, magnification: 80-fold).

resection rate was 77.7% for 127 patients with nonlifting adenomas. The overall complication rate was 9.9% and included perforation, fistula, bleeding and appendicitis; the rate of emergency surgery was 2.2%[42].

CONCLUSION

Polypectomy and EMR remain the standard treatment options for the removal of most colorectal neoplasia. They are relatively easy and quick to perform in terms of technique and have an acceptable complication rate. New developments are underway with cold snare resection as a method that might be associated with even shorter procedure times and lower complication rates. In addition, ESD has the potential for the *en bloc* resection of larger lesions; it should probably be reserved for larger lesions suspicious of high grade dysplasia or early invasive cancer. Finally, smaller difficult-to-resect lesions can now be treated effectively by EFTR.
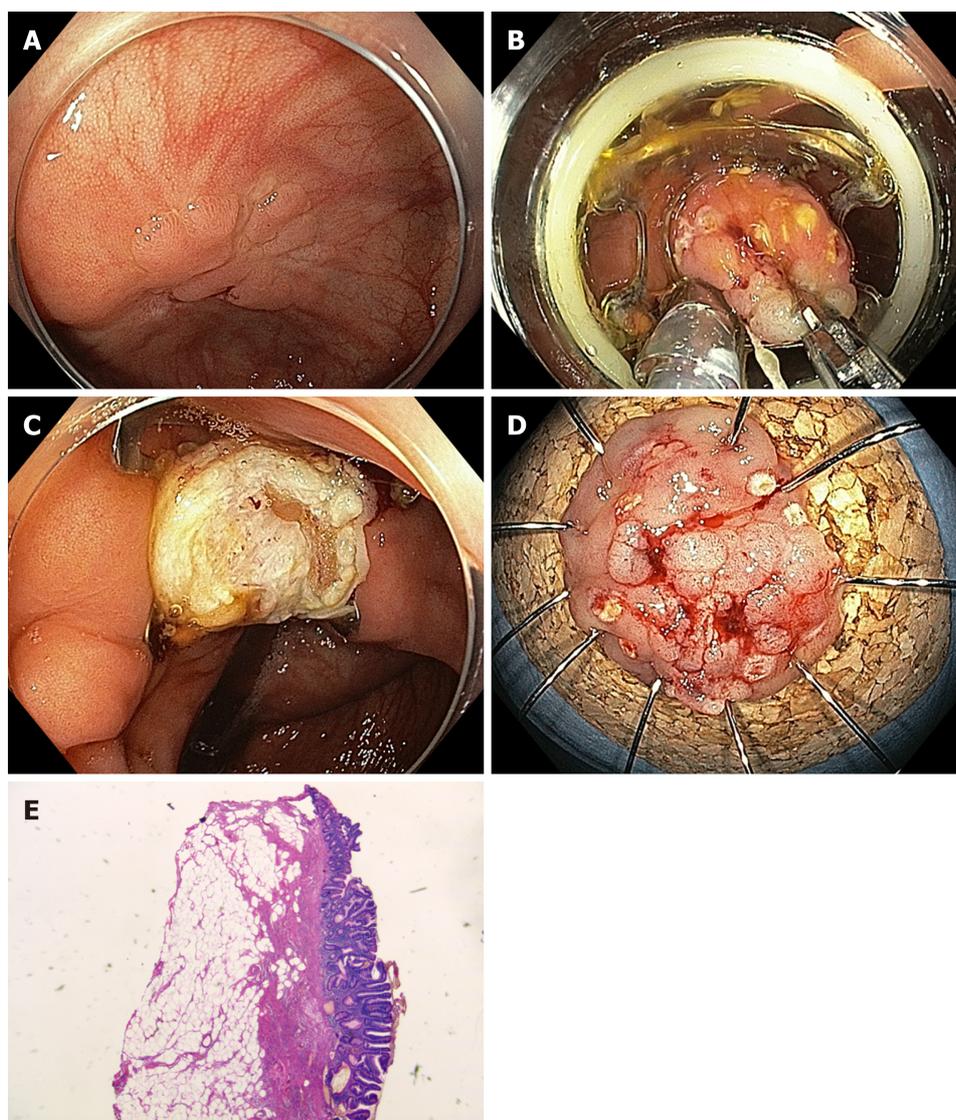
Figure 3 Endoscopic full-thickness resection with the full thickness resection device. A: Endoscopic aspect of a recurrence after piecemeal endoscopic mucosal resection in the ascending colon. B: The lesion is marked and retracted into the resection cap using a grasping forceps. C: Resection bed with over the scope clip in situ. Note the periluminal fat within the clip. D: Resected specimen on corkboard. E: Histopathology: full-thickness resection specimen with tubulovillous adenoma/low-grade intraepithelial neoplasia (hematoxylin/eosine, magnification 80-fold).

REFERENCES

1   **Zauber AG**, Winawer SJ, O'Brien MJ, Lansdorp-Vogelaar I, van Ballegooijen M, Hankey BF, Shi W, Bond JH, Schapiro M, Panish JF, Stewart ET, Waye JD. Colonoscopic polypectomy and long-term prevention of colorectal-cancer deaths. *N Engl J Med* 2012; **366**: 687-696 [PMID: 22356322 DOI: 10.1056/NEJMoa1100370]

2   **Bénard F**, Barkun AN, Martel M, von Renteln D. Systematic review of colorectal cancer screening guidelines for average-risk adults: Summarizing the current global recommendations. *World J Gastroenterol* 2018; **24**: 124-138 [PMID: 29358889 DOI: 10.3748/wjg.v24.i1.124]

3   **Rex DK**, Johnson DA, Anderson JC, Schoenfeld PS, Burke CA, Inadomi JM; American College of Gastroenterology. American College of Gastroenterology guidelines for colorectal cancer screening 2009 [corrected]. *Am J Gastroenterol* 2009; **104**: 739-750 [PMID: 19240699 DOI: 10.1038/ajg.2009.104]

4   **Tanaka S**, Kashida H, Saito Y, Yahagi N, Yamano H, Saito S, Hisabe T, Yao T, Watanabe M, Yoshida M, Kudo SE, Tsuruta O, Sugihara K, Watanabe T, Saitoh Y, Igarashi M, Toyonaga T, Ajioka Y, Ichinose M, Matsui T, Sugita A, Sugano K, Fujimoto K, Tajiri H. JGES guidelines for colorectal endoscopic submucosal dissection/endoscopic mucosal resection. *Dig Endosc* 2015; **27**: 417-434 [PMID: 25652022 DOI: 10.1111/den.12456]

5   **Schmiegel W**, Buchberger B, Follmann M, Graeven U, Heinemann V, Langer T, Nothacker M, Porschen R, Rödel C, Rösch T, Schmitt W, Wesselmann S, Pox C. S3-Leitlinie – Kolorektales Karzinom. *Z Gastroenterol* 2017; **55**: 1344-1498 [PMID: 29212104 DOI: 10.1055/s-0043-121106]

6   **Ferlitsch M**, Moss A, Hassan C, Bhandari P, Dumonceau JM, Paspatis G, Jover R, Langner C, Bronzwaer M, Nalankilli K, Fockens P, Hazzan R, Gralnek IM, Gschwantler M, Waldmann E, Jeschek P, Penz D, Heresbach D, Moons L, Lemmers A, Paraskeva K, Pohl J, Ponchon T, Regula J,

Repici A, Rutter MD, Burgess NG, Bourke MJ. Colorectal polypectomy and endoscopic mucosal resection (EMR): European Society of Gastrointestinal Endoscopy (ESGE) Clinical Guideline. *Endoscopy* 2017; **49**: 270-297 [PMID: 28212588 DOI: 10.1055/s-0043-102569]

7   **Gaglia A**, Sarkar S. Evaluation and long-term outcomes of the different modalities used in colonic endoscopic mucosal resection. *Ann Gastroenterol* 2017; **30**: 145-151 [PMID: 28243034 DOI: 10.20524/aog.2016.0104]

8   **Shinozaki S**, Kobayashi Y, Hayashi Y, Sakamoto H, Lefor AK, Yamamoto H. Efficacy and safety of cold versus hot snare polypectomy for resecting small colorectal polyps: Systematic review and meta-analysis. *Dig Endosc* 2018; **30**: 592-599 [PMID: 29675857 DOI: 10.1111/den.13173]

9   **Ito A**, Suga T, Ota H, Tateiwa N, Matsumoto A, Tanaka E. Resection depth and layer of cold snare polypectomy versus endoscopic mucosal resection. *J Gastroenterol* 2018; **53**: 1171-1178 [PMID: 29516270 DOI: 10.1007/s00535-018-1446-2]

10 **Piraka C**, Saeed A, Waljee AK, Pillai A, Stidham R, Elmunzer BJ. Cold snare polypectomy for non-pedunculated colon polyps greater than 1cm. *Endosc Int Open* 2017; **5**: E184-E189 [PMID: 28331902 DOI: 10.1055/s-0043-101696]

11 **Tate DJ**, Awadie H, Bahin FF, Desomer L, Lee R, Heitman SJ, Goodrick K, Bourke MJ. Wide-field piecemeal cold snare polypectomy of large sessile serrated polyps without a submucosal injection is safe. *Endoscopy* 2018; **50**: 248-252 [PMID: 29169195 DOI: 10.1055/s-0043-121219]

12 **Jung YS**, Park CH, Nam E, Eun CS, Park DI, Han DS. Comparative efficacy of cold polypectomy techniques for diminutive colorectal polyps: a systematic review and network meta-analysis. *Surg Endosc* 2018; **32**: 1149-1159 [PMID: 28812188 DOI: 10.1007/s00464-017-5786-4]

13 **Moss A**, Williams SJ, Hourigan LF, Brown G, Tam W, Singh R, Zanati S, Burgess NG, Sonson R, Byth K, Bourke MJ. Long-term adenoma recurrence following wide-field endoscopic mucosal resection (WF-EMR) for advanced colonic mucosal neoplasia is infrequent: results and risk factors in 1000 cases from the Australian Colonic EMR (ACE) study. *Gut* 2015; **64**: 57-65 [PMID: 24986245 DOI: 10.1136/gutjnl-2013-305516]

14 **Holmes I**, Friedland S. Endoscopic Mucosal Resection versus Endoscopic Submucosal Dissection for Large Polyps: A Western Colonoscopist's View. *Clin Endosc* 2016; **49**: 454-456 [PMID: 27561263 DOI: 10.5946/ce.2016.077]

15 **Bahin FF**, Rasouli KN, Byth K, Hourigan LF, Singh R, Brown GJ, Zanati SA, Moss A, Raftopoulos S, Williams SJ, Bourke MJ. Prediction of Clinically Significant Bleeding Following Wide-Field Endoscopic Resection of Large Sessile and Laterally Spreading Colorectal Lesions: A Clinical Risk Score. *Am J Gastroenterol* 2016; **111**: 1115-1122 [PMID: 27296942 DOI: 10.1038/ajg.2016.235]

16 **Belderbos TD**, Leenders M, Moons LM, Siersema PD. Local recurrence after endoscopic mucosal resection of nonpedunculated colorectal lesions: systematic review and meta-analysis. *Endoscopy* 2014; **46**: 388-402 [PMID: 24671869 DOI: 10.1055/s-0034-1364970]

17 **Briedigkeit A**, Sultanie O, Sido B, Dumoulin FL. Endoscopic mucosal resection of colorectal adenomas > 20 mm: Risk factors for recurrence. *World J Gastrointest Endosc* 2016; **8**: 276-281 [PMID: 26981180 DOI: 10.4253/wjge.v8.i5.276]

18 **Knabe M**, Pohl J, Gerges C, Ell C, Neuhaus H, Schumacher B. Standardized long-term follow-up after endoscopic resection of large, nonpedunculated colorectal lesions: a prospective two-center study. *Am J Gastroenterol* 2014; **109**: 183-189 [PMID: 24343549 DOI: 10.1038/ajg.2013.419]

19 **Tate DJ**, Desomer L, Klein A, Brown G, Hourigan LF, Lee EY, Moss A, Ormonde D, Raftopoulos S, Singh R, Williams SJ, Zanati S, Byth K, Bourke MJ. Adenoma recurrence after piecemeal colonic EMR is predictable: the Sydney EMR recurrence tool. *Gastrointest Endosc* 2017; **85**: 647-656.e6 [PMID: 27908600 DOI: 10.1016/j.gie.2016.11.027]

20 **Robertson DJ**, Lieberman DA, Winawer SJ, Ahnen DJ, Baron JA, Schatzkin A, Cross AJ, Zauber AG, Church TR, Lance P, Greenberg ER, Martínez ME. Colorectal cancers soon after colonoscopy: a pooled multicohort analysis. *Gut* 2014; **63**: 949-956 [PMID: 23793224 DOI: 10.1136/gutjnl-2012-303796]

21 **Wang J**, Zhang XH, Ge J, Yang CM, Liu JY, Zhao SL. Endoscopic submucosal dissection vs endoscopic mucosal resection for colorectal tumors: a meta-analysis. *World J Gastroenterol* 2014; **20**: 8282-8287 [PMID: 25009404 DOI: 10.3748/wjg.v20.i25.8282]

22 **Arezzo A**, Passera R, Marchese N, Galloro G, Manta R, Cirocchi R. Systematic review and meta-analysis of endoscopic submucosal dissection vs endoscopic mucosal resection for colorectal lesions. *United European Gastroenterol J* 2016; **4**: 18-29 [PMID: 26966519 DOI: 10.1177/2050640615585470]

23 **Takeuchi Y**, Iishi H, Tanaka S, Saito Y, Ikematsu H, Kudo SE, Sano Y, Hisabe T, Yahagi N, Saitoh Y, Igarashi M, Kobayashi K, Yamano H, Shimizu S, Tsuruta O, Inoue Y, Watanabe T, Nakamura H, Fujii T, Uedo N, Shimokawa T, Ishikawa H, Sugihara K. Factors associated with technical difficulties and adverse events of colorectal endoscopic submucosal dissection: retrospective exploratory factor analysis of a multicenter prospective cohort. *Int J Colorectal Dis* 2014; **29**: 1275-1284 [PMID: 24986141 DOI: 10.1007/s00384-014-1947-2]

24 **Nishizawa T**, Yahagi N. Endoscopic mucosal resection and endoscopic submucosal dissection: technique and new directions. *Curr Opin Gastroenterol* 2017; **33**: 315-319 [PMID: 28704212 DOI: 10.1097/MOG.0000000000000388]

25 **Uraoka T**, Parra-Blanco A, Yahagi N. Colorectal endoscopic submucosal dissection: is it suitable in western countries? *J Gastroenterol Hepatol* 2013; **28**: 406-414 [PMID: 23278302 DOI: 10.1111/jgh.12099]

26 **Yang DH**, Jeong GH, Song Y, Park SH, Park SK, Kim JW, Jung KW, Kim KJ, Ye BD, Myung SJ, Yang SK, Kim JH, Park YS, Byeon JS. The Feasibility of Performing Colorectal Endoscopic Submucosal Dissection Without Previous Experience in Performing Gastric Endoscopic Submucosal Dissection. *Dig Dis Sci* 2015; **60**: 3431-3441 [PMID: 26088371 DOI: 10.1007/s10620-015-3755-0]

27 **Berr F**, Wagner A, Kiesslich T, Friesenbichler P, Neureiter D. Untutored learning curve to establish endoscopic submucosal dissection on competence level. *Digestion* 2014; **89**: 184-193 [PMID: 24714421 DOI: 10.1159/000357805]

28 **Sauer M**, Hildenbrand R, Oyama T, Sido B, Yahagi N, Dumoulin FL. Endoscopic submucosal dissection for flat or sessile colorectal neoplasia >20mm: A European single-center series of 182 cases. *Endosc Int Open* 2016; **4**: E895-E900 [PMID: 27540580 DOI: 10.1055/s-0042-111204]

29 **Probst A**, Ebigbo A, Märkl B, Schaller T, Anthuber M, Fleischmann C, Messmann H. Endoscopic

submucosal dissection for early rectal neoplasia: experience from a European center. *Endoscopy* 2017; **49**: 222-232 [PMID: 27842423 DOI: 10.1055/s-0042-118449]

30   **ASGE Technology Committee**. Maple JT, Abu Dayyeh BK, Chauhan SS, Hwang JH, Komanduri S, Manfredi M, Konda V, Murad FM, Siddiqui UD, Banerjee S. Endoscopic submucosal dissection. *Gastrointest Endosc* 2015; **81**: 1311-1325 [PMID: 25796422 DOI: 10.1016/j.gie.2014.12.010]

31   **Bhatt A**, Abe S, Kumaravel A, Vargo J, Saito Y. Indications and Techniques for Endoscopic Submucosal Dissection. *Am J Gastroenterol* 2015; **110**: 784-791 [PMID: 25623656 DOI: 10.1038/ajg.2014.425]

32   **Bahin FF**, Heitman SJ, Rasouli KN, Mahajan H, McLeod D, Lee EYT, Williams SJ, Bourke MJ. Wide-field endoscopic mucosal resection versus endoscopic submucosal dissection for laterally spreading colorectal lesions: a cost-effectiveness analysis. *Gut* 2018; **67**: 1965-1973 [PMID: 28988198 DOI: 10.1136/gutjnl-2017-313823]

33   **Kiriyama S**, Saito Y, Yamamoto S, Soetikno R, Matsuda T, Nakajima T, Kuwano H. Comparison of endoscopic submucosal dissection with laparoscopic-assisted colorectal surgery for early-stage colorectal cancer: a retrospective analysis. *Endoscopy* 2012; **44**: 1024-1030 [PMID: 23012216 DOI: 10.1055/s-0032-1310259]

34   **Ahlenstiel G**, Hourigan LF, Brown G, Zanati S, Williams SJ, Singh R, Moss A, Sonson R, Bourke MJ; Australian Colonic Endoscopic Mucosal Resection (ACE) Study Group. Actual endoscopic versus predicted surgical mortality for treatment of advanced mucosal neoplasia of the colon. *Gastrointest Endosc* 2014; **80**: 668-676 [PMID: 24916925 DOI: 10.1016/j.gie.2014.04.015]

35   **Nakamura F**, Saito Y, Sakamoto T, Otake Y, Nakajima T, Yamamoto S, Murakami Y, Ishikawa H, Matsuda T. Potential perioperative advantage of colorectal endoscopic submucosal dissection versus laparoscopy-assisted colectomy. *Surg Endosc* 2015; **29**: 596-606 [PMID: 25037724 DOI: 10.1007/s00464-014-3705-5]

36   **Jayanna M**, Burgess NG, Singh R, Hourigan LF, Brown GJ, Zanati SA, Moss A, Lim J, Sonson R, Williams SJ, Bourke MJ. Cost Analysis of Endoscopic Mucosal Resection vs Surgery for Large Laterally Spreading Colorectal Lesions. *Clin Gastroenterol Hepatol* 2016; **14**: 271-278.e1-2 [PMID: 26364679 DOI: 10.1016/j.cgh.2015.08.037]

37   **Schurr MO**, Baur FE, Krautwald M, Fehlker M, Wehrmann M, Gottwald T, Prosst RL. Endoscopic full-thickness resection and clip defect closure in the colon with the new FTRD system: experimental study. *Surg Endosc* 2015; **29**: 2434-2441 [PMID: 25318369 DOI: 10.1007/s00464-014-3923-x]

38   **Fähndrich M**, Sandmann M. Endoscopic full-thickness resection for gastrointestinal lesions using the over-the-scope clip system: a case series. *Endoscopy* 2015; **47**: 76-79 [PMID: 25221859 DOI: 10.1055/s-0034-1377975]

39   **Richter-Schrag HJ**, Walker C, Thimme R, Fischer A. [Full thickness resection device (FTRD). Experience and outcome for benign neoplasms of the rectum and colon]. *Chirurg* 2016; **87**: 316-325 [PMID: 26438202 DOI: 10.1007/s00104-015-0091-z]

40   **Backes Y**, Kappelle WFW, Berk L, Koch AD, Groen JN, de Vos Tot Nederveen Cappel WH, Schwartz MP, Kerkhof M, Siersema PD, Schröder R, Tan TG, Lacle MM, Vleggaar FP, Moons LMG; T1 CRC Working Group. Colorectal endoscopic full-thickness resection using a novel, flat-base over-the-scope clip: a prospective study. *Endoscopy* 2017; **49**: 1092-1097 [PMID: 28753696 DOI: 10.1055/s-0043-114730]

41   **Al-Bawardy B**, Rajan E, Wong Kee Song LM. Over-the-scope clip-assisted endoscopic full-thickness resection of epithelial and subepithelial GI lesions. *Gastrointest Endosc* 2017; **85**: 1087-1092 [PMID: 27569858 DOI: 10.1016/j.gie.2016.08.019]

42   **Schmidt A**, Beyna T, Schumacher B, Meining A, Richter-Schrag HJ, Messmann H, Neuhaus H, Albers D, Birk M, Thimme R, Probst A, Faehndrich M, Frieling T, Goetz M, Riecken B, Caca K. Colonoscopic full-thickness resection using an over-the-scope device: a prospective multicentre study in various indications. *Gut* 2018; **67**: 1280-1289 [PMID: 28798042 DOI: 10.1136/gutjnl-2016-313677]

MINIREVIEWS

Elastography-based screening for esophageal varices in patients with advanced chronic liver disease

Rafael Paternostro, Thomas Reiberger, Theresa Bucsics

ORCID number: Rafael Paternostro (0000-0002-1813-5769); Thomas Reiberger (0000-0002-4590-3583); Theresa Bucsics (0000-0003-3901-4111).

Rafael Paternostro, Thomas Reiberger, Theresa Bucsics, Department of Medicine III, Division of Gastroenterology and Hepatology, Medical University of Vienna, Vienna A-1090, Austria

Corresponding author: Thomas Reiberger, MD, Associate Professor, Department of Internal Medicine III, Division of Gastroenterology and Hepatology, Medical University of Vienna, Spitalgasse 23, Vienna, A-1090, Austria. thomas.reiberger@meduniwien.ac.at
Telephone: +43-140-40047410
Fax: +43-140-40047350

Abstract

Elastography-based liver stiffness measurement (LSM) is a non-invasive tool for estimating liver fibrosis but also provides an estimate for the severity of portal hypertension in patients with advanced chronic liver disease (ACLD). The presence of varices and especially of varices needing treatment (VNT) indicates distinct prognostic stages in patients with compensated ACLD (cACLD). The Baveno VI guidelines suggested a simple algorithm based on LSM < 20 kPa (by transient elastography, TE) and platelet count > 150 G/L for ruling-out VNT in patients with cACLD. These (and other) TE-based LSM cut-offs have been evaluated for VNT screening in different liver disease etiologies. Novel point shear-wave elastography (pSWE) and two-dimensional shear wave elastography (2D-SWE) methodologies for LSM have also been evaluated for their ability to screen for "any" varices and for VNT. Finally, the measurement of spleen stiffness (SSM) by elastography (mainly by pSWE and 2D-SWE) may represent another valuable screening tool for varices. Here, we summarize the current literature on elastography-based prediction of "any" varices and VNT. Finally, we have summarized the published LSM and SSM cut-offs in clinically useful scale cards.

Key words: Elastography; Liver stiffness; Spleen stiffness; Shear wave; Magnetic resonance elastography; Varices; Portal hypertension; Cirrhosis; Advanced chronic liver disease

Core tip: Elastography-based measurement of liver stiffness (LSM) and spleen stiffness (SSM) represent an important non-invasive screening tool for esophageal varices (EVs). Transient elastography (TE) is most widely validated, and the combined TE-based LSM < 20 kPa and platelet count (PLT) > 150 G/L algorithm has been adopted by newest guidelines as a tool to rule-out varices-needing-treatment (VNTs). While LSM and SSM

by novel shear wave elastography devices and magnetic resonance elastography (MRE) may be more accurate to reflect the risk of EV and VNT, their value in clinical practice remains to be established.

INTRODUCTION

In 2015, the Baveno VI consensus defined the term "compensated advanced chronic liver disease" (cACLD) in order to better define the spectrum of advanced fibrosis and cirrhosis in asymptomatic patients[1]. In patients with chronic liver diseases, transient elastography (TE) is recommended to screen for cACLD, with values between 10-15 kPa being suggestive and > 15 kPa being highly suggestive for cACLD[1]. Importantly, patients with cACLD should be evaluated for the presence of clinically significant portal hypertension (CSPH) and undergo regular surveillance for hepatocellular carcinoma (HCC). Detection of CSPH most commonly relies on endoscopic screening for esophageal varices (EV) but may be (earlier) identified by hepatic venous pressure gradient (HVPG) measurements showing HVPG ≥ 10 mmHg. Screening for EV is a cornerstone in the management of cirrhotic patients, since the presence of EV indicates a distinct inferior prognosis within cACLD patients. Moreover, varices-needing-treatment (VNT) are defined by large size (≥ 5 mm) but also include small varices (< 5 mm) in case of Child-C cirrhosis or if red spot signs are present (1,4). Patients with VNTs should receive primary prophylaxis of varices bleeding in order to prevent variceal bleeding, and reduce the risk of decompensation and death[2-4].

Fibrosis-induced increases of hepatic vascular resistance represents the main causative factor for CSPH. Consequently, CSPH leads to development of portosystemic collaterals, such as esophageal-, umbilical-, fundal- and/or rectal-varices. Thus, in cACLD patients the degree of hepatic fibrosis, *i.e.*, LSM results are highly suggestive of CSPH and thus, for EV and VNT. Pathophysiologically, CSPH precludes the formation of EV and can be present in compensated patients that have not yet developed EV[5]. However, due to the limited availability of HVPG, CSPH is clinically most often diagnosed only after EV are detected by upper-gastrointestinal endoscopy[1,5]. Nevertheless, endoscopy is an invasive procedure, requiring training and specialized infrastructure and is not well perceived by patients. Therefore in recent years, several studies have investigated liver elastography as a non-invasive method for the diagnosis of EV and VNT. The Baveno VI consensus statement defined non-invasive criteria based on liver stiffness measurement (LSM) by transient elastography and platelet count by which patients can safely avoid screening endoscopy[1]. In this comprehensive literature review, we summarize current knowledge on non-invasive elastography-based methods for the detection of EV and VNT and its implications in daily clinical practice.

Esophageal varices

Referring to our national guidelines[5], EV should be graded as: absent, small (< 5mm of diameter) or large (> 5 mm of diameter), and the presence of red spots should be indicated for risk stratification[5]. While international guidelines also discriminate between small, medium and large varices[1,3] this discrimination is neither clinically useful, as the international recommendations for the management of medium-to-large varices are similar but only different to small varices and there is considerable inter-observer disagreement during endoscopical assessment of variceal size. Thus, we define for the purpose of this review the following categories: "any EV" as any EV detected on endoscopy (including small varices) and "varices-needing-treatment" (VNT) as all (medium)/large varices (≥ 5mm) and small varices found in patients with Child-Pugh C cirrhosis or small varices presenting red spot signs. Accordingly, the capability of non-invasive elastography methods to detect "any varices" and "VNT" was analyzed seperately.

ELASTOGRAPHY METHODS

Over the years, several methods to non-invasively stage fibrosis have been implemented: vibration-controlled or transient elastography (TE), point shear-wave-elastography (pSWE), two dimensional shear wave elastography (2D-SWE) and magnetic resonance elastography (MRE).

Elastography assesses tissue elasticity, which is defined as the tendency of tissue that resists deformation when force is applied and the return to its original form once the force is removed[6]. To calculate stiffness certain formulas are used that include variables for tissue elasticity, tissue density and shear wave velocity[7]. In SWE, dynamic stress is applied to the tissue via mechanical vibrations in TE, and acoustic radiation impulses in pSWE and 2D-SWE[6]. Shear waves generated by the device are propagated by the underlying tissue, and measured perpendicular to the acoustic radiation force or parallel to the one-dimensional TE impulse[6]. The shear wave propagation speed varies between tissue densities. This propagation velocity is then measured by the device and reflects tissue elasticity[6]. In MRE, a passive driver, stimulated by acoustic waves enacts physical pressure pulses on the right abdomen and thus, the liver, which is captured and visualized using specific magnetic resonance sequences and software algorithms. In contrast to TE and ultrasound-based SWE that evaluate liver stiffness only locally in small, defined areas limited to a few mm² (pSWE, TE) or up to 4 cm² (2D-SWE), MRE is able to assess stiffness within the entire volume of the liver (3D-SWE). MRE has been reported to be highly reproducible and very accurate in differentiating between low stages of liver fibrosis[8,9].

While most studies on TE, pSWE, 2D-SWE and MRE have focused on correlation with liver fibrosis on histology, several other studies have focused on their potential to non-invasively predict the presence of EV and VNT. We summarized the most important studies in Table 1 (TE), Table 2 (pSWE), Table 3 (2D-SWE) and Table 4 (MRE). We furthermore created graphical charts marking important cut-offs for each method, that can easily be implemented in daily clinical practice (see Figure 1 for TE-, Figure 2 for pSWE- , Figure 3A for 2D-SWE- and Figure 3B for MRE-derived cut-offs).

TE

TE is a one dimensional SWE method that measures liver (LSM) or spleen (SSM) stiffness at a depth of 2.5-6.5 cm beneath the skin with an exploration volume of 3 cm²[6]. The propagation velocity of the shear wave is directly proportional to the stiffness of the liver, which in other words means "the faster, the stiffer"[10]. Results measured by SWE are usually presented as either m/s (tissue velocity) or kPa (estimated tissue elasticity). To secure reliability and validity, at least ten measurements should be performed and results must fulfill established quality criteria (median/interquartile range ratio ≤ 30%)[10,11]. However, LSM results obtained in obese patients and patients with ascites have to be interpreted with caution; in some rare cases, valid measurements cannot be obtainable by TE-based LSM[10]. For obese patients, a separate probe (XL) has been developed that increases the proportion of (obese) patients in whom valid LSM can be obtained since measurements are read at high depth and recommendation to use the XL-probe are based on higher skin-to-liver-capsule distances. However, the LSM results obtained by the TE-XL probe may slightly deviate from the standard TE-M probe[12-14].

One of the first studies to report LSM cut-offs for predicting EV was Kazemi *et al*. in 2006[15]. In a prospective cohort with mixed etiologies, the authors identified 13.9 kPa for any varices (including small varices) and 19.0 kPa for VNT as the suitable cut-offs. In the same year, Foucher *et al*[16] published a cut-off of 27.5 kPa for ruling-out VNT, also in a mixed cohort of patients. Since then, several studies have been published (Table 1); unfortunately, results on optimal LSM cut-offs vary exceedingly. For the prediction of presence of varices of any size ("any varices"), cut-offs between 6.8 kPa[17] and 28.0 kPa[18] were reported. For the prediction of VNT, which should not be missed by non-invasive screening, values ranged between 14 kPa[19] and 43 kPa[20]. One of the main issues for the highly variable results are diverse aims and approaches of the authors: in studies with a focus on ruling in the presence of EV reporting positive-predictive values (PPV) > 90%, cut-offs range from 15 kPa[21] to 28kPa[18], whereas studies focusing on ruling out EV and reporting negative-predictive values (NPV) > 90%, results ranged between 19 kPa[15] and 48 kPa[20].

In 2015 the Baveno VI consensus report on the treatment of portal hypertension[1] was published. These guidelines proposed that in cACLD patients with LSM values < 20 kPa and platelet count (PLT) > 150 G/L, screening endoscopy for esophageal varices can be omitted, since these patients have a very low risk for VNT. Since then, multiple studies validating these criteria have been published[19,22-24]. Finally, in a meta-analysis by Marot[25] analyzing data of 3364 patients, the LSM cut-off of 20 kPa (alone)

Table 1 Studies on transient elastography for the prediction of varices

Author, journal, year of publication	Country	Study design	Etiology	N Patients included % with EV % with VNT		TE-Cut-offs and AUC EV/VNT	Main conclusions (Specificity/Sensitivity, PPV/NPV)
Foucher, *Gut*, 2006[16]	France	Prospective	Mixed	EV: VNT:	144 42 (29%) 85 (59%)	LSM: n/a 27.5 kPa, AUC 0.73	LSM: EV: n/a VNT: Sens. 88%, Spec. 53%, PPV: 45%, NPV: 90%
Kazemi, *J Hepatol*, 2006[15]	France	Prospective	Mixed	EV: VNT	Total: 165 74 (44.8%) 47 (28.5%)	LSM: 13.9 kPa, AUC: 0.84 19.0 kPa, AUC 0.83,	LSM: EV: Sens. 92%, Spec. 39%, PPV 55%, NPV 85% VNT: Sens. 89%, Spec. 59%, PPV 47%, NPV: 93%
Vizzutti, *Hepatology*, 2007[80]	Italy	Prospective	HCV	EV: VNT	Total: 61 30 (49.2%) 18 (38.2%)	LSM: 17.6 kPa, AUC 0.76 27.4 kPa, AUC 0.76	LSM: EV: Sens. 90%, spec. 43%, PPV 77%, NPV 66% VNT: Sens. 70%, spec. 78%, PPV 90%, NPV 55%
Bureau, *Aliment Pharmacol Ther*, 2008[81]	France	Prospective	Mixed	EV: VNT	Total: 150 64 (42.6%) 43 (28.6%)	LSM: EV: 21.1 kPa, AUC 0.85 VNT/large: 29.3 kPa, AUC 0.76	LSM: EV: sens. 84%, spec. 71% VNT: sens. 81%, spec. 61%
Castéra, *J Hepatol*, 2009[82]	France	Prospective	HCV	EV: VNT	Total: 70 25 (35.7%) 15 (21.4%)	LSM: 13.9 kPa, 17.6 kPa, 21.5 kP; AUC 0.96 19 kPa, 21.5 kPa; 30 kPa, AUC 0.87	LSM: Cut-off 13.9 kPa: Sens. 96%, Spec. 39%, PPV 49%, NPV 94% Cut-off 17.6 kPa: Sens. 84%, Spec. 61%, PPV 57%, NPV 86% Cut-off 21.5 kPa: Sens. 76%, Spec. 78%, PPV 68%, NPV 84% Cut-off 19.0 kPa: Sens. 85%, Spec. 62%, PPV 35%, NPV 94% Cut-off 21.5 kPa: Sens. 85%, Spec. 68%, PPV 39%, NPV 95% Cut-off 30.5 kPa: Sens. 77%, Spec. 5%, PPV 56%, NPV 94%10
Nguyen-Khac, *Alcohol Clin Exp Res*; 2010[20]	France	Prospective	Mixed	EV: VNT	Total: 183 NR 41 (22%)	LSM: 48 kPa; AUC 0.75 ALD: 47.2 kPa, AUC 0.77 Viral: 19.8 kPa, AUC 0.73	LSM: Sens. 73%, Spec. 73%, PPV 44%, NPV 90% ALD: Sens. 85%, Spec. 64%, PPV 44%, NPV 93% Viral: Sens. 89%, Spec. 55%, PPV 27%, NPV 96%
Stefanescu, *J Gastroenterol Hepatol*, 2011[18]	Romania	Prospective	ALD and/or HCV or healthy controls	EV: VNT	Total: 137 116 (85%) 60 (44%)	LSM: EV: 28 kPa, AUC 0.75 SSM: EV: 46.4 kPa, AUC 0.78 LSM + SSM: EV: LSM 19 kPa, SSM 55 kPa NR	LSM: Sens. 74%, Spec. 64%, PPV 92%, NPV 31% SSM: Sens. 84%, Spec. 71%, PPV 94%, NPV 46% LSM (19 kPa) + SSM (55 kPa): Sens. 93%, Spec. 40%, PPV 95%, NPV 33% NR

Stefanescu, *J Gastrointestin Liver Dis*, 2011[83]	Romania	Prospective	ALD and/or HCV	EV: VNT	Total: 231 157 (68%) 68 (30%)	LSM: 19 kPa, AUC 0.66 38 kPa, AUC 0.69	LSM: Sens. 84%, Spec. 32%, PPV 72%, NPV 49% Sens. 56%, Spec. 75%, PPV 47%, NPV 81%
Chen, *J Gastroenterol Hepatol*, 2012[84]	China	Prospective	HBV	EV: VNT	Total: 222 96 (43%) 82 (40%)	LSM: NR All 17.1 kPa, AUC 0.73 ALT >5 x ULN: 36.1 kPa, AUC 0.92 CPC A, rule-out EV : 7.9 kPa, AUC 0.79 CPC A, rule-in 34.6 kPa, AUC 0.79	LSM: NR Cut-off 17.1 kPa: Sens. 90%, Spec. 44%, PPV 47%, NPV: 88% Cut-off 36.1 kPa: PPV 73%, NPV 100% Cut-off 7.9 kPa: Sens. 97%, NPV 95% Cut-off 34.6 kPa: Spec. 94%, PPV 73% LSPS: Cut-off 3.5: Sens. 78%, NPV 86% (exclusion) Cut-off 5.5: Spec. 90%, PPV 76% (inclusion)
Wang, *J Gastroenterol Hepatol*, 2012[85]	Taiwan	Prospective	HBV	EV: VNT	Total: 126 48 (38%) 13 (10%)	LSM: 12.0 kPa, AUC 0.79 21.0 kPa, AUC 0.87	LSM: Sens. 67%, Spec. 77%, PPV 64%, NPV 79% Sens. 77%, Spec. 87%, PPV 40%, NPV 97%
Colecchia, *Gastroenterology*, 2012[32]	Italy	Prospective	HCV	EV: VNT:	Total: 100 53 (53%) 26 (26%)	LSM (AUC 0.90): cut-off 16.4 kPa cut-off 25.0 kPa SSM (AUC 0.94): cut-off 41.3 kPa cut-off 55.0 kPa NR	LSM: Sens. 96%, Spec. 60% (rule out) Sens. 57%, Spec. 98% (rule in) SSM: Sens. 98%, Spec. 66% (rule out) Sens. 72%, Spec. 96% (rule in) NR
Sporea, *Med Ultrason*, 2013[86]	Romania	Prospective	Viralalcoholic	EV: VNT:	Total: 697 387 (54.5%) 273 (39.1%)	NR All: 29.5 kPa (0.871) Alcohol: 32.5 kPa (0.836) Viral: 24.8 kPa (0.867)	NR Sens. 77.5%, Spec. 86.9% Sens. 85.0%, Spec. 74.6% Sens. 81.0%, Spec. 80.7%
Calvaruso, *J Viral Hepat*, 2013[33]	Italy	Prospective	HCV	EV: VNT:	Total: 96 54 (56.3%) 26 (27.1%)	LSM:17.0 kPa, AUC 0.71 Modified SSM (0-150kPa): 50.0kPa, AUC 0.70 LSM: 19.0 kPa, AUC 0.71 Modified SSM (0-150kPa): 54.0 kPa, AUC 0.82	LSM: Sens. 71%, Spec. 57%, PPV 67%, NPV 62% Modified SSM: Sens. 65%, Spec. 61%, PPV: 69%, NPV: 57% LSM: Sens. 72% Spec. 55%, PPV 38%, NPV 84% Modified SSM: Sens. 80%, Spec. 70%, PPV: 47%, NPV: 90%
Shi, *Liver Int*, 2013[87]	China	Meta-analysis	Mixed Sub-analyses for viral etiologies	EV: VNT:	Total: 3644 1786 (49.0%) 1166 (32.0%)	LSM (pooled): 15.1-28.0 kPa; AUC 0.84 17.8-48.0 kPa; AUC 0.78	LSM (pooled): Sens. 87%, Spec. 53%, PPV 79%, NPV 64% Sens. 86%, Spec. 59%,, PPV 79%, NPV 66%
Sharma, *Am J Gastroenterol*, 2013[30]	India	Prospective	Mixed	EV: VNT:	Total: 174 124 (71.3%) 78 (44.8%)	LSM: 27.3 kPa, AUC 0.91; SSM: 40.8 kPa, AUC 0.90 NR	LSM: Sens. 91%, Spec. 72%, PPV 89%, NPV 76%, SSM: Sens. 94%, Spec. 76%, PPV 91%, NPV 84%

Hassan, *Gastroenterol Hepatol*, 2014[88]	Egypt	Prospective	HCV	EV: VNT:	Total: 62 50 (81%) 32 (52%)	LSM: 18.2 kPa, AUC 0.79 22.4 kPa, AUC 0.80	LSM: Sens. 82%, Spec. 73%, PPV 89%, NPV 49% Sens. 84%, Spec. 72%, PPV 84%, NPV 72%
Binţinţan, *Med Ultrason*, 2015[21]	Romania	Prospective	ViralALD	EV: VNT:	Total: 60 47 (78%) 32 (53%)	LSM: 15 kPa, AUC 0.96 28.8 kPa, AUC 0.90	LSM: Sens. 95%, Spec. 100%, PPV 100%, NPV 86% Sens. 87%, Spec. 83%, PPV: 84%, NPV: 86%
Hu, *Ultrasound Med Biol*, 2015[89]	China	Prospective	Viral	EV: VNT:	Total: 200 110 (55%) 69 (35%)	LSM: 20.3 kPa, AUC 0.84 25.6 kPa, AUC 0.86	LSM: Sens. 84%, Spec. 73%, PPV 72%, NPV: 91% Sens. 86%, Spec. 72%, PPV 79%, NPV: 81%
Li *et al. Rev Esp Enferm Dig* 2016[90]	International	Meta-analysis	Mixed	EV: VNT:	Total: 2,994 Studies: 20 NR NR	LSM NR 14.5-48.0 kPa (0.83)	LSM Sens 81%, Spec 71%,
Wong, *J Dig Dis*, 2016[17]	Hong Kong	Prospective	Chronic HBV	EV: VNT:	Total: 144 31 (21.5%) 2 (1.4%)	LSM: (0.690) Rule out: 6.8 kPa Rule in: 20.8 kPa SSM: (0.736) Rule out: 21.4 kPa Rule in: 50.5 kPa NR	Sens. 90.3%, Spec 29.2%, PPV 25.9%, NPV 91.7% Sens. 29.0%, Spec. 90.3%, PPV 45.0%, NPV 82.3% Sens. 90.3%, Spec 43.4%, PPV 30.4%, NPV 94.2% Sens. 45.2%, Spec. 90.3%, PPV 56.0%, NPV 85.7% NR
Maurice, *J Hepatol*, 2016[22]	United Kingdom	Retrospective	Mixed	EV: VNT:	Total: 310 72 (23%) 15 (5%)	LSM: 20 kPa, AUC 0.686 LSM (20 kPa) and PLT (150 G/L): AUC 0.746	Sens. 67%, Spec. 55%, PPV 7%, NPV 97% Sens. 87%, Spec. 34%, PPV 6%, NPV 98%
Abraldes, *Hepatology*, 2016[19]	International	Retrospective	Mixed	EV: VNT:	Total: 518 217 (42%) 67 (13%)	NR (AUC 0.71) LSM: 14.0 kPa (AUC 0.67) LSM (20 kPa) and PLT (150 G/L): AUC 0.76	NR NR NR
Marot, *Liver Int*, 2017[25]	International	Meta-analysis	Mixed	EV: VNT	Total: 3364 NR (49.0%) NR (32.0%)	LSM: 20 kPa: AUC: NR LSM (20 kPa) and PLT (150 G/L): AUC: NR	LSM and PLT (150 G/L): Sens. 89%, Spec. 38%, PPV: 43%, NPV: 86% Sens. 93%, Spec. 30%, PPV 14%, NPV 97%
Pu, *World J Gastroenterol*, 2017[26]	International	Meta-analysis	Mixed	EV: VNT:	Total: 2697 NR NR	LSM (pooled): 20 kPa, AUC 0.83 30 kPa, AUC: 0.83	LSM: Pooled: Sens. 84%, Spec. 62%, Cut-off 20 kPa: Sens. 83%, Spec. 68%, PPV: n/a, NPV: n/a Pooled: Sens. 78%, Spec. 76%, Cut-off 30 kPa: Sens. 73%, Spec. 74%, PPV: n/a, NPV: n/a
Llop, *J Gastroenterol Hepatol*, 2017[23]	Spain	Retrospective analysis of prospective data	Mixed	EV: VNT:	Total: 161 25 (15.5%) NR	LSM: 20.0 kPa, AUC: NR LSM (20 kPa) and Plt (150 G/L), AUC: NR	LSM: Sens. 76%, Spec. 71%, PPV: 32%, NPV: 94% LSM+Plt: Sens. 88%, Spec. 38%, PPV 21%, NPV 94%

Wong, *Liver Int*, 2018[27]	Hong Kong	Prospective	Mixed	EV: VNT:	TE exam.: 264 51 (18.6%) 11 (4.0%)	LSM:20.0 kPa, AUC: NR LSM (20 kPa) and Plt (150 G/L): AUC: NR SSM: 41.3 kPa; AUC: NR	LSM: Sens: 96%, Spec.: 26%, PPV: 47%, NPV: 91% LSM+PLT: Sens. 91%, Spec.: 18.1%, PPV: 10%, NPV: 96% NR
Manatsathit, *J Gastroenterol Hepatol*, 2018[31]	USA	Meta-analysis	Mixed	EV: VNT:	LSM: 4,337 SSM: 1,1119 LSM: 1681 (56%) SSM: 968 (51%) LSM: 1466 (34%) SSM: 383 (34%)	LSM (pooled): cut-offs NR; AUC 0.82 SSM (pooled): cut-offs NR; AUC: 0.90 LSM (pooled): cut-offs NR; AUC 0.83 SSM (pooled): cut-offs NR; AUC 0.81	LSM (pooled): Sens. 84%, Spec. 64% SSM (pooled): Sens. 91% Spec. 66% LSM: Sens. 85%, Spec. 64% SSM: Sens. 90%, Spec. 73% LSM: Sens. 85%, Spec. 63% SSM: Sens. 87%, Spec. 52%
Petta, *J Hepatol*, 2018[28]	Italy	Retrospective analysis of prospective data	NAFLD/NASH	EV: VNT:	Total: 790 249 (31.5%) 91 (11.5%)	NR LSM: 20 kPa + Plt 150 G/L: AUC LSM 25 kPa + Plt 110 G/L: AUC LSM 30 kPa + Plt 110 G&L:	NR Validation set: Sens. 37%, spec. 96%, PPV:18%, NPV:0.96 XL probe, Validation set: Sens. 93%, spec. 51%, PPV: 18%, NPV:98% M probe, validation set: Sens. 78%, spec. 68%, PPV:27%, NPV:96%
Colecchia, *J Hepatol*, 2018[34]	Italy	Prospective + retrospective validation cohort	Mixed	EV: VNT:	Total: 498 252 (50.6%) 100 (20.1%)	NR LSM: AUC: 0.768 LSM (20 kPa) + Plt (150 G/L): AUC 0.732 SSM: 46 kPa: AUC 0.847 LSM (20 kPa)+Plt (150 G/L)+SSM (46 kPa):AUC 0.787	NR NR Sens. 98%, Spec. 26%, NPV 98% Sens. 98%, Spec. 44%, NPV 99% Sens. 96%, Spec. 53%, NPV 98%

AUC: Area under the (receiver operating) curve; CSPH: Clinically significant portal hypertension; LSM: Liver stiffness measurement; L-SWE: Liver shear wave elastography esophageal varices; TE: Transient elastography; Plt: Platelet count; VNT: Varices needing treatment; Se: Sensitivity; SSM: Spleen stiffness measurement; Sp: Specificity; +LR: Positive likelihood ratio; -LR: Negative likelihood ratio; NR: Not reported; S-SWE: Spleen share wave elastography; ASPS: ARFI-spleen diameter to platelet ratio; ARFI: Acoustic radiation force impulse; PRED: Prediction of significant EV score.

was found to predict the presence of EV with a PPV of 43% and a NPV of 86%. Importantly, another meta-analysis by Pu including 2697 patients reported similar results with a sensitivity of 84% and a specificity of 68% (PPV and NPV not reported)[26].

In summary, LSM is a very valuable non-invasive tool for non-invasive exclusion of VNT. However, due to the high variance of results (cut-offs, PPV and NPV values) reported in the literature, we cannot recommend to rely on TE as a single tool for the prediction of EV or VNT, but advise using combination algorithms instead.

TE: combination algorithms

Since the publication of the Baveno VI guidelines[1], most studies reported data on the combination algorithm of LSM + PLT (commonly at the cutoff 150G/L) to rule-out VNT. One of the first studies was the 'Anticipate study'[19]; however, with an AUC of 0.76, results for this algorithm were rather disappointing. Maurice *et al*[22] evaluated these criteria in 310 patients and reported a PPV of 6% and a NPV of 98%, indicating that these criteria be highly accurate for ruling out VNT as intended. Wong *et al*[27] prospectively analyzed 274 patients and found similar results with a PPV of 9.5% and a NPV of 95.5%. Most recently, the Baveno VI criteria were tested in a large cohort of NAFLD patients and performed very well, missing only 0.9% of large EV[28]. Moreover, a large meta-analysis by Marot including 3364 patients with mixed etiologies of liver disease reported an excellent NPV for ruling out VNT (98%) using the cut-offs proposed by the Baveno VI consensus[25].

However, according to a recent study by Augustín *et al*, 40% of all endoscopies performed when applying the Baveno VI criteria to rule out VNTs did not detect

A Diagnosis of "any varices" by TE and LSM

Kazemi, *J Hepatol* 2006; *n* = 165 — 13.9 kPa

Vizutti, *Hepatology* 2007; *n* = 61 — 17.6 kPa

Bureau, *AP & T* 2008; *n* = 150 — 21.1 kPa

Castera, *J Hepatol* 2009; *n* = 70 — 13.8 kPa, 21.5 kPa

Stefanescu, *J Gastroenterol Hepatol* 2011; *n* = 137 — 28 kPa

Stefanescu, *J Gastro Liv Dis* 2011; *n* = 231 — 19 kPa

Wang, *J Gastroenterol Hepatol* 2012; *n* = 126 — 12 kPa

Colecchia, *Gastroenterology* 2012; *n* = 100 — 16.4 kPa, 25 kPa

Calvaruso, *J Viral Hepatitis* 2013; *n* = 96 — 17 kPa

Sharma, *Am J Gastro* 2013; *n* = 174 — 27.3 kPa

Hassan, *Gastro y Hepatol* 2014; *n* = 62 — 18.2 kPa

Bintintan, *Med Ultrasongraphy* 2015; *n* = 60 — 15 kPa

Hu, *Ultrasound in Medicine and Biology* 2015; *n* = 200 — 20.3 kPa

Wong, *J Dig Dis* 2016; *n* = 144 — 6.8 kPa, 20.8 kPa

Llop, *J Gastroenterol Hepatol* 2017; *n* = 161 — 20 kPa*

Wong, *Liver Int* 2018; *n* = 264 — 20 kPa*

(x-axis: 0 kPa 5 10 12.5 kPa Rule-out 15 20 25 30 70 75 kPa)

B Diagnosis of "varices needing treatment" by TE and LSM

Foucher, *Gut* 2006; *n* = 144 — 27.5 kPa

Kazemi, *J Hepatol* 2006; *n* = 165 — 19 kPa

Vizutti, *Hepatology* 2007; *n* = 61 — 27.4 kPa

Bureau, *AP & T* 2008; *n* = 150 — 29.3 kPa

Castera, *J Hepatol* 2009; *n* = 70 — 19 kPa, 30 kPa

Nguyen-Khac, *Alcoholism: Clin and Exp Res* 2010; *n* = 183 — 43 kPa

Stefanescu, *J Gastroenterol Hepatol* 2011; *n* = 231 — 38 kPa

Wang, *J Gastroenterol Hepatol* 2012; *n* = 126 — 21 kPa

Chen, *J Gastroenterol Hepatol* 2012; *n* = 222 — 17.1 kPa

Sporea, *Medical Ultrasound* 2013; *n* = 697 — 29.5 kPa

Calvaruso, *J Viral Hep* 2013; *n* = 96 — 19.0 kPa

Hassan, *Gastroenteroly Hepatol* 2014; *n* = 62 — 22.4 kPa

Bintintan, *Medical Ultrasonography* 2015; *n* = 60 — 28.8 kPa

Hu, *Ultrasound in Med Biol* 2015; *n* = 200 — 25.6 kPa

Maurice, *J Hepatol* 2016; *n* = 310 — 20 kPa*

(x-axis: 0 kPa 5 10 15 20 kPa Rule-out 25 30 35 40 45 70 75 kPa)

C Diagnosis of "any varices" by TE and SSM

Stefanescu, *J Gastroenterol Hepatol* 2011; *n* = 137 — 46.6 kPa

Colecchia, *Gastroenterology* 2012; *n* = 100 — 41.3 kPa, 55 kPa

Calvaruso, *J Viral Hepatitis* 2013; *n* = 96 — 50 kPa

Sharma, *Am J Gastro* 2013; *n* = 174 — 40.8 kPa

Wong, *J Dig Dis* 2016; *n* = 144 — 21.4 kPa, 50.5 kPa

(x-axis: 0 kPa 5 10 15 20 25 30 35 40 kPa Rule-out 45 50 55 70 75 kPa 150 kPa)

Diagnosis of "varices needing treatment" by TE and SSM

Calvaruso, *J Viral Hepatitis* 2013; *n* = 96 — 54 kPa

Wong, *Liver Int* 2018; *n* = 264 — 41.3 kPa

Colecchia, *J Hepatol* 2018; *n* = 498 — 46 kPa

(x-axis: 0 kPa 5 10 15 20 25 30 35 40 kPa Rule-out 45 50 55 70 75 kPa 150 kPa)

Figure 1 Summary of studies that reported transient elastography derived cut-offs on the non-invasive diagnosis of any varices (A), varices needing treatment (B) using liver stiffness measurement and spleen stiffness measurement respectively (C).

varices. The surprisingly low number of spared endoscopies could be increased by raising the cut-off for LSM to 25kPa and lowering the PLT threshold to 110 G/L ('*expanded Baveno VI criteria*')[24]. Also Jangouk *et al*. refined and redefined the Baveno VI criteria by applying the 'Meld-6' rule, where patients that did not fulfill the Baveno VI criteria due to PLT < 150 G/L but had a MELD of six (*i.e.*, normal/preserved liver function) were all not found with VNT, proposing that the number of spared endoscopies could be increased by this adaption of the Baveno VI criteria[29].

In 2013, Sharma *et al*[30] identified not only LSM, but also spleen stiffness measurement (SSM) as a non-invasive surrogate parameter for the prediction of EV. Indeed, several studies have subsequently investigated the predictive value of SSM using TE[27,30-34]. Importantly, SSM is also able to capture portal hypertension that is due to pre-sinusoidal or pre-hepatic causes that may not be detected by LSM. SSM has universally been shown to be at least equal, if not superior to LSM in regard to the detection of EV as well as of VNT[27,30-34]. This includes a very recent meta-analysis from 2018 by Manatsathit[31] including 4337 patients of mixed etiologies who calculated a pooled AUC of 0.90 for SSM for the detection of any EV as compared to a pooled AUC of 0.82 for LSM, and a pooled AUC of 0.81 *vs* 0.83 for the detection of VNT for LSM and SSM, respectively. Sharma *et al*[30] even concluded in their study that, in contrast to LSM, SSM can differentiate between small and large varices.

However, there is a limitation to SSM, as routine TE units (Fibroscan®, Echosens, France) are generally capped at a fibrosis value of 75 kPa. While LSM mostly remains within this range in cACLD patients, in severe portal hypertension SSM can exceed this threshold, especially in patients at highest risk of VNT. For this reason, in a study by Calvaruso *et al*[33] investigating SSM for the prediction of VNT, the authors used a modified TE unit with a maximum stiffness limit of 150 kPa, demonstrating superior ability of SSM to predict VNT with an AUC of 0.80 as compared to LSM with an AUC of 0.71, respectively. Accordingly, Stefanescu *et al*[18] combined LSM (cutoff 19 kPa) and SSM (cutoff: 55kPa) into a simple diagnostic algorithm to rule-in any EV with a sensibility of 93% and a PPV of 95%.

In conclusion, combining TE-based LSM with other non-invasive parameters such as PLT or SSM significantly increases the diagnostic accuracy for predicting the presence of EV. Given the convincing evidence, the combined Baveno VI criteria to rule out VNT at TE-based LSM < 20kPa and PLT > 150G/L have already been adapted into national guidelines[5].

Point shear wave elastography

In contrast to TE as a 1D-SWE that uses vibration-controlled dynamic stress, pSWE and 2D-SWE are based on the ultrasound-based acoustic radiation force impulse (ARFI) technology[6]. In pSWE, ARFI is used to generate a high-intensity short-duration acoustic pulse that slightly displaces liver tissue at one specific point[6,35]. As ARFI is usually implemented into modified ultrasound probes, one of the major advantages compared to TE is the availability to visualize liver tissue via B-Mode[6,10]. Furthermore, the tissue is being displaced directly in the liver with focus on the ROI rather than on the body surface, making the technique less prone to ascites or obesity[6,10]. However, pSWE is limited by the small region of interest (ROI) compared to other SWE modalities, which makes it more prone to "sample" bias and to artefacts, *e.g.*, due to patient movements[10]. In 2014, Salzl *et al*[36] reported an AUC of 0.855 for the prediction of CSPH and an AUC of 0.743 for the prediction of EV using pSWE (as compared to EV prediction by TE with an AUC of 0.802). Similar results were found in a Japanese cohort of patients with mixed etiologies with an AUC 0.833 for the prediction of CSPH, an AUC of 0.789 for any varices and AUC an 0.788 for VNT respectively[37]. Most recently LSM via pSWE was found to predict presence of EV with an AUC of 0.913, as compared to pSWE-based SSM with an AUC of 0.675[38], however, only 21 patients with "low-grade EVs" and none with VNT have been included.

After the promising result of TE-based SSM, several studies have been published on the value of pSWE-based SSM for the diagnosis of CSPH and for EV[35]. The AUC of pSWE-based SSM ranged from 0.578[39] to 0.959[40] for any EV and between 0.580[41] to 0.955[37] for VNT. In a large cohort of 340 patients with mixed etiologies, SSM had the best diagnostic accuracy for the identification of patients with any EV (AUC 0.937 for viral, AUC 0.923 for non-viral etiologies) or VNT (AUC 0.924 for viral, 0.944 for non-viral etiologies) when compared to other non-invasive parameters (such as LSM, spleen diameter and PLT)[42].

Table 2 Point shear wave elastography for the prediction of varices

Ref.	Country	Study design	N	Etiology	Device	Cut-off (AUC) for EV	Sens/Spec/ +LR/-LR/p for EV	Cut-off (AUC) for VNT	Se/Sp/+LR/ -LR/p for VNT	Comments
Vermehren, *Liver International* 2011[41]	Germany	Prospective	166	Mixed	Acuson S2000	NR	NR	L-SWE: (0.58) S-SWE: (0.58) Youden: 4.13 m/s Highest NPV: 3.04 m/s	NR Youden: 35%/83%/2.06/0.78/PPV 54%/NPV 69% Highest NPV: 90%/25%/1.19/0,4/PPV 40%/NPV 81%	Cut-offs only calculated for S-SWE and TE, but not for L-SWE
Bota, *Annals of Hepatology*, 2012[39]	Romania	Prospective	145 Cirrhosis: 24	Mixed, healthy	Acuson S2000	NR	NR	L-SWE: 2.25 m/s (0.596) S-SWE: 2.55 m/s (0.578) PRED: 0.395 (0.721)	LSM: 93.4%/28.9 %/PPV48.5 %/NPV:85.7 % SSM: 96.7%/21%/ PPV:47.6%/ NPV:53.1% PRED: 75%/61.8%/ PPV:61.4%/ NPV:69.6%/ p=0.0001	VNT: Varices ≥grade 2
Ye, *Journal of Ultrasound in Medicine*, 2012[91]	China	Prospective	264, cirrhosis: 141	Chronic HBV, healthy	Acuson S2000	L-SWE: 3.16 m/s (0.83)	84.1%/81.0 %/NR	L-SWE: 3.39 m/s (0.83)	78.9%/78.3 %	Main focus on liver stiffness evaluation VNT: Varices ≥grade 3
Takuma *et al*. *Gastroenterology* 2013[42]	Japan	Prospecttive	340	Mixed	Acuson S2000	S-SWE: cirrhosis: 3.17 m/s (0.933) Comp.: 3.18 m/s (0.934) Decomp: 3.22 m/s (0.936) Viral: 3.18 m/s (0.937) Nonviral: 3.24 m/s (0.923) L-SWE: NR (0.746)	98.4%/60.1 %/2.468/0.0 25/PPV 61.0%/NPV 98.4%/acc. 75.0% 98.4%/63.4 %/2.689/0.0 25/PPV: 50.4%/NPV: 99.0%/acc: 73.0% 98.6%/50.0 %/1.971/0.0 29/PPV: 75.8%/NPV: 85.7%/acc: 79.8% 98.9%/59.9 %/2.464/0.0 19/PPV: 57.5%/NPV: 99.0%/acc: 73.7% 97.7%/65.2 %/2.808/0.0 36/PPV: 57.5%/NPV: 99.0%/acc: 73.7%	S-SWE: cirrhosis: 3.30 m/s (0.930) Comp: 3.30 m/s (0.921) Decomp: 3.45 m/s (0.934); S-Viral: 3.30 m/s (0.924); Nonviral: 3.41 m/s (0.944)	98.9%/62.9 %/2.661/0.0 18/PPV 47.8%/NPV 99.4%/acc. 72.1% 97.5%/66.7 %/2.925/0.0 38/PPV: 38.6%/NPV: 99.2%/acc: 72.1% 97.9%/73.1 %/3.643/0.0 29/PPV: 71.9%/NPV: 98.0%/acc: 83.3% 98.2%/63.8 %/2.243/0.0 29/PPV: 43.2%/NPV: 99.2%/acc: 71.3% 96.9%/71.9 %/2.267/0.0 43/PPV: 66.0%/NPV: 97.6%/acc: 80.9%	No cut-offs for L-SWE reported - significantly superior S-SWE results
Mori, *BioMed Research International* 2013[92]	Japan	Prospective	33 cirrhosis: 24	Mixed, including healthy	Acuson 2000	NR	NR	NR	NR	Neither liver nor spleen stiffness correlated with presence of EV

Salzl, *Ultraschall in der Medizin*, 2014[36]	Austria	Prospective	88	Mixed	Acuson S2000	L-SWE: 2.74 m/s (0.743)	62.5%/89.5 %/PPV: 91.5%/NPV: 56.9%	NR	NR	Size of EV was not defined
Morishita, *Journal of Gastroenterology* 2014[93]	Japan	Prospective	181	Chronic HCV	Acuson S2000	L-SWE: 2.05 m/s (0.890)	Training set: 83%/76%/PPV: 78%/NPV: 81% Validation set: 83%/77%/PPV 59%/NPV: 92%	L-SWE: 2.39 m/s (0.868)	Training set: 81%/82%/PPV: 69%/NPV: 89% Validation set: 83%/77%/PPV: 59%/NPV: 92%	
Park, *PloS ONE*, 2015[94]	South Korea	Prospective	143	Mixed	Acuson S2000	L-SWE: 2.08 m/s (0.769) ASPS: 1.67 (0.903)	64.9%/81.1 %/3.44/0.43 /PPV 54.5%/NPV: 86.9% 81.1%/84.0 %/5.06/0.23 /PPV 63.8%/NPV: 92.7%	L-SWE: 1.90 (0.786) ASPS: 2.83 (0.946)	85%/67.5%/ 2.61/0.22/P PV: 29.8%/NPV: 96.5% 90%/94.3%/ 15.81/0.11/ PPV: 72.0%/NPV: 98.3%	High discriminative power of ASPS confirmed in validation cohort
Attia, *Ultraschall in der Medizin*, 2015[95]	Germany	Prospective	78	Mixed	Acuson S2000	L-SWE (HVPG ≥10mmHg): 2.29 m/s (0.840) L-SWE (HVPG ≥12mmHg): 2.70 m/s (0.878) S-SWE (HVPG≥10m mHg):2.55 m/s(0.899) S-SWE (HVPG≥12m mHg):2.71 m/s (9.31)	91%/85%/6. 08/0.1/<0.0 01/PPV 95%/NPV 74% 93%/77%/4 00/0.09/<0. 001/PPV 89%/NPV 85% 95%/90%/9. 06/0.05/<0. 001/PPV 97%/NPV 85% 95%/92%/1 1.86/0.06/< 0.001/PPV9 7%/NPV 89%	NR	NR	SSM independently predicted presence of CSPH+EV
Kim, *Medicine*, 2015[96]	Korea	Prospective	125	Mixed	Acuson S2000	L-SWE: cutoff NR (0.747) S-SWE: 3.16 m/s(0.785)	NR 87.0%/60.4 %/PPV 77.9%/NPV 64.4%	L-SWE: cutoff NR (0.687) S-SWE: 3.40 m/s (0.762)	NR 78.9%/63.0 %/PPV 60.3%/NPV 80.7%	VNT: medium-large varices
Park, *Medical Ultrasound*, 2016[97]	South Korea	Prospective	366	ALD or viral	iU22	L-SWE: NR S-SWE: 29.9 kPa (0.859)	L-SWE:NR S-SWE: 58.1%/79.1 %/<0.001/P PV:81.6%/N PV:82.8%	NR	NR	High rate of unreliable results (25%) No significant correlation with L-SWE
Wiles, *Clinical Radiology*, 2018[98]	UK	Prospective	58	Mixed	Acuson S2000	NR	NR	NR	NR	ARFI not suitable to predict GOV (*P* = 0.15)
Lucchina *et al*. *Ultrasound Med Biol* 2018[38]	Italy	Prospective	42	Mixed	iU22	L-SWE: 12.27 kPa (0.913)S-SWE: 23.87kPa (0.675)	100%/66.67 %/NR 73,81%/59.5 2%/NR	NR	NR	High rate of inconclusive results (22%)

AUC: Area under the (receiver operating) curve; CSPH: Clinically significant portal hypertension; LSM: Liver stiffness measurement; L-SWE: Liver shear wave elastography esophageal varices; TE: Transient elastography; Plt: Platelet count; VNT: Varices needing treatment; Se: Sensitivity; SSM: Spleen stiffness measurement; Sp: Specificity; +LR: Positive likelihood ratio; -LR: Negative likelihood ratio; NR: Not reported; S-SWE: Spleen share wave elastography; ASPS: ARFI-spleen diameter to platelet ratio; ARFI: Acoustic radiation force impulse; PRED: Prediction of significant EV score.

Importantly, while TE-based elastography is a simple technique that can be
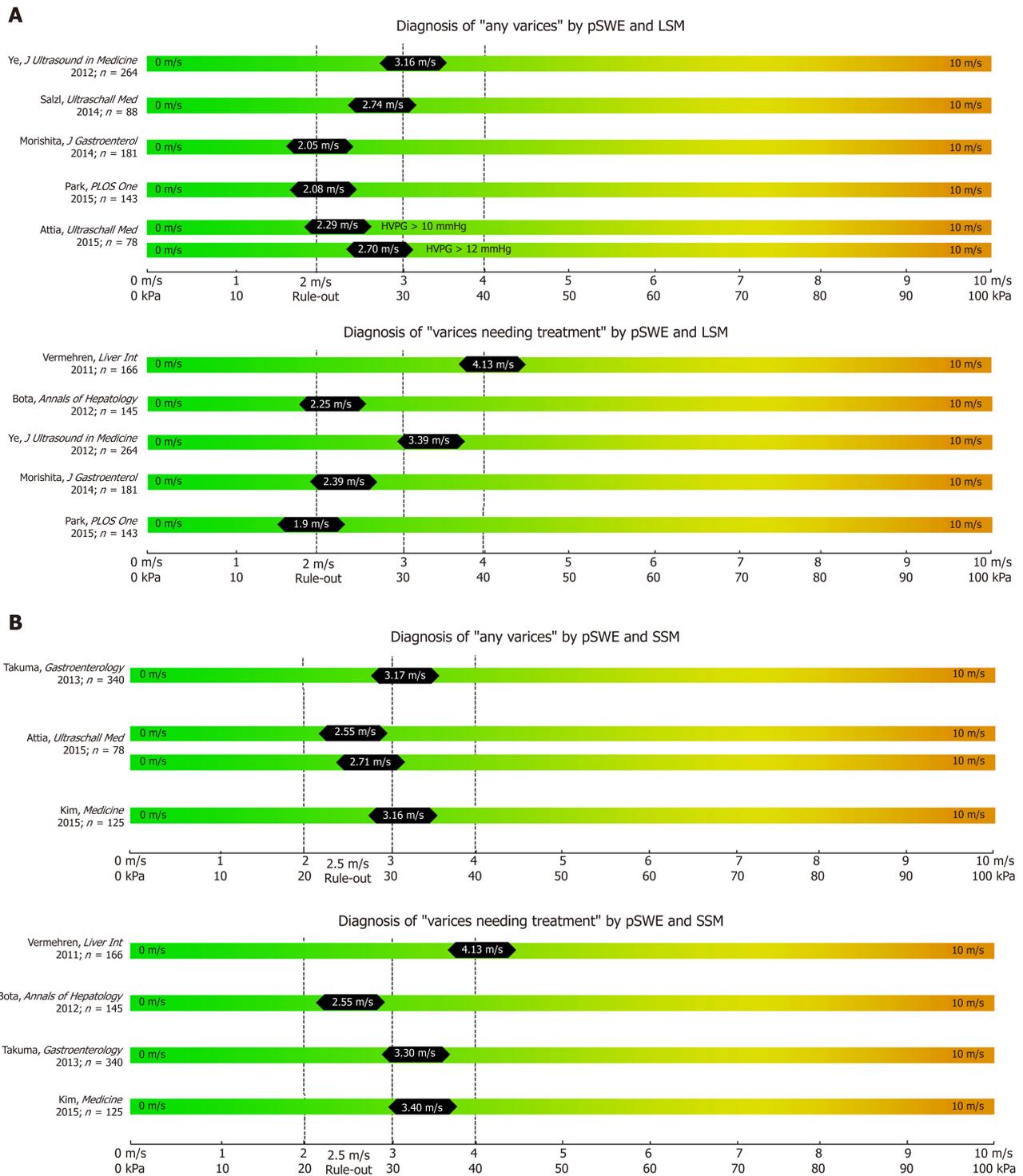
Figure 2 Summary of studies that reported point shear wave elastography derived cut-offs on the non-invasive diagnosis of any varices and varices needing treatment (A) using liver stiffness measurement and spleen stiffness measurement respectively (B).

performed by trained personal (*e.g.* nurses), while ultrasound-based pSWE (and 2D-SWE) is critically dependent on the experience of the ultrasound operator[43]. In addition, the accuracy of pSWE-based assessment of LSM and SSM can be improved by following quality criteria[44].

In synopsis, pSWE has been widely evaluated for the prediction of EV, mostly through SSM. Nevertheless this technique might not be available everywhere, AUC of SSM vary and too few studies have been published about pSWE-LSM to predict presence of EV.

2D shear wave elastography
In contrast to pSWE , 2D-SWE uses two-dimensional measurement of shear wave

Table 3 Two-dimensional shear wave elastography for the prediction of varices

Ref.	Country	Study design	Nr.	Etiology	Model	Cut-off (AUC) for EV	Sens/Spec/+LR/-LR/p for EV	Cut-off (AUC) for VNT	Se/Sp/+LR/-LR/p for VNT	Comment
Kim, *Liver International*, 2015[51]	Korea	Prospective	92	Mixed	Aixplorer	L-SWE: All patients: 26.3 kPa (0.683) Compensated cirrhosis: 14.2 kPa (0.925)	L-SWE: All patients: 61.4%/75.0%/PPV 89.6%/NPV 35.7%/P = 0.004 Compensated cirh.: 87.5%/90.0%/PPV 93.3%/NPV 81.8%/ P < 0.001	NR	NR	Main focus on prediction of PHT/CSPH
Grgurevic, *Croatian Medical Journal* 2015[53]	Croatia	Retrospective	44	Mixed	Aixplorer	L-SWE: 19.7 kPa (0.796) S-SWE: 30.3 kPa (0.790)	L-SWE: 83.3%/66.6%/2.5/0.25/0.037 S-SWE: 79.6%/75.8%/3.3/0.27/0.009	NR	NR	
Kasai *Journal of Medical Ultrasonics*, 2015[54]	Japan	Retrospective	273	Mixed	Aixplorer	Cut-off: NR AUC: (0.807)	NR	NR	NR	No cut-offs or sensitivity analyses reported; varices: ≥ grade 2
Elkrief *et al.* *Radiology* 2015[56]	France	Prospective	79	Mixed	Aixplorer	NR	NR	NR	NR	EV not evaluated; Neither L-SWE, nor S-SWE, nor L-TE, nor LSPS predictive of VNT, but predictive of CSPH
Cassinotto, *Digestive Liver Disease* 2015[99]	France	Prospective	401	Mixed	Aixplorer	NR	NR	L-SWE: 12.8 (0.70) S-SWE: 25.6 (0.75)	L-SWE: 92%/36%/1.44/0.22/NR /PPV: 44%/NPV: 90% S-SWE: 94%/36%/1.47/0-17/NR/PPV:50%/NPV:90%	
Kim *et al.* *Journal of Ultrasound in Medicine* 2016[55]	Korea	Retrospective	103	Mixed	Aixplorer	L-SWE: 13.9 kPa (0.887)	75%/88.9%/6.75/0.28/< 0.001	16.1 kPa (0.880)	84.6%/85.6%/5.86/0.18 /< 0.001	

AUC: Area under the (receiver operating) curve; CLD: Chronic liver disease; CSPH: Clinically significant portal hypertension; L-SWE: Liver shear wave elastography esophageal varices; TE: Transient elastography; Plt: Platelet count; VNT: Varices needing treatment; Se: Sensitivity; Sp: Specificity; +LR: Positive likelihood ratio; -LR: Negative likelihood ratio; NR: Not reported; S-SWE: Spleen share wave elastography.

speed and multiple focal zones are measured[6]. Furthermore, real-time measurement - as displayed "on-screen" - is possible[10,35]. This enables the operator to analyze a larger amount of liver tissue in real-time and improves the applicability of elastography[10]. Nevertheless, 2D-SWE has not yet been introduced into clinical routine and are limited to specialized centers and should be only performed by experienced operators[35]. Importantly, there are not established/accepted quality criteria for 2D-
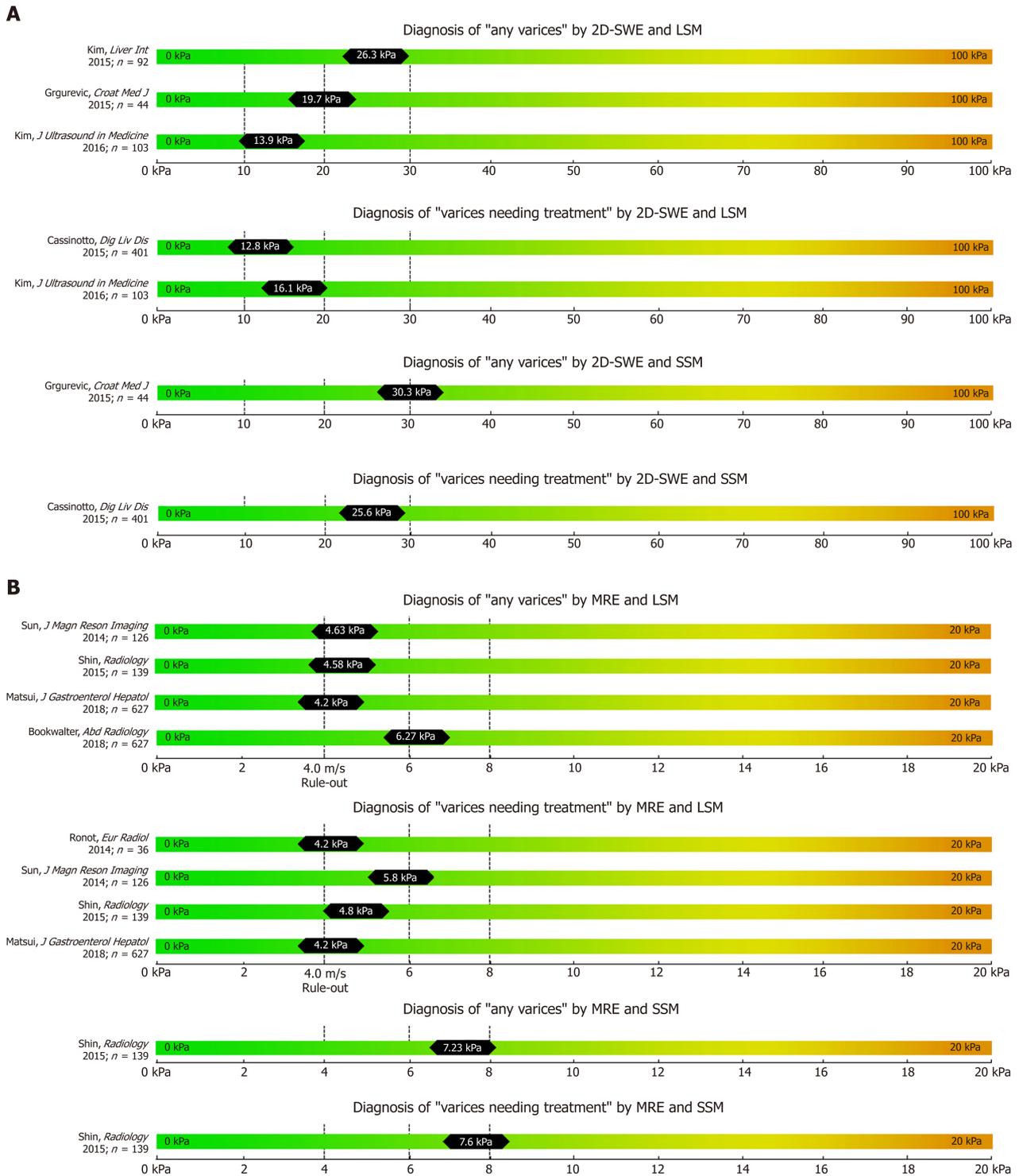
**Figure 3 Summary of studies that reported two-dimensional shear wave elastography (A) and magnetic resonance elastography (B) derived cut-offs on the non-invasive diagnosis of any varices and varices needing treatment using liver stiffness measurement and spleen stiffness measurement respectively.**

SWE measurements for LSM and/or SSM[35].

2D-SWE-based LSM has been validated as a valid tool for non-invasive assessment of fibrosis in several studies[45-48]. The reliability of 2D-SWE-based LSM measurements was significantly higher as compared to the widely established TE-based LSM[49]: The AUC for 2D-SWE-based LSM for prediction of F ≥ 2 (cut-off 8.03 kPa) and F4 (cut-off 13.1 kPa) were 0.832 and 0.915, respectively. Indeed, most recently, two meta-analysis on 2D-SWE including 1134 patient[48] and 746 patients[50] have been published that both reported superior accuracy to detect significant fibrosis or cirrhosis using 2D-SWE as compared to TE.

Kim *et al*[51] evaluated 2D-SWE for the prediction of CSPH and reported an AUC of

Table 4 Magnetic resonance elastography for prediction of varices

Author, Journal, Year	Liver/Spleen	Patient N	Etiology	Cut-offs for EV (AUC)	EV: Sens/Spec/+LR/-LR/acc/p	Cut-offs for VNT (AUC)	VNT: Sens/Spec/+LR/-LR/acc/p	Prevalence of EV and VNT	Comment
Ronot *et al. Eur Radiol* 2014[63]	yes/yes	36	mixed	NR	NR	Gl, 84 Hz: 4.2 kPa (0.93)	54%/100%/PPV: 33%/NPV: 79%/*P* = 0.001	Any EV: 75%; VNT: 72%	Liver MRE not predictive of EV or VNT. Advantage of 3D multifrequency MRE
Sun *et al. J Magn Reson Imaging* 2014[62]	yes/no	126	mixed	L-MRE: 4.63 kPa (0.859)	NR	L-MRE: 5.803 kPa (0.810)	L-MRE: 96%/60%/n.r.	Any EV: 49%; VNT: 19%	Pearson correlation coefficient between liver stiffness and EV: 0.63 (*P* < 0.0001).
Shin *et al. Radiology* 2014[61]	yes/yes	139	mixed	L-MRE: 4.58 kPa (0.821) S-MRE: 7.23 kPa (0.833)	L-MRE: 87.4%/65.6%/n.r. S-MRE: 85.8%/65.4%/n.r.	L-MRE: 4.81 kPa (0.755) S-MRE: 7.60 kPa (0.750)	L-MRE: 84.4%/56.7%/n.r. S-MRE: 68.3%/61.6%/n.r.	Any EV: 56%; VNT: 32%	Data cross-validated; several false-positive diagnoses of EV and VNT due to high liver stiffness and non-esophageal collaterals; 11 cases of false-negative diagnoses of EV: pre-hepatic PHT, iron deposition, large ascites.
Matsui, *Journal of Gastroenterology and Hepatology,* 2018[100]	yes/no	627	mixed	MRE: 4.2 kPa (0.85) PLT: 18*10⁴ (0.77)	MRE: 85%/69%/PPV 32%/NPV 96% MRE + PLT: 93%/43%/PPV 22%/NPV 96%	MRE: 4.2 kPa (0.85) PLT: 18*10⁴ (0.77)	MRE: 94%/65%/PPV 17%/ NPV 99% MRE + PLT: 100%/35%/PPV 10%/ NPV 100%	Any EV: 15.6% VNT: 4.5%	3T device; also validated Baveno VI criteria (1) and modified Baveno VI criteria (30); excellent performance in NAFLD and viral hepatitis
Bookwalter, *Abdominal Radiology,* 2018[101]	yes/no	55	PSC	6.27 kPa (NR)	Sens. 100%/Spec. 76.7%	NR	NR	NR	Several sequences, 2D and 3D modes, at 1,5T and 3T; Varices assessed by global LSM
Kim, *European Radiologist,* 2017[102]	yes/no	84	NR	GRE-MRE: (0.948) SE-EPI-MRE: (0.914)	NR	GRE-MRE: 4.493 kPa (0.752) SE-EPI-MRE: 5.880 kPa (0.839)	NR	Any EV: 17.9% VNT: 8.3%	Neither SE-EPI-, nor GRE-MRE reached significance regarding diagnostic performance

AUC: Area under the (receiver operating) curve; CSPH: Clinically significant portal hypertension; LSM: Liver stiffness measurement; EV: Esophageal varices; MRE: Magnetic resonance elastography; TE: Transient elastography; Plt: Platelet count; VNT: Varices needing treatment; NR: Not reported; SSM: Spleen stiffness measurement; SE-EPI: Spin-echo echoplanar imaging; GRE: Gradient recalled echo.

0.819 at a 2D-SWE LSM cut-off of 15.2 kPa in 115 cirrhotic patients undergoing

measurement of portal pressure by hepatic venous pressure gradient (HVPG). Importantly, a recent meta-analysis by Suh[50] showed an excellent diagnostic performance of 2D-SWE for predicting the presence of CSPH with sensitivity and specificity around 85%[50].

Studies reporting on the performance of 2D-SWE based non-invasive screening for EV are scarce. In a large prospective study investigating 2D-SWE-based liver (L-SWE) and spleen (S-SWE) for the diagnosis of CSPH yielded an AUC of 0.861 for L-SWE (24.6 kPa) and of 0.837 for S-SWE (26.3 kPa), respectively[52].

A Croatian study reported a cut-off of 19.7 for L-SWE (AUC 0.796) and 30.3 kPa for S-SWE (AUC 0.790) for the prediction of any EV in a cohort of 44 patients with cACLD[53]. Kasai *et al*[54] found significantly higher L-SWE values in 16 patients with EV than in 257 patients without EV, with similar AUC of 0.807. In a retrospective cohort of 103 cACLD patients 2D-SWE of L-SWE yielded an AUC of 0.887 (cut-off 13.9 kPa) for any EV and 0.880 (cut-off 16.1 kPa) for VNT[55]. Interestingly, a prospective study published in 2015 including 79 patients found no difference between LSM and SSM values (measured by 2D-SWE and by TE respectively) between patients with VNT and patients without VNT[56]. The resulting AUCs of 2D-SWE for detection of VNT were consequently unacceptably low with an AUC of 0.600 for L-SWE and an AUC of 0.580 for S-SWE, respectively[56].

In conclusion, while there is strong evidence for the value of 2D-SWE-based LSM for fibrosis assessment, studies on the value of 2D-SWE based LSM and SSM for the screening of EVs are limited. Larger studies using 2D-SWE-based liver and spleen stiffness measurement for the assessment of patients with cACLD are needed to establish its value for the prediction of any EV and of VNTs in daily clinical practice.

Magnetic resonance elastography

Several studies have been already been published on the correlation of MRE with liver fibrosis and found high diagnostic accuracies (> 90%) for the diagnosis of advanced fibrosis and cirrhosis[10,57,58]. Most recently, few studies on the value of MRE for the prediction of EV have been published with data on both liver MRE (L-MRE) and spleen MRE (S-MRE). Major advantages of MRE are its capability to evaluate the whole liver three-dimensionally (3D-SWE) and its excellent diagnostic accuracy for staging fibrosis[10]. Furthermore, failure rate is low and was reported to be mostly due to physical "non-fitting" into the MR device, claustrophobia or low hepatic signal related to iron overload[10,59]. Importantly, MRE shows excellent inter-observer and intra-observer agreement[60]. The main limitations of MRE include its high costs, limited availability and the need for specialized infrastructure and equipment. Shin *et al*[61] reported MRE data on 139 cirrhotic patients: Any EV were predicted by an L-MRE cut-off at 4.58 kPa (AUC 0.821) and by an S-MRE cut-off at 7.23 kPa (AUC 0.833). Furthermore, VNT were predicted by an L-MRE cut-off at 4.81 kPa (AUC 0.755) and a S-MRE cut-off at 7.6 kPa (AUC: 0.750).

In a South-Korean cohort of 126 patients[62], L-MRE cut offs were 4.63 kPa (AUC 0.859) for any EV, and 5.8 kPa (AUC 0.81) for VNT, respectively. Finally, Ronot *et al*[63] reported data on a small cohort of 36 patients and found 4.2 kPa (AUC 0.93) as an optimal cut-off for ruling out VNT (PPV 33%, NPV 79%).

Despite these promising results of MRE-based LSM and SSM for predicting any EV or VNT, more prospective studies are needed before implementing MRE for the non-invasive screening of EV/VNT in clinical practice. Furthermore, the feasibility of MRE is limited due to its inherent high costs, long examination times and considerable need for radiological expertise. Considering the limited data on MRE-based screening for EV/VNTs, as of now TE, pSWE and 2D-SWE are likely the first choice for screening of EV/VNTs in clinical practice – given their wider availability and lower costs.

CONCLUSION

In this review we summarized the current knowledge on elastography-based methods for the non-invasive prediction of any EVs and VNTs in adult patients with advanced chronic liver disease.

TE is an easy to use device with good applicability and well-trained nursing staff can usually perform LSM after training. Nevertheless the area of TE-based LSM is small and values can be significantly altered or even impossible to obtain in patients with obesity or ascites. Importantly, the combined TE-based LSM < 20 kPa plus PLT > 150 G/L has become a widely accepted non-invasive algorithm for ruling out VNTs[1,5]

Following TE-based LSM, pSWE and 2D-SWE have been developed as novel ultrasound-based elastography methods. Importantly, next to LSM also SSM - mostly

by pSWE and 2D-SWE have been additionally introduced as a valuable screening tool for EV/VNTs. Both pSWE and 2D-SWE methods have the benefit of "seeing what you measure", given the integration of the technique in standard ultrasound machines. However, the operator performing pSWE and 2D-SWE needs to be well-trained in ultrasound sonography and quality criteria for valid LSM and SSM have to be rigorously followed. Nevertheless there are some potential limiting factors that may hamper interpretation of results irrespective of operators experience and elastography method. It is known that in states of chronic inflammation such as viral hepatitis[64,65],autoimmune hepatitis[66] and alcoholic steatohepatitis[67] and in cases of acute liver damage[68] liver stiffness can be false positively increased. Furthermore increased LSM has also been described due to mechanical cholestasis[69]. Lastly hepatic congestion due congestive heart failure[70,71] and Budd-Chiari syndrome[72,73] thus generally speaking through increased venous pressure[74] is also known to increase elastography-based LSM values[75]. In a recent review by Lemmer *et al*[75] non-invasive methods to diagnose fibrosis in patients with congestive hepatopathy were discussed and conclusions were quite disillusioning since only very limited data exists. In a study that evaluated LSM in 32 patients with valvular heart disease that underwent valve operation, LSM was found to be consistently higher than in the control group, even though none of the participants were found with evidence of underlying chronic liver disease[76]. Furthermore LSM at baseline was significantly positively correlated with NT-proBNP, and central venous pressure during the operation and negatively with left ventricular ejection fraction[76]. Ninety days after surgery LSM values significantly decreased compared to 7 d after surgery (8.4 kPa *vs* 6.0 kPa, $P = 0.026$). On the other hand a study evaluating MRE-LSM and -SSM in congestive hepatopathy found promising results and reported significant correlation of LSM ($r = 0.74$, $P = 0.02$) and SSM ($r = 0.97$, $P = 0.002$) with fibrosis stage, although liver biopsy results were only available in 8 patients[77]. Therefore, given the potential pitfalls, we suggest that irrespective of the elastography method used, clinical signs of chronic liver disease, laboratory data and other co-morbidities should always be taken into account when performing LSM or SSM respectively.

Our extensive literature search revealed significant discrepancies between published LSM and SSM cut-offs using pSWE and 2D-SWE for EV/VNT screening. The absence of generally-accepted quality criteria for pSWE and 2D-SWE remains and validated cut-offs for ruling-in/out EVs/VNTs calls for further research on the clinical applicability of pSWE and 2D-SWE for the screening of EVs/VNTs. Moreover, presence of esophageal varices may be relied on cofounding factors, other than liver stiffness. Most recently, patients with large or even small portosystemic shunting were found to have an increased prevalence of esophageal varices[78], and although grade of portosystemic shunting was related to liver dysfunction, varices might be missed by transient elastography in those cases. Interestingly patients with preserved liver function (defined as MELD 6-9 or Child Pugh Stage A) and portosystemic shunting showed higher HVPG values and were found with significantly more portal hypertension related complications such as bleeding or ascites than in those without shunting[78] and this emphasizes even more that especially in those patients, where LSM might be low, esophageal varices might be missed. Furthermore, in the era of successful and highly efficient treatment of hepatitis C, nowadays quite a lot of cirrhotic patients present without the initial trigger for their underlying liver disease and it has been shown that directly acting antivirals significantly lower portal pressure[79]. Concerning this matter, no study has up to date evaluated applicability of elastography-based methods to predict esophageal varices in this cohort, and therefore it is not known whether published cut-offs work in this large subgroup of patients.

More recently, MRE-based LSM has been introduced as a very accurate method to stage liver fibrosis and with concomitant MRE-based LSM and SSM yielding excellent performance for non-invasive diagnosis of EV/VNTs. Consequently, MRE seems to be a highly accurate screening method for EVs/VNTs, however, studies are scarce and further evidence is needed.

In conclusion a vast amount of studies on the diagnostic performance of elastography-based methods for the presence of EV/VNTs have been published, mostly reporting data on TE. Both pSWE and 2D-SWE-based LSM and SSM represent promising tools for EV/VNT screening but further clinical studies and evaluation of specific cut-offs are required. MRE-based LSM and SSM-based screening of EV/VNT holds promise but is limited by its high costs. At the moment we strongly recommend to use the combined TE-LSM < 20 kPa and PLT > 150 G/L algorithm to rule-out VNTs. Considering the promising data on SSM and the ability of SSM to capture pre-sinusoidal/pre-hepatic components of CSPH, we strongly encourage further research on SSM for screening of CSPH and EV/VNTs. Finally, we have summarized the currently available data and published cut-offs for EV/VNT prediction by TE, pSWE,

2D-SWE and MRE on scale-cards for clinical practice.

REFERENCES

1. **de Franchis R**; Baveno VI Faculty. Expanding consensus in portal hypertension: Report of the Baveno VI Consensus Workshop: Stratifying risk and individualizing care for portal hypertension. *J Hepatol* 2015; **63**: 743-752 [PMID: 26047908 DOI: 10.1016/j.jhep.2015.05.022]

2. **Tsochatzis EA**, Bosch J, Burroughs AK. Liver cirrhosis. *Lancet* 2014; **383**: 1749-1761 [PMID: 24480518 DOI: 10.1016/s0140-6736(14)60121-5]

3. **Garcia-Tsao G**, Abraldes JG, Berzigotti A, Bosch J. Portal hypertensive bleeding in cirrhosis: Risk stratification, diagnosis, and management: 2016 practice guidance by the American Association for the study of liver diseases. *Hepatology* 2017; **65**: 310-335 [PMID: 27786365 DOI: 10.1002/hep.28906]

4. **Reiberger T**, Ulbrich G, Ferlitsch A, Payer BA, Schwabl P, Pinter M, Heinisch BB, Trauner M, Kramer L, Peck-Radosavljevic M; Vienna Hepatic Hemodynamic Lab. Carvedilol for primary prophylaxis of variceal bleeding in cirrhotic patients with haemodynamic non-response to propranolol. *Gut* 2013; **62**: 1634-1641 [PMID: 23250049 DOI: 10.1136/gutjnl-2012-304038]

5. **Reiberger T**, Püspök A, Schoder M, Baumann-Durchschein F, Bucsics T, Datz C, Dolak W, Ferlitsch A, Finkenstedt A, Graziadei I, Hametner S, Karnel F, Krones E, Maieron A, Mandorfer M, Peck-Radosavljevic M, Rainer F, Schwabl P, Stadlbauer V, Stauber R, Tilg H, Trauner M, Zoller H, Schöfl R, Fickert P. Austrian consensus guidelines on the management and treatment of portal hypertension (Billroth III). *Wien Klin Wochenschr* 2017; **129**: 135-158 [PMID: 29063233 DOI: 10.1007/s00508-017-1262-3]

6. **Sigrist RMS**, Liau J, Kaffas AE, Chammas MC, Willmann JK. Ultrasound Elastography: Review of Techniques and Clinical Applications. *Theranostics* 2017; **7**: 1303-1329 [PMID: 28435467 DOI: 10.7150/thno.18650]

7. **Xie LT**, Yan CH, Zhao QY, He MN, Jiang TA. Quantitative and noninvasive assessment of chronic liver diseases using two-dimensional shear wave elastography. *World J Gastroenterol* 2018; **24**: 957-970 [PMID: 29531460 DOI: 10.3748/wjg.v24.i9.957]

8. **Venkatesh SK**, Ehman RL. Magnetic resonance elastography of abdomen. *Abdom Imaging* 2015; **40**: 745-759 [PMID: 25488346 DOI: 10.1007/s00261-014-0315-6]

9. **Horowitz JM**, Venkatesh SK, Ehman RL, Jhaveri K, Kamath P, Ohliger MA, Samir AE, Silva AC, Taouli B, Torbenson MS, Wells ML, Yeh B, Miller FH. Evaluation of hepatic fibrosis: a review from the society of abdominal radiology disease focus panel. *Abdom Radiol (NY)* 2017; **42**: 2037-2053 [PMID: 28624924 DOI: 10.1007/s00261-017-1211-7]

10. **Friedrich-Rust M**, Poynard T, Castera L. Critical comparison of elastography methods to assess chronic liver disease. *Nat Rev Gastroenterol Hepatol* 2016; **13**: 402-411 [PMID: 27273167 DOI: 10.1038/nrgastro.2016.86]

11. **Schwabl P**, Bota S, Salzl P, Mandorfer M, Payer BA, Ferlitsch A, Stift J, Wrba F, Trauner M, Peck-Radosavljevic M, Reiberger T. New reliability criteria for transient elastography increase the number of accurate measurements for screening of cirrhosis and portal hypertension. *Liver Int* 2015; **35**: 381-390 [PMID: 24953516 DOI: 10.1111/liv.12623]

12. **Şirli R**, Sporea I, Deleanu A, Culcea L, Szilaski M, Popescu A, Dănilă M. Comparison between the M and XL probes for liver fibrosis assessment by transient elastography. *Med Ultrason* 2014; **16**: 119-122 [PMID: 24791843]

13. **Sporea I**, irli R, Mare R, Popescu A, Ivacu SC. Feasibility of Transient Elastography with M and XL probes in real life. *Med Ultrason* 2016; **18**: 7-10 [PMID: 26962547 DOI: 10.11152/mu.2013.2066.181.xsi]

14. **Bazerbachi F**, Haffar S, Wang Z, González JC, Arias-Loste MT, Crespo J, Darwish-Murad S, Ikram MA, Olynyk JK, Gan E, Petta S, Berzuini A, Prati D, de Lédinghen V, Wai-Sun Wong V, Del Poggio P, Chávez-Tapia NC, Chen YP, Cheng PN, Yuen MF, Das K, Chowdhury A, Caballeria L, Fabrellas N, Ginès P, Kumar M, Sarin SK, Conti F, Andreone P, Sirli R, Cortez-Pinto H, Carvalhana S, Sugihara T, Kim SU, Parikh P, Chayama K, Corpechot C, Kim KM, Papatheodoridis G, Alsebaey A, Kamath PS, Murad MH, Watt KD. Range of Normal Liver Stiffness and Factors Associated With Increased Stiffness Measurements in Apparently Healthy Individuals. *Clin Gastroenterol Hepatol* 2018; Epub ahead of print [PMID: 30196155 DOI: 10.1016/j.cgh.2018.08.069]

15. **Kazemi F**, Kettaneh A, N'kontchou G, Pinto E, Ganne-Carrie N, Trinchet JC, Beaugrand M. Liver stiffness measurement selects patients with cirrhosis at risk of bearing large oesophageal varices. *J Hepatol* 2006; **45**: 230-235 [PMID: 16797100 DOI: 10.1016/j.jhep.2006.04.006]

16. **Foucher J**, Chanteloup E, Vergniol J, Castéra L, Le Bail B, Adhoute X, Bertet J, Couzigou P, de Lédinghen V. Diagnosis of cirrhosis by transient elastography (FibroScan): a prospective study. *Gut* 2006; **55**: 403-408 [PMID: 16020491 DOI: 10.1136/gut.2005.069153]

17. **Wong GL**, Kwok R, Chan HL, Tang SP, Lee E, Lam TC, Lau TW, Ma TM, Wong BC, Wong VW. Measuring spleen stiffness to predict varices in chronic hepatitis B cirrhotic patients with or without receiving non-selective beta-blockers. *J Dig Dis* 2016; **17**: 538-546 [PMID: 27185358 DOI: 10.1111/1751-2980.12359]

18. **Stefanescu H**, Grigorescu M, Lupsor M, Procopet B, Maniu A, Badea R. Spleen stiffness measurement using Fibroscan for the noninvasive assessment of esophageal varices in liver cirrhosis patients. *J Gastroenterol Hepatol* 2011; **26**: 164-170 [PMID: 21175810 DOI: 10.1111/j.1440-1746.2010.06325.x]

19. **Abraldes JG**, Bureau C, Stefanescu H, Augustin S, Ney M, Blasco H, Procopet B, Bosch J, Genesca J, Berzigotti A; Anticipate Investigators. Noninvasive tools and risk of clinically significant portal hypertension and varices in compensated cirrhosis: The "Anticipate" study. *Hepatology* 2016; **64**: 2173-2184 [PMID: 27639071 DOI: 10.1002/hep.28824]

20. **Nguyen-Khac E**, Saint-Leger P, Tramier B, Coevoet H, Capron D, Dupas JL. Noninvasive diagnosis of large esophageal varices by Fibroscan: strong influence of the cirrhosis etiology. *Alcohol Clin Exp Res* 2010; **34**: 1146-1153 [PMID: 20477777 DOI: 10.1111/j.1530-0277.2010.01191.x]

21. **Bintintan A**, Chira RI, Bintintan VV, Nagy GA, Manzat-Saplacan MR, Lupsor-Platon M,

Stefanescu H, Duma MM, Valean SD, Mircea PA. Value of hepatic elastography and Doppler indexes for predictions of esophageal varices in liver cirrhosis. *Med Ultrason* 2015; **17**: 5-11 [PMID: 25745650 DOI: 10.11152/mu.2013.2066.171.abric]

22   **Maurice JB**, Brodkin E, Arnold F, Navaratnam A, Paine H, Khawar S, Dhar A, Patch D, O'Beirne J, Mookerjee R, Pinzani M, Tsochatzis E, Westbrook RH. Validation of the Baveno VI criteria to identify low risk cirrhotic patients not requiring endoscopic surveillance for varices. *J Hepatol* 2016; **65**: 899-905 [PMID: 27388923 DOI: 10.1016/j.jhep.2016.06.021]

23   **Llop E**, Lopez M, de la Revilla J, Fernandez N, Trapero M, Hernandez M, Fernández-Carrillo C, Pons F, Martinez JL, Calleja JL. Validation of noninvasive methods to predict the presence of gastroesophageal varices in a cohort of patients with compensated advanced chronic liver disease. *J Gastroenterol Hepatol* 2017; **32**: 1867-1872 [PMID: 28295587 DOI: 10.1111/jgh.13781]

24   **Augustin S**, Pons M, Maurice JB, Bureau C, Stefanescu H, Ney M, Blasco H, Procopet B, Tsochatzis E, Westbrook RH, Bosch J, Berzigotti A, Abraldes JG, Genescà J. Expanding the Baveno VI criteria for the screening of varices in patients with compensated advanced chronic liver disease. *Hepatology* 2017; **66**: 1980-1988 [PMID: 28696510 DOI: 10.1002/hep.29363]

25   **Marot A**, Trépo E, Doerig C, Schoepfer A, Moreno C, Deltenre P. Liver stiffness and platelet count for identifying patients with compensated liver disease at low risk of variceal bleeding. *Liver Int* 2017; **37**: 707-716 [PMID: 27862856 DOI: 10.1111/liv.13318]

26   **Pu K**, Shi JH, Wang X, Tang Q, Wang XJ, Tang KL, Long ZQ, Hu XS. Diagnostic accuracy of transient elastography (FibroScan) in detection of esophageal varices in patients with cirrhosis: A meta-analysis. *World J Gastroenterol* 2017; **23**: 345-356 [PMID: 28127208 DOI: 10.3748/wjg.v23.i2.345]

27   **Wong GLH**, Kwok R, Hui AJ, Tse YK, Ho KT, Lo AOS, Lam KLY, Chan HCH, Lui RA, Au KHD, Chan HLY, Wong VWS. A new screening strategy for varices by liver and spleen stiffness measurement (LSSM) in cirrhotic patients: A randomized trial. *Liver Int* 2018; **38**: 636-644 [PMID: 28853196 DOI: 10.1111/liv.13560]

28   **Petta S**, Sebastiani G, Bugianesi E, Viganò M, Wong VW, Berzigotti A, Fracanzani AL, Anstee QM, Marra F, Barbara M, Calvaruso V, Cammà C, Di Marco V, Craxì A, de Ledinghen V. Non-invasive prediction of esophageal varices by stiffness and platelet in non-alcoholic fatty liver disease cirrhosis. *J Hepatol* 2018; **69**: 878-885 [PMID: 29802949 DOI: 10.1016/j.jhep.2018.05.019]

29   **Jangouk P**, Turco L, De Oliveira A, Schepis F, Villa E, Garcia-Tsao G. Validating, deconstructing and refining Baveno criteria for ruling out high-risk varices in patients with compensated cirrhosis. *Liver Int* 2017; **37**: 1177-1183 [PMID: 28160373 DOI: 10.1111/liv.13379]

30   **Sharma P**, Kirnake V, Tyagi P, Bansal N, Singla V, Kumar A, Arora A. Spleen stiffness in patients with cirrhosis in predicting esophageal varices. *Am J Gastroenterol* 2013; **108**: 1101-1107 [PMID: 23629600 DOI: 10.1038/ajg.2013.119]

31   **Manatsathit W**, Samant H, Kapur S, Ingviya T, Esmadi M, Wijarnpreecha K, McCashland T. Accuracy of liver stiffness, spleen stiffness, and LS-spleen diameter to platelet ratio score in detection of esophageal varices: Systemic review and meta-analysis. *J Gastroenterol Hepatol* 2018; **33**: 1696-1706 [PMID: 29736946 DOI: 10.1111/jgh.14271]

32   **Colecchia A**, Montrone L, Scaioli E, Bacchi-Reggiani ML, Colli A, Casazza G, Schiumerini R, Turco L, Di Biase AR, Mazzella G, Marzi L, Arena U, Pinzani M, Festi D. Measurement of spleen stiffness to evaluate portal hypertension and the presence of esophageal varices in patients with HCV-related cirrhosis. *Gastroenterology* 2012; **143**: 646-654 [PMID: 22643348 DOI: 10.1053/j.gastro.2012.05.035]

33   **Calvaruso V**, Bronte F, Conte E, Simone F, Craxì A, Di Marco V. Modified spleen stiffness measurement by transient elastography is associated with presence of large oesophageal varices in patients with compensated hepatitis C virus cirrhosis. *J Viral Hepat* 2013; **20**: 867-874 [PMID: 24304456 DOI: 10.1111/jvh.12114]

34   **Colecchia A**, Ravaioli F, Marasco G, Colli A, Dajti E, Di Biase AR, Bacchi Reggiani ML, Berzigotti A, Pinzani M, Festi D. A combined model based on spleen stiffness measurement and Baveno VI criteria to rule out high-risk varices in advanced chronic liver disease. *J Hepatol* 2018; **69**: 308-317 [PMID: 29729368 DOI: 10.1016/j.jhep.2018.04.023]

35   **Berzigotti A**. Non-invasive evaluation of portal hypertension using ultrasound elastography. *J Hepatol* 2017; **67**: 399-411 [PMID: 28223101 DOI: 10.1016/j.jhep.2017.02.003]

36   **Salzl P**, Reiberger T, Ferlitsch M, Payer BA, Schwengerer B, Trauner M, Peck-Radosavljevic M, Ferlitsch A. Evaluation of portal hypertension and varices by acoustic radiation force impulse imaging of the liver compared to transient elastography and AST to platelet ratio index. *Ultraschall Med* 2014; **35**: 528-533 [PMID: 24871695 DOI: 10.1055/s-0034-1366506]

37   **Takuma Y**, Nouso K, Morimoto Y, Tomokuni J, Sahara A, Takabatake H, Matsueda K, Yamamoto H. Portal Hypertension in Patients with Liver Cirrhosis: Diagnostic Accuracy of Spleen Stiffness. *Radiology* 2016; **279**: 609-619 [PMID: 26588019 DOI: 10.1148/radiol.2015150690]

38   **Lucchina N**, Recaldini C, Macchi M, Molinelli V, Montanari M, Segato S, Novario R, Fugazzola C. Point Shear Wave Elastography of the Spleen: Its Role in Patients with Portal Hypertension. *Ultrasound Med Biol* 2018; **44**: 771-778 [PMID: 29352618 DOI: 10.1016/j.ultrasmedbio.2017.11.019]

39   **Bota S**, Sporea I, Sirli R, Focsa M, Popescu A, Danila M, Strain M. Can ARFI elastography predict the presence of significant esophageal varices in newly diagnosed cirrhotic patients? *Ann Hepatol* 2012; **11**: 519-525 [PMID: 22700634]

40   **Rizzo L**, Attanasio M, Pinzone MR, Berretta M, Malaguarnera M, Morra A, L'Abbate L, Balestreri L, Nunnari G, Cacopardo B. A new sampling method for spleen stiffness measurement based on quantitative acoustic radiation force impulse elastography for noninvasive assessment of esophageal varices in newly diagnosed HCV-related cirrhosis. *Biomed Res Int* 2014; **2014**: 365982 [PMID: 24729970 DOI: 10.1155/2014/365982]

41   **Vermehren J**, Polta A, Zimmermann O, Herrmann E, Poynard T, Hofmann WP, Bojunga J, Sarrazin C, Zeuzem S, Friedrich-Rust M. Comparison of acoustic radiation force impulse imaging with transient elastography for the detection of complications in patients with cirrhosis. *Liver Int* 2012; **32**: 852-858 [PMID: 22222050 DOI: 10.1111/j.1478-3231.2011.02736.x]

42   **Takuma Y**, Nouso K, Morimoto Y, Tomokuni J, Sahara A, Toshikuni N, Takabatake H, Shimomura H, Doi A, Sakakibara I, Matsueda K, Yamamoto H. Measurement of spleen stiffness by acoustic radiation force impulse imaging identifies cirrhotic patients with esophageal varices. *Gastroenterology* 2013; **144**: 92-101.e2 [PMID: 23022955 DOI: 10.1053/j.gastro.2012.09.049]

43   **Grădinaru-Taşcău O**, Sporea I, Bota S, Jurchiş A, Popescu A, Popescu M, Şirli R, Szilaski M. Does experience play a role in the ability to perform liver stiffness measurements by means of supersonic shear imaging (SSI)? *Med Ultrason* 2013; **15**: 180-183 [PMID: 23979612]

44   **Ferraioli G**, De Silvestri A, Reiberger T, Taylor-Robinson SD, de Knegt RJ, Maiocchi L, Mare R, Bucsics T, Atzori S, Tinelli C, Sporea I. Adherence to quality criteria improves concordance between transient elastography and ElastPQ for liver stiffness assessment-A multicenter retrospective study. *Dig Liver Dis* 2018; **50**: 1056-1061 [PMID: 29705030 DOI: 10.1016/j.dld.2018.03.033]

45   **Zhang W**, Zhu Y, Zhang C, Ran H. Diagnostic Accuracy of 2-Dimensional Shear Wave Elastography for the Staging of Liver Fibrosis: A Meta-analysis. *J Ultrasound Med* 2018; Epub ahead of print [PMID: 30171621 DOI: 10.1002/jum.14760]

46   **Zheng J**, Guo H, Zeng J, Huang Z, Zheng B, Ren J, Xu E, Li K, Zheng R. Two-dimensional shear-wave elastography and conventional US: the optimal evaluation of liver fibrosis and cirrhosis. *Radiology* 2015; **275**: 290-300 [PMID: 25575116 DOI: 10.1148/radiol.14140828]

47   **Gerber L**, Kasper D, Fitting D, Knop V, Vermehren A, Sprinzl K, Hansmann ML, Herrmann E, Bojunga J, Albert J, Sarrazin C, Zeuzem S, Friedrich-Rust M. Assessment of liver fibrosis with 2-D shear wave elastography in comparison to transient elastography and acoustic radiation force impulse imaging in patients with chronic liver disease. *Ultrasound Med Biol* 2015; **41**: 2350-2359 [PMID: 26116161 DOI: 10.1016/j.ultrasmedbio.2015.04.014]

48   **Herrmann E**, de Lédinghen V, Cassinotto C, Chu WC, Leung VY, Ferraioli G, Filice C, Castera L, Vilgrain V, Ronot M, Dumortier J, Guibal A, Pol S, Trebicka J, Jansen C, Strassburg C, Zheng R, Zheng J, Francque S, Vanwolleghem T, Vonghia L, Manesis EK, Zoumpoulis P, Sporea I, Thiele M, Krag A, Cohen-Bacrie C, Criton A, Gay J, Deffieux T, Friedrich-Rust M. Assessment of biopsy-proven liver fibrosis by two-dimensional shear wave elastography: An individual patient data-based meta-analysis. *Hepatology* 2018; **67**: 260-272 [PMID: 28370257 DOI: 10.1002/hep.29179]

49   **Bota S**, Paternostro R, Etschmaier A, Schwarzer R, Salzl P, Mandorfer M, Kienbacher C, Ferlitsch M, Reiberger T, Trauner M, Peck-Radosavljevic M, Ferlitsch A. Performance of 2-D shear wave elastography in liver fibrosis assessment compared with serologic tests and transient elastography in clinical routine. *Ultrasound Med Biol* 2015; **41**: 2340-2349 [PMID: 26004669 DOI: 10.1016/j.ultrasmedbio.2015.04.013]

50   **Suh CH**, Kim KW, Park SH, Lee SS, Kim HS, Tirumani SH, Lee JG, Pyo J. Shear Wave Elastography as a Quantitative Biomarker of Clinically Significant Portal Hypertension: A Systematic Review and Meta-Analysis. *AJR Am J Roentgenol* 2018; **210**: W185-W195 [PMID: 29570374 DOI: 10.2214/ajr.17.18367]

51   **Kim TY**, Jeong WK, Sohn JH, Kim J, Kim MY, Kim Y. Evaluation of portal hypertension by real-time shear wave elastography in cirrhotic patients. *Liver Int* 2015; **35**: 2416-2424 [PMID: 25875718 DOI: 10.1111/liv.12846]

52   **Jansen C**, Bogs C, Verlinden W, Thiele M, Möller P, Görtzen J, Lehmann J, Vanwolleghem T, Vonghia L, Praktiknjo M, Chang J, Krag A, Strassburg CP, Francque S, Trebicka J. Shear-wave elastography of the liver and spleen identifies clinically significant portal hypertension: A prospective multicentre study. *Liver Int* 2017; **37**: 396-405 [PMID: 27569696 DOI: 10.1111/liv.13243]

53   **Grgurević I**, Bokun T, Mustapić S, Hara T, Trkulja V, Heinzl R, Banić M, Puljiz Ž, Lukšić B, Kujundžić M. Real-time two-dimensional shear wave ultrasound elastography of the liver is a reliable predictor of clinical outcomes and the presence of esophageal varices in patients with compensated liver cirrhosis. *Croat Med J* 2015; **56**: 470-481 [PMID: 26526884]

54   **Kasai Y**, Moriyasu F, Saito K, Hara T, Kobayashi Y, Nakamura I, Sugimoto K. Value of shear wave elastography for predicting hepatocellular carcinoma and esophagogastric varices in patients with chronic liver disease. *J Med Ultrason (2001)* 2015; **42**: 349-355 [PMID: 26576786 DOI: 10.1007/s10396-014-0603-3]

55   **Kim TY**, Kim TY, Kim Y, Lim S, Jeong WK, Sohn JH. Diagnostic Performance of Shear Wave Elastography for Predicting Esophageal Varices in Patients With Compensated Liver Cirrhosis. *J Ultrasound Med* 2016; **35**: 1373-1381 [PMID: 27208198 DOI: 10.7863/ultra.15.07024]

56   **Elkrief L**, Rautou PE, Ronot M, Lambert S, Dioguardi Burgio M, Francoz C, Plessier A, Durand F, Valla D, Lebrec D, Vilgrain V, Castéra L. Prospective comparison of spleen and liver stiffness by using shear-wave and transient elastography for detection of portal hypertension in cirrhosis. *Radiology* 2015; **275**: 589-598 [PMID: 25469784 DOI: 10.1148/radiol.14141210]

57   **Wang QB**, Zhu H, Liu HL, Zhang B. Performance of magnetic resonance elastography and diffusion-weighted imaging for the staging of hepatic fibrosis: A meta-analysis. *Hepatology* 2012; **56**: 239-247 [PMID: 22278368 DOI: 10.1002/hep.25610]

58   **Singh S**, Venkatesh SK, Wang Z, Miller FH, Motosugi U, Low RN, Hassanein T, Asbach P, Godfrey EM, Yin M, Chen J, Keaveny AP, Bridges M, Bohte A, Murad MH, Lomas DJ, Talwalkar JA, Ehman RL. Diagnostic performance of magnetic resonance elastography in staging liver fibrosis: a systematic review and meta-analysis of individual participant data. *Clin Gastroenterol Hepatol* 2015; **13**: 440-451.e6 [PMID: 25305349 DOI: 10.1016/j.cgh.2014.09.046]

59   **Huwart L**, Sempoux C, Vicaut E, Salameh N, Annet L, Danse E, Peeters F, ter Beek LC, Rahier J, Sinkus R, Horsmans Y, Van Beers BE. Magnetic resonance elastography for the noninvasive staging of liver fibrosis. *Gastroenterology* 2008; **135**: 32-40 [PMID: 18471441 DOI: 10.1053/j.gastro.2008.03.076]

60   **Runge JH**, Bohte AE, Verheij J, Terpstra V, Nederveen AJ, van Nieuwkerk KM, de Knegt RJ, Baak BC, Jansen PL, Sinkus R, Stoker J. Comparison of interobserver agreement of magnetic resonance elastography with histopathological staging of liver fibrosis. *Abdom Imaging* 2014; **39**: 283-290 [PMID: 24366108 DOI: 10.1007/s00261-013-0063-z]

61   **Shin SU**, Lee JM, Yu MH, Yoon JH, Han JK, Choi BI, Glaser KJ, Ehman RL. Prediction of esophageal varices in patients with cirrhosis: usefulness of three-dimensional MR elastography with echo-planar imaging technique. *Radiology* 2014; **272**: 143-153 [PMID: 24620910 DOI: 10.1148/radiol.14130916]

62   **Sun HY**, Lee JM, Han JK, Choi BI. Usefulness of MR elastography for predicting esophageal varices in cirrhotic patients. *J Magn Reson Imaging* 2014; **39**: 559-566 [PMID: 24115368 DOI: 10.1002/jmri.24186]

63   **Ronot M**, Lambert S, Elkrief L, Doblas S, Rautou PE, Castera L, Vilgrain V, Sinkus R, Van Beers

BE, Garteiser P. Assessment of portal hypertension and high-risk oesophageal varices with liver and spleen three-dimensional multifrequency MR elastography in liver cirrhosis. *Eur Radiol* 2014; **24**: 1394-1402 [PMID: 24626745 DOI: 10.1007/s00330-014-3124-y]

64   **Vispo E**, Barreiro P, Del Valle J, Maida I, de Ledinghen V, Quereda C, Moreno A, Macías J, Castera L, Pineda JA, Soriano V. Overestimation of liver fibrosis staging using transient elastography in patients with chronic hepatitis C and significant liver inflammation. *Antivir Ther* 2009; **14**: 187-193 [PMID: 19430093]

65   **Arena U**, Vizzutti F, Corti G, Ambu S, Stasi C, Bresci S, Moscarella S, Boddi V, Petrarca A, Laffi G, Marra F, Pinzani M. Acute viral hepatitis increases liver stiffness values measured by transient elastography. *Hepatology* 2008; **47**: 380-384 [PMID: 18095306 DOI: 10.1002/hep.22007]

66   **Hartl J**, Denzer U, Ehlken H, Zenouzi R, Peiseler M, Sebode M, Hübener S, Pannicke N, Weiler-Normann C, Quaas A, Lohse AW, Schramm C. Transient elastography in autoimmune hepatitis: Timing determines the impact of inflammation and fibrosis. *J Hepatol* 2016; **65**: 769-775 [PMID: 27238753 DOI: 10.1016/j.jhep.2016.05.023]

67   **Mueller S**, Millonig G, Sarovska L, Friedrich S, Reimann FM, Pritsch M, Eisele S, Stickel F, Longerich T, Schirmacher P, Seitz HK. Increased liver stiffness in alcoholic liver disease: differentiating fibrosis from steatohepatitis. *World J Gastroenterol* 2010; **16**: 966-972 [PMID: 20180235]

68   **Sagir A**, Erhardt A, Schmitt M, Häussinger D. Transient elastography is unreliable for detection of cirrhosis in patients with acute liver damage. *Hepatology* 2008; **47**: 592-595 [PMID: 18098325 DOI: 10.1002/hep.22056]

69   **Millonig G**, Reimann FM, Friedrich S, Fonouni H, Mehrabi A, Büchler MW, Seitz HK, Mueller S. Extrahepatic cholestasis increases liver stiffness (FibroScan) irrespective of fibrosis. *Hepatology* 2008; **48**: 1718-1723 [PMID: 18836992 DOI: 10.1002/hep.22577]

70   **Lebray P**, Varnous S, Charlotte F, Varaut A, Poynard T, Ratziu V. Liver stiffness is an unreliable marker of liver fibrosis in patients with cardiac insufficiency. *Hepatology* 2008; **48**: 2089 [PMID: 19003902 DOI: 10.1002/hep.22594]

71   **Frulio N**, Laumonier H, Balabaud C, Trillaud H, Bioulac-Sage P. Hepatic congestion plays a role in liver stiffness. *Hepatology* 2009; **50**: 1674-1675 [PMID: 19670411 DOI: 10.1002/hep.23109]

72   **Mukund A**, Pargewar SS, Desai SN, Rajesh S, Sarin SK. Changes in Liver Congestion in Patients with Budd-Chiari Syndrome following Endovascular Interventions: Assessment with Transient Elastography. *J Vasc Interv Radiol* 2017; **28**: 683-687 [PMID: 28153486 DOI: 10.1016/j.jvir.2016.11.091]

73   **Wang HW**, Shi HN, Cheng J, Xie F, Luo YK, Tang J. Real-time shear wave elastography (SWE) assessment of short- and long-term treatment outcome in Budd-Chiari syndrome: A pilot study. *PLoS One* 2018; **13**: e0197550 [PMID: 29847588 DOI: 10.1371/journal.pone.0197550]

74   **Millonig G**, Friedrich S, Adolf S, Fonouni H, Golriz M, Mehrabi A, Stiefel P, Pöschl G, Büchler MW, Seitz HK, Mueller S. Liver stiffness is directly influenced by central venous pressure. *J Hepatol* 2010; **52**: 206-210 [PMID: 20022130 DOI: 10.1016/j.jhep.2009.11.018]

75   **Lemmer A**, VanWagner LB, Ganger D. Assessment of Advanced Liver Fibrosis and the Risk for Hepatic Decompensation in Patients With Congestive Hepatopathy. *Hepatology* 2018; **68**: 1633-1641 [PMID: 29672883 DOI: 10.1002/hep.30048]

76   **Chon YE**, Kim SU, Park JY, Kim DY, Ahn SH, Han KH, Chon CY, Lee S. Dynamics of the liver stiffness value using transient elastography during the perioperative period in patients with valvular heart disease. *PLoS One* 2014; **9**: e92795 [PMID: 24670988 DOI: 10.1371/journal.pone.0092795]

77   **Poterucha JT**, Johnson JN, Qureshi MY, O'Leary PW, Kamath PS, Lennon RJ, Bonnichsen CR, Young PM, Venkatesh SK, Ehman RL, Gupta S, Smyrk TC, Dearani JA, Warnes CA, Cetta F. Magnetic Resonance Elastography: A Novel Technique for the Detection of Hepatic Fibrosis and Hepatocellular Carcinoma After the Fontan Operation. *Mayo Clin Proc* 2015; **90**: 882-894 [PMID: 26059757 DOI: 10.1016/j.mayocp.2015.04.020]

78   **Simón-Talero M**, Roccarina D, Martínez J, Lampichler K, Baiges A, Low G, Llop E, Praktiknjo M, Maurer MH, Zipprich A, Triolo M, Vangrinsven G, Garcia-Martinez R, Dam A, Majumdar A, Picón C, Toth D, Darnell A, Abraldes JG, Lopez M, Kukuk G, Krag A, Bañares R, Laleman W, La Mura V, Ripoll C, Berzigotti A, Trebicka J, Calleja JL, Tandon P, Hernandez-Gea V, Reiberger T, Albillos A, Tsochatzis EA, Augustin S, Genescà J; Baveno VI-SPSS group from the Baveno Cooperation. Association Between Portosystemic Shunts and Increased Complications and Mortality in Patients With Cirrhosis. *Gastroenterology* 2018; **154**: 1694-1705.e4 [PMID: 29360462 DOI: 10.1053/j.gastro.2018.01.028]

79   **Mandorfer M**, Kozbial K, Schwabl P, Freissmuth C, Schwarzer R, Stern R, Chromy D, Stättermayer AF, Reiberger T, Beinhardt S, Sieghart W, Trauner M, Hofer H, Ferlitsch A, Ferenci P, Peck-Radosavljevic M. Sustained virologic response to interferon-free therapies ameliorates HCV-induced portal hypertension. *J Hepatol* 2016; **65**: 692-699 [PMID: 27242316 DOI: 10.1016/j.jhep.2016.05.027]

80   **Vizzutti F**, Arena U, Romanelli RG, Rega L, Foschi M, Colagrande S, Petrarca A, Moscarella S, Belli G, Zignego AL, Marra F, Laffi G, Pinzani M. Liver stiffness measurement predicts severe portal hypertension in patients with HCV-related cirrhosis. *Hepatology* 2007; **45**: 1290-1297 [PMID: 17464971 DOI: 10.1002/hep.21665]

81   **Bureau C**, Metivier S, Peron JM, Selves J, Robic MA, Gourraud PA, Rouquet O, Dupuis E, Alric L, Vinel JP. Transient elastography accurately predicts presence of significant portal hypertension in patients with chronic liver disease. *Aliment Pharmacol Ther* 2008; **27**: 1261-1268 [PMID: 18397389 DOI: 10.1111/j.1365-2036.2008.03701.x]

82   **Castéra L**, Le Bail B, Roudot-Thoraval F, Bernard PH, Foucher J, Merrouche W, Couzigou P, de Lédinghen V. Early detection in routine clinical practice of cirrhosis and oesophageal varices in chronic hepatitis C: comparison of transient elastography (FibroScan) with standard laboratory tests and non-invasive scores. *J Hepatol* 2009; **50**: 59-68 [PMID: 19013661 DOI: 10.1016/j.jhep.2008.08.018]

83   **Stefanescu H**, Grigorescu M, Lupsor M, Maniu A, Crisan D, Procopet B, Feier D, Badea R. A new and simple algorithm for the noninvasive assessment of esophageal varices in cirrhotic patients using serum fibrosis markers and transient elastography. *J Gastrointest Liver Dis* 2011; **20**: 57-64 [PMID: 21451799]

84   **Chen YP**, Zhang Q, Dai L, Liang XE, Peng J, Hou JL. Is transient elastography valuable for high-risk esophageal varices prediction in patients with hepatitis-B-related cirrhosis? *J Gastroenterol Hepatol* 2012; **27**: 533-539 [PMID: 21871027 DOI: 10.1111/j.1440-1746.2011.06889.x]

85   **Wang JH**, Chuah SK, Lu SN, Hung CH, Chen CH, Kee KM, Chang KC, Tai WC, Hu TH. Transient elastography and simple blood markers in the diagnosis of esophageal varices for compensated patients with hepatitis B virus-related cirrhosis. *J Gastroenterol Hepatol* 2012; **27**: 1213-1218 [PMID: 22432969 DOI: 10.1111/j.1440-1746.2012.07132.x]

86   **Sporea I**, Grădinaru-Taşcău O, Bota S, Popescu A, Şirli R, Jurchiş A, Popescu M, Dănilă M. How many measurements are needed for liver stiffness assessment by 2D-Shear Wave Elastography (2D-SWE) and which value should be used: the mean or median? *Med Ultrason* 2013; **15**: 268-272 [PMID: 24286089]

87   **Shi KQ**, Fan YC, Pan ZZ, Lin XF, Liu WY, Chen YP, Zheng MH. Transient elastography: a meta-analysis of diagnostic accuracy in evaluation of portal hypertension in chronic liver disease. *Liver Int* 2013; **33**: 62-71 [PMID: 22973991 DOI: 10.1111/liv.12003]

88   **Hassan EM**, Omran DA, El Beshlawey ML, Abdo M, El Askary A. Can transient elastography, Fib-4, Forns Index, and Lok Score predict esophageal varices in HCV-related cirrhotic patients? *Gastroenterol Hepatol* 2014; **37**: 58-65 [PMID: 24365388 DOI: 10.1016/j.gastrohep.2013.09.008]

89   **Hu Z**, Li Y, Li C, Huang C, Ou Z, Guo J, Luo H, Tang X. Using Ultrasonic Transient Elastometry (FibroScan) to Predict Esophageal Varices in Patients with Viral Liver Cirrhosis. *Ultrasound Med Biol* 2015; **41**: 1530-1537 [PMID: 25817781 DOI: 10.1016/j.ultrasmedbio.2015.02.005]

90   **Li T**, Qu Y, Yang B, Xue Y, Wang L. Evaluation of large esophageal varices in cirrhotic patients by transient elastography: a meta-analysis. *Rev Esp Enferm Dig* 2016; **108**: 464-472 [PMID: 27444047 DOI: 10.17235/reed.2016.3980/2015]

91   **Ye XP**, Ran HT, Cheng J, Zhu YF, Zhang DZ, Zhang P, Zheng YY. Liver and spleen stiffness measured by acoustic radiation force impulse elastography for noninvasive assessment of liver fibrosis and esophageal varices in patients with chronic hepatitis B. *J Ultrasound Med* 2012; **31**: 1245-1253 [PMID: 22837289]

92   **Mori K**, Arai H, Abe T, Takayama H, Toyoda M, Ueno T, Sato K. Spleen stiffness correlates with the presence of ascites but not esophageal varices in chronic hepatitis C patients. *Biomed Res Int* 2013; **2013**: 857862 [PMID: 23984413 DOI: 10.1155/2013/857862]

93   **Morishita N**, Hiramatsu N, Oze T, Harada N, Yamada R, Miyazaki M, Yakushijin T, Miyagi T, Yoshida Y, Tatsumi T, Kanto T, Takehara T. Liver stiffness measurement by acoustic radiation force impulse is useful in predicting the presence of esophageal varices or high-risk esophageal varices among patients with HCV-related cirrhosis. *J Gastroenterol* 2014; **49**: 1175-1182 [PMID: 24005957 DOI: 10.1007/s00535-013-0877-z]

94   **Park Y**, Kim SU, Park SY, Kim BK, Park JY, Kim DY, Ahn SH, Tak WY, Kweon YO, Han KH. A novel model to predict esophageal varices in patients with compensated cirrhosis using acoustic radiation force impulse elastography. *PLoS One* 2015; **10**: e0121009 [PMID: 25826654 DOI: 10.1371/journal.pone.0121009]

95   **Attia D**, Schoenemeier B, Rodt T, Negm AA, Lenzen H, Lankisch TO, Manns M, Gebel M, Potthoff A. Evaluation with Liver and Spleen Stiffness with Acoustic Radiation Force Impulse Quantification Elastography for Diagnosing Clinically Significant Portal Hypertension. *Ultraschall Med* 2015; **36**: 603-610 [PMID: 26565516 DOI: 10.1055/s-0041-107971]

96   **Kim HY**, Jin EH, Kim W, Lee JY, Woo H, Oh S, Seo JY, Oh HS, Chung KH, Jung YJ, Kim D, Kim BG, Lee KL. The Role of Spleen Stiffness in Determining the Severity and Bleeding Risk of Esophageal Varices in Cirrhotic Patients. *Medicine (Baltimore)* 2015; **94**: e1031 [PMID: 26091449 DOI: 10.1097/md.0000000000001031]

97   **Park J**, Kwon H, Cho J, Oh J, Lee S, Han S, Lee SW, Baek Y. Is the spleen stiffness value acquired using acoustic radiation force impulse (ARFI) technology predictive of the presence of esophageal varices in patients with cirrhosis of various etiologies? *Med Ultrason* 2016; **18**: 11-17 [PMID: 26962548 DOI: 10.11152/mu.2013.2066.181.sff]

98   **Wiles R**, Patanwala I, Hankinson B, Healey P, Farrell C, Griffin C, Bonnett L, Richardson P. Can acoustic radiation force imaging of the liver and spleen predict the presence of gastroesophageal varices? *Clin Radiol* 2018; **73**: 1046-1051 [PMID: 30245070 DOI: 10.1016/j.crad.2018.07.199]

99   **Cassinotto C**, Charrie A, Mouries A, Lapuyade B, Hiriart JB, Vergniol J, Gaye D, Hocquelet A, Charbonnier M, Foucher J, Laurent F, Chermak F, Montaudon M, de Ledinghen V. Liver and spleen elastography using supersonic shear imaging for the non-invasive diagnosis of cirrhosis severity and oesophageal varices. *Dig Liver Dis* 2015; **47**: 695-701 [PMID: 25959234 DOI: 10.1016/j.dld.2015.04.008]

100   **Matsui N**, Imajo K, Yoneda M, Kessoku T, Honda Y, Ogawa Y, Tomeno W, Fujisawa N, Misumi T, Kazumi K, Saito S, Nakajima A. Magnetic resonance elastography increases usefulness and safety of non-invasive screening for esophageal varices. *J Gastroenterol Hepatol* 2018; **33**: 2022-2028 [PMID: 29869419 DOI: 10.1111/jgh.14298]

101   **Bookwalter CA**, Venkatesh SK, Eaton JE, Smyrk TD, Ehman RL. MR elastography in primary sclerosing cholangitis: correlating liver stiffness with bile duct strictures and parenchymal changes. *Abdom Radiol (NY)* 2018; **43**: 3260-3270 [PMID: 29626258 DOI: 10.1007/s00261-018-1590-4]

102   **Kim YS**, Song JS, Kannengiesser S, Seo SY. Comparison of spin-echo echoplanar imaging and gradient recalled echo-based MR elastography at 3 Tesla with and without gadoxetic acid administration. *Eur Radiol* 2017; **27**: 4120-4128 [PMID: 28289936 DOI: 10.1007/s00330-017-4781-4]

Basic Study

NKX6.3 protects against gastric mucosal atrophy by downregulating β-amyloid production

Jung Hwan Yoon, Yeon Soo Lee, Olga Kim, Hassan Ashktorab, Duane T Smoot, Suk Woo Nam, Won Sang Park

ORCID number: Jung Hwan Yoon (0000-0001-7770-2965); Yeon Soo Lee (0000-0002-1653-6315); Olga Kim (0000-0001-5110-2523); Hassan Ashktorab (0000-0002-4048-4666); Duane T Smoot (0000-0002-8416-7419); Suk Woo Nam (0000-0001-5767-8291); Won Sang Park (0000-0002-9090-0584).

Jung Hwan Yoon, Olga Kim, Suk Woo Nam, Won Sang Park, Department of Pathology, College of Medicine, The Catholic University of Korea, Seoul 06591, South Korea

Jung Hwan Yoon, Suk Woo Nam, Won Sang Park, Functional RNomics Research Center, College of Medicine, The Catholic University of Korea, Seoul 06591, South Korea

Yeon Soo Lee, Department of Hospital Pathology, College of Medicine, The Catholic University of Korea, Seoul 06591, South Korea

Hassan Ashktorab, Department of Medicine, Howard University, Washington, DC 20060, United States

Duane T Smoot, Department of Medicine, Meharry Medical Center, Nashville, TN 37208, United States

Corresponding author: Won Sang Park, MD, PhD, Doctor, Professor, Department of Pathology, College of Medicine, The Catholic University of Korea, 222 Banpo-daero, Seocho-gu, Seoul 06591, South Korea. wonsang@catholic.ac.kr
Telephone: +82-2-22587310
Fax: +82-2-5376586

Abstract

BACKGROUND
Atrophic gastritis is characterized by loss of appropriate glands and reduction in gastric secretory function due to chronic inflammatory processes in gastric mucosa. Moreover, atrophic gastritis is considered as a precancerous condition of gastric cancer. However, little is known about the molecular mechanism underlying gastric mucosal atrophy and its contribution to gastric carcinogenesis. Thus, we hypothesized that transcription factor NKX6.3 might be involved in maintaining gastric epithelial homeostasis by regulating amyloid β (Aβ) production.

AIM
To determine whether NKX6.3 might protect against gastric mucosal atrophy by regulating Aβ production.

METHODS
We identified NKX6.3 depletion induced cell death by cell count and Western blot assay. Production and mechanism of Aβ oligomer were analyzed by enzyme-linked immunosorbent assay, Western blot, immunoprecipitation, real-time

quantitative polymerase chain reaction and immunofluorescence analysis. We further validated the correlation between expression of NKX6.3, *Helicobacter pylori* CagA, Aβ oligomer, apolipoprotein E (ApoE), and β-secretase 1 (Bace1) in 55 gastric mucosae.

RESULTS

NKX6.3 depletion increased both adherent and floating cell populations in HFE-145 cells. Expression levels of cleaved caspase-3, -9, and poly ADP ribose polymerase were elevated in floating HFE-145$^{shNKX6.3}$ cells. NKX6.3 depletion produced Aβ peptide oligomers, and increased expression of ApoE, amyloid precursor protein, Aβ, Bace1, low-density lipoprotein receptor, nicastrin, high mobility group box1, and receptor for advanced glycosylation end product proteins. In immunoprecipitation assay, γ-secretase complex was stably formed only in HFE-145$^{shNKX6.3}$ cells. In gastric mucosae with atrophy, expression of Aβ peptide oligomer, *ApoE*, and *Bace1* was detected and inversely correlated with NKX6.3 expression. Treatment with recombinant Aβ 1-42 produced Aβ oligomeric forms and decreased cell viability in HFE-145$^{shNKX6.3}$ cells. Additionally, NKX6.3 depletion increased expression of inflammatory cytokines and cyclooxygenase-2.

CONCLUSION

NKX6.3 inhibits gastric mucosal atrophy by regulating Aβ accumulation and inflammatory reaction in gastric epithelial cells.

Key words: NKX6.3; Gastric mucosa; Atrophy; Amyloid β; Gastrokine 1

Core tip: In human gastric epithelial cells, NKX6.3 depletion induced production of amyloid β (Aβ) oligomers, and also increased expression of apolipoprotein E (ApoE), Aβ, β-secretase 1 (Bace1), nicastrin, and receptor for advanced glycosylation end product proteins. Moreover, NKX6.3 depletion leads to stably formed of γ-secretase complex and binding to Bace1 protein. In gastric mucosae with atrophy, expression of Aβ oligomer, ApoE, and Bace1 was detected and inversely correlated with NKX6.3 expression. Additionally, treatment with recombinant Aβ 1-42 produced oligomeric forms of Aβ and significantly decreased cell viability in NKX6.3 depleting cells. These observations provide evidences that NKX6.3 can inhibit gastric mucosal atrophy by regulating Aβ peptide accumulation and inflammatory reaction in gastric epithelial cells.

INTRODUCTION

Atrophic gastritis is characterized by loss of appropriate glands and reduction in gastric secretory function due to chronic inflammatory processes in gastric mucosa[1]. In South Korea, the prevalence of atrophic gastritis is relatively high. It is 59.4% in people older than 60 years[2], and the crude incidence for cancer is 1.7% in atrophic gastritis[3]. It has been widely accepted that chronic inflammation of the stomach can initiate histopathologic progression from chronic gastritis to gastric atrophy, intestinal metaplasia, dysplasia and finally gastric cancer[4-6]. Thus, atrophic gastritis is considered as a precancerous condition of gastric cancer. However, little is known about the molecular mechanism underlying gastric mucosal atrophy and its contribution to gastric carcinogenesis.

Amyloid β peptide (Aβ) plays a key role in pathogenesis of Alzheimer's disease. It is a 4-kDa metalloprotein with 39- to 43-amino acids derived from proteolytic cleavage of amyloid precursor protein (APP) by β- and γ-secretase[7]. In contrast, α-secretase ADAM10, a metalloprotease, cleaves APP within the Aβ domain, thus

preventing Aβ generation[8]. It has been reported that β-site amyloid precursor protein cleaving enzyme (BACE) is a novel transmembrane aspartic protease that exhibits properties of β-secretase[9]. γ-secretase is a high molecular weight complex minimally composed of four components: presenilin (PS), nicastrin (NCT), anterior pharynx-defective-1 (APH-1), and presenilin enhancer-2 (PEN2)[10-13]. BACE1 cleaves APP not processed by α-secretase to generate carboxy-terminal fragments of 99 amino acids. This is further processed by γ-secretase to Aβ40 and Aβ42 that are transported to the cell surface which they are secreted *via* recycling vesicle[14]. In addition, receptor for advanced glycation end products (RAGE) is one of receptors that medicate Aβ effects on neurons and microglia[15] and is implicated in a wide spectrum of pathological responses, including inflammation and cancer[16]. Apolipoprotein E (ApoE) increases oligomerization of Aβ peptide in an isoform-dependent manner[17] and major ApoE receptors belong to low-density lipoprotein (LDL) receptor family[18]. It has been proposed that accumulated Aβ proteins can generate oligomers and induce synaptic dysfunction and death of neurons[19,20].

NKX family of homeodomain transcription factors are involved in a variety of developmental processes, and the NKX6.3 member is expressed in epithelium of the most distal stomach[21,22]. Previously, we have reported that NKX6.3 functions as a master regulator of gastric differentiation by modulating SOX2 and CDX2 expression and as a tumor suppressor by inhibiting cell proliferation and inducing apoptosis[23,24]. Interestingly, gastric tumor suppressor gastrokine 1 (GKN1), a downstream target of NKX6.3, interacts with APP and inhibits polymerization of Aβ[25,26]. Thus, we hypothesized that transcription factor NKX6.3 might be involved in maintaining gastric epithelial homeostasis by regulating Aβ production. Here, we provide the first evidence that NKX6.3 may protect gastric mucosal epithelial cells from atrophy by inhibiting Aβ production and polymerization.

MATERIALS AND METHODS

Samples
A total of 55 patients with sporadic gastric cancer who underwent a gastrectomy at Chonnam National University Hwasun Hospital were included. Fresh-frozen non-neoplastic gastric mucosae remote (≥ 5 cm) from the tumor were used in this study. In addition, gastric mucosal tissues adjacent to each frozen specimen were fixed in formalin and stained with hematoxylin-eosin. Patients with a history of familial gastric cancer were excluded. Two expert gastrointestinal pathologists independently assessed the histologic specimens according to the updated Sydney system and the reached a consensus for all specimens[27]. Atrophy was defined as loss of appropriate glands and a periodic acid Schiff staining was used to identify intestinal metaplasia. Gastric mucosae with atrophy and intestinal metaplasia were considered as atrophic gastritis. The presence of *Helicobacter pylori* (*H. pylori*) CagA was determined by Western blot analysis[28]. This study was approved by the Institutional Review Board (IRB) of The Catholic University of Korea, College of Medicine (approval number: MC16SISI0130).

Cell culture and transfection of NKX6.3
HFE-145 immortalized gastric epithelial cell line expressing NKX6.3 was cultured at 37 °C and 5% CO_2 in RPMI-1640 medium supplemented with 10% heat-inactivated fetal bovine serum. shNKX6.3 was cloned into pSilencer 3.1 H1-neo (Invitrogen, Carlsbad, CA, United States). We generated stable shNKX6.3 transfectants of HFE-145 cells (HFE-145[shNKX6.3] cells), stably silencing human NKX6.3 expression, as well as shControl transfectants of HFE-145[shCtrl] cells as described previously[24]. Expression levels of NKX6.3 in HFE-145[shCtrl] and HFE-145[shNKX6.3] cells were confirmed by Western blot analysis. The *CagA* gene of *H. pylori* was cloned into a pSP65SRalpha vector containing a hemagglutinin (HA) tag, and the HFE-145 cells were transfected with *CagA* gene, as described previously[24]. The *CagA* construct was kindly provided by Dr. Hatakeyama (Tokyo University, Tokyo, Japan).

Cell count of floating and adherent cells
HFE-145[shCtrl] and HFE-145[shNKX6.3] cells in complete medium were seeded onto 12-well plates at a density of 1×10^4 cells per well. Floating and adherent cells were harvested after 48 h of culture and counted using a hemocytometer.

Cell viability and proliferation assay
For cell viability analysis, MTT assay were performed for HFE-145 immortalized gastric epithelial cells at 24, 48, 72, and 96 h after treatment with recombinant Aβ (1 μg/mL, rAβ, Sigma, St. Louis, MO, United States). Absorbance at 540 nm was

measured using a spectrophotometer and cell viability was expressed relative to non-treated cells.

Measurement of caspase 3/7 activity

To analyze the effect of NKX6.3 on apoptosis, caspase-3 and -7 activities were examined using an Apo-One Homogeneous caspase 3/7 assay kit (Promega Corporation, Madison, WI, United States) as described previously[28].

Measurement of NKX6.3, ApoE, Bace1, and inflammatory cytokine expression

Expression levels of *NKX6.3*, *ApoE*, and *Bace1* mRNA transcripts were examined in 55 gastric mucosal tissues by real-time RT-PCR. In addition, to investigate whether ablation of NKX6.3 might contributed to inflammatory cytokine expression, the expression of *IL-1β*, *IL-6*, *IL-8*, and *COX-2* mRNAs in HFE-145[shCtrl] and HFE-145[shNKX6.3] cells were analyzed by real-time RT-PCR. The effects of *ApoE* silencing with *siApoE* on expression levels of inflammatory cytokines were also examined. After quantification of total RNA extracted from 55 frozen gastric mucosal tissues, HFE-145[shCtrl], and HFE-145[shNKX6.3] cells, RT-PCR was carried out using SYBR Green Q-PCR Master Mix (Bio-Rad, Hercules, CA, United States) according to the manufacturer's protocol. The mRNA expression of these genes was quantified by quantitative real-time reverse transcription PCR (QRT-PCR) and normalized to mRNA level of *β-actin*. Primer sequences are presented in Supplementary Table 1. Data are reported as relative quantities according to an internal calibrator using a $2^{-\Delta\Delta CT}$ method[23]. The standard curve method was used for quantification of the relative amounts of gene expression products. This method provides unit-less normalized expression values that can be used for direct comparison of the relative amount of RNA in different samples.

Immunoblot and immunofluorescent studies

Primary anti-Aβ antibody (Merck-millipore, Darmstadt, Germany), anti-BACE1 (Abcam, Cambridge, United Kingdom) and secondary anti-alexa-488 conjugated goat anti-mouse IgG antibody (Invitrogen, CA, United States) were used to visualize immunoreactivity. The specificity of reactions was tested by incubation with non-immune mouse serum (Invitrogen).

We examined expression levels of NKX6.3 and Aβ-related genes in cell lysates by Western blot analysis. We separated equal amounts of cell lysates by 12.5% SDS-PAGE and transferred them to Hybond-polyvinylidene difluoride transfer membranes (Amersham Biosciences, NJ, United States). After blocking with 0.5% skim milk, we blotted the membranes with the primary antibodies and then incubated them with horseradish peroxidase-conjugated secondary antibodies. We detected the protein bands using westernsure ECL substrate (LI-COR Biosciences, NE, United States) and visualized the intensity of bands using a LAS 4000 image analyzer (Fuji Film, Japan). The antibody list is described in Supplementary Table 2.

Chromatin immunoprecipitation assay

For assessing the NKX6.3 binding activity to the promoter regions of *ApoE* and *Bace1*, chromatin immunoprecipitation (ChIP) assays were performed using the Thermo Scientific Pierce Agarose ChIP kit (Thermo Scientific Pierce, Rockford, IL, United States), as previously described[24]. Briefly, HFE-145[shCtrl] and HFE-145[shNKX6.3] cells were cultured in a 10-cm dish for 4 d. The cells were fixed with 1% formaldehyde in PBS for 10 min, washed twice with ice-cold PBS and re-suspended in lysis buffer. Nuclei were recovered by centrifugation and MNase digestion was carried out at 37 °C for 15 min. Nuclei were lysed and the extracts were immunoprecipitated with 4 μg of antibody against NKX6.3 at 4 °C overnight. Normal rabbit IgG was used as a negative control. Protein-bound DNA was recovered using affinity chromatography purification columns according to the manufacturer's protocol (Thermo Scientific), and 5 μL of lysed nuclei were also purified under the same procedure and used as input. DNA amplification was performed by PCR using primers for the *ApoE* and *Bace1* promoters described in Supplementary Table 1. Amplification products were separated on a 2% agarose gel.

Aβ ELISAs

ELISAs for measuring Aβ42 peptide were performed using commercial kits (Invitrogen) following the manufacturer's instructions. Briefly, Aβ42 ELISAs were performed using 6E10 as a capture antibody and anti-Aβ42 HRP-conjugated antibodies (Covance, Dedham, MA, United States) as detection antibodies. Synthetic Aβ42 were used to generate a standard curve for each experiment. The plates were developed using TMB substrate kit (Pierce, Rockford, IL, United States) and the reaction was stopped by addition of equal volume of 1 mol/L HCl. The results were read using a Spectramax colorimetric plate reader (Molecular Devices, Sunnyvale,

CA, United States).

Immunoprecipitation

For coimmunoprecipitation experiments, cells were harvested in PBS, centrifuged at 800 g for 10 min, and lysed in 125 mmol/L NaCl, 50 mmol/L Hepes, pH 7.4 (supplemented with 1% Triton X-100 or CHAPS and Complete protease inhibitors) for 30 min at 4 °C. After centrifugation at 16000 g for 15 min, cleared cell extracts were incubated overnight at 4 °C with protein A/G-agarose (Santa Cruz Biotechnology, Santa Cruz, CA, United States) and anti-PSN1 or anti-rabbit IgG beads. Immunoprecipitated proteins were resolved on 12% SDS-polyacrylamide gels and transferred to PVDF membranes (Bio-Rad, Richmond, CA, United States). The membranes were blocked for 1 h in PBS containing 0.1% Tween 20 (PBS-T) and 5% non-fat dry milk (Sigma) and reacted with antibodies against PSN1, each diluted 1:1000. The membranes were washed with PBS-T, then incubated for 1 h at room temperature with horseradish peroxidase-conjugated anti-rabbit IgG antibody (Sigma), diluted 1:5000, and developed with westernsure ECL substrate (LI-COR Biosciences). Immunoreactive bands were identified by co-migration of prestained protein size markers (Fermentas, Glen Burnie, MD, United States). To confirm equivalent protein loading and transfer, the blots were stripped and re-probed for GAPDH (Santa Cruz Biotechnology).

Statistical analyses

Pearson and Student's *t*-tests were used to analyze the correlation between expression of NKX6.3, GKN1, Aβ peptide oligomer, ApoE, and BACE1. We performed all experiments in duplicate to verify the reproducibility of the findings. Data are expressed as means ± SD from two independent experiments. A *P*-value < 0.05 was considered to be the limit of statistical significance.

RESULTS

Loss of NKX6.3 expression induces both cell death and proliferation

During cell culture, NKX6.3 depletion in HFE-145[shNKX6.3] cells increased populations of both adherent and floating cells compared to HFE-145[shCtrl] cells (Figure 1A). Since previously we have reported that NKX6.3 depletion increases cell population of HFE-145 cells[24], here we focused on the increase of floating HFE-145[shNKX6.3] cells. When we examined the effects of NKX6.3 depletion on cell death, caspase 3/7 activity was significantly increased only in floating HFE-145[shNKX6.3] cells (Figure 1B). Interestingly, NKX6.3 depletion did not affect expression of apoptosis markers including caspase-3, -9, and PARP in attached cells. However, expression levels of cleaved forms of caspase-3, -9, and PARP were increased in floating HFE-145[shNKX6.3] cells compared with those in floating HFE-145[shCtrl] cells (Figure 1C). Thus, it is likely that NKX6.3 may inhibit both cell proliferation and apoptotic cell death in gastric epithelial cells.

NKX6.3 inhibits Aβ accumulation by regulating ApoE, β-, and γ-secretase

Next, we examined whether NKX6.3 was involved in Aβ production in HFE-145 cells. Interestingly, NKX6.3 depletion markedly induced expression of ApoE, APP, Aβ peptide, BACE1, LDLR, NCT, high-mobility group box 1 (HMGB1), and RAGE proteins but decreased expression of presenilin1 (PSN1) protein in HFE-145 cells (Figure 2A). There are three distinct pools of Aβ species: monomers, soluble oligomers, and insoluble fibrils[29]. Interestingly, HFE-145[shCtrl] cells only expressed Aβ monomer, while NKX6.3 depleted HFE-145[shNKX6.3] cells induced production of Aβ oligomers and increased expression of Aβ monomer (Figure 2A). When we examined the effect of NKX6.3 on γ-secretase assembly by immunoprecipitation assay, γ-secretase complex, including PSN1, PSN2, NCT, and PEN2 was stably formed and binding to BACE1 protein only in NKX6.3 depleted HFE-145[shNKX6.3] cells (Figure 2B). In immunofluorescence analysis, strong expression of Aβ peptides were detected in the cytoplasm of NKX6.3 depleted HFE-145[shNKX6.3] cells (Figure 2C). Notably, aggregated Aβ peptide was not detected in HFE-145[shCtrl] cells expressing NKX6.3 whereas NKX6.3 depletion significantly increased concentrations of the aggregated Aβ peptide in both cell lysate and culture media (Figure 2D). In NKX6.3 depleted HFE-145[shNKX6.3] cells, mRNA expression of *ApoE* and *Bace1* genes were significantly increased (Figure 2E) while binding capacity of NKX6.3 to promoter regions of *ApoE* and *Bace1* genes was dramatically decreased in ChIP assay (Figure 2F), suggesting that NKX6.3 might be a transcriptional repressor of *ApoE* and *Bace1* genes. When we treated HFE-145[shCtrl] and HFE-145[shNKX6.3] cells with recombinant Aβ 1-42 (rAβ 1-42), ApoE and oligomeric forms of Aβ were detected in NKX6.3 depleted HFE-145[shNKX6.3] cells (Figure 2G). Taken together, these results suggest that NKX6.3 may inhibit accumulation and
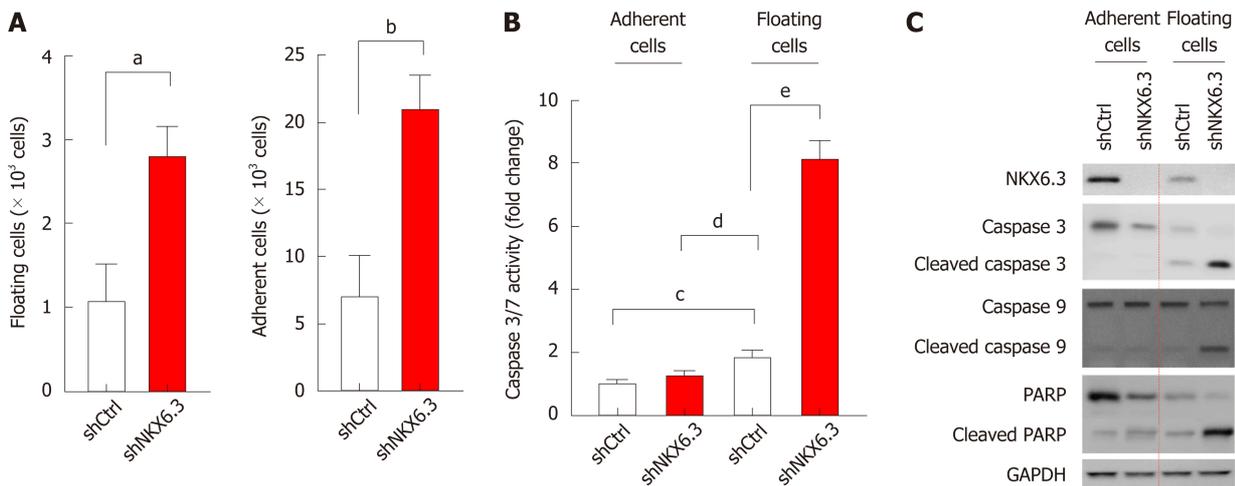
Figure 1 NKX6.3 inhibits both cell proliferation and apoptotic cell death in gastric epithelial cells. A: NKX6.3 depletion in HFE-145[shNKX6.3] cells increased both adherent and floating cell populations. Shown are the means ± SEM from three experiments. Superscript letter represents significant difference ([a]*P* < 0.005). B: Caspase 3/7 activity was significantly increased in floating HFE-145[shNKX6.3] cells. Shown are the means ± SEM from three experiments. Superscript letter significant difference ([b]*P* < 0.0001). C: In Western blot analysis, expression of cleaved forms of caspase-3, -9, and poly ADP ribose polymerase (PARP) was increased in floating HFE-145[shNKX6.3] cells.

oligomerization of Aβ peptide in gastric epithelial cells.

Aβ oligomerization is strongly associated with gastric mucosal atrophy

Histologically, gastric mucosal atrophy was found in 18 (32.7%) of 55 gastric mucosae. In Western blot analysis, Aβ oligomers, including tetramer, were mainly expressed in gastric mucosae with atrophy. In addition, expression levels of ApoE, Bace1, and cleaved form of caspase-3 were increased in atrophic gastric mucosae along with reduced NKX6.3 expression (Figure 3A). To further confirm the effect of NKX6.3 on ApoE and Bace1 expression, we compared expression levels of *NKX6.3* with *ApoE* and *Bace1* mRNA expression levels in 55 non-neoplastic gastric mucosae by real-time RT-PCR. Previously, NKX6.3 expression has been found to be significantly reduced in the cases with atrophy[23]. As expected, mRNA expression levels of *ApoE* and *Bace1* were significantly higher in gastric mucosae with atrophy (Figure 3B), showing inverse correlations with *NKX6.3* expression (*P* = 0.0001) (Figure 3C). In addition, reduced expression of NKX6.3 protein, expression of Aβ oligomer, Bace1, ApoE, and cleaved caspase-3 proteins, and CagA were significantly associated with gastric mucosal atrophy. The expression of Aβ oligomer was positively correlated with expression of Bace1, ApoE, cleaved caspase-3, and CagA (Figure 3D). We also measured aggregated Aβ peptide concentrations in 55 gastric mucosae by ELISA and found significantly higher Aβ peptide concentrations in gastric mucosae with atrophy (1.20 ± 0.60 μg/mL) than those in gastric mucosae without atrophy (0.09 ± 0.09 μg/mL; Figure 3E). When we transfected HFE-145 cells with CagA, ectopic expression of CagA reduced the expression of NKX6.3 but increased Aβ oligomerization and expression of ApoE, Bace1, and cleaved caspase-3 (Figure 3F). Next, we examined Aβ oligomer expression in 6 non-neoplastic gastric mucosae with atrophy (*n* = 3) and without atrophy (*n* = 3) using specific antibody against Aβ oligomer by immunofluorescent assay. Consistent with above result, expression of Aβ oligomer was detected in gastric mucosae with atrophy in immunofluorescent assay (Figure 3G). Interestingly, Aβ oligomer was present only in gastric mucosal epithelial cells, but not in extracellular matrix including inflammatory cells (Figure 3G).

Aβ induces cell death in gastric epithelial cells

Next, to investigate whether oligomeric forms of Aβ were associated with gastric mucosal atrophy, we analyzed cell viability of gastric epithelial cells after treatment with rAβ 1-42. Because we found 1.18 ± 0.57 μg/mL of aggregated Aβ peptide in gastric mucosae with atrophy (Figure 3), we treated HFE-145[shCtrl] and HFE-145[shNKX6.3] cells with 1 μg/mL of rAβ for 4 d. As shown in Figure 4A, treatment with rAβ 1-42 produced oligomeric forms of Aβ only in HFE-145[shNKX6.3] cells, but not in HFE-145[shCtrl] cells (Figure 4A). In addition, recombinant GKN1 (rGKN1) partially reduced expression of Aβ oligomers (Figure 4A). In HFE-145[shNKX6.3] cells, treatment with rAβ 1-42 significantly reduced cell viability but markedly increased floating cell population in HFE-145[shNKX6.3] cells (Figure 4B and C). Notably, rGKN1 partially revoked the effect of rAβ on cell viability (Figure 4D). However, treatment with rAβ 1-42 did not affect
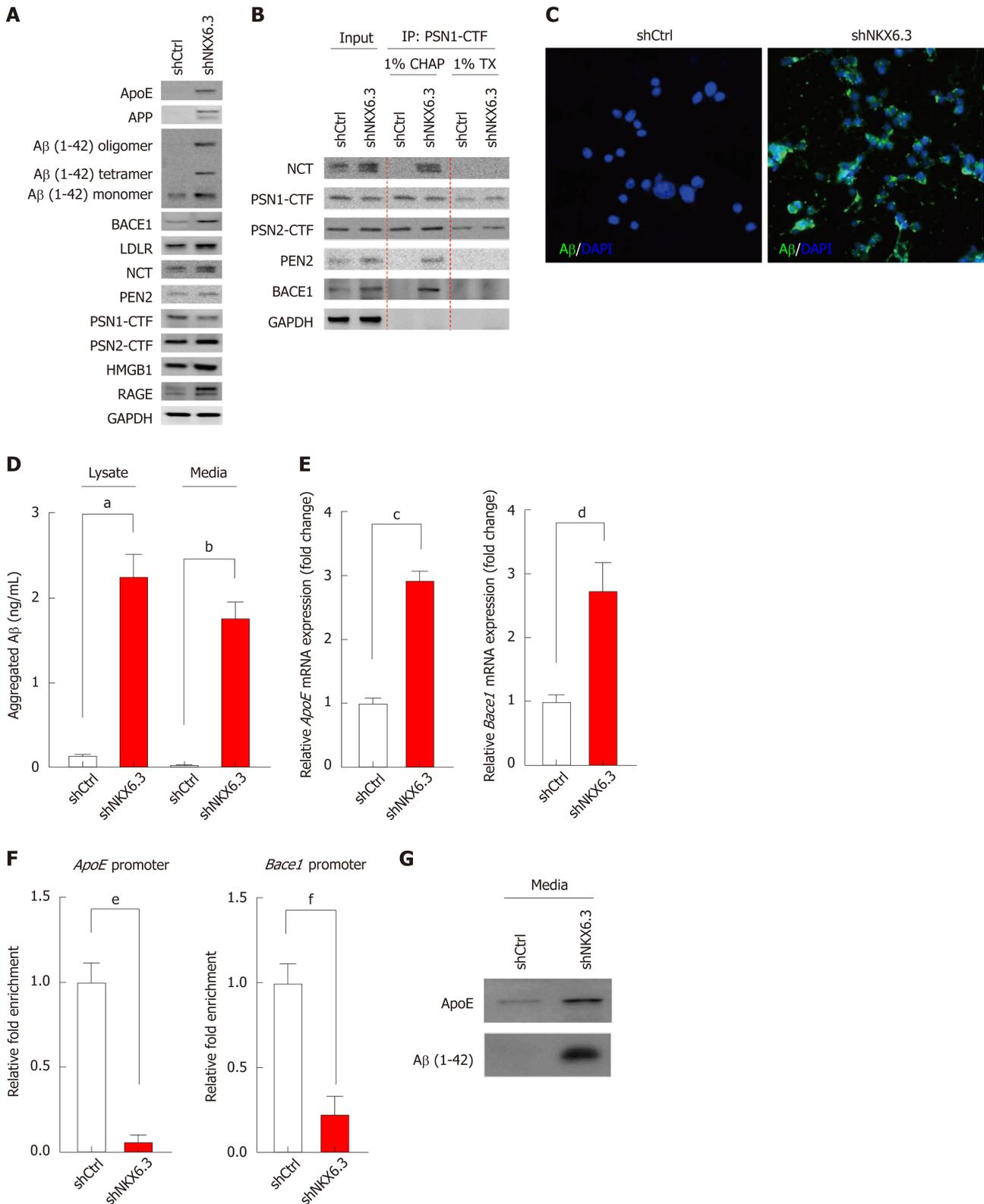
Figure 2 NKX6.3 inhibits amyloid β accumulation by regulating apolipoprotein E, β-, and γ-secretase. A: Western blot analysis showing increased expression of apolipoprotein E (ApoE), amyloid precursor protein (APP), amyloid β (Aβ), β-secretase 1 (Bace1), low-density lipoprotein receptor (LDLR), nicastrin (NCT), high mobility group box1 (HMGB1), and receptor for advanced glycosylation end product (RAGE) proteins but decreased expression of presenilin 1 (PSN1)- C-terminal (CTF) protein in NKX6.3 depleted HFE-145 cells. Interestingly, HFE-145[shCtrl] cells expressed only Aβ monomer whereas NKX6.3 depleted HFE-145[shNKX6.3] cells induced production of oligomers of Aβ and increased expression of Aβ monomer. B: In immunoprecipitation assay, γ-secretase complex including PSN1-CTF and 2-CTF, NCT, and presenilin enhancer 2 (PEN2) was stably formed, binding to Bace1 protein only in NKX6.3 depleted HFE-145[shNKX6.3] cells. C: Immunofluorescence images showing strong expression of Aβ protein in the cytoplasm of NKX6.3 depleted HFE-145[shNKX6.3] cells. D: In Aβ42 enzyme-linked immunosorbent assay, NKX6.3 depletion significantly increased concentrations of aggregated Aβ in both cell lysate and culture media. Shown are the means ± SEM from three experiments. Superscript letter significant difference ([a]$P < 0.0001$). E: Increased mRNA expression of *ApoE* and *Bace1* genes was detected in NKX6.3 depleted HFE-145[shNKX6.3] cells. Shown are the means ± SEM from three experiments. Superscript letter represents significant difference ([b]$P < 0.005$ and [c]$P < 0.0001$). F: In chromatin immunoprecipitation assay, the binding capacity of NKX6.3 to promoter regions of *ApoE* and *Bace1* genes was dramatically decreased. Shown are the means ± SEM

from three experiments. Superscript letter represents significant difference ($^dP < 0.005$ and $^eP < 0.0001$). G: When we treated HFE-145[shCtrl] and HFE-145[shNKX6.3] cells with Aβ 1-42 recombinant protein (rAβ 1-42), expression levels of ApoE and oligomeric forms of Aβ were makedly increased in NKX6.3 depleted HFE-145[shNKX6.3] cells. CHAP: Chaps buffer; TX: Triton-100; ApoE: Apolipoprotein E; APP: Amyloid precursor protein; Aβ: Amyloid β; Bace1: β-secretase 1; LDLR: Low-density lipoprotein receptor; NCT: Nicastrin; HMGB1: High mobility group box1; RAGE: Receptor for advanced glycosylation end product; PSN1: Presenilin 1; CTF: C-terminal; PEN2: Presenilin enhancer 2; rAβ 1-42: Aβ 1-42 recombinant protein.

cell viability of HFE-145[shCtrl] cells (Figure 4B). These results suggest that Aβ oligomerization prompted by NKX6.3 depletion may induce cell death in gastric epithelial cells.

NKX6.3 depletion induces inflammatory cytokine expression in gastric epithelial cells

It is known that Aβ accumulation in human nerve cells leads to synthesis of proinflammatory cytokines and activation of inflammatory pathways[30]. Thus, we further examined the expression of inflammatory markers including IL-1β, -6, -8, and COX-2 by real-time RT-PCR. Expectedly, NKX6.3 depletion in HFE-145[shNKX6.3] cells dramatically increased the expression of these inflammatory cytokines and COX-2 (Figure 5A). In HFE-145[shNKX6.3] cells, silencing of ApoE with *siApoE* markedly inhibited oligomerization and aggregation of Aβ peptide. It also suppressed expression of NF-κB p-p65 and inflammatory cytokines (Figure 5B and C). This suggests that ApoE plays an important role in Aβ oligomerization and synthesis of inflammatory cytokines.

DISCUSSION

Inflammatory disorders have been well recognized as key risk factor for many types of cancers. Stages of precancerous cascade for gastric adenocarcinoma are a series of histologically discernible changes in gastric mucosa with the following sequence: non-atrophic gastritis, multifocal atrophic gastritis, intestinal metaplasia (IM), and dysplasia[31]. *H. pylori* infection has been identified as the causative agent of chronic gastric inflammation, such as atrophic gastritis and metaplastic gastritis[32]. However, molecular mechanisms underlying gastric mucosal atrophy still remain to be determined for the prevention and early diagnosis of gastric cancer. Since intracellular generation of the Aβ protein is known to lead to neuronal death[19] while NKX6.3 expression is confined to the gut and caudal hindbrain[33]. Thus, we hypothesized that NKX6.3 could protect gastric mucosa from atrophic changes by inhibiting Aβ accumulation.

We first examined whether NKX6.3 was involved in proliferation and death of gastric mucosa. As shown in Figure 1A, NKX6.3 depletion in HFE-145[shNKX6.3] cells significantly increased proportions of both adherent and floating cells. In addition, increased caspase 3/7 activity was found in floating HFE-145[shNKX6.3] cells (Figure 1B). In Western blot analysis, NKX6.3 did not affect expression of apoptosis markers, including PARP, caspase-3, or caspase-9 in adherent HFE-145[shNKX6.3] cells, but NKX6.3 depletion induced expression of these apoptotic markers (Figure 1C), providing an intriguing scenario where NKX6.3 might be a key regulator of gastric mucosal homeostasis by inhibiting both cell proliferation and death. Here, we focused on the inhibitory activity of NKX6.3 on death of gastric mucosal epithelial cells.

In general, regulation of proteolysis plays a crucial role in many processes of development, cell proliferation and death. Dysregulation of proteolytic system can destroy cellular homeostasis by accumulation of specific proteins, thus contributing to disease pathogenesis. Amyloid aggregates have been found to be associated with disruption of several cellular functions, including mitochondrial activity[34], oxidative stress[35,36], and apoptosis[37]. Aβ acts as a neurotoxin that directly induces oxidative stress whereas RAGE mediates Aβ-induced oxidative stress and inflammatory response. Increased expression of RAGE has been implicated in the pathogenesis of neuronal dysfunction and death[15]. In the present study, we hypothesized that Aβ peptide accumulation caused by NKX6.3 depletion could induce gastric epithelial cell death which subsequently could contribute to gastric mucosal atrophy. Interestingly, depletion of NKX6.3 induced Aβ peptide accumulation in the cytoplasm of HFE-145[shNKX6.3] cells and increased expression of Aβ in cell lysate and culture medium (Figure 2). These results suggest that NKX6.3 may inhibit accumulation and oligomerization of Aβ peptide in gastric epithelial cells.

Cleavage of APP by Bace1 produces a large soluble ectodomain form and a membrane-bound 99-amino acid C-terminal fragment. Subsequently, the γ-secretase
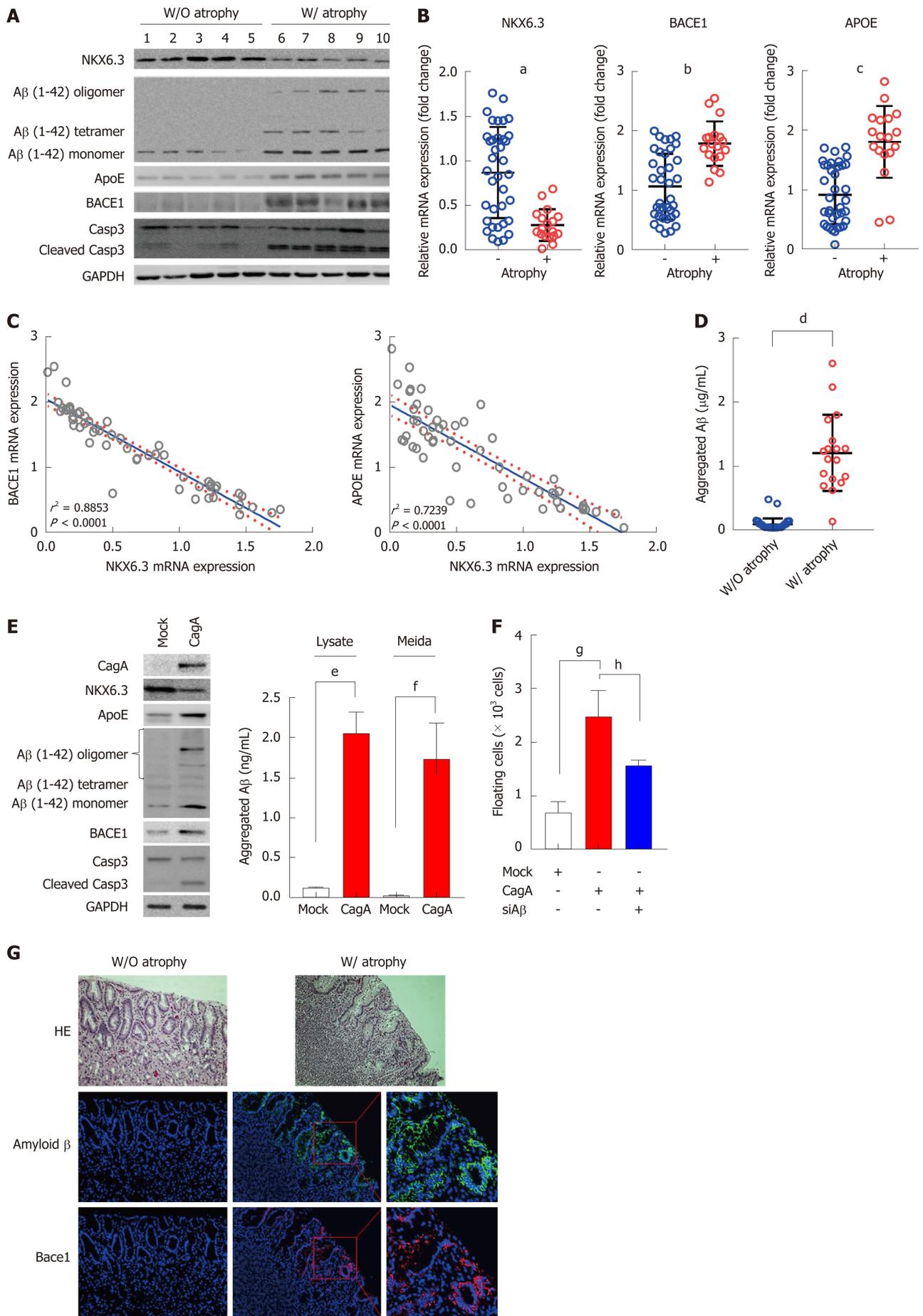
Figure 3 Amyloid β oligomerization is strongly associated with gastric mucosal atrophy. A: In Western blot analysis, amyloid β (Aβ) oligomers were expressed only in gastric mucosae with atrophy. Expression of apolipoprotein E (ApoE), β-secretase 1 (Bace1), and cleaved form of caspase-3 were increased in atrophic gastric

mucosae with reduced NKX6.3 expression. B and C: Expression levels of *ApoE* and *Bace1* mRNAs were significantly higher in gastric mucosae with atrophy (B), showing inverse correlations with NKX6.3 expression ($P < 0.0001$, C). Shown are the means ± SEM from three experiments. Superscript letter represents significant difference ([a]$P < 0.0001$, [b]$P < 0.0001$ and [c]$P < 0.0001$). D: In Aβ42 enzyme-linked immunosorbent assay, concentrations of aggregated Aβ were significantly increased in gastric mucosa with (W/) atrophy (1.20 ± 0.60 μg/mL) compared to without (W/O) atrophy (0.09 ± 0.09 μg/mL). Shown are the means ± SEM from three experiments. Superscript letter represents significant difference ([d]$P < 0.0001$). E: Western blot analysis showing decreased expression of NKX6.3 and increased expression of ApoE, Aβ oligomer, Bace1, and cleaved caspase-3 proteins in CagA transfected HFE-145 cells. In addition, CagA significantly increased concentrations of aggregated Aβ in both cell lysate and culture media. Shown are the means ± SEM from three experiments. Superscript letter represents significant difference ([e]$P < 0.005$ and [f]$P < 0.0001$). F: Knock-down of Aβ inhibited CagA-induced floating cells populations. Shown are the means ± SEM from three experiments. Superscript letter represents significant difference ([g]$P < 0.005$ and [h]$P < 0.0001$). G: Immunofluorescence analysis showing expression of Aβ oligomer and Bace1 only in gastric mucosae with atrophy, but not in gastric mucosa without atrophy. Right panel is a higher magnification of the Aβ oligomer and Bace1 in the inlet in gastric mucosa with atrophy. ApoE: Apolipoprotein E; Aβ: Amyloid β; Bace1: β-secretase 1; W/: With atrophy; W/O: Without atrophy.

protein complex will cleave the C-terminus of C99 to produce a 40- to 42-amino acid Aβ-peptide[38]. After sequential cleavage of APP by β- and γ-secretases[38,39], Aβ monomer can aggregate to form oligomers, protofibrils, and fibrils that deposit as amyloid plaque[40]. RAGE and HMGB1 are involved in activating NF-κB[41], and the interaction of RAGE and HMGB1 can be lined to necrosis and a proinflammatory response in cells[42]. Here, we found that NKX6.3 depletion induced expression of ApoE, APP, Aβ, Bace1, LDLR, NCT, HMGB1, and RAGE proteins in HFE-145[shNKX6.3] cells (Figure 2A). In addition, NKX6.3 inhibited the γ-secretase complex assembly (Figure 2B) and down-regulated expression of the *APOE* and *Bace1* genes by acting as a transcriptional repressor (Figure 2D and E). In gastric mucosae with atrophy, oligomeric forms of Aβ and Bace1 were detected by immunofluorescent and Western blot analyses (Figure 3A and G), and the increased expression of *APOE* and *Bace1* was inversely correlated with NKX6.3 expression (Figure 3B and C). Interestingly, expression of Aβ oligomer, Bace1, ApoE, cleaved caspase-3, and *H. pylori* CagA was closely associated with gastric mucosal atrophy and inversely correlated with NKX6.3 expression ($P < 0.0001$, Table 1). Furthermore, Aβ peptide concentrations were significantly higher in gastric mucosae with atrophy (1.18 ± 0.57 μg/ml) than those in gastric mucosae without atrophy (0.07 ± 0.04 μg/ml; Figure 3D). In HFE-145 cells, *H. pylori* CagA increased the expression of ApoE, Bace1, and cleaved caspase-3 and induced oligomerization and aggregation of Aβ peptide (Figure 3E). Notably, *siAβ* markedly inhibited CagA effect of cell viability (Figure 3F), indicating that Aβ be involved in CagA-induced cell death in non-neoplastic gastric epithelial cells. Taken together, these results suggest that NKX6.3 may prevent gastric mucosal atrophy by regulating Aβ degradation or clearance pathway.

Recent studies have shown that soluble oligomeric species of Aβ have direct adverse effects, whereas fibrillar or monomeric Aβ seems to be less harmful *in vitro* and in animal models[43-45]. Soluble Aβ oligomers can produce cognitive deficits in the absence of plaques[46] while blocking the Aβ oligomerization can protect cells from toxicity[47], suggesting that oligomerization of Aβ peptide may be a key event in the development of cerebral atrophy. In addition, it has been reported that Aβ oligomers can induce inflammation through RAGE receptor[48] and inhibition of RAGE has therapeutic potential to prevent Aβ-induced inflammatory damage to the brain[49]. NF-κB, a key regulator of inflammation, is activated by Aβ which then transcriptionally regulates IL-6 and IL-8[50]. HMGB1 binds to RAGE receptor to activate a multitude of proinflammatory genes[51]. Recent studies have shown that GKN1 can prevent amyloid aggregation and fibril formation and block the access of γ-secretase to APP *in vitro*[26,52]. Experimental studies showed that partial atrophy of the gastric mucosa in aging rat is not related to the inflammation and gastric mucosa of aging rat has increased susceptibility to injury by a variety of damaging agents[53,54]. Previously, we have reported that NKX6.3 transcriptionally suppresses reactive oxygen production and NF-κB activation which is required for expression of IL-6 and IL-8[55]. Here, we found that treatment with rAβ 1-42 produced oligomeric forms of Aβ and significantly decreased cell viability of HFE-145[shNKX6.3] cells (Figure 4A and B). In addition, NKX6.3 depletion dramatically increased expression of inflammatory cytokines and COX-2 by upregulating ApoE (Figure 5). These results are consistent with our previous report showing that NKX6.3 transcriptionally suppresses reactive oxygen production and NF-κB activation which is required for expression of IL-6 and IL-8[55]. Thus, upregulation of ApoE prompted by NKX6.3 depletion might play an important role in Aβ oligomerization and gastric mucosal inflammation. These findings suggest that depletion of NKX6.3 may account for increased susceptibility of gastric epithelial cells to Aβ-induced cytotoxicity and contribute to gastric mucosal atrophy.

In conclusion, NKX6.3 is a key regulator of gastric mucosal homeostasis *via* inhibiting both cell proliferation and apoptotic cell death. Aβ accumulation was
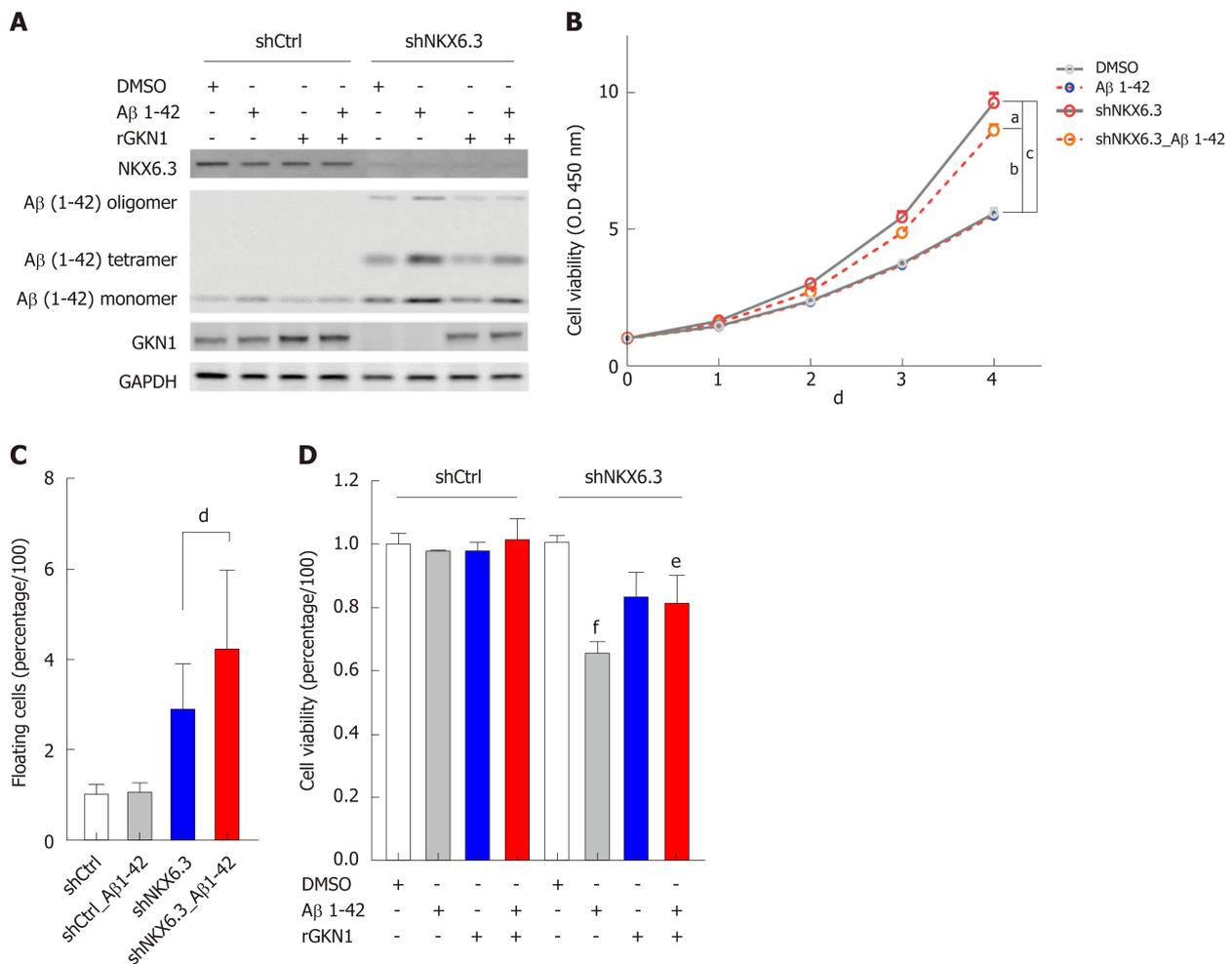
Figure 4 Amyloid β induces cell death in gastric epithelial cells. A: Treatment with recombinant amyloid β (rAβ) 1-42 produced oligomeric forms of Aβ in HFE-145[shNKX6.3] cells, but not in HFE-145[shCtrl] cells. Recombinant gastrokine 1 (rGKN1) partially reduced expression of Aβ oligomers. B: Treatment with rAβ 1-42 did not affect viability of HFE-145[shCtrl] cells, although it significantly decreased viability of HFE-145[shNKX6.3] cells in a time dependent manner. Shown are the means ± SEM from three experiments. Superscript letter represents significant difference ([a]$P < 0.05$, [b]$P < 0.005$ and [c]$P < 0.0001$). C: Floating cell population was markedly increased in HFE-145[shNKX6.3] cells treated with rAβ 1-42. Shown are the means ± SEM from three experiments. Superscript letter represents significant difference ([d]$P < 0.001$). D: In HFE-145[shNKX6.3] cells, treatment with rAβ 1-42 for 72 hrs decreased cell viability while treatment with rGKN1 revoked the effect of rAβ on cell viability. Shown are the means ± SEM from three experiments. Superscript letter represents significant difference ([e]$P < 0.05$ and [f]$P < 0.005$). rAβ: Recombinant amyloid β; rGKN1: Recombinant gastrokine 1; Aβ: Amyloid β.

detected in the cytoplasm of HFE-145[shNKX6.3] cells and gastric mucosae with atrophy. NKX6.3 inhibited accumulation and oligomerization of Aβ peptide in gastric epithelial cells by regulating Aβ degradation or clearance pathways. Finally, NKX6.3 suppressed gastric mucosal inflammation by modulating ApoE-induced NF-κB and expression of cytokines. These observations provide evidence that NKX6.3 can restrain gastric mucosal atrophy by regulating Aβ accumulation and inflammatory reaction in gastric epithelial cells (Figure 6).

Table 1 Protein expression of amyloid β oligomer, β-secretase 1, apolipoprotein E, cleaved caspase-3, and *Helicobacter pylori* CagA was significantly associated with gastric mucosal atrophy and inversely correlated with NKX6.3 expression

		Atrophy			NKX6.3			Aβ oligomer			Bace1			ApoE			Cleaved Casp3		
		+	-	*P* value	+	-	*P* value	+	-	*P* value	+	-	*P* value	+	-	*P* value	+	-	*P* value
NKX6.3	+	3	33	0.0001															
	-	15	4																
Aβ oligomer	+	17	2	0.0001	3	16	0.0001												
	-	1	35		33	3													
Bace1	+	16	5	0.0001	2	19	0.0001	18	3	0.0001									
	-	2	32		34	0		1	33										
ApoE	+	18	5	0.0001	4	19	0.0001	19	4	0.0001	21	2	0.0001						
	-	0	32		32	0		0	32		0	32							
Cleaved Casp3	+	16	8	0.0001	5	19	0.0001	19	5	0.0001	21	3	0.0001	22	2	0.0001			
	-	2	29		31	0		0	31		0	31		1	30				
CagA	+	14	12	0.0041	9	17	0.0001	16	10	0.0002	19	7	0.0001	19	7	0.0001	21	5	0.0001
	-	4	25		27	2		3	26		2	27		4	25		3	26	

Aβ: Amyloid β; ApoE: Apolipoprotein E; Bace1: β-secretase 1; Casp3: Caspase-3.
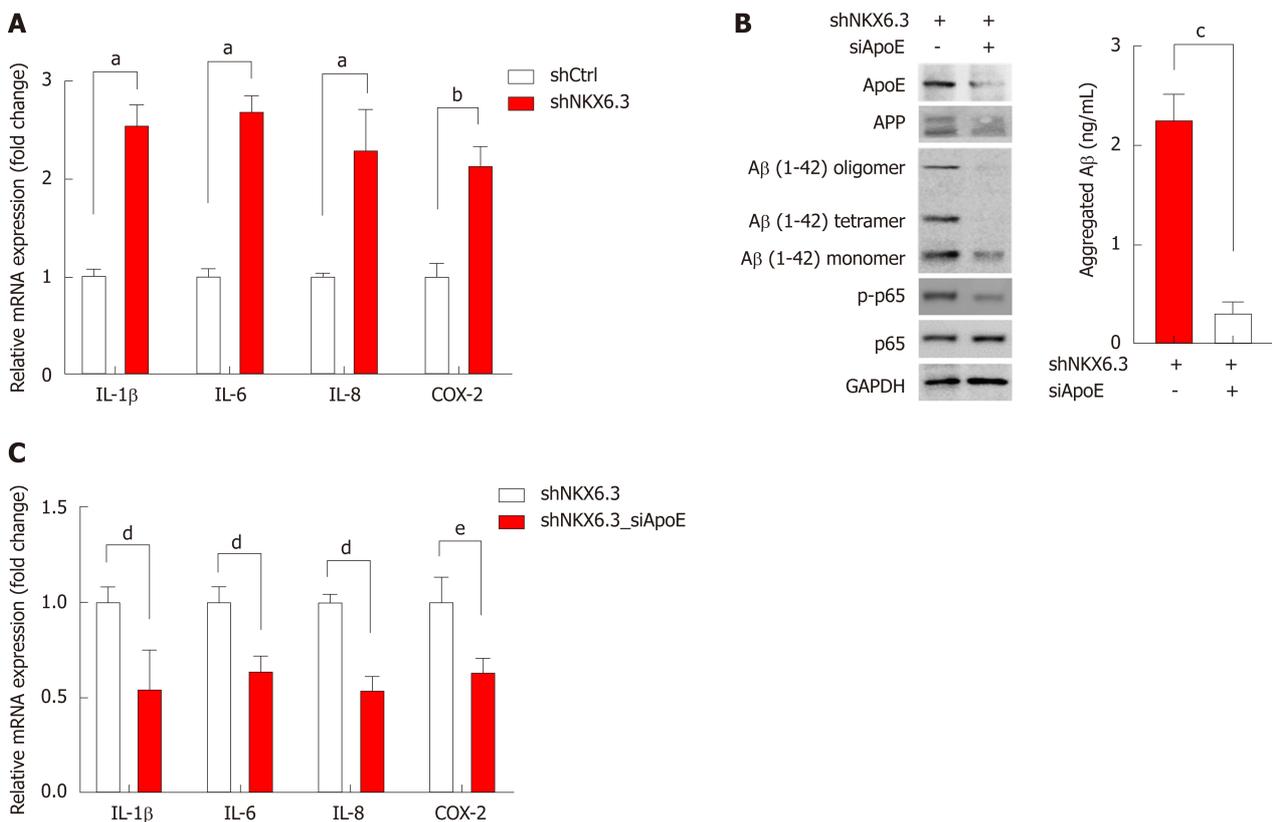
Figure 5 NKX6.3 depletion induces inflammatory cytokine expression in gastric epithelial cells. A: NKX6.3 depletion in HFE-145[shNKX6.3] cells dramatically increased expression of inflammatory cytokines, including interleukin (IL)-1β, IL-6, and IL-8, and cyclooxygenase-2. Shown are the means ± SEM from three experiments. Superscript letter represents significant difference ([a]$P < 0.005$ and [b]$P < 0.001$). B and C: In HFE-145[shNKX6.3] cells, silencing of apolipoprotein E (ApoE) with *siApoE* markedly inhibited oligomerization and aggregation of amyloid β and expression of nuclear factor kappa B p-p65 and inflammatory cytokines. Shown are the means ± SEM from three experiments. Superscript letter represents significant difference ([c]$P < 0.05$, [d]$P < 0.005$ and [e]$P < 0.0001$). IL: Interleukin; COX-2: Cyclooxygenase-2; ApoE: Apolipoprotein E; Aβ: Amyloid β; NF-κB: Nuclear factor kappa B.
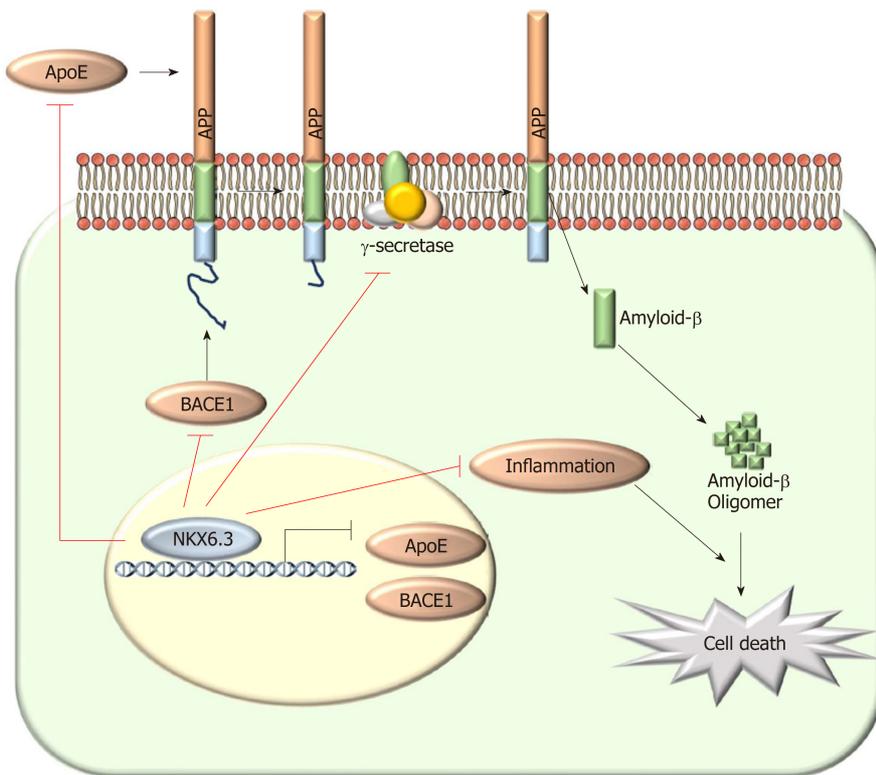
Figure 6 Schematic model of the role of NKX6.3 in gastric mucosal atrophy. In gastric mucosal cells, NKX6.3 prevents gastric mucosal atrophy by regulating amyloid β (Aβ) peptide accumulation and oligomerization through inhibiting the γ-secretase complex formation and the expression of apolipoprotein E (ApoE), and β-secretase 1. In addition, NKX6.3 suppresses gastric mucosal inflammation by modulating ApoE-induced nuclear factor kappa B activity and expression of cytokines. Aβ: Amyloid β; ApoE: Apolipoprotein E; Bace1: β-secretase 1; NF-κB: Nuclear factor kappa B.

ARTICLE HIGHLIGHTS

Research background

Atrophic gastritis is characterized by loss of appropriate glands and considered as a precancerous condition of gastric cancer. However, little is known about the molecular mechanism underlying gastric mucosal atrophy. NKX6.3 plays a key role in the maintaining gastric epithelial homeostasis. Amyloid β (Aβ) acts as a neurotoxin that directly induces oxidative stress and receptor for advanced glycation end products (RAGE) mediates Aβ-induced oxidative stress and inflammatory response. Increased expression of RAGE has been implicated in the pathogenesis of neuronal cell death. Interestingly, gastrokine 1, a downstream target of NKX6.3, interacts with amyloid precursor protein (APP) and inhibits polymerization of Aβ.

Research motivation

A better understanding of molecular mechanism underlying gastric mucosal atrophy could protect against gastric mucosal atrophy and gastric carcinogenesis.

Research objectives

To investigate whether NKX6.3 might play a critical role in the development of gastric mucosal atrophy by regulating Aβ production.

Research methods

We examined whether NKX6.3 depletion induces cell death by cell count and Western blot assay. Production and mechanism of Aβ oligomer were analyzed by enzyme-linked immunosorbent assay, Western blot, immunoprecipitation, real-time quantitative polymerase chain reaction and immunofluorescence analysis in HFE-145 non-neoplastic gastric epithelial cells and gastric mucosal tissues. We further validated the correlation between expression of NKX6.3, *Helicobacter pylori* CagA, Aβ oligomer, apolipoprotein E (ApoE), and β-secretase 1 (Bace1) in gastric mucosae.

Research results

We found that NKX6.3 depletion increased floating cell populations in HFE-145 cells and induced production of Aβ peptide oligomers. In addition, NKX6.3 depletion increased expression of APP, Aβ, and RAGE proteins. In gastric mucosae with atrophy, expression of Aβ peptide oligomer, *ApoE*, and *Bace1* was detected and inversely correlated with NKX6.3 expression. Treatment with rAβ 1-42 produced oligomeric forms of Aβ and significantly

decreased cell viability only in HFE-145[shNKX6.3] cells. Furthermore, NKX6.3 depletion in HFE-145[shNKX6.3] cells increased expression of inflammatory cytokines and cyclooxygenase-2.

Research conclusions

These data strongly suggest that NKX6.3 inhibit gastric mucosal atrophy by regulating Aβ accumulation and inflammatory reaction in gastric epithelial cells.

Research perspectives

Additional studies are needed to validate the results obtained. Identification of molecular mechanism underlying gastric mucosal atrophy could contribute to the prevention of atrophic gastritis and gastric cancer.

ACKNOWLEDGEMENTS

REFERENCES

1   **Watari J**, Chen N, Amenta PS, Fukui H, Oshima T, Tomita T, Miwa H, Lim KJ, Das KM. Helicobacter pylori associated chronic gastritis, clinical syndromes, precancerous lesions, and pathogenesis of gastric cancer development. *World J Gastroenterol* 2014; **20**: 5461-5473 [PMID: 24833876 DOI: 10.3748/wjg.v20.i18.5461]

2   **Joo YE**, Park HK, Myung DS, Baik GH, Shin JE, Seo GS, Kim GH, Kim HU, Kim HY, Cho SI, Kim N. Prevalence and risk factors of atrophic gastritis and intestinal metaplasia: a nationwide multicenter prospective study in Korea. *Gut Liver* 2013; **7**: 303-310 [PMID: 23710311 DOI: 10.5009/gnl.2013.7.3.303]

3   **Song JH**, Kim SG, Jin EH, Lim JH, Yang SY. Risk Factors for Gastric Tumorigenesis in Underlying Gastric Mucosal Atrophy. *Gut Liver* 2017; **11**: 612-619 [PMID: 28531911 DOI: 10.5009/gnl16488]

4   **Uemura N**, Okamoto S, Yamamoto S, Matsumura N, Yamaguchi S, Yamakido M, Taniyama K, Sasaki N, Schlemper RJ. Helicobacter pylori infection and the development of gastric cancer. *N Engl J Med* 2001; **345**: 784-789 [PMID: 11556297 DOI: 10.1056/NEJMoa001999]

5   **Fox JG**, Wang TC. Helicobacter pylori--not a good bug after all. *N Engl J Med* 2001; **345**: 829-832 [PMID: 11556306 DOI: 10.1056/NEJM200109133451111]

6   **Ohata H**, Kitauchi S, Yoshimura N, Mugitani K, Iwane M, Nakamura H, Yoshikawa A, Yanaoka K, Arii K, Tamai H, Shimizu Y, Takeshita T, Mohara O, Ichinose M. Progression of chronic atrophic gastritis associated with Helicobacter pylori infection increases risk of gastric cancer. *Int J Cancer* 2004; **109**: 138-143 [PMID: 14735480 DOI: 10.1002/ijc.11680]

7   **Cappai R**, White AR. Amyloid beta. *Int J Biochem Cell Biol* 1999; **31**: 885-889 [PMID: 10533280]

8   **Lichtenthaler SF**. Alpha-secretase cleavage of the amyloid precursor protein: proteolysis regulated by signaling pathways and protein trafficking. *Curr Alzheimer Res* 2012; **9**: 165-177 [PMID: 21605033]

9   **Vassar R**, Bennett BD, Babu-Khan S, Kahn S, Mendiaz EA, Denis P, Teplow DB, Ross S, Amarante P, Loeloff R, Luo Y, Fisher S, Fuller J, Edenson S, Lile J, Jarosinski MA, Biere AL, Curran E, Burgess T, Louis JC, Collins F, Treanor J, Rogers G, Citron M. Beta-secretase cleavage of Alzheimer's amyloid precursor protein by the transmembrane aspartic protease BACE. *Science* 1999; **286**: 735-741 [PMID: 10531052]

10   **Yu G**, Nishimura M, Arawaka S, Levitan D, Zhang L, Tandon A, Song YQ, Rogaeva E, Chen F, Kawarai T, Supala A, Levesque L, Yu H, Yang DS, Holmes E, Milman P, Liang Y, Zhang DM, Xu DH, Sato C, Rogaev E, Smith M, Janus C, Zhang Y, Aebersold R, Farrer LS, Sorbi S, Bruni A, Fraser P, St George-Hyslop P. Nicastrin modulates presenilin-mediated notch/glp-1 signal transduction and betaAPP processing. *Nature* 2000; **407**: 48-54 [PMID: 10993067 DOI: 10.1038/35024009]

11   **Goutte C**, Tsunozaki M, Hale VA, Priess JR. APH-1 is a multipass membrane protein essential for the Notch signaling pathway in Caenorhabditis elegans embryos. *Proc Natl Acad Sci USA* 2002; **99**: 775-779 [PMID: 11792846 DOI: 10.1073/pnas.022523499]

12   **Li YM**, Xu M, Lai MT, Huang Q, Castro JL, DiMuzio-Mower J, Harrison T, Lellis C, Nadin A, Neduvelil JG, Register RB, Sardana MK, Shearman MS, Smith AL, Shi XP, Yin KC, Shafer JA, Gardell SJ. Photoactivated gamma-secretase inhibitors directed to the active site covalently label presenilin 1. *Nature* 2000; **405**: 689-694 [PMID: 10864326 DOI: 10.1038/35015085]

13   **Ahn K**, Shelton CC, Tian Y, Zhang X, Gilchrist ML, Sisodia SS, Li YM. Activation and intrinsic gamma-secretase activity of presenilin 1. *Proc Natl Acad Sci USA* 2010; **107**: 21435-21440 [PMID: 21115843 DOI: 10.1073/pnas.1013246107]

14   **Baranello RJ**, Bharani KL, Padmaraju V, Chopra N, Lahiri DK, Greig NH, Pappolla MA, Sambamurti K. Amyloid-beta protein clearance and degradation (ABCD) pathways and their role in Alzheimer's disease. *Curr Alzheimer Res* 2015; **12**: 32-46 [PMID: 25523424]

15   **Yan SD**, Chen X, Fu J, Chen M, Zhu H, Roher A, Slattery T, Zhao L, Nagashima M, Morser J, Migheli A, Nawroth P, Stern D, Schmidt AM. RAGE and amyloid-beta peptide neurotoxicity in Alzheimer's disease. *Nature* 1996; **382**: 685-691 [PMID: 8751438 DOI: 10.1038/382685a0]

16   **Schmidt AM**, Yan SD, Yan SF, Stern DM. The multiligand receptor RAGE as a progression factor amplifying immune and inflammatory responses. *J Clin Invest* 2001; **108**: 949-955 [PMID: 11581294 DOI: 10.1172/JCI14002]

17   **Hashimoto T**, Serrano-Pozo A, Hori Y, Adams KW, Takeda S, Banerji AO, Mitani A, Joyner D, Thyssen DH, Bacskai BJ, Frosch MP, Spires-Jones TL, Finn MB, Holtzman DM, Hyman BT. Apolipoprotein E, especially apolipoprotein E4, increases the oligomerization of amyloid β peptide. *J Neurosci* 2012; **32**: 15181-15192 [PMID: 23100439 DOI: 10.1523/JNEUROSCI.1542-12.2012]

18   **Kanekiyo T**, Xu H, Bu G. ApoE and Aβ in Alzheimer's disease: accidental encounters or partners? *Neuron* 2014; **81**: 740-754 [PMID: 24559670 DOI: 10.1016/j.neuron.2014.01.045]

19   **LaFerla FM**, Hall CK, Ngo L, Jay G. Extracellular deposition of beta-amyloid upon p53-dependent neuronal cell death in transgenic mice. *J Clin Invest* 1996; **98**: 1626-1632 [PMID: 8833912 DOI: 10.1172/JCI118957]

20   **Manczak M**, Reddy PH. Abnormal interaction of oligomeric amyloid-β with phosphorylated tau: implications to synaptic dysfunction and neuronal damage. *J Alzheimers Dis* 2013; **36**: 285-295 [PMID: 23594602 DOI: 10.3233/JAD-130275]

21   **Alanentalo T**, Chatonnet F, Karlen M, Sulniute R, Ericson J, Andersson E, Ahlgren U. Cloning and analysis of Nkx6.3 during CNS and gastrointestinal development. *Gene Expr Patterns* 2006; **6**: 162-170 [PMID: 16326147 DOI: 10.1016/j.modgep.2005.06.012]

22   **Choi MY**, Romer AI, Wang Y, Wu MP, Ito S, Leiter AB, Shivdasani RA. Requirement of the tissue-restricted homeodomain transcription factor Nkx6.3 in differentiation of gastrin-producing G cells in the stomach antrum. *Mol Cell Biol* 2008; **28**: 3208-3218 [PMID: 18347062 DOI: 10.1128/MCB.01737-07]

23   **Yoon JH**, Choi SS, Kim O, Choi WS, Park YK, Nam SW, Lee JY, Park WS. Inactivation of NKX6.3 in the stomach leads to abnormal expression of CDX2 and SOX2 required for gastric-to-intestinal transdifferentiation. *Mod Pathol* 2016; **29**: 194-208 [PMID: 26743476 DOI: 10.1038/modpathol.2015.150]

24   **Yoon JH**, Choi WS, Kim O, Choi SS, Lee EK, Nam SW, Lee JY, Park WS. NKX6.3 controls gastric differentiation and tumorigenesis. *Oncotarget* 2015; **6**: 28425-28439 [PMID: 26314965 DOI: 10.18632/oncotarget.4952]

25   **Yoon JH**, Choi YJ, Choi WS, Ashktorab H, Smoot DT, Nam SW, Lee JY, Park WS. GKN1-miR-185-DNMT1 axis suppresses gastric carcinogenesis through regulation of epigenetic alteration and cell cycle. *Clin Cancer Res* 2013; **19**: 4599-4610 [PMID: 23846337 DOI: 10.1158/1078-0432.CCR-12-3675]

26   **Di Stadio CS**, Altieri F, Minopoli G, Miselli G, Rippa E, Arcari P. Role of human GKN1 on APP processing in gastric cancer. *Biochimie* 2017; **135**: 149-153 [PMID: 28214529 DOI: 10.1016/j.biochi.2017.02.007]

27   **Choi WS**, Seo HS, Song KY, Yoon JH, Kim O, Nam SW, Lee JY, Park WS. Gastrokine 1 expression in the human gastric mucosa is closely associated with the degree of gastritis and DNA methylation. *J Gastric Cancer* 2013; **13**: 232-241 [PMID: 24511419 DOI: 10.5230/jgc.2013.13.4.232]

28   **Yoon JH**, Seo HS, Choi SS, Chae HS, Choi WS, Kim O, Ashktorab H, Smoot DT, Nam SW, Lee JY, Park WS. Gastrokine 1 inhibits the carcinogenic potentials of Helicobacter pylori CagA. *Carcinogenesis* 2014; **35**: 2619-2629 [PMID: 25239641 DOI: 10.1093/carcin/bgu199]

29   **Goure WF**, Krafft GA, Jerecic J, Hefti F. Targeting the proper amyloid-beta neuronal toxins: a path forward for Alzheimer's disease immunotherapeutics. *Alzheimers Res Ther* 2014; **6**: 42 [PMID: 25045405 DOI: 10.1186/alzrt272]

30   **Currais A**, Quehenberger O, M Armando A, Daugherty D, Maher P, Schubert D. Amyloid proteotoxicity initiates an inflammatory response blocked by cannabinoids. *NPJ Aging Mech Dis* 2016; **2**: 16012 [PMID: 28721267 DOI: 10.1038/npjamd.2016.12]

31   **Correa P**, Piazuelo MB. The gastric precancerous cascade. *J Dig Dis* 2012; **13**: 2-9 [PMID: 22188910 DOI: 10.1111/j.1751-2980.2011.00550.x]

32   **Atherton JC**. The pathogenesis of Helicobacter pylori-induced gastro-duodenal diseases. *Annu Rev Pathol* 2006; **1**: 63-96 [PMID: 18039108 DOI: 10.1146/annurev.pathol.1.110304.100125]

33   **Nelson SB**, Janiesch C, Sander M. Expression of Nkx6 genes in the hindbrain and gut of the developing mouse. *J Histochem Cytochem* 2005; **53**: 787-790 [PMID: 15928328 DOI: 10.1369/jhc.5B6619.2005]

34   **Palmblad M**, Westlind-Danielsson A, Bergquist J. Oxidation of methionine 35 attenuates formation of amyloid beta -peptide 1-40 oligomers. *J Biol Chem* 2002; **277**: 19506-19510 [PMID: 11912198 DOI: 10.1074/jbc.M112218200]

35   **Butterfield DA**, Drake J, Pocernich C, Castegna A. Evidence of oxidative damage in Alzheimer's disease brain: central role for amyloid beta-peptide. *Trends Mol Med* 2001; **7**: 548-554 [PMID: 11733217]

36   **Martins RN**, Harper CG, Stokes GB, Masters CL. Increased cerebral glucose-6-phosphate dehydrogenase activity in Alzheimer's disease may reflect oxidative stress. *J Neurochem* 1986; **46**: 1042-1045 [PMID: 3950618]

37   **Wei W**, Norton DD, Wang X, Kusiak JW. Abeta 17-42 in Alzheimer's disease activates JNK and caspase-8 leading to neuronal apoptosis. *Brain* 2002; **125**: 2036-2043 [PMID: 12183349]

38   **Sathya M**, Premkumar P, Karthick C, Moorthi P, Jayachandran KS, Anusuyadevi M. BACE1 in Alzheimer's disease. *Clin Chim Acta* 2012; **414**: 171-178 [PMID: 22926063 DOI: 10.1016/j.cca.2012.08.013]

39   **Chow VW**, Mattson MP, Wong PC, Gleichmann M. An overview of APP processing enzymes and products. *Neuromolecular Med* 2010; **12**: 1-12 [PMID: 20232515 DOI: 10.1007/s12017-009-8104-z]

40   **Hardy J**, Selkoe DJ. The amyloid hypothesis of Alzheimer's disease: progress and problems on the road to therapeutics. *Science* 2002; **297**: 353-356 [PMID: 12130773 DOI: 10.1126/science.1072994]

41   **Luan ZG**, Zhang H, Yang PT, Ma XC, Zhang C, Guo RX. HMGB1 activates nuclear factor-κB signaling by RAGE and increases the production of TNF-α in human umbilical vein endothelial cells. *Immunobiology* 2010; **215**: 956-962 [PMID: 20163887 DOI: 10.1016/j.imbio.2009.11.001]

42   **Li G**, Liang X, Lotze MT. HMGB1: The Central Cytokine for All Lymphoid Cells. *Front Immunol* 2013; **4**: 68 [PMID: 23519706 DOI: 10.3389/fimmu.2013.00068]

43   **Kayed R**, Head E, Thompson JL, McIntire TM, Milton SC, Cotman CW, Glabe CG. Common structure of soluble amyloid oligomers implies common mechanism of pathogenesis. *Science*

2003; **300**: 486-489 [PMID: 12702875 DOI: 10.1126/science.1079469]

44   **Walsh DM**, Klyubin I, Fadeeva JV, Cullen WK, Anwyl R, Wolfe MS, Rowan MJ, Selkoe DJ. Naturally secreted oligomers of amyloid beta protein potently inhibit hippocampal long-term potentiation in vivo. *Nature* 2002; **416**: 535-539 [PMID: 11932745 DOI: 10.1038/416535a]

45   **Shankar GM**, Li S, Mehta TH, Garcia-Munoz A, Shepardson NE, Smith I, Brett FM, Farrell MA, Rowan MJ, Lemere CA, Regan CM, Walsh DM, Sabatini BL, Selkoe DJ. Amyloid-beta protein dimers isolated directly from Alzheimer's brains impair synaptic plasticity and memory. *Nat Med* 2008; **14**: 837-842 [PMID: 18568035 DOI: 10.1038/nm1782]

46   **Gandy S**, Simon AJ, Steele JW, Lublin AL, Lah JJ, Walker LC, Levey AI, Krafft GA, Levy E, Checler F, Glabe C, Bilker WB, Abel T, Schmeidler J, Ehrlich ME. Days to criterion as an indicator of toxicity associated with human Alzheimer amyloid-beta oligomers. *Ann Neurol* 2010; **68**: 220-230 [PMID: 20641005 DOI: 10.1002/ana.22052]

47   **De Felice FG**, Vieira MN, Saraiva LM, Figueroa-Villar JD, Garcia-Abreu J, Liu R, Chang L, Klein WL, Ferreira ST. Targeting the neurotoxic species in Alzheimer's disease: inhibitors of Abeta oligomerization. *FASEB J* 2004; **18**: 1366-1372 [PMID: 15333579 DOI: 10.1096/fj.04-1764com]

48   **Minter MR**, Taylor JM, Crack PJ. The contribution of neuroinflammation to amyloid toxicity in Alzheimer's disease. *J Neurochem* 2016; **136**: 457-474 [PMID: 26509334 DOI: 10.1111/jnc.13411]

49   **Sengupta U**, Nilson AN, Kayed R. The Role of Amyloid-β Oligomers in Toxicity, Propagation, and Immunotherapy. *EBioMedicine* 2016; **6**: 42-49 [PMID: 27211547 DOI: 10.1016/j.ebiom.2016.03.035]

50   **Park SY**, Jin ML, Kim YH, Kim Y, Lee SJ. Anti-inflammatory effects of aromatic-turmerone through blocking of NF-κB, JNK, and p38 MAPK signaling pathways in amyloid β-stimulated microglia. *Int Immunopharmacol* 2012; **14**: 13-20 [PMID: 22728094 DOI: 10.1016/j.intimp.2012.06.003]

51   **Sims GP**, Rowe DC, Rietdijk ST, Herbst R, Coyle AJ. HMGB1 and RAGE in inflammation and cancer. *Annu Rev Immunol* 2010; **28**: 367-388 [PMID: 20192808 DOI: 10.1146/annurev.immunol.021908.132603]

52   **Pavone LM**, Del Vecchio P, Mallardo P, Altieri F, De Pasquale V, Rea S, Martucci NM, Di Stadio CS, Pucci P, Flagiello A, Masullo M, Arcari P, Rippa E. Structural characterization and biological properties of human gastrokine 1. *Mol Biosyst* 2013; **9**: 412-421 [PMID: 23319233 DOI: 10.1039/c2mb25308a]

53   **Tarnawski A**, Pai R, Deng X, Ahluwalia A, Khomenko T, Tanigawa T, Akahoshi T, Sandor Z, Szabo S. Aging gastropathy-novel mechanisms: hypoxia, up-regulation of multifunctional phosphatase PTEN, and proapoptotic factors. *Gastroenterology* 2007; **133**: 1938-1947 [PMID: 18054565 DOI: 10.1053/j.gastro.2007.08.037]

54   **Tarnawski AS**, Ahluwalia A, Jones MK. Increased susceptibility of aging gastric mucosa to injury: the mechanisms and clinical implications. *World J Gastroenterol* 2014; **20**: 4467-4482 [PMID: 24782600 DOI: 10.3748/wjg.v20.i16.4467]

55   **Yoon JH**, Kim O, Nam SW, Lee JY, Park WS. NKX6.3 Regulates Reactive Oxygen Species Production by Suppressing NF-kB and DNMT1 Activities in Gastric Epithelial Cells. *Sci Rep* 2017; **7**: 2807 [PMID: 28584243 DOI: 10.1038/s41598-017-02901-y]

Basic Study

Effects of positive acceleration (+Gz stress) on liver enzymes, energy metabolism, and liver histology in rats

Bin Shi, Xian-Qiang Wang, Wei-Dong Duan, Guo-Dong Tan, Han-Jing Gao, Ying-Wei Pan, Qing-Jun Guo, Hong-Yi Zhang

ORCID number: Bin Shi (0000-0002-1524-1574); Xian-Qiang Wang (0000-0002-3279-8411); Wei-Dong Duan (0000-0002-9405-6720); Guo-Dong Tan (0000-0001-9558-9994); Han-Jing Gao (0000-0002-9460-2525); Ying-Wei Pan (0000-0002-5852-8727); Qing-Jun Guo (0000-0002-9108-489X); Hong-Yi Zhang (0000-0002-7521-5247).

Bin Shi, Hong-Yi Zhang, Department of Hepatobiliary Surgery, Air Force Medical Center, PLA, Beijing 100142, China

Xian-Qiang Wang, Department of Pediatrics, Chinese PLA General Hospital and PLA Medical School, Beijing 100853, China

Wei-Dong Duan, Ying-Wei Pan, Department of Hepatobiliary Surgery, Chinese PLA General Hospital and PLA Medical School, Beijing 100853, China

Guo-Dong Tan, Outpatient Department, Air Command Headquarters, Beijing 100038, China

Han-Jing Gao, Department of Ultrasound, Chinese PLA General Hospital and PLA Medical School, Beijing 100853, China

Qing-Jun Guo, Department of Endocrinology, Changhai Hospital, Second Military Medical University, Shanghai 200433, China

Corresponding author: Hong-Yi Zhang, MD, Professor, Department of Hepatobiliary Surgery, Air Force Medical Center, PLA, No. 30, Fucheng Road, Haidian District, Beijing 100142, China. qhcgzhy@163.com
Telephone: +86-10-66928312
Fax: +86-10-66928312

Abstract

BACKGROUND
Exposure to high sustained +Gz (head-to-foot inertial load) is known to have harmful effects on pilots' body in flight. Although clinical data have shown that liver dysfunction occurs in pilots, the precise cause has not been well defined.

AIM
To investigate rat liver function changes in response to repeated +Gz exposure.

METHODS
Ninety male Wistar rats were randomly divided into a blank control group (BC group, $n = 30$), a +6 Gz/5 min stress group (6GS group, $n = 30$), and a +10 Gz/5min stress group (10GS group, $n = 30$). The 6GS and 10GS groups were exposed to +6 Gz and +10 Gz, respectively, in an animal centrifuge. The onset rate of +Gz was 0.5 G/s. The sustained time at peak +Gz was 5 min for each exposure (for 5 exposures, and 5-min intervals between exposures for a total exposure and non-exposure time of 50 min). We assessed liver injury by

measuring the portal venous flow volume, serum alanine aminotransferase (ALT) and aspartate aminotransferase (AST), liver tissue malondialdehyde (MDA), Na+-K+-ATPase, and changes in liver histology. These parameters were recorded at 0 h, 6 h, and 24 h after repeated +Gz exposures.

RESULTS
After repeated +Gz exposures in the 6GS and the 10GS groups, the velocity and flow signal in the portal vein (PV) were significantly decreased as compared to the BC group at 0 h after exposure. Meanwhile, we found that the PV diameter did not change significantly. However, rats in the 6GS group had a much higher portal venous flow volume than the 10GS group at 0 h after exposure. The 6GS group had significantly lower ALT, AST, and MDA values than the 10GS group 0 h and 6 h post exposure. The Na+-K+-ATPase activity in the 6GS group was significantly higher than that in the 10GS group 0 h and 6 h post exposure. Hepatocyte injury, determined pathologically, was significantly lower in the 6GS group than in the 10GS group.

CONCLUSION
Repeated +Gz exposures transiently cause hepatocyte injury and affect liver metabolism and morphological structure.

Key words: Positive acceleration; +Gz; Liver function; Animal models; Liver metabolism; Ischemia-reperfusion injury

Core tip: Some clinical data showed that liver dysfunction was observed in pilots. However, the reason was not clear. We conducted this experimental study to investigate rat liver function changes in response to repeated +Gz exposures, and to observe the portal venous flow volume, liver function indexes, liver tissue malondialdehyde, Na+-K+-ATPase activity, and changes in liver histology. We found that repeated +Gz exposures transiently cause hepatocyte injury and affect liver metabolism and morphological structure.

INTRODUCTION

Exposure to high sustained +Gz (head-to-foot inertial load) is known to have harmful effects on pilots' body in flight[1]. Along with fast developments in aviation and aerospace technologies, pilots are required to undertake sustained high G-acceleration stress. The characteristics of modern high performance aircraft flight in particular involve high acceleration (>9 Gz) that occurs repeatedly and is continued for 15-45 s, and may transcend the physiological tolerance of flight personnel, even resulting in pilot incapacitation and subsequent loss of life[2,3]. Repeated high-acceleration force exposures may result in cumulative adverse stress responses in the body[4]. Accordingly, safe flying is an issue that is attracting broad attention[5].

The vascular beds that ensure hepatic circulation include two vascular systems, the portal vein (PV) and hepatic artery (HA)[6]. Fighter pilots are frequently exposed to high Gz acceleration with the vector oriented in the foot-head direction. Under these conditions, blood and fluids are redistributed in the body and into the lower body[7]. There are some clinical reports in which liver dysfunction has been observed in pilots[8]. However, the reason for these abnormalities remains unclear. An important question to address is whether or not changes in the blood flow direction after +Gz exposure impairs liver function. Moreover, the manner in which portal venous hemodynamics changes after repeated +Gz exposures, and whether or not oxidative stress parameters increase the duration of these changes, are additional questions

awaiting answers. To answer these questions, further studies on liver damage and the mechanisms of liver damage induced by high +Gz exposure are needed to provide evidence for effective preventative measures. In recent years, studies on the effects of high +Gz on the heart, brain, and lung have been addressed in considerable numbers of human and animal studies[9-11]. With the above in mind, we attempted to research the effects of acceleration on liver blood flow, function, and histology.

MATERIALS AND METHODS

Animals

Healthy male Wistar rats, weighing 200-250 g, were raised in comfortable environment, and fed and water naturally. All animal experiments and procedures performed in this study were conducted in accordance with the Nursing Guidelines and Usage Specification.

Experimental groups and animal exposure to acceleration

In this experiment, we chose +6 and +10 Gz as the acceleration test parameters, as reported previously[12,13]. Ninety rats were divided randomly into three groups: blank control group (BC group, *n* = 30), +6 Gz/5 min stress group (6GS group, *n* = 30), and +10 Gz/5 min stress group (10GS group, *n* = 30). The animal centrifuge used has a diameter of 2 m and has the capacity to generate a wide series of gravities, between +1 Gz and +15 Gz, with an initial rate of 0.1-6 Gz/s[14]. In the 6GS and 10GS groups, rats were repeatedly exposed to +6 Gz or +10 Gz stress (each time for 5 min, initial rate of approximately 1 G/s, 5 times with 0 Gz, at 5-min intervals), respectively. The rats in the blank control group were placed in the centrifuge arm and were subjected to the same process as the test groups, but were not exposed to acceleration. For sample collection, the combined exposure and interval time was 50 min. At 0, 6 h, or 24 h after the last centrifuge run, experimental rats were harvested and blood samples were obtained from the infra-hepatic vena cava to measure hepatic enzyme levels (*n* = 10 per measurement point). Half of liver lobe was instantly stored in liquid nitrogen and stored at -80 °C. The other half was fixed in 4% formalin, stained with hematoxylin and eosin, and analyzed by a microscopic examination. At the end of the observation period, all the rats were ultimately killed using chloral hydrate.

Determination of portal blood flow

Using color Doppler ultrasound, we evaluated blood vessel diameter and the blood flow velocity in the PV. The blood flow volume of the PV was calculated with the flow equation: $Q = \pi \times (D/2)2 \times Vmean \times 60$ (Q: flow volume per minute; Vmean: mean blood flow velocity; D: vessel diameter).

Liver function tests

The extent of liver damage and activity changes in serum alanine aminotransferase (ALT) and aspartate aminotransferase (AST) were quantified.

Malondialdehyde (MDA) level measurements

MDA is involved in the metabolism of lipid peroxidation products. The MDA content was determined using a standardized MDA assay kit (Nanjing Jiancheng Biotechnology Institute, Nanjing, China), in accordance with the operation manual. A peach red color is generated during the condensation reaction between thiobarbituric acid (TBA) and MDA. The results are expressed as nmol/mg protein.

Measurement of Na+-K+-ATPase activity levels

Hepatic Na^+-K^+-ATPase activity was measured using an ATPase assay kit (Nanjing Jiancheng Biotechnology Institute, Nanjing, China). The measurement of the Na^+-K^+-ATPase activity was based on the quantification of inorganic phosphate that is formed by adenosine triphosphate decomposition[15].

Morphological assessment

Liver specimens were deparaffinized for morphological assessment. The histologic damage severity was stratified using Suzuki's criteria[16]. Liver tissue slices were microscopically examined in a blinded method by an experienced histologist.

Statistical analysis

Statistical analyses were performed using SPSS version 13.0 statistical software (SPSS, Chicago, IL, United States). Experimental results are expressed as the mean ± standard deviation (SD). Differences were regarded as statistically significant at $P < 0.05$.

RESULTS

Portal venous flow after repeated +Gz exposures

The normal portal venous flow in Wistar rats was 11.468 ± 0.237 mL/min. After repeated +Gz exposures in the 6GS and the 10GS groups, the velocity and flow signals in the PV were significantly reduced compared to the BC group ($P < 0.01$ at 0 h post exposure; Figure 1). Meanwhile, we found that the PV diameter did not change significantly. However, rats in the 6GS group had a much higher portal venous flow volume than those in the 10GS group ($P < 0.01$ at 0 h post exposure). All rats exhibited normal portal venous flow 6 h after repeated +Gz exposure. To summarize, as the G force increased, the portal venous blood flow decreased significantly, but transiently.

Liver function after repeated +Gz exposures

To assess liver cell damage in rats, plasma ALT and AST levels were determined 0, 6, and 24 h after repeated +Gz exposures. ALT and AST levels in the BC group were 46.6 ± 4.7 IU/L and 110.5 ± 7.6 IU/L, respectively.

After repeated +Gz exposures, ALT and AST values in the 6GS and the 10GS groups were higher than those in the BC group ($P < 0.01$ at 0 and 6 h time-points after exposure). However, rats in the 6GS group exhibited lower ALT and AST levels than those in the 10GS group at 0 and 6 h post exposure ($P < 0.01$, 6GS group *vs* 10GS group). The experimental groups showed normal ALT and AST levels 24 h after exposure (Figure 2). These consequences display that the degree of damage to the liver function positively correlated with the increase in G-value, but the abnormalities were transient.

Tissue MDA levels after repeated +Gz exposures

MDA concentration in both the 6GS and the 10GS groups had increased 0 h and 6 h after exposure. The MDA concentration in the 6GS group was lower than that in the 10GS group at 0 h (2.89 ± 0.24 nmol/mg protein *vs* 3.32 ± 0.25 nmol/mg protein, $P < 0.01$) and 6 h (2.64 ± 0.18 *vs* 3.18 ± 0.19; $P < 0.01$) post exposure (Figure 3). Notably, the 6GS and 10GS group MDA concentrations did not recover to normal 24 h after exposure. Based on these data, it was concluded that repeated +Gz exposures may induce lipid peroxidation in the rat liver.

Evaluation of Na+-K+-ATPase activity

Na+-K+-ATPase is a cell membrane enzyme that is highly susceptible to lipid membrane peroxidation and free radical reactions[17]. Loss of its activity is a signal of indirect membrane damage. Na+-K+-ATPase activity decreased significantly after exposure in both the 6GS and the 10GS groups, compared to the BC group. The 6GS group had higher Na+-K+-ATPase activity than the 10GS group at 0 h (0.85 ± 0.04 μmolPi/mg protein/h *vs* 0.73 ± 0.05 μmolPi/mg protein/h, $P < 0.01$) and 6 h (0.87 ± 0.03 μmolPi/mg protein/h *vs* 0.78 ± 0.05 μmolPi/mg protein/h, $P < 0.01$) post exposure. There was no significant difference between the 6GS and the 10GS groups at 24 h after exposure (Figure 4).

Histopathological observations in the liver after repeated +Gz exposures

The hepatic pathological injury after repeated +Gz exposures was assessed and scored according to Suzuki's criteria[16]. The structures of the hepatic lobules and liver antrum were clear, and cellular edema was not obvious in the BC group (Figure 5B, Suzuki's score = 2.12 ± 0.35). At the 0 h time-point after exposure, the hepatic sinus cord-like structure was maintained in the 6GS group (Figure 5C, Suzuki's score = 3.21 ± 0.13), whereas it was less well maintained in the 10GS group, which presented with hepatocyte edema (Figure 5D, Suzuki's score = 4.63 ± 0.25). At the 6 h time-point post exposure, hepatocyte edema had been significantly relieved in the 10GS group (Figure 5F, Suzuki's score = 3.53 ± 0.31, $P < 0.01$). There was no significant score difference between the 0 and 6 h time-points after exposure in the 6GS group (Figure 5C and E, Suzuki's score = 3.21 ± 0.13 *vs* 3.24 ± 0.28, $P < 0.01$). The hepatic histology profiles in both the 6GS and the 10GS groups were nearly normal 24 h after exposure (Figure 5G, Suzuki's score = 2.14 ± 0.33; Figure 5H, Suzuki's score = 2.13 ± 0.36).

DISCUSSION

In this study, the effects of high +Gz acceleration on rat liver function was investigated. To this end, we devised an animal model of short-term repeated +Gz exposures. We chose Wistar rats as the experimental subjects because the human Glisson's capsule is similar to that of rats and the model is simple and easy to control. Hepatic energy metabolism and an optimal intracellular environment rely on an
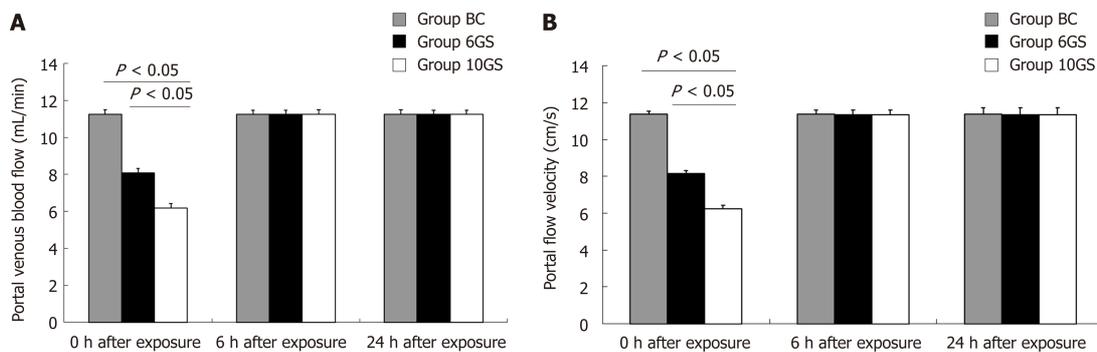
Figure 1 Comparison of the rat portal venous blood flow at 0, 6, and 24 h after repeated +Gz exposures in the blank control group, +6 Gz/5 min stress group, and +10 Gz/5 min stress group. A: Portal vein blood flow; B: Portal flow velocity.

adequate blood supply. Hepatocytes are very sensitive to ischemia and/or hypoxia in liver tissue[18,19]. Therefore, factors related to ischemia and/or hypoxia will definitely influence their metabolism[20]. Direct action and stress reaction caused by +Gz exposure can result in obvious hemodynamic changes between the upper and the lower body, in important organs, and on the body surface, which is similar to hepatic ischemia-reperfusion (I/R). Indeed, repeated +Gz exposures may cause hepatic I/R. Ischemia is defined as inadequate blood supply to an organ or part of an organ as a result of obstructed blood flow[21]. Our findings were consistent with those reported effects, with some significant differences between the acceleration exposed and the control rats observed.

Color Doppler ultrasound is a well-established method for assessing hemodynamic changes in liver circulation that occur under various physiological conditions[22,23]. As described by Kim *et al*[24], exposure to high +Gz accelerating force acting along the body axis from the head to the feet severely reduces blood supply to the internal organs.

Levels of ALT and AST can be used as measures of hepatic damage, and were used in this study to assess damage incurred due to repeated +Gz exposures. The 6GS group was associated with less cellular damage than the 10GS analogue; this was reflected by the lower serum ALT and AST levels. The results indicated that the degree of functional liver damage increased gradually with increasing G value. Zhang *et al*[25] reported that repeated +10 Gz stress had some impact on the oxygen radical metabolism in the rat liver. MDA is widely used as an indicator of oxidative stress, which is one of the end products of lipid peroxidation in the liver[26]. The results of our study displayed that rats in the 10GS group had more hepatic MDA than those in the 6GS group. After repeated +10 Gz exposures, the oxygen and nutrients supplied to the liver were reduced. After exposure, rats in the 6GS group presented with less oxidative stress-induced damage than rats in the 10GS group, as manifested by the lower MDA levels. In this study, changes in the MDA levels were in accordance with those caused by ischemia and/or hypoxia in rat livers[27], which also points toward ischemia or hypoxia as one of the main causes of high +Gz stress-induced liver injury.

Early research in this field found that positive acceleration affected the physiological indexes of the liver. Daligcon *et al*[28] reported that hyper-G stress increased levels of circulating catecholamines and glucagon, both effective stimulators of hepatic gluconeogenesis, and that continued hyperglycemia may be due, in part, to the control of the insulin-stimulated uptake by muscle tissues. They also found that hyper-G stress not only increased circulating and blood glucose levels, but also increased the content of liver glycogen. This was attributed to an increased rate of gluconeogenesis and the key role that epinephrine plays during the beginning of centrifugation exposure[29]. Later research reported that hypergravity exposure caused significant injury to the liver[30].

Our study has some limitations. First, we did not measure the blood flow changes in the HA due to technical limitations. This may be possible through technical advances in the future or the use of larger animal models, and we plan to actively pursue this research avenue in the near future. Additionally, other serum liver parameters such as alkaline phosphatase, gamma-glutamyl transferase, bilirubin, and serum lactate were not measured. We also plan to assess these parameters in future work. Moreover, physiological differences between rats and humans may render the data obtained herein non-transferable to human pilots under similar conditions of exposure.

In summary, the main findings of the study can be summarized as follows: first,
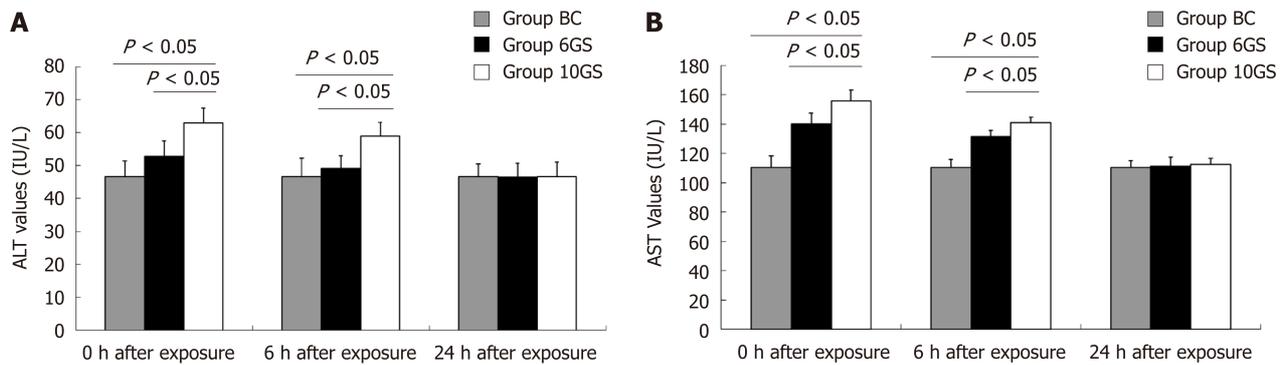
Figure 2 Comparison of rat serum alanine aminotransferase and aspartate aminotransferase levels at 0, 6, and 24 h after repeated +Gz exposures in the blank control group, +6 Gz/5 min stress group, and +10 Gz/5 min stress group. A: Alanine aminotransferase; B: Aspartate aminotransferase. ALT: Alanine aminotransferase; AST: Aspartate aminotransferase.

short-term repeated exposures to either +6 Gz or +10 Gz temporarily reduced the portal venous flow. Second, ALT and AST levels only slightly increased in response to G exposure and soon reverted back to normal. An increase in G force resulted in additional liver damage. Third, evidence of oxidative damage was found, which may have been due to liver ischemia. Finally, repeated exposures were associated with a transient decrease of the liver energy, as indicated by the decrease in Na^+-K^+-ATPase activity. Although the rat data may not be directly extended to that of pilots, because of similar conditions of +Gz exposure, this model may be helpful in identifying more potential adverse effects of high +Gz stress on the human liver, and help develop practical effective protective measures. In the future, we will further expand our study to explore the effects of +Gz exposure over longer durations on liver function, with a view to elucidating the underlying pathophysiological mechanisms and proposing feasible protection to decrease adverse +Gz effects. This could be accomplished by applying an understanding of aviation medicine to aeronautical engineering technology development. This would be significant in aviation progress by ensuring flight safety, extending pilot flying-life, promoting good performance of combat aircrafts, and improving fighting capacity. These factors are essential for the development of a new generation of high-performance fighter aircrafts.
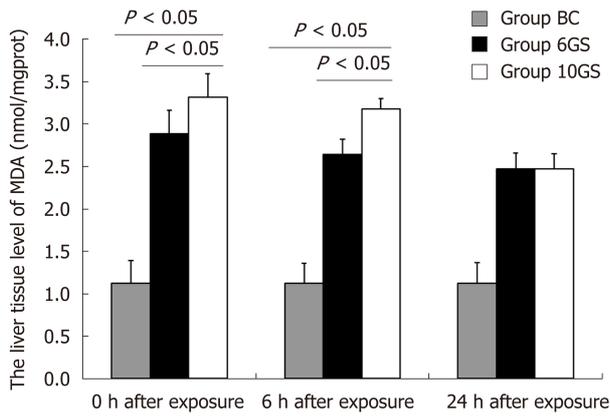
Figure 3 Comparison of the liver tissue malondialdehyde levels at 0, 6, and 24 h after repeated +Gz exposures in the blank control group, +6 Gz/5 min stress group, and +10 Gz/5 min stress group. MDA: Malondialdehyde.
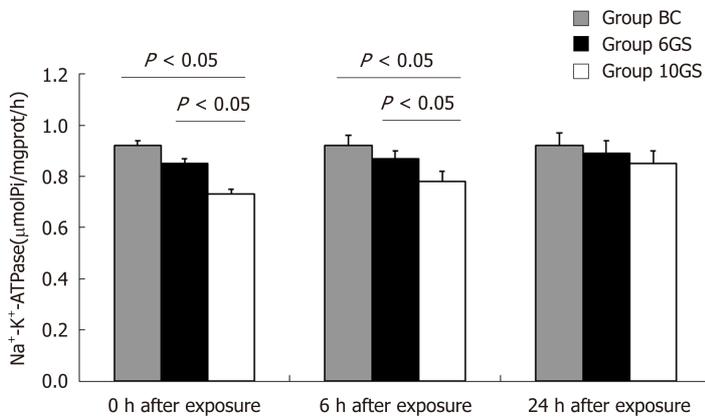
**Figure 4 Comparison of the rat liver Na+-K+-ATPase activity at 0, 6, and 24 h after repeated +Gz exposures in the blank control group, +6 Gz/5 min stress group, and +10 Gz/5 min stress group.**
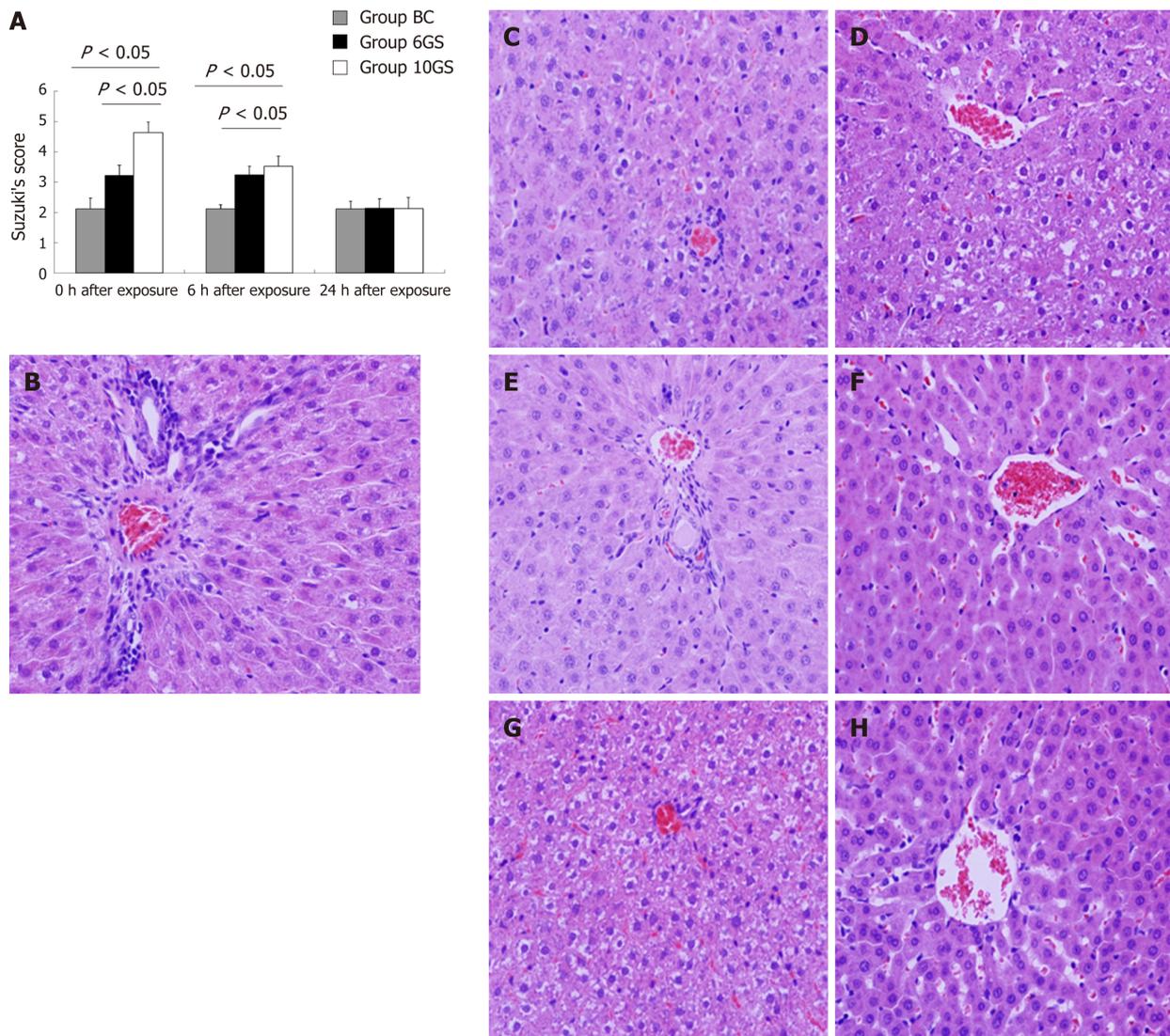
Figure 5 Pathological changes in the liver tissue at 0, 6, and 24 h after repeated +Gz exposures in the blank control group, +6 Gz/5 min stress group, and +10 Gz/5 min stress group. A: The hepatic pathological injury after repeated +Gz exposures was assessed and scored according to Suzuki's criteria. B: The structures of the hepatic lobules and liver antrum were clear, and cellular edema was not obvious in the BC group. C: At the 0 h time-point after exposure, the hepatic sinus cord-like structure was maintained in the 6GS group. D: It was less well maintained in the 10GS group, which presented with hepatocyte edema. E: There was no significant score difference between the 0 and 6 h time-points after exposure in the 6GS group. F: At the 6 h time-point post exposure, hepatocyte edema had been significantly relieved in the 10GS group. G and H: The hepatic histology profiles in both the 6GS and the 10GS groups were nearly normal 24 h after exposure.

ARTICLE HIGHLIGHTS

Research background
Some clinical data show that liver dysfunction was observed in pilots. However, there are many reasons for this: hepatitis virus, drug abuse, excessive drinking and so on. The objective of this study was to probe into whether positive acceleration affects rat liver function.

Research motivation
Exposure to high sustained +Gz (head-to-foot inertial load) is conclusively known to have harmful effects on the human body during aviation activities. High-acceleration force exposures, particularly when occurring repeatedly, may result in accumulative adverse stress responses in the body, and safe flying is a social problem that has attracted broad attention. An important question to address is whether changes in the blood flow direction after +Gz exposure impair liver function in rats. Moreover, the manner in which the portal venous hemodynamics changes after repeated +Gz exposures, and whether oxidative stress parameters increase the duration of these changes are additional questions awaiting answers. To clarify these questions, further studies on liver damage and the mechanisms of liver damage induced by high +Gz exposures are needed, and this will provide evidence to take effective preventive measures.

Research objectives
In this article, an animal centrifuge model was used to study whether positive acceleration

impairs liver function. This research may help find more potential adverse effects of high +Gz stress on the human liver, and help develop practical, effective protective measures. In the future, we will further expand our study to explore the effects of +Gz exposures of longer duration on the liver function, to illuminate the pathophysiological mechanisms that are involved.

Research methods

Completely random grouping design and exploratory experimental research were performed based on the experimental animals. We adopted the method of acceleration exposure in rats. The difference of experimental data was detected by analysis of variance using SPSS version 13.0 statistical software (SPSS, Chicago, IL, United States). Experimental results are expressed as the mean ± standard deviation.

Research results

The main findings of the study showed that repeated +Gz exposures not only transiently impair liver function but also affect liver metabolism and morphological structure. Although there are some gaps between experimental animal model and real flight environment, this research may help find more potential adverse effects of high +Gz stress on the human liver, and help develop practical effective protective measures.

Research conclusions

While fighter pilots are frequently exposed to high Gz acceleration with the vector in the foot-head direction, the blood and fluid of the body will be redistributed and flow along the direction of inertia force to the lower body. Many studies have demonstrated the harmful effects of repeated +Gz stress on the cardiac ultrastructure, metabolism, and function. It was, however, of scarcity that to investigate the effect of high +Gz exposure on the hepatobiliary system. Therefore, we propose some doubts: Do high +Gz exposures impair liver function of rats? How does the portal venous hemodynamics change after repeated +Gz exposures? Do oxidative stress parameters increase? Well then, should the changes of blood flow direction after +Gz exposure cause hepatic ischemia, so as to affect the liver function? We hypothesized that repeated +Gz exposures could transiently impair the liver function in rats.

The main findings of the study can be summarized as follows: First, short-term repeated exposures to either +6 Gz or +10 Gz reduced the portal venous flow. Blood redistribution between the liver and body surface or other organs is similar to liver ischemia reperfusion. Repeat +Gz exposures may result in liver ischemia-reperfusion injury. Second, alanine aminotransferase and aspartate aminotransferase levels were only slightly increased and could soon revert back to normal. With an increase in the G force, additional damage also occurred in the liver function of the rats. The results showed that this damage should be functional and reversible. Third, oxidative damage might be engaged in the pathophysiologic process during liver ischemia. After repeated +Gz exposures, the blood and nutrient substance supplied to the liver were reduced. The exposed group had oxidative stress injury, as reflected in the higher malondialdehyde (MDA) levels. In addition, the MDA levels increased as the G value increased. Fourth, repeated +Gz exposures had something to do with a temporary reduction of the liver metabolism, as indicated by a decrease in the Na^+-K^+-ATPase activity. The main role of the Na^+-K^+-ATPase is to maintain the structure and function of mitochondria. When the activities of the Na^+-K^+-ATPase decline, the structure of mitochondria is likely to change. Morphologically mitochondria became swelling and matrix density decreased.

Research perspectives

Although trained pilots may not use the same way as the rats under similar conditions of exposure due to species difference, the research method in rats may help in investigating the pathophysiological mechanism of high +Gz stress in humans. In addition, this research may aid discovery of more potentially harmful effects of high +Gz stress on the human liver, and subsequently, help to prevent liver injury. Flight crews will be the research subject of the project in the future. Prospective study will be the best research method.

REFERENCES

1   **Evans JM**, Knapp CF, Goswami N. Artificial Gravity as a Countermeasure to the Cardiovascular Deconditioning of Spaceflight: Gender Perspectives. *Front Physiol* 2018; **9**: 716 [PMID: 30034341 DOI: 10.3389/fphys.2018.00716]

2   **Akparibo IY**, Chumbley E. Aerospace, Gravitational Effects, High Performance. 2018; Epub ahead of print [PMID: 28613519]

3   **Öztürk C**, İlbasmış MS, Akın A. Cardiac responses to long duration and high magnitude +Gz exposure in pilots: an observational study. *Anadolu Kardiyol Derg* 2012; **12**: 668-674 [PMID: 22968302 DOI: 10.5152/akd.2012.219]

4   **Perrier E**, Leduc PA, Manen O, Lerecouvreux M, Deroche J, Paris JF, Doireau P, Quiniou G, Geffroy S, Carlioz R. [The heart and aerobatics]. *Arch Mal Coeur Vaiss* 2005; **98**: 47-52 [PMID: 15724419]

5   **Scott JM**, Esch BT, Goodman LS, Bredin SS, Haykowsky MJ, Warburton DE. Cardiovascular consequences of high-performance aircraft maneuvers: implications for effective countermeasures and laboratory-based simulations. *Appl Physiol Nutr Metab* 2007; **32**: 332-339 [PMID: 17486177 DOI: 10.1139/h06-087]

6   **Greenway CV**, Stark RD. Hepatic vascular bed. *Physiol Rev* 1971; **51**: 23-65 [PMID: 5543903 DOI: 10.1152/physrev.1971.51.1.23]

7   **Pattarini JM**, Blue RS, Aikins LT, Law J, Walshe AD, Garbino A, Turney MW, Clark JB. Flat spin and negative Gz in high-altitude free fall: pathophysiology, prevention, and treatment. *Aviat Space Environ Med* 2013; **84**: 961-970 [PMID: 24024308 DOI: 10.3357/ASEM.3648.2013]

8   **Mitchell SJ**, Evans AD. Flight safety and medical incapacitation risk of airline pilots. *Aviat Space Environ Med* 2004; **75**: 260-268 [PMID: 15018295]

9   **Lu WH**, Hsieh KS, Li MH, Ho CW, Wu YC, Ger LP, Wang JS, Chu H. Heart status following high G exposure in rats and the effect of brief preconditioning. *Aviat Space Environ Med* 2008; **79**: 1086-1090 [PMID: 19070302 DOI: 10.3357/ASEM.2353.2008]

10   **Nishida Y**, Maruyama S, Shouji I, Kemuriyama T, Tashiro A, Ohta H, Hagisawa K, Hiruma M, Yokoe H. Effects and biological limitations of +Gz acceleration on the autonomic functions-related circulation in rats. *J Physiol Sci* 2016; **66**: 447-462 [PMID: 27262847 DOI: 10.1007/s12576-016-0461-4]

11   **Lauritzsen LP**, Pfitzner J. Pressure breathing in fighter aircraft for G accelerations and loss of cabin pressurization at altitude--a brief review. *Can J Anaesth* 2003; **50**: 415-419 [PMID: 12670822 DOI: 10.1007/BF03021042]

12   **Cao XS**, Sun XQ, Zhang S, Wang B, Wu YH, Liu TS, Wu XY. Acceleration after-effects on learning and memory in rats: +10 Gz or +6 Gz for 3 min. *Neurosci Lett* 2007; **413**: 245-248 [PMID: 17175101 DOI: 10.1016/j.neulet.2006.11.055]

13   **Zhou Y**, Wang B, Wang YC, Wu YH, Zhang S, Geng J, Sun XQ. [Apoptosis in myocyte after repeated + Gz exposures in rats]. *Zhongguo Ying Yong Sheng Li Xue Za Zhi* 2010; **26**: 275-277 [PMID: 21038668]

14   **Sun XQ**, Zhang LF, Wu XY, Jiang SZ. Effect of repeated +Gz exposures on energy metabolism and some ion contents in brain tissues of rats. *Aviat Space Environ Med* 2001; **72**: 422-426 [PMID: 11346006]

15   **Sousa L**, Pessoa MTC, Costa TGF, Cortes VF, Santos HL, Barbosa LA. Iron overload impact on P-ATPases. *Ann Hematol* 2018; **97**: 377-385 [PMID: 29307086 DOI: 10.1007/s00277-017-3222-4]

16   **Suzuki S**, Toledo-Pereyra LH, Rodriguez FJ, Cejalvo D. Neutrophil infiltration as an important factor in liver ischemia and reperfusion injury. Modulating effects of FK506 and cyclosporine. *Transplantation* 1993; **55**: 1265-1272 [PMID: 7685932 DOI: 10.1097/00007890-199306000-00011]

17   **Bonatsos V**, Kappas I, Birbas K, Vlachodimitropoulos D, Toutouzas K, Karampela E, Syrmos N, Bonatsos G, Papalois AE. Effects of U-74389G (21-Lazaroid) and Ascorbic Acid on Liver Recovery After Acute Ischemia and Reperfusion in Rats. *In Vivo* 2015; **29**: 585-594 [PMID: 26359418]

18   **Cannistrà M**, Ruggiero M, Zullo A, Gallelli G, Serafini S, Maria M, Naso A, Grande R, Serra R, Nardo B. Hepatic ischemia reperfusion injury: A systematic review of literature and the role of current drugs and biomarkers. *Int J Surg* 2016; **33** Suppl 1: S57-S70 [PMID: 27255130 DOI: 10.1016/j.ijsu.2016.05.050]

19   **de Oliveira THC**, Marques PE, Poosti F, Ruytinx P, Amaral FA, Brandolini L, Allegretti M, Proost P, Teixeira MM. Intravital Microscopic Evaluation of the Effects of a CXCR2 Antagonist in a Model of Liver Ischemia Reperfusion Injury in Mice. *Front Immunol* 2018; **8**: 1917 [PMID: 29379500 DOI: 10.3389/fimmu.2017.01917]

20   **Peralta C**, Jiménez-Castro MB, Gracia-Sancho J. Hepatic ischemia and reperfusion injury: effects on the liver sinusoidal milieu. *J Hepatol* 2013; **59**: 1094-1106 [PMID: 23811302 DOI: 10.1016/j.jhep.2013.06.017]

21   **Chu MJ**, Premkumar R, Hickey AJ, Jiang Y, Delahunt B, Phillips AR, Bartlett AS. Steatotic livers are susceptible to normothermic ischemia-reperfusion injury from mitochondrial Complex-I dysfunction. *World J Gastroenterol* 2016; **22**: 4673-4684 [PMID: 27217699 DOI: 10.3748/wjg.v22.i19.4673]

22   **Heller MT**, Tublin ME. The role of ultrasonography in the evaluation of diffuse liver disease. *Radiol Clin North Am* 2014; **52**: 1163-1175 [PMID: 25444098 DOI: 10.1016/j.rcl.2014.07.013]

23   **Iranpour P**, Lall C, Houshyar R, Helmy M, Yang A, Choi JI, Ward G, Goodwin SC. Altered Doppler flow patterns in cirrhosis patients: an overview. *Ultrasonography* 2016; **35**: 3-12 [PMID: 26169079 DOI: 10.14366/usg.15020]

24   **Kim HS**, Kim YW. Expression of phosphorylated extracellular signal-regulated kinase in rat kidneys exposed to high +Gz. *Bosn J Basic Med Sci* 2012; **12**: 269-272 [PMID: 23198944 DOI: 10.17305/bjbms.2012.2453]

25   **Chen LE**, Wu F, Zhao A, Ge H, Zhan H. Protection Efficacy of the Extract of Ginkgo biloba against the Learning and Memory Damage of Rats under Repeated High Sustained +Gz Exposure. *Evid Based Complement Alternat Med* 2016; **2016**: 6320586 [PMID: 27069491 DOI: 10.1155/2016/6320586]

26   **Luczaj W**, Skrzydlewska E. [The present-day look at lipid peroxidation]. *Postepy Biochem* 2006; **52**: 173-179 [PMID: 17078507]

27   **Nakagawa K**, Kato S, Miyazawa T. Determination of Phosphatidylcholine Hydroperoxide (PCOOH) as a Marker of Membrane Lipid Peroxidation. *J Nutr Sci Vitaminol (Tokyo)* 2015; **61** Suppl: S78-S80 [PMID: 26598897 DOI: 10.3177/jnsv.61.S78]

28   **Daligcon BC**, Oyama J. Hyper-G stress-induced hyperglycemia in rats mediated by glucoregulatory hormones. *Aviat Space Environ Med* 1985; **56**: 37-42 [PMID: 3883981]

29   **Daligcon BC**, Oyama J, Hannak K. Increased gluconeogenesis in rats exposed to hyper-G stress. *Life Sci* 1985; **37**: 235-241 [PMID: 4010477 DOI: 10.1016/0024-3205(85)90649-6]

30   **Niu ZY**, Zhang JZ, Shi SG, Wu B, Li D, Dang P, Kan GH. Effect of hypergravity on expression of c-fos gene in hepatocytes of Rhesus macaque. *Shijie Huaren Xiaohua Zazhi* 2006; **14**: 2793-2795 [DOI: 10.11569/wcjd.v14.i28.2793]

Retrospective Study

Incidence and treatment of mediastinal leakage after esophagectomy: Insights from the multicenter study on mediastinal leaks

Uberto Fumagalli, Gian Luca Baiocchi, Andrea Celotti, Paolo Parise, Andrea Cossu, Luigi Bonavina, Daniele Bernardi, Giovanni de Manzoni, Jacopo Weindelmayer, Giuseppe Verlato, Stefano Santi, Giovanni Pallabazzer, Nazario Portolani, Maurizio Degiuli, Rossella Reddavid, Stefano de Pascale

ORCID number: Uberto Fumagalli (0000-0001-5163-4546); Gian Luca Baiocchi (0000-0003-2402-2178); Andrea Celotti (0000-0003-2246-0684); Paolo Parise (0000-0003-0404-4118); Andrea Cossu (0000-0002-4239-3194); Luigi Bonavina (0000-0002-4880-1670); Daniele Bernardi (0000-0002-1109-7974); Giovanni de Manzoni (0000-0002-6787-164X); Jacopo Weindelmayer (0000-0002-9859-6038); Giuseppe Verlato (0000-0001-5262-8818); Stefano Santi (0000-0002-1613-5896); Giovanni Pallabazzer (0000-0003-2495-7635); Nazario Portolani (0000-0003-2606-0020); Maurizio Degiuli (0000-0002-9812-7020); Rossella Reddavid (0000-0003-0603-9953); Stefano de Pascale (0000-0002-2722-822X).

Author contributions: Fumagalli U and de Pascale S conceived and designed the study; Fumagalli U implemented the study and drafted the article; Celotti A made substantial contributions to the acquisition and analysis of data; Baiocchi GL made substantial contributions to the analysis and interpretation of data; Verlato G reviewed the statistical analysis. All authors substantially contributed to the interpretation of data, made critical revisions related to important intellectual content of the manuscript, and approved the final version of the manuscript.

Uberto Fumagalli, Department of Digestive Surgery, IEO European Institute of Oncology IRCCS, Milano 20141, Italy

Gian Luca Baiocchi, Nazario Portolani, Department of Clinical and Experimental Studies, Surgical Clinic, University of Brescia, Brescia 25123, Italy

Andrea Celotti, Stefano de Pascale, General Surgery 2, ASST Spedali Civili di Brescia, Brescia 25123, Italy

Paolo Parise, Andrea Cossu, Department of Gastrointestinal Surgery, San Raffaele Hospital, Vita-Salute San Raffaele University, Milano 20132, Italy

Luigi Bonavina, Daniele Bernardi, Department of Surgery, IRCCS Policlinico San Donato, University of Milan, Milano 20122, Italy

Giovanni de Manzoni, Jacopo Weindelmayer, General and Upper GI Surgery Division, University of Verona, Verona 37134, Italy

Giuseppe Verlato, Department of Diagnostics and Public Health, University of Verona, Verona 37134, Italy

Stefano Santi, Giovanni Pallabazzer, Esophageal Surgery Unit, Tuscany Regional Referral Center for the Diagnosis and Treatment of Esophageal Disease, Cisanello Hospital, Pisa 56124, Italy

Maurizio Degiuli, Rossella Reddavid, University of Turin, Department of Oncology, Surgical Oncology and Digestive Surgery, San Luigi University Hospital, Orbassano 10043, Italy

Corresponding author: Uberto Fumagalli, MD, Director, Surgical Oncologist, Department of Digestive Surgery, IEO European Institute of Oncology IRCCS, Via Ripamonti 435, Milano 20141, Italy. ubertofumagalliromario@gmail.com
Telephone: +39-2-57489680
Fax: +39-2-57489930

Abstract

BACKGROUND
Mediastinal leakage (ML) is one of the most feared complications of esophagectomy. A standard strategy for its diagnosis and treatment has been

difficult to establish because of the great variability in their incidence and mortality rates reported in the existing series.

AIM

To assess the incidence, predictive factors, treatment, and associated mortality rate of mediastinal leakage using the standardized definition of mediastinal leaks recently proposed by the Esophagectomy Complications Consensus Group (ECCG).

METHODS

Seven Italian surgical centers (five high-volume, two low-volume) affiliated with the Italian Society for the Study of Esophageal Diseases designed and implemented a retrospective study including all esophagectomies (n = 501) with intrathoracic esophagogastric anastomosis performed from 2014 to 2017. Anastomotic MLs were defined according to the classification recently proposed by the ECCG.

RESULTS

Fifty-nine cases of ML were recorded, yielding an overall incidence of 11.8% (95%CI: 9.1%-14.9%). The surgical approach significantly influenced the occurrence of ML: the proportion of leakage was 10.5% and 9% after open and hybrid esophagectomy (HE), respectively, and doubled (20%) after totally minimally invasive esophagectomy (TMIE) (P = 0.016). No other predictive factors were found. The 30- and 90-d overall mortality rates were 1.4% and 3.2%, respectively; the 30- and 90-d leak-related mortality rates were 5.1% and 10.2%, respectively; the 90-d mortality rates for TMIE and HE were 5.9% and 1.8%, respectively. Endoscopy was the first-line treatment in 49% of ML cases, with the need for retreatment in 17.2% of cases. Surgery was needed in 44.1% of ML cases. Endoscopic treatment had the lowest mortality rate (6.9%). Removal of the gastric tube with stoma formation was necessary in 8 (13.6%) cases.

CONCLUSION

The incidence of ML after esophagectomy was high mainly in the TMIE group. However, the general and specific (leak-related) mortality rates were low. Early treatment (surgical or endoscopic) of severe leaks is mandatory to limit related mortality.

Key words: Transthoracic esophagectomy; Minimally invasive esophagectomy; Mediastinal leak; Esophagectomy complications

Core tip: Anastomotic mediastinal leaks represent one of the most feared complications of esophageal resection. The incidence of mediastinal leaks and their associated mortality rates are reported with great variability, and a standard strategy for the diagnosis and treatment has been difficult to establish. Data on all esophagectomies performed in seven Italian centers from 2014 to 2017 were collected and analyzed. The two take-home messages of our multicenter retrospective study are as follows: (1) the surgical approach significantly influenced the rate of mediastinal leaks, with the highest leakage rate occurring after totally minimally invasive esophagectomy and lowest rate occurring after hybrid esophagectomy; and (2) early (surgical or endoscopic) treatment of mediastinal leaks is an essential tool to address this complication and prevent other major complications of esophagectomy.

INTRODUCTION

Cancer of the esophagus is a highly malignant disease with a poor prognosis. Surgical treatment is usually indicated for localized disease. Notwithstanding recent improvements in perioperative care, esophagectomy is still a highly invasive surgical procedure, with significant morbidity rates ranging from 50% to 60%[1-3] and 30- and 90-d mortality rates as high as 3% and 7.4%, respectively[4].

Minimally invasive esophagectomy was introduced with the aim of improving postoperative morbidity rates[5]. However, the application of this approach may require a modification of the technique for esophagogastric anastomosis, possibly affecting the results of esophagectomy in terms of the leakage rate[6].

Anastomotic mediastinal leakage (ML) represents one of the most feared complications of esophageal resection. MLs are associated with a wide spectrum of complications, such as mediastinitis, sepsis, and acute respiratory distress syndrome, in addition to prolonged hospitalization and decreased quality of life. Studies have also shown that MLs are associated with a reduced life expectancy[7,8]. The incidence, the associated mortality rates, and the treatment strategies of MLs reported in the literature vary widely[5].

Additionally, a variety of factors have been described as correlated with this complication[9,10]. Therefore, a standard strategy for both the diagnosis and treatment of MLs remains difficult to establish.

In this context, studies using standardized and commonly agreed upon definitions of postoperative complications and relying on large and comprehensive datasets of esophagectomies are very welcome. The aim of this retrospective study [multicenter study on mediastinal leaks (MuMeLe)] was to evaluate the incidence, predictive factors, treatments, and associated mortality rates of ML after transthoracic esophagectomy in seven Italian surgical centers (5 high-volume and 2 low-volume), which are members of the Italian Society for the Study of Esophageal Diseases (SISME) and form a representative sample of Italian centers with surgical teams having significant expertise in esophageal resection.

MATERIALS AND METHODS

Ethics

The study was approved by the Institutional Review Board of the Department of Clinical and Experimental Sciences of the University of Brescia, Italy. Informed consent for the surgical procedure was obtained from the patients after explaining to them that they were suitable candidates for transthoracic esophagectomy with intrathoracic esophagogastric anastomosis given their diagnosis. Patients were not required to provide informed consent for the study because the analysis used anonymous clinical data that were obtained after each patient agreed to treatment by written consent.

Patients and surgical procedures

A total of 501 patients (416 men and 85 women; Table 1) were identified by retrospective review of the prospectively maintained medical databases of the seven Italian surgical centers participating in this study. Five centers were considered high-volume centers, performing more than 20 esophagectomies per year. The global database included all patients who underwent transthoracic esophagectomy with intrathoracic esophagogastric anastomosis from 2014 to 2017. Esophago-jejunal, esophago-colic, and neck anastomoses were excluded.

Most (78.6%) patients had adenocarcinoma. Neoadjuvant treatment was administered to 62.7% of the patients. Body mass index (BMI) ranged from 15 to 35 kg/m^2.

Common approaches for performing transthoracic esophagectomy were laparotomy and thoracotomy (152 patients), laparoscopy and thoracotomy [hybrid esophagectomy (HE); 244 patients], and laparoscopy and thoracoscopy [totally minimally invasive esophagectomies (TMIE); 105 patients]. Minimally invasive techniques were routinely used in four surgical centers, whereas robotic surgery was a routine procedure in one center. These four centers had a large experience with the hybrid technique, whereas the number of totally minimally invasive esophagectomies should be considered to be still in the learning curve for all 7 centers. One center had the largest experience with TMIE including more than 60 cases.

Mechanical, semimechanical, and manual anastomosis was performed according to thoracic access and the surgeon's preference at each center. Most (90.3%) patients did not undergo any pyloric procedures during surgery. Nutritional jejunostomy was

Table 1 Patients' characteristics and perioperative information

	Number of patients	Patients with ML *n* (%)	*P* value
Total	501	59 (11.8)	
ASA score			0.43
1-2	266	32 (12.0)	
3-4	158	24 (15.2)	
Histology			0.96
Adenocarcinoma	385	44 (11.4)	
Squamous carcin.	101	12 (11.8)	
Other	7	2 (28.5)	
T			0.34
1-2	212	34 (16.0)	
3-4	280	34 (12.1)	
N			0.098
0	200	36 (18.0)	
+	274	31 (11.3)	
Neoadjuvant chemotherapy			0.89
Yes	314	37 (11.8)	
No	187	22 (11.8)	
Pyloric procedure			0.14
Yes	53	10 (18.9)	
No	448	49 (10.9)	
	Patients with no ML	Patients with ML	*P* value
Median body mass index (range)	25 (15-33.3)	27.5 (17.7-35)	0.0328
Median surgery duration (range)	360 (127-700)	330 (173-615)	0.6707

ML: Mediastinal leakage.

routinely positioned in only some surgical centers.

Standardization of the definitions of major postoperative complications is a fundamental step for delivering accurate analyses and facilitating global comparisons, which are prerequisites for proposing quality improvement strategies[11,12]. Therefore, anastomotic leakages were defined here according to the taxonomy recently proposed by the Esophagectomy Complications Consensus Group[11]: Full thickness GI defect involving the esophagus, anastomosis, staple line, or conduit irrespective of presentation or method of identification and graded into 3 types: Type I - local defect requiring no change in therapy or treated medically or with dietary modification; Type II - localized defect requiring interventional but not surgical therapy, for example, interventional radiology drain, stent or bedside opening, and packing of incision; Type III - localized defect requiring surgical therapy.

Statistical analysis

The following variables were coded and analyzed to assess their correlation with ML development: patient ASA score and BMI, tumor histology and stage, use of neoadjuvant treatment, pyloric procedure, duration of surgery, surgical approach, and anastomotic technique.

The Mann-Whitney *U* test was used to compare continuous variables not normally distributed [presented as the median and interquartile range (IQR)]. The normality of the distribution of variables was determined using the D'Agostino-Pearson test. Chi-square or Fisher's exact tests, when appropriate, were used to compare categorical variables. Statistical analysis was performed with statistical software for biomedical research (MedCalc Software for Windows).

The statistical methods of this study were reviewed by Giuseppe Verlato, Professor of Biostatics, Department of Diagnostics and Public Health, University of Verona, Verona, Italy.

RESULTS

The analysis of the entire set of 501 esophagectomies performed from 2014 to 2017 in seven Italian centers with expertise in esophageal resection delivered the following findings.

First, the overall incidence of ML was 11.8%, with a leakage rate varying across centers from 1.6% to 20% (Table 2). Leakage incidence did not correlate with center volume.

The median postoperative day of diagnosis of the ML was the third postoperative day (range: 1-58) (Table 3). Leaks were diagnosed as follows: 38 radiologically, 18 endoscopically, 2 clinically, and 1 surgically.

Second, the 30- and 90-d total mortality rates were 1.4% and 3.2%, respectively. Meanwhile, the 30- and 90-d leak-related mortality rates were 0.6% and 1.8%, respectively. Among the patients who developed this postoperative complication, the 30- and 90-d mortality rates were 5.1% and 10.2, respectively.

Third, the ASA score, tumor histology and stage, use of preoperative (neoadjuvant) treatment, and duration of surgery did not correlate with the occurrence of ML. BMI was significantly correlated with an increased risk of ML ($P = 0.032$) (Table 1).

Fourth, the surgical approach significantly influenced the incidence rate of ML (Table 4): the proportion of leakages was 10.5% and 9% after open Ivor Lewis esophagectomy (IL) and HE, respectively, and doubled (20%) after TMIE ($P = 0.016$). The 30-d mortality rates for TMIE and HE were 5.9% and 1.8%, respectively ($P = 0.03$). Most anastomoses in TMIE were performed with a semimechanical linear side-to-side technique, whereas only a few were performed manually.

Fifth, conservative treatment was the first-line treatment in 13.6% of ML cases (Table 5). Endoscopy was the first-line treatment in 49% of ML cases; most of these patients either had an endoscopic stent or a nasoesophageal extraluminal drain placed. Other endoscopic treatments (clips or glue) were seldom used. Surgery, as a first-line treatment, consisting of surgical debridement with or without stent placement, re-anastomosis or demontage, was performed in 37.3% of patients. Surgery was generally the preferred treatment for very early leaks when a redo anastomosis was considered the elective treatment before septic signs would appear. The presence of ischemic tissue at the anastomotic site or septic patients with non-contained leaks represented the other instances in which surgery was considered the recommended treatment and, as such, it was performed. Surgery was also performed when conservative treatment had failed.

Endoscopy had the highest rate of retreatment (17.2%) but the lowest mortality rate (6.9%). Surgery as a primary, secondary, or tertiary treatment was needed globally in 44.1% of ML cases. Removal of the gastric tube with stoma formation was considered necessary in 8 (13.6%) cases.

DISCUSSION

The MuMeLe study group, consisting of 5 high-volume and 2 low-volume surgical centers affiliated with the Italian Society for the Study of Esophageal Diseases, serves as a representative sample of the Italian surgical community with expertise in esophageal resection. Similar to a recent worldwide trend[3,13], minimally invasive techniques were used in a significantly high percentage of the total number (349/501, 69.6%) of esophagectomies performed in these seven Italian surgical centers from 2014 to 2017.

The incidence of ML reported in the MuMeLe series (11.8%) was higher than expected (although widely varying across the seven surgical centers) and higher than rates reported in other recent western series[7,14], which vary from 6.8% to 9.3% (the incidence of ML in the Swedish database including 559 patients undergoing surgery from 2001 to 2005 was 7.9%[8]). The western series, however, display incidence rates of ML that are significantly higher than those in eastern series (Table 6): for example, Guo *et al*[15] recently reported an incidence rate of ML after esophagectomy of 1.8%, significantly lower than the 6.3% reported in the latest results from the United Kingdom National Oesophago-Gastric Cancer Audit[14].

The main novel finding from the analysis of our series is that technical aspects of esophageal resection, more specifically the use of a minimally invasive approach, seem to be one of the two predictive factors for the occurrence of ML (BMI being the other). In contrast, other factors, such as tumor histology and stage, multimodality treatment, and duration of surgery, did not seem to influence the occurrence of this postoperative surgical complication. From this perspective, the findings from our series are consistent with similar findings in the literature. More specifically, Rutegård *et al*[8] found no statistically significant predictive factors for the occurrence of ML; however, the period examined in that series did not include minimally invasive IL

Table 2 Number of esophagectomies and leaks by center								
Center	**1**	**2**	**3**	**4**	**5**	**6**	**7**	**All**
Number of esophagectomies	64	66	16	127	62	151	15	501
Number of leaks	1	3	1	10	11	30	3	59
Leak/esophagectomies (%)	1.6	4.5	6.3	7.9	17.7	19.9	20.0	11.8

Centers 1, 2, 4, 5, and 6 are high-volume centers, whereas centers 3 and 7 are low- volume centers.

(MIIL) esophagectomies. Another study found that neoadjuvant therapy did not seem to carry an inherent risk of esophageal leakage greater than the baseline risk[16].

Other predictive factors for anastomotic leakage have been reported in the literature, such as factors involved in vascularization of the gastric tube, associated diseases (cardiovascular diseases, diabetes, renal insufficiency), active smoking, corticosteroid use[9], center volume for esophagectomy[17], intraoperative hypotensive episodes[18], intraoperative blood loss, and anastomosis site (cervical *vs* thoracic). Given these findings, strategies to reduce the incidence of ML include techniques for improving the detection of gastric tube vascularization. Intraoperative tools for detecting vascular insufficiency of the gastric tube are now being used routinely in some centers; a significant advantage in reducing the rate of ML with the use of these tools has been reported in the literature[19-22].

In our series, the main predictive factor for ML occurrence was the use of a totally minimally invasive approach. One can speculate that such approaches require the introduction of a new technique for constructing the anastomosis, thus generating a learning curve before reaching satisfactory results in terms of the rate of ML. Interestingly, in a recently published paper on the MIIL approach, the reported mean incidence of anastomotic leakage was 18.8% during the learning curve and 4.5% after the plateau had been reached[23]. The length of the learning curve for preventing anastomotic leakage using the MIIL approach was 119 cases. The four centers performing TMIE are still in the learning curve for this type of procedure, and this factor may partly explain the higher incidence of ML with this approach.

There is still no consensus on the safest anastomotic technique in the MIIL approach; some studies argue that a semimechanical side-to-side anastomotic approach is better[24], whereas other studies maintain that an end-to-side circular anastomosis, though technically more complex, may be safer[25]. Robotic anastomosis may be a suitable alternative[26]. However, data on the different techniques are scant and cannot be used for clinical evidence.

In our series (Table 3), the time of ML diagnosis (median = 3 d) was earlier than that (median = 7 d; range: 3-18) reported in other studies[7], even if the range was definitely wider (1-58 d), with 13 leaks being diagnosed later than 10 d postoperatively. Earlier diagnosis supports the hypothesis that a technical problem during construction of the anastomosis was likely the factor associated with the occurrence of the complication (vascular insufficiency of the gastric tube is usually considered responsible for later leaks[27]).

The 30- and 90-d mortality rates (total and leak-related) in our series can be compared to the corresponding rates reported recently in the literature (Table 7).

The early diagnosis and treatment of ML are key factors for achieving a low mortality rate[28] because one can treat the cause of contamination and sepsis, which in turn increase the mortality rate. MLs are generally associated with a high rate of postoperative mortality, even in a series with a low incidence of ML, which reported a mortality rate of 21.2%[15]. The overall 90-d mortality rate for all patients undergoing esophagectomy was 2.1% in Dent's series[28], quite close to our 90-d mortality rate of 3.2%, which is lower than corresponding values reported in other series.

Even in the totally minimally invasive Ivor Lewis group in our series, in which the incidence of ML was higher than the incidence reported in other series, the ML-related mortality rate was lower than those previously reported in the literature. This means that either the leaks in our series were different (less severe) or the treatment of this complication was quite effective. This latter scenario is in line with the concept of rescuing patients from severe complications. From this perspective, other factors beyond the occurrence of a severe complication such as ML need to be considered: for example, the surgeon and hospital volume[29], the nurse-to-patient ratio, and the multidisciplinary approach to the treatment of the complication can definitely be important in reducing the mortality rate[30].

In our series, most patients with a leak were initially treated either conservatively or endoscopically (Table 5). Endoscopic treatment was usually limited to either

Table 3 Mediastinal leaks and mortality rates in the multicenter study on mediastinal leaks

	TEG	30-d mortality		90-d mortality		Post-op day of diagnosis[1]
		Leak *n* (%)	All *n* (%)	Leak *n* (%)	All *n* (%)	
Patients	501	3 (0.6)	7 (1.4)	9 (1.8)	16 (3.2)	
Leaks[2]	59 (11.8)	3 (5.1)		6 (10.2)		3 (1-58)
Necrosis[2]						
Type I	5			0		8 (4-8)
Type II	30			2 (6.7)	2 (6.7)	4 (1-28)
Type III	24	3 (12.5)		7 (29.2)	10 (41.7)	7 (4-58)
P value		0.038		< 0.001		

[1]Median values for the postoperative day on which the mediastinal leak was diagnosed;
[2]Mediastinal leak was defined according to the taxonomy recently proposed by the Esophageal Complications Consensus Group[11]. TEG: Transthoracic esophagectomy with intrathoracic anastomosis.

endoscopic stenting or nasoesophageal extraluminal drainage because Eso-SPONGE is not yet commercially available in Italy. This factor, as well as the fact that several leaks were diagnosed earlier than the typical timing reported in the literature (indicating a possible technical problem in the construction of the anastomosis), may explain the relatively high number of redo anastomoses.

The need for surgery was similar in our study and in other reported series[15,31], even if the rate of esophageal diversion was higher in our series. Surgical intervention is recommended for septic patients with uncontained leaks or when conservative treatment has failed. Based on our experience and the insights from the analysis of our large series, it is extremely important not to delay the decision to perform surgery in patients with sepsis persisting after conservative treatment. In patients who need surgery when extensive necrosis of the tube is found and/or when the patient's general condition is critical, removal of the gastric tube by cervical esophagostomy and delayed reconstruction should be an option. The anastomosis can be reconstructed only when the gastric tube is well vascularized.

Similar to what has been reported in other studies[16], the mortality rate was higher among patients with leaks treated surgically than among patients with leaks treated endoscopically; this is likely a selection effect because the medical conditions of patients with surgical indications are more severe and patients undergoing surgery have more severe local conditions. We acknowledge that, like other retrospective analyses of prospectively collected data, our study has limitations. In addition, the ML treatment strategies differed among the seven surgical centers, which makes it difficult to recommend a specific treatment strategy for this severe complication. However, the MuMeLe study group is a representative sample of Italian surgical centers with expertise in esophageal resection and, as such, can serve as an important benchmark for future studies. It is also noteworthy that the reported mortality rates in our series are definitely low, which means that the therapeutic choices were overall quite effective despite differing among centers.

In summary, our series shows that the incidence of ML after esophagectomy was high. ML occurred mainly in the group of patients undergoing TMIE, suggesting that technical problems during the initial phase of the learning curve are likely the main drivers behind the occurrence of ML. General and specific (leak-related) mortality rates were, however, low, demonstrating that the therapeutic choices were correct. Based on our experience and the analysis of our series, we strongly believe that the early treatment (surgical or endoscopic) of severe leaks, presenting either directly as severe or causing persistent sepsis after initial conservative treatment, is mandatory, and that there should be no hesitation before reoperation if the first attempt of conservative management fails.

Table 4 Mediastinal leakage rate by surgical technique

	Surgical technique			Total	*P* value
	Open IL	Hybrid IL	MIIL[1]		
Number of TEG	152	244	105	501	
Number of leaks	16	22	21	59	
Leakage rate (%)	10.5	9.0	20.0	11.8	
Necrosis - type I	1	4	0	5	
Necrosis - type II	9	10	11	30	
Necrosis - type III	6	8	10	24	
Hybrid *vs* MI					0.0072
Open *vs* MI					0.0520
Open + hybrid *vs* MI					0.0560

[1]Minimally invasive Ivor Lewis (MIIL) procedure performed in 4 of the 7 surgical centers. Anastomoses in MIIL are mainly semi-mechanical (highest leaking rate compared to manual and mechanical). TEG: Transthoracic esophagectomy with intrathoracic anastomosis; MIIL: Minimally invasive Ivor Lewis; IL: Ivor Lewis; MI: Minimally invasive.

Table 5 Treatment of mediastinal leaks

	Conservative		Endoscopic		Surgical		
	NGT antibiotics	NED	ES	Other	Deb	Redo A	Dem
Primary, *n*	8[1]	11	12	6[2]	6	10	6
Primary, %	13.6		49.2		37.3		
Retreat, *n*	1	2	1	2	2		
Retreat, %	12.5		17.2		9.1		
Secondary	1 stent	2 end stent	1 restent	1 surg+stent; 1 stent	1 redo A 1 restent		
Tertiary		1 reanast		1 reanast; 1 restent	1 dem		
Total leaks	7		26		26		
Mortality	2		2			3	2
Mortality (%)	25		6.9		22.7		

[1]Eight patients: radiologically guided drainage (pleural/mediastinal collections).
[2]One patient transferred to another hospital. NED: Naso-esophageal extraluminal drainage. ES: Endoscopic stent; Other: Other endoscopic treatment (clip, glue); Deb: Surgical debridment with or without stent; Redo A: Redo anastomosis; Dem: Demontage.

Table 6 Mediastinal leakage and mortality rates: Multicenter study on mediastinal leaks and other studies

	Patients	Mortality rates		Leakage rates	Leak-related mortality rates	
Price's in 2013	268	3.7[1]		5.9		
Dent *et al*[28] 2016	377	0[1]		7.2	0	
Van Daele *et al*[9] 2016	412			2.9		
Guo *et al*[15] 2014	1867			1.8	18.2	
		30-d	90-d		30-d	90-d
Rutegård *et al*[8] 2012[2]	559		6.2	7.9		
Kassis *et al*[16] 2013[3]	1559	3.6		9.3		
MuMeLe study[4]	501	1.4	3.2	11.8	5.0	15.3

[1]Operative mortality rate;
[2]Multicenter prospective study;
[3]Multicenter retrospective study;
[4]Multicenter retrospective study. MuMeLe: Multicenter study on mediastinal leaks.

Table 7 Mediastinal leakage and mortality rates by minimally invasive technique: Multicenter study on mediastinal leaks and other studies

Technique	Study	Patients	Operative mortality rate	Mediastinal leakage rate
MIIL	van Workum *et al*[23] 2019	646	2.3	14.4
	Schmidt *et al*[13] 2017	49	6.1	6.1
	Zhang's in 2017	15		0.0
	Mungo *et al*[25] 2016	52	3.8	14.0
	MuMeLe study	105	5.9	20.0
Hybrid	Woodard's in 2017	143	2.5	2.5
	MuMeLe study	244	1.8	9.0

MIIL: Minimally invasive Ivor Lewis; Hybrid: Hybrid Ivor Lewis; MuMeLe: Multicenter study on mediastinal leaks.

ARTICLE HIGHLIGHTS

Research background

Cancer of the esophagus is a highly malignant disease with a poor prognosis. Esophagectomy is still a highly invasive surgical procedure, with significant morbidity rates and mortality rates. Minimally invasive esophagectomy was introduced with the aim of improving postoperative morbidity rates, yet possibly affecting the leakage rate. In fact, anastomotic mediastinal leakage (ML) represents one of the most feared complications of esophageal resection, being associated with mediastinitis, sepsis, acute respiratory distress syndrome, prolonged hospitalization, decreased quality of life, and reduced life expectancy.

Research motivation

A standard strategy for both the diagnosis and treatment of MLs remains difficult to establish because the incidence, the underlying risk factors, the associated mortality rates, and the treatment strategies of MLs reported in the literature vary widely. This heterogeneity in the reported findings is partly explained by the fact that different series and studies use different definitions of ML, which make it difficult to compare their findings, and, hence, to derive clear indications regarding the best strategy for the diagnosis and treatment of MLs.

Research objectives

The aim of our retrospective study was to evaluate the incidence, predictive factors, treatments, and associated mortality rates of ML after transthoracic esophagectomy using a standardized and commonly agreed upon definition of ML recently proposed by the Esophagectomy Complications Consensus Group (ECCG) and relying on a large, multicenter and comprehensive dataset of esophagectomies.

Research methods

The data include all transthoracic esophagectomies intrathoracic esophagogastric anastomosis performed from 2014 to 2017 in seven Italian surgical centers (5 high-volume and 2 low-volume), which form a representative sample of Italian centers with surgical teams having significant expertise in esophageal resection. A total of 501 patients were identified by retrospective review of the prospectively maintained medical databases. MLs, patient ASA score and body mass index (BMI), tumor histology and stage, use of neoadjuvant treatment, pyloric procedure, duration of surgery, surgical approach, and anastomotic technique were coded. The Mann-Whitney U test was used to compare continuous variables not normally distributed [presented as the median and interquartile range (IQR)]. The normality of the distribution of variables was determined using the D'Agostino-Pearson test. Chi-square or Fisher's exact tests, when appropriate, were used to compare categorical variables.

Research results

The overall incidence of ML was 11.8%, with a leakage rate varying across centers from 1.6% to 20%. Leakage incidence did not correlate with center volume. The 30- and 90-d total mortality rates were 1.4% and 3.2%. Meanwhile, the 30- and 90-d leak-related mortality rates were 0.6% and 1.8%. The ASA score, tumor histology and stage, use of preoperative (neoadjuvant) treatment, and duration of surgery did not correlate with the occurrence of ML. BMI was significantly correlated with an increased risk of ML (P = 0.032). The surgical approach significantly influenced the incidence rate of ML: the proportion of leakages was 10.5% and 9% after open Ivor Lewis esophagectomy and hybrid esophagectomy, respectively, and doubled (20%) after total minimally invasive esophagectomy (P = 0.016). Conservative treatment was the first-line treatment in 13.6% of ML cases. Endoscopy was the first-line treatment in 49% of ML cases. Surgery, as a first-line treatment, consisting of surgical debridement with or without stent placement, re-anastomosis or demontage, was performed in 37.3% of patients. Endoscopy had the highest rate of retreatment (17.2%) but the lowest mortality rate (6.9%).

Research conclusions

The main novel finding from the analysis of our series is that technical aspects of esophageal resection, more specifically the use of a minimally invasive approach, seem to be one of the two predictive factors for the occurrence of ML (BMI being the other). In contrast, other factors, such as tumor histology and stage, multimodality treatment, and duration of surgery, did not seem to influence the occurrence of this postoperative surgical complication.

Research perspectives

Our series shows that ML occurred mainly in the group of patients undergoing totally minimally invasive esophagectomy, suggesting that technical problems during the initial phase of the learning curve are likely the main drivers behind the occurrence of ML. The take-home message of our study is that early treatment of severe leaks, presenting either directly as severe or causing persistent sepsis after initial conservative treatment, is mandatory, and that there should be no hesitation before reoperation if the first attempt of conservative management fails. Further studies using large and comprehensive datasets from other countries yet relying on the same standardized definition of ML recently proposed through international consensus by the ECCG will enable to compare different series in a meaningful way. This in turn will significantly improve the understanding of the risk factors, incidence and treatment strategies for mediastinal leaks after esophageal resection.

REFERENCES

1   **Yoshida N**, Baba Y, Watanabe M, Ida S, Ishimoto T, Karashima R, Iwagami S, Imamura Y, Sakamoto Y, Miyamoto Y, Baba H. Original scoring system for predicting postoperative morbidity after esophagectomy for esophageal cancer. *Surg Today* 2015; **45**: 346-354 [PMID: 24997754 DOI: 10.1007/s00595-014-0958-5]

2   **Jiang R**, Liu Y, Ward KC, Force SD, Pickens A, Sancheti MS, Javidfar J, Fernandez FG, Khullar OV. Excess Cost and Predictive Factors of Esophagectomy Complications in the SEER-Medicare Database. *Ann Thorac Surg* 2018; **106**: 1484-1491 [PMID: 29944881 DOI: 10.1016/j.athoracsur.2018.05.062]

3   **Low DE**, Kuppusamy MK, Alderson D, Cecconello I, Chang AC, Darling G, Davies A, D'Journo XB, Gisbertz SS, Griffin SM, Hardwick R, Hoelscher A, Hofstetter W, Jobe B, Kitagawa Y, Law S, Mariette C, Maynard N, Morse CR, Nafteux P, Pera M, Pramesh CS, Puig S, Reynolds JV, Schroeder W, Smithers M, Wijnhoven BPL. Benchmarking Complications Associated with Esophagectomy. *Ann Surg* 2019; **269**: 291-298 [PMID: 29206677 DOI: 10.1097/SLA.0000000000002611]

4   **Rutegård M**, Lagergren P, Johar A, Lagergren J. Time shift in early postoperative mortality after oesophagectomy for cancer. *Ann Surg Oncol* 2015; **22**: 3144-3149 [PMID: 25649859 DOI: 10.1245/s10434-015-4394-6]

5   **Allum WH**, Bonavina L, Cassivi SD, Cuesta MA, Dong ZM, Felix VN, Figueredo E, Gatenby PA, Haverkamp L, Ibraev MA, Krasna MJ, Lambert R, Langer R, Lewis MP, Nason KS, Parry K, Preston SR, Ruurda JP, Schaheen LW, Tatum RP, Turkin IN, van der Horst S, van der Peet DL, van der Sluis PC, van Hillegersberg R, Wormald JC, Wu PC, Zonderhuis BM. Surgical treatments for esophageal cancers. *Ann N Y Acad Sci* 2014; **1325**: 242-268 [PMID: 25266029 DOI: 10.1111/nyas.12533]

6   **Maas KW**, Biere SS, Scheepers JJ, Gisbertz SS, Turrado Rodriguez VT, van der Peet DL, Cuesta MA. Minimally invasive intrathoracic anastomosis after Ivor Lewis esophagectomy for cancer: a review of transoral or transthoracic use of staplers. *Surg Endosc* 2012; **26**: 1795-1802 [PMID: 22294057 DOI: 10.1007/s00464-012-2149-z]

7   **Crestanello JA**, Deschamps C, Cassivi SD, Nichols FC, Allen MS, Schleck C, Pairolero PC. Selective management of intrathoracic anastomotic leak after esophagectomy. *J Thorac Cardiovasc Surg* 2005; **129**: 254-260 [PMID: 15678033 DOI: 10.1016/j.jtcvs.2004.10.024]

8   **Rutegård M**, Lagergren P, Rouvelas I, Lagergren J. Intrathoracic anastomotic leakage and mortality after esophageal cancer resection: a population-based study. *Ann Surg Oncol* 2012; **19**: 99-103 [PMID: 21769467 DOI: 10.1245/s10434-011-1926-6]

9   **Van Daele E**, Van de Putte D, Ceelen W, Van Nieuwenhove Y, Pattyn P. Risk factors and consequences of anastomotic leakage after Ivor Lewis oesophagectomy†. *Interact Cardiovasc Thorac Surg* 2016; **22**: 32-37 [PMID: 26433973 DOI: 10.1093/icvts/ivv276]

10   **Messager M**, Warlaumont M, Renaud F, Marin H, Branche J, Piessen G, Mariette C. Recent improvements in the management of esophageal anastomotic leak after surgery for cancer. *Eur J Surg Oncol* 2017; **43**: 258-269 [PMID: 27396305 DOI: 10.1016/j.ejso.2016.06.394]

11   **Low DE**, Alderson D, Cecconello I, Chang AC, Darling GE, DJourno XB, Griffin SM, Hölscher AH, Hofstetter WL, Jobe BA, Kitagawa Y, Kucharczuk JC, Law SY, Lerut TE, Maynard N, Pera M, Peters JH, Pramesh CS, Reynolds JV, Smithers BM, van Lanschot JJ. International Consensus on Standardization of Data Collection for Complications Associated With Esophagectomy: Esophagectomy Complications Consensus Group (ECCG). *Ann Surg* 2015; **262**: 286-294 [PMID: 25607756 DOI: 10.1097/SLA.0000000000001098]

12   **Baiocchi GL**, Giacopuzzi S, Marrelli D, Reim D, Piessen G, Matos da Costa P, Reynolds JV, Meyer HJ, Morgagni P, Gockel I, Lara Santos L, Jensen LS, Murphy T, Preston SR, Ter-Ovanesov M, Fumagalli Romario U, Degiuli M, Kielan W, Mönig S, Kołodziejczyk P, Polkowski W, Hardwick R, Pera M, Johansson J, Schneider PM, de Steur WO, Gisbertz SS, Hartgrink H, van Sandick JW, Portolani N, Hölscher AH, Botticini M, Roviello F, Mariette C, Allum W, De Manzoni G. International consensus on a complications list after gastrectomy for cancer. *Gastric Cancer* 2019; **22**: 172-189 [PMID: 29846827 DOI: 10.1007/s10120-018-0839-5]

13   **Schmidt HM**, Gisbertz SS, Moons J, Rouvelas I, Kauppi J, Brown A, Asti E, Luyer M, Lagarde SM, Berlth F, Philippron A, Bruns C, Hölscher A, Schneider PM, Raptis DA, van Berge Henegouwen MI, Nafteux P, Nilsson M, Räsanen J, Palazzo F, Rosato E, Mercer S, Bonavina L,

Nieuwenhuijzen G, Wijnhoven BPL, Schröder W, Pattyn P, Grimminger PP, Gutschow CA. Defining Benchmarks for Transthoracic Esophagectomy: A Multicenter Analysis of Total Minimally Invasive Esophagectomy in Low Risk Patients. *Ann Surg* 2017; **266**: 814-821 [PMID: 28796646 DOI: 10.1097/SLA.0000000000002445]

14   **Fischer C**, Lingsma H, Klazinga N, Hardwick R, Cromwell D, Steyerberg E, Groene O. Volume-outcome revisited: The effect of hospital and surgeon volumes on multiple outcome measures in oesophago-gastric cancer surgery. *PLoS One* 2017; **12**: e0183955 [PMID: 29073140 DOI: 10.1371/journal.pone.0183955]

15   **Guo J**, Chu X, Liu Y, Zhou N, Ma Y, Liang C. Choice of therapeutic strategies in intrathoracic anastomotic leak following esophagectomy. *World J Surg Oncol* 2014; **12**: 402 [PMID: 25547979 DOI: 10.1186/1477-7819-12-402]

16   **Kassis ES**, Kosinski AS, Ross P Jr, Koppes KE, Donahue JM, Daniel VC. Predictors of anastomotic leak after esophagectomy: an analysis of the society of thoracic surgeons general thoracic database. *Ann Thorac Surg* 2013; **96**: 1919-1926 [PMID: 24075499 DOI: 10.1016/j.athoracsur.2013.07.119]

17   **Markar S**, Gronnier C, Duhamel A, Bigourdan JM, Badic B, du Rieu MC, Lefevre JH, Turner K, Luc G, Mariette C. Pattern of Postoperative Mortality After Esophageal Cancer Resection According to Center Volume: Results from a Large European Multicenter Study. *Ann Surg Oncol* 2015; **22**: 2615-2623 [PMID: 25605511 DOI: 10.1245/s10434-014-4310-5]

18   **Fumagalli U**, Melis A, Balazova J, Lascari V, Morenghi E, Rosati R. Intra-operative hypotensive episodes may be associated with post-operative esophageal anastomotic leak. *Updates Surg* 2016; **68**: 185-190 [PMID: 27146868 DOI: 10.1007/s13304-016-0369-9]

19   **Ohi M**, Toiyama Y, Mohri Y, Saigusa S, Ichikawa T, Shimura T, Yasuda H, Okita Y, Yoshiyama S, Kobayashi M, Araki T, Inoue Y, Kusunoki M. Prevalence of anastomotic leak and the impact of indocyanine green fluorescein imaging for evaluating blood flow in the gastric conduit following esophageal cancer surgery. *Esophagus* 2017; **14**: 351-359 [PMID: 28983231 DOI: 10.1007/s10388-017-0585-5]

20   **Kumagai Y**, Hatano S, Sobajima J, Ishiguro T, Fukuchi M, Ishibashi KI, Mochiki E, Nakajima Y, Ishida H. Indocyanine green fluorescence angiography of the reconstructed gastric tube during esophagectomy: efficacy of the 90-second rule. *Dis Esophagus* 2018; **31** [PMID: 29897432 DOI: 10.1093/dote/doy052]

21   **Noma K**, Shirakawa Y, Kanaya N, Okada T, Maeda N, Ninomiya T, Tanabe S, Sakurama K, Fujiwara T. Visualized Evaluation of Blood Flow to the Gastric Conduit and Complications in Esophageal Reconstruction. *J Am Coll Surg* 2018; **226**: 241-251 [PMID: 29174858 DOI: 10.1016/j.jamcollsurg.2017.11.007]

22   **Baiocchi GL**, Diana M, Boni L. Indocyanine green-based fluorescence imaging in visceral and hepatobiliary and pancreatic surgery: State of the art and future directions. *World J Gastroenterol* 2018; **24**: 2921-2930 [PMID: 30038461 DOI: 10.3748/wjg.v24.i27.2921]

23   **van Workum F**, Stenstra MHBC, Berkelmans GHK, Slaman AE, van Berge Henegouwen MI, Gisbertz SS, van den Wildenberg FJH, Polat F, Irino T, Nilsson M, Nieuwenhuijzen GAP, Luyer MD, Adang EM, Hannink G, Rovers MM, Rosman C. Learning Curve and Associated Morbidity of Minimally Invasive Esophagectomy: A Retrospective Multicenter Study. *Ann Surg* 2019; **269**: 88-94 [PMID: 28857809 DOI: 10.1097/SLA.0000000000002469]

24   **Irino T**, Tsai JA, Ericson J, Nilsson M, Lundell L, Rouvelas I. Thoracoscopic side-to-side esophagogastrostomy by use of linear stapler-a simplified technique facilitating a minimally invasive Ivor-Lewis operation. *Langenbecks Arch Surg* 2016; **401**: 315-322 [PMID: 26960591 DOI: 10.1007/s00423-016-1396-1]

25   **Mungo B**, Lidor AO, Stem M, Molena D. Early experience and lessons learned in a new minimally invasive esophagectomy program. *Surg Endosc* 2016; **30**: 1692-1698 [PMID: 26123339 DOI: 10.1007/s00464-015-4343-2]

26   **Cerfolio RJ**, Bryant AS, Hawn MT. Technical aspects and early results of robotic esophagectomy with chest anastomosis. *J Thorac Cardiovasc Surg* 2013; **145**: 90-96 [PMID: 22910197 DOI: 10.1016/j.jtcvs.2012.04.022]

27   **Griffin SM**, Lamb PJ, Dresner SM, Richardson DL, Hayes N. Diagnosis and management of a mediastinal leak following radical oesophagectomy. *Br J Surg* 2001; **88**: 1346-1351 [PMID: 11578290 DOI: 10.1046/j.0007-1323.2001.01918.x]

28   **Dent B**, Griffin SM, Jones R, Wahed S, Immanuel A, Hayes N. Management and outcomes of anastomotic leaks after oesophagectomy. *Br J Surg* 2016; **103**: 1033-1038 [PMID: 27146631 DOI: 10.1002/bjs.10175]

29   **Fumagalli U**, Bersani M, Russo A, Melis A, de Pascale S, Rosati R. Volume and outcomes after esophageal cancer surgery: the experience of the Region of Lombardy-Italy. *Updates Surg* 2013; **65**: 271-275 [PMID: 23943409 DOI: 10.1007/s13304-013-0227-y]

30   **Liou DZ**, Serna-Gallegos D, Mirocha J, Bairamian V, Alban RF, Soukiasian HJ. Predictors of Failure to Rescue After Esophagectomy. *Ann Thorac Surg* 2018; **105**: 871-878 [PMID: 29397102 DOI: 10.1016/j.athoracsur.2017.10.022]

31   **Schaheen L**, Blackmon SH, Nason KS. Optimal approach to the management of intrathoracic esophageal leak following esophagectomy: a systematic review. *Am J Surg* 2014; **208**: 536-543 [PMID: 25151186 DOI: 10.1016/j.amjsurg.2014.05.011]

Retrospective Study

Predicting gastroesophageal varices through spleen magnetic resonance elastography in pediatric liver fibrosis

Haesung Yoon, Hyun Joo Shin, Myung-Joon Kim, Seok Joo Han, Hong Koh, Seung Kim, Mi-Jung Lee

ORCID number: Haesung Yoon (0000-0003-0581-8656); Hyun Joo Shin (0000-0002-7462-2609); Myung-Joon Kim (0000-0002-4608-0275); Seok Joo Han (0000-0001-5224-1437); Hong Koh (0000-0002-3660-7483); Seung Kim (0000-0003-4373-9828); Mi-Jung Lee (0000-0003-3244-9171).

Haesung Yoon, Hyun Joo Shin, Myung-Joon Kim, Mi-Jung Lee, Department of Radiology, Severance Hospital, Severance Pediatric Liver Disease Research Group, Research Institute of Radiological Science, Yonsei University College of Medicine, Seoul 03722, South Korea

Seok Joo Han, Department of Surgery, Severance Hospital, Severance Pediatric Liver Disease Research Group, Yonsei University College of Medicine, Seoul 03722, South Korea

Hong Koh, Seung Kim, Division of Gastroenterology, Hepatology and Nutrition, Department of Pediatrics, Severance Children's Hospital, Severance Pediatric Liver Disease Research Group, Yonsei University College of Medicine, Seoul 03722, South Korea

Corresponding author: Mi-Jung Lee, MD, PhD, Assistant Professor, Department of Radiology, Severance Hospital, Severance Pediatric Liver Disease Research Group, Research Institute of Radiological Science, Yonsei University College of Medicine, 50-1 Yonsei-ro, Seodaemun-gu, Seoul 03722, South Korea. mjl1213@yuhs.ac
Telephone: +82-2-22287400
Fax: +82-2-3933035

Author contributions: Yoon H and Lee MJ designed the research; Yoon H, Shin HJ and Lee MJ performed the research and wrote the manuscript; Yoon H, Shin HJ and Lee MJ analyzed the data; Kim MJ, Han SJ, Koh H and Kim S contributed analytic tools; Yoon H, Shin HJ, Kim MJ, Han SJ, Koh H, Kim S and Lee MJ revised and approved the final version.

Institutional review board statement: This study was reviewed and approved by the local ethics committee of the Severance Hospital, Yonsei University.

Informed consent statement: Because of the retrospective and anonymous character of this study, the need for informed consent was waived by the institutional review board.

Conflict-of-interest statement: All authors declare no conflicts-of-interest related to this article.

Data sharing statement: No additional data are available.

Open-Access: This is an open-access article that was selected by an in-house editor and fully peer-reviewed by external reviewers. It is distributed in accordance with

Abstract

BACKGROUND
A recent retrospective study confirmed that hepatic stiffness and splenic stiffness measured with magnetic resonance elastography (MRE) are strongly associated with the presence of esophageal varices. In addition, strong correlations have been reported between splenic stiffness values measured with MRE and hepatic venous pressure gradients in animal models. However, most studies have been conducted on adult populations, and previous pediatric MRE studies have only demonstrated the feasibility of MRE in pediatric populations, while the actual clinical application of spleen MRE has been limited.

AIM
To assess the utility of splenic stiffness measurements by MRE to predict gastroesophageal varices in children.

METHODS
We retrospectively reviewed abdominal MRE images taken on a 3T system in pediatric patients. Patients who had undergone Kasai operations for biliary atresia were selected for the Kasai group, and patients with normal livers and spleens were selected for the control group. Two-dimensional spin-echo echo-planar MRE acquisition centered on the liver, with a pneumatic driver at 60 Hz and a low amplitude, was performed to obtain hepatic and splenic stiffness values. Laboratory results for aspartate aminotransferase to platelet ratio index

(APRI) were evaluated within six months of MRE, and the normalized spleen size ratio was determined with the upper normal size limit. All Kasai group patients underwent gastroesophageal endoscopy during routine follow-up. The Mann-Whitney U test, Kendall's tau b correlation and diagnostic performance analysis using the area under the curve (AUC) were performed for statistical analysis.

RESULTS
The median spleen MRE value was 5.5 kPa in the control group (n = 9, age 9-18 years, range 4.7-6.4 kPa) and 8.6 kPa in the Kasai group (n = 22, age 4-18 years, range 5.0-17.8 kPa). In the Kasai group, the APRI, spleen size ratio and spleen MRE values were higher in patients with portal hypertension (n = 11) than in patients without (n = 11) (all $P < 0.001$) and in patients with gastroesophageal varices (n = 6) than in patients without (n = 16) (all $P < 0.05$), even though their liver MRE values were not different. The APRI (τ = 0.477, P = 0.007), spleen size ratio (τ = 0.401, P = 0.024) and spleen MRE values (τ = 0.426, P = 0.016) also correlated with varices grades. The AUC in predicting gastroesophageal varices was 0.844 at a cut-off of 0.65 (100% sensitivity and 75% specificity) for the APRI, and 0.844 at a cut-off of 9.9 kPa (83.3% sensitivity and 81.3% specificity) for spleen MRE values.

CONCLUSION
At a cut-off of 9.9 kPa, spleen MRE values predicted gastroesophageal varices as well as the APRI and spleen size ratio in biliary atresia patients after the Kasai operation. However, liver MRE values were not useful for this purpose.

Key words: Biliary atresia; Magnetic resonance elastography; Kasai operation; Splenic stiffness; Portal hypertension

Core tip: Non-invasive monitoring of portal hypertension is important in children with hepatic fibrosis. Spleen magnetic resonance elastography (MRE) values predicted gastroesophageal varices at a cut-off of 9.9 kPa in biliary atresia patients after the Kasai operation, and the diagnostic performance was comparable to that of the aspartate aminotransferase to platelet ratio index and the spleen size ratio. However, liver MRE values did not differ in patients with and without portal hypertension or gastroesophageal varices.

INTRODUCTION

Biliary atresia is a perinatal disease of unclear etiology characterized by inflammatory obstruction of the biliary tree, leading to biliary cirrhosis and early death if left untreated. The Kasai hepatoportoenterostomy is the first surgical step aimed at restoring bile flow. Performing the Kasai operation earlier increases its chance of success[1]. However, even if the Kasai operation is performed in the first month of life, up to 60% of children who receive the operation will require liver transplantation before the age of 20 years due to liver cirrhosis[2,3]. In 70% of children with successfully established bile drainage, the disease progresses, presenting as fibrosis, portal hypertension and cirrhosis[3]. Therefore, regular long-term monitoring of fibrosis and cholestasis is important for patients with biliary atresia[4].

Liver biopsy is the reference standard for evaluating hepatic fibrosis. However, repeated monitoring with liver biopsy is difficult because of its invasive nature, relatively high cost, small sampling size, interpretational variability and limited patient acceptance, especially in children[5-8]. As a result of these limitations, many investigators have focused on identifying alternative, noninvasive methods to assess

hepatic fibrosis. Magnetic resonance elastography (MRE) is an imaging technique that assesses tissue stiffness by measuring the speed of shear wave propagation within the parenchyma. MRE can quantitatively measure the stiffness of the liver parenchyma to facilitate safe, rapid, cost-effective and noninvasive evaluations of a wide range of hepatic diseases. MRE hepatic stiffness values correlate well with hepatic fibrosis, and thus play a crucial role in monitoring disease progression in adults with chronic liver disease[9-11]. Through the use of MRE, it is possible to measure both hepatic stiffness and splenic stiffness and comprehensively assess liver fibrosis and portal hypertension.

Previous studies have revealed that splenic stiffness best correlates with the presence of gastroesophageal varices observed upon endoscopy in chronic liver disease[12,13]. A recent retrospective study confirmed that hepatic stiffness and splenic stiffness measured with MRE are strongly associated with the presence of esophageal varices[14]. In addition, strong correlations have been reported between splenic stiffness values measured with MRE and hepatic venous pressure gradients in animal models[15,16]. However, most studies have been conducted on adult populations, and previous pediatric MRE studies have only demonstrated the feasibility of MRE in pediatric populations, while the actual clinical application of spleen MRE has been limited.

Therefore, the primary aim of this study was to evaluate the utility of MRE for hepatic and splenic stiffness assessments to evaluate portal hypertension in pediatric patients with biliary atresia after the Kasai operation.

MATERIALS AND METHODS

Patients

Our institutional review board approved this study and waived the requirement for informed consent because of its retrospective nature. From January 2015 to December 2016, we retrospectively reviewed patients who were under the age of 18 and had undergone liver magnetic resonance imaging (MRI), including MRE and T2* mapping, due to various indications. Patients with a history of biliary atresia who had undergone the Kasai operation, with lab results obtained within six months of MRE imaging, were included in the Kasai group. Patients without any previous medical or surgical history who had undergone liver MRI to evaluate the possibility of fatty liver, and who were thereby found to have no liver pathology, were included in the control group. The normal criteria for liver MRI were a hepatic fat fraction < 6%[17], liver MRE values < 2.71 kPa[18,19] and a liver T2* value > 6.7 msec[20].

Clinical charts were reviewed to determine the absence or presence of clinical portal hypertension (PHT). Clinically evident PHT was defined as being present when there was either a history of a complication of PHT (esophageal or gastric variceal bleed, ascites or hepatopulmonary syndrome) or clinical findings consistent with PHT in terms of both splenomegaly and thrombocytopenia (platelet count < 150000 cells/mL)[21]. The modified aspartate aminotransferase to platelet ratio index (APRI) was calculated[22]. In the Kasai group, all patients had previous endoscopy results, which were reviewed by one gastroenterologist to determine the presence of varices. The varices grade was classified as 0, no varices; 1, varices running straight; 2, varices with a beaded appearance; and 3, varices running obliquely and tortuously, with a tumor-like appearance[23].

Liver MRI with MRE

Liver MRI was performed with a 3T system (Discovery 750w; GE Healthcare, Milwaukee, WI, United States). The routine liver MRI protocol included coronal and axial single-shot fast spin-echo T2-weighted images for morphological liver assessment, a three-dimensional volumetric multi-echo gradient sequence (IDEAL-IQ; GE Healthcare) for fat quantification using the proton density fat fraction and T2* decay assessment, and MRE. Spleen size was measured as the longest diameter of the spleen on either a coronal or axial image. The spleen size ratio was calculated as the spleen length divided by the suggested upper normal limit of spleen length at each age[24], to compensate for growth effects due to age. The total scan time was less than 15 min, and the imaging study was done without sedation. All patients fasted for at least 4 h prior to MRE.

For MRE, a 19-cm diameter passive pneumatic driver was positioned over the right anterior abdominal wall and attached to an acoustic waveform generator. The driver amplitude power was reduced by 20%, and a 60 Hz waveform was applied to the driver to prevent abdominal wall discomfort and pain in pediatric patients[25]. A two-dimensional spin-echo-based echo-planar MRE sequence was acquired with the

following parameters: repetitive time/echo time = 1000/62, 60 Hz magnetization encoding gradient, 64 × 64 matrix and 8-mm slice thickness with a 2-mm gap and a 38-cm field of view. Four slices were obtained, including the level of the porta hepatis, during a 24-s breath hold. If the patient could not hold his or her breath, the scan was performed while the patient was breathing freely, with a single average rather than multiple averages. Wave images and MRE images with cross-hatching were automatically generated on the operating console.

The inversion algorithm used for stiffness map calculation involved a multi-scale direct inversion. Hepatic stiffness was measured by one experienced radiologist. A single maximum region of interest (ROI) was placed on each stiffness map, mainly in the right hepatic lobe, avoiding large vessels and areas with inadequate wave propagation or cross-hatching marks. The cross-reference tool in our system was used for guidance. The average of four stiffness maps was used to represent the hepatic stiffness of each patient, and the mean values were recorded in kilopascals (kPa). Splenic stiffness was measured through the placement of a free-hand single maximum ROI at each visible splenic area on the stiffness map. The average of the spleen ROIs was used to represent the splenic stiffness of each patient and was recorded in kPa.

Statistical analysis

Data management and statistical calculations were performed with MedCalc software (version 18.10.2, Ostend, Belgium). The Mann-Whitney *U* test was performed for group comparisons. For the varices grade groups, the Kruskal-Wallis test was used for group comparisons, and Kendall's tau b test was used for correlation analysis. Area under the curve (AUC) analyses were also performed to evaluate the diagnostic performance for gastroesophageal varices. *P* values less than 0.05 were considered significant.

RESULTS

Group comparison between the Kasai and control groups

During the study period, 26 biliary atresia patients who had previously undergone the Kasai operation underwent liver MRI including MRE. Four of these patients were excluded: three had a history of splenic artery embolization, and one did not have a spleen MRE value because the spleen was outside the field of view. Thus, a total of 22 patients (10 male and 12 female) were enrolled in the Kasai group, with ages ranging from 4 to 18 years (median age of 10 years). None of the patients had difficulty holding their breath during the liver MRI. All 22 patients had a native liver, and none had a clinical or radiological diagnosis of a hepatic tumor. For the control group, 10 patients met the inclusion criteria. However, one was excluded because the spleen was outside the field of view during MRE. Therefore, nine patients (five male and four female, age 9-18 years with a median of 14 years) were ultimately included in the control group.

Table 1 displays the clinical and radiological results of both groups. The body mass index, hepatic fat fraction and liver T2* values did not differ between the two groups. However, the Kasai group had higher APRI (median 0.61 *vs* 0.33, *P* = 0.033), spleen size (median 11.8 cm *vs* 9.5 cm, *P* = 0.009), spleen size ratio (median 1.03 *vs* 0.83, *P* = 0.004), liver MRE (median 3.4 kPa *vs* 2.2 kPa, *P* < 0.001) and spleen MRE values (median 9.0 kPa *vs* 5.5 kPa, *P* < 0.001) than the control group. The range of spleen MRE values in the control group was 4.7-6.4 kPa.

Group comparison with and without portal hypertension in the Kasai group

In the Kasai group, 11 patients (11/22, 50%) had clinical PHT. The patients with and without PHT (Table 2) did not differ in age (median 10.0 years *vs* 10.0 years, *P* = 0.797). The APRI (median 1.17 *vs* 0.30, *P* < 0.001), spleen size (median 14.6 cm *vs* 9.6 cm, *P* < 0.001), spleen size ratio (median 1.30 *vs* 0.91, *P* < 0.001), and spleen MRE values (median 11.1 kPa *vs* 7.6 kPa, *P* < 0.001) were higher in the patients with PHT than in those without PHT. However, the liver MRE values did not differ between these groups (median 3.7 kPa *vs* 3.1 kPa, *P* = 0.056).

Gastroesophageal varices evaluation in the Kasai group

Six patients were found to have esophageal or gastric varices upon endoscopy. The endoscopies were performed within 0-104 mo of the liver MRI (median 52 mo) in all patients, and within 0-98 mo (median 15 mo) in patients with varices. Four patients had grade 1 esophageal varices, one patient had grade 2 esophageal varices and one patient had grade 2 gastric varices.

When patients with and without gastroesophageal varices were compared (Table 3), the APRI (median 1.21 *vs* 0.40, *P* = 0.013), spleen size ratio (median 1.33 *vs* 0.95, *P* =

Table 1 Patient characteristics in the Kasai group and control group

		Kasai group (*n* = 22)	Control group (*n* = 9)	*P* value[1]
Clinical and laboratory findings	Age (yr)	10.0 (4.0-18.0)	14.0 (9.0-18.0)	0.012
	BMI (kg/m^2)	17.1 (14.8-29.9)	20.6 (14.7-24.2)	0.593
	APRI	0.61 (0.18-5.00)	0.33 (0.18-0.51)	0.033
	Varices	*n* = 6	*n* = 0	
Liver MRI findings	Spleen size (cm)	11.8 (7.1-19.0)	9.5 (7.9-10.1)	0.009
	Spleen size ratio	1.03 (0.63-1.73)	0.83 (0.68-0.92)	0.004
	Liver fat fraction (%)	3.0 (1.0-18.0)	3.1 (2.5-5.8)	0.313
	Liver T2* value (msec)	23.5 (15.0-64.1)	25.6 (12.0-30.0)	0.824
	Liver MRE value (kPa)	3.4 (2.5-6.0)	2.2 (1.6-2.5)	< 0.001
	Spleen MRE value (kPa)	9.0 (5.0-17.8)	5.5 (4.7-6.4)	< 0.001

[1]From the Mann-Whitney *U* test. The values are the median (range). BMI: Body mass index; APRI: Aspartate aminotransferase to platelet ratio index; MRE: Magnetic resonance elastography; MRI: Magnetic resonance imaging.

0.027) and spleen MRE values (median 12.0 kPa *vs* 8.4 kPa, *P* = 0.013) were found to be significantly higher in patients with varices. However, the liver MRE values did not differ between these groups (median 3.7 kPa *vs* 3.3 kPa, *P* = 0.541).

When the groups were compared according to the varices grade, only the APRI (median 0.40, 1.10 and 3.72 for grades 0, 1 and 2; *P* = 0.029) and spleen MRE values (median 8.4, 12.2 and 12.0 for grades 0, 1 and 2; *P* = 0.045) differed among the different grade groups (Figure 1). However, the spleen size (*P* = 0.183) and spleen size ratio (*P* = 0.084) did not differ in this comparison. In the correlation analysis between the measurement variables and varices grades, the APRI (*τ* = 0.477, *P* = 0.007), spleen size ratio (*τ* = 0.401, *P* = 0.024) and spleen MRE values (*τ* = 0.426, *P* = 0.016) correlated with the varices grade (Figure 2).

Table 4 summarizes the diagnostic performance of the APRI, spleen size ratio and spleen MRE values. The APRI had 100% sensitivity and 75.0% specificity for predicting varices when a cut-off value of 0.65 was used (AUC = 0.844). The cut-off value for the spleen size ratio was 1.08, with 83.3% sensitivity and 75.0% specificity (AUC = 0.813). The AUC of the spleen MRE values in predicting varices was 0.844 at a cut-off value of 9.9 kPa. When the AUCs of these three methods were compared, the diagnostic performance was not found to differ among them (Figure 3).

DISCUSSION

The results of our study indicate that spleen MRE values can predict gastroesophageal varices as well as the APRI and spleen size ratio in biliary atresia patients after the Kasai operation. However, liver MRE values did not differ between patients with and without portal hypertension and patients with and without varices. These results are in good agreement with a previous study in adults, which also demonstrated that splenic stiffness values were superior to hepatic stiffness values for identifying the presence of varices in patients with chronic liver disease[26].

One of the major complications of biliary atresia is the development of PHT. Often, PHT is defined by the development of complications, or by endoscopic findings. However, surveillance endoscopy of children with cirrhosis is not undertaken by many pediatric gastroenterologists[21]. Therefore, a clinically accessible and reproducible modality for surveillance is required. Monitoring the APRI or splenomegaly can be an easy way for clinicians to predict liver cirrhosis. In 2011, Chongsrisawat *et al*[27] demonstrated that the APRI (at a cut-off value of 1.92) had 84% sensitivity and 83% specificity for predicting varices in 73 biliary atresia patients after operation. They also found that splenomegaly had high sensitivity and specificity (92% and 85%, respectively). Another study revealed that the APRI (*r* = 0.5, *P* < 0.001) and spleen size (*r* = 0.38, *P* < 0.001) correlated with portal venous pressure in Kasai patients, but had limitations as prognostic factors for variceal development[28]. The APRI (at a cut-off value of 0.6) also had greater predictive accuracy than liver stiffness measurements for esophageal varices in pediatric patients with various liver diseases[29]. Our study also demonstrated the high diagnostic performance of the APRI and spleen size ratio for predicting gastroesophageal varices in biliary atresia patients. However, the APRI is an indirect method of evaluating portal hypertension, and a

Table 2 Characterisics of biliary atresia patients with and without portal hypertension

		With PHT (*n* = 11)	Without PHT (*n* = 11)	*P* value[1]
Clinical and laboratory findings	Age (yr)	10.0 (7.0-18.0)	10.0 (4.0-15.0)	0.797
	BMI (kg/m^2)	16.6 (15.1-25.6)	17.4 (14.8-29.9)	0.797
	APRI	1.17 (0.47-5.00)	0.30 (0.18-1.82)	< 0.001
Liver MRI findings	Spleen size (cm)	14.6 (10.9-19.0)	9.6 (7.1-12.1)	< 0.001
	Spleen size ratio	1.30 (0.97-1.73)	0.91 (0.63-1.06)	< 0.001
	Liver fat fraction (%)	3.0 (1.6-7.0)	2.0 (1.0-18.0)	0.300
	Liver T2* value (msec)	22.5 (15.0-38.8)	24.1 (17.5-64.1)	0.654
	Liver MRE value (kPa)	3.7 (2.9-6.0)	3.1 (2.5-5.7)	0.056
	Spleen MRE value (kPa)	11.1 (7.1-17.8)	7.6 (5.0-9.6)	< 0.001

[1]From the Mann-Whitney *U* test. The values are the median (range). BMI: Body mass index; APRI: Aspartate aminotransferase to platelet ratio index; MRE: Magnetic resonance elastography; MRI: Magnetic resonance imaging; PHT: Portal hypertension.

wide range of cut-off values were reported in the previous studies. Furthermore, to obtain the spleen size ratio, precise anatomical imaging is essential.

Several quantitative elastography technologies using ultrasound such as transient elastography (TE), acoustic radiation force impulse (ARFI) imaging and supersonic shear wave elastography (SSWE) have been used to evaluate liver fibrosis in pediatric patients and showed good correlation between liver fibrosis and elastographic values[30-32]. However, TE has many pitfalls such as more technical failures in children and inability to avoid other structures such as liver vessels and bile ducts[33]. Unlike TE, real-time elastographic methods such as ARFI and SSWE have been integrated to conventional diagnostic ultrasound. However, ARFI cannot produce a real-time quantitative map of liver tissue stiffness, and only a few studies have been performed in children to predict liver fibrosis using SSWE[31,34]. In our study, we performed short liver MRI, including an anatomical sequence and MRE, which could be completed in less than 15 min and did not require sedation. This allowed us to perform a minimal and noninvasive study to evaluate the status of the liver and combined complications during follow-up in patients with biliary atresia after the Kasai operation. We could not only measure spleen size, evaluate anatomical lesions such as morphological cirrhosis and identify biliary complications such as bile cysts or masses, but also perform a functional evaluation using hepatic and splenic stiffness measurements. The spleen size ratio measured from MRI images and spleen MRE values had a good diagnostic performance for predicting gastroesophageal varices in children. However, liver MRE values were not useful for this purpose.

In previous studies, hepatic fibrosis has been found to correlate with liver MRE values in adult patients[35] and children[36]. However, although liver MRE values appear to be a reliable surrogate for liver biopsies in identifying hepatic fibrosis, the pathophysiological basis for their correlation with PHT remains poorly defined. Hepatic stiffness can reflect increased intrahepatic vascular resistance caused by anatomical changes, but it is not likely to be sensitive to changes in portal pressure due to functional vascular changes[37]. Our study revealed no difference in liver MRE values between patients with and without PHT or gastroesophageal varices.

This is the first report of spleen MRE values in children. We obtained spleen MRE values during routine liver MRI with the driver placed on the right side of the abdomen. The normal range of spleen MRE values in our control group (aged 9-18 years) was 4.7-6.4 kPa, with a median of 5.5 kPa. In a previous study in which a 1.5T MRI system was used, the mean spleen MRE value in healthy adult volunteers was 3.6 kPa (ranging from 2.4 to 4.4 kPa) with the driver placed on the right side of the abdomen, and 4.3 kPa (ranging from 3.2 to 5.6 kPa) with the driver on the left side of the abdomen[38]. This indicates that the location of the driver can affect the stiffness value, and this factor needs to be considered when results are interpreted in each clinic.

Our study also demonstrated the clinical usefulness of spleen MRE values in pediatric patients with biliary atresia. Spleen MRE values were higher in patients with portal hypertension than in patients without (median 11.1 kPa *vs* 7.6 kPa, *P* < 0.001) and in patients with gastroesophageal varices than in patients without (median 12.0 kPa *vs* 8.4 kPa, *P* = 0.013). The diagnostic performance of spleen MRE values in predicting gastroesophageal varices was comparable to that of the APRI and spleen size ratio. Therefore, clinicians may start gastroesophageal endoscopy in patients with spleen MRE values above the cut-off value of 9.9 kPa. Moreover, spleen MRE values

Table 3 Characteristics of biliary atresia patients with and without gastroesophageal varices

		With varices (*n* = 6)	Without varices (*n* = 16)	*P* value[1]
Clinical and laboratory findings	Age (yr)	9.0 (7.0-11.0)	10.0 (4.0-18.0)	0.203
	BMI (kg/m^2)	17.1 (15.3-25.6)	17.1 (14.8-29.9)	0.914
	APRI	1.21 (0.83-5.00)	0.40 (0.18-3.39)	0.013
Liver MRI findings	Spleen size (cm)	14.1 (10.9-17.2)	11.1 (7.1-19.0)	0.070
	Spleen size ratio	1.33 (0.97-1.52)	0.95 (0.63-1.73)	0.027
	Liver fat fraction (%)	3.0 (2.2-7.0)	2.8 (1.0-18.0)	0.294
	Liver T2* value (msec)	24.7 (15.0-38.8)	23.5 (17.2-64.1)	0.791
	Liver MRE value (kPa)	3.7 (2.9-4.6)	3.3 (2.5-6.0)	0.541
	Spleen MRE value (kPa)	12.0 (7.1-17.8)	8.4 (5.0-11.4)	0.013

[1]From the Mann-Whitney *U* test. The values are the median (range). BMI: Body mass index; APRI: Aspartate aminotransferase to platelet ratio index; MRE: Magnetic resonance elastography; MRI: Magnetic resonance imaging.

were different at different varices grades, even though the number of patients in each grade was small (four in grade 1 and two in grade 2). Thus, clinicians can use this method to monitor PHT noninvasively.

Although our experience suggests that liver MRI including spleen MRE is a promising tool for assessing biliary atresia patients after the Kasai operation, there are some limitations to this study. First, this was a retrospective study with a limited number of patients in a single center. Also, we lacked portal venous pressure measurements with hepatic venous pressure gradients. At our institution, hepatic venous pressure measurements are not performed in routine practice for patients with biliary atresia after the Kasai operation, and we did not perform an additional invasive procedure for this retrospective analysis. A future study with a large number of patients involving multiple institutions should be considered. Second, there were varying time intervals between gastroesophageal endoscopy and MRE, even though most patients were stable during follow-up. Third, we could not control other factors that can influence hepatic elasticity, since hepatic stiffness reflects not only fibrosis, but also inflammation. Despite these limitations, our study suggests the clinical utility of spleen MRE in pediatric patients with biliary atresia. A further study with a large number of patients with variable varices grades is needed to validate these results.

In conclusion, the median value of normal spleen MRE was 5.5 kPa in children, with a maximum of 6.4 kPa. Spleen MRE values predicted gastroesophageal varices at a cut-off of 9.9 kPa in biliary atresia patients after the Kasai operation, and the diagnostic performance was comparable to that of the APRI and the spleen size ratio. However, liver MRE values did not differ in patients with and without PHT or gastroesophageal varices.

Table 4 Diagnostic performance in assessing the presence of gastroesophageal varices

Parameter	AUC	95%CI	Cut-off value	Sensitivity (%)	Specificity (%)
APRI	0.844	0.627-0.961	> 0.65	100.0	75.0
Spleen size ratio	0.813	0.591-0.945	> 1.08	83.3	75.0
Spleen MRE (kPa)	0.844	0.627-0.961	> 9.9	83.3	81.3

APRI: Aspartate aminotransferase to platelet ratio index; MRE: Magnetic resonance elastography; AUC: Area under the curve.
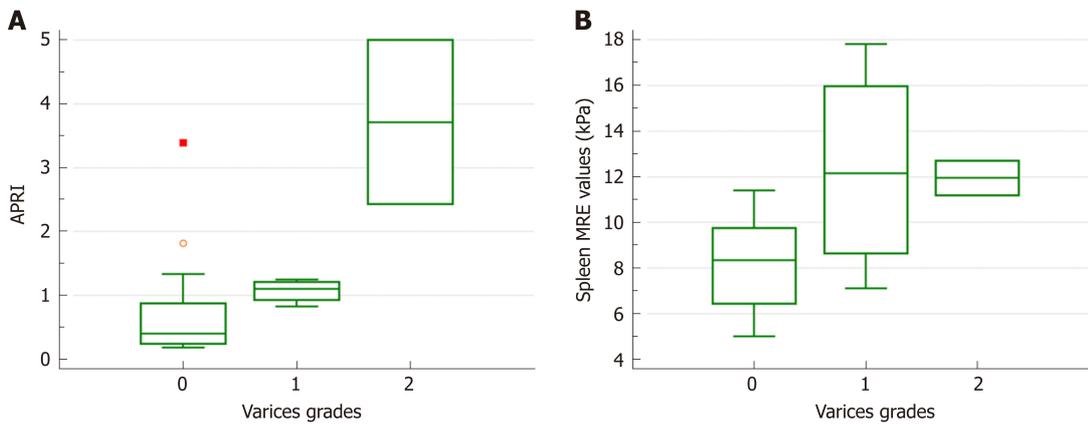

Figure 1 Box-and-whisker plots for the comparison of varices grades. The graphs are shown for (A) the aspartate aminotransferase to platelet ratio index (APRI) and (B) spleen magnetic resonance elastography (MRE) values according to the grade of gastroesophageal varices. Among the different varices grades, there were significant differences in the APRI (P = 0.029) and spleen MRE values (P = 0.045), but not in the spleen size ratio (P = 0.084) or liver MRE values (P = 0.795). MRE: Magnetic resonance elastography; APRI: Aspartate aminotransferase to platelet ratio index.
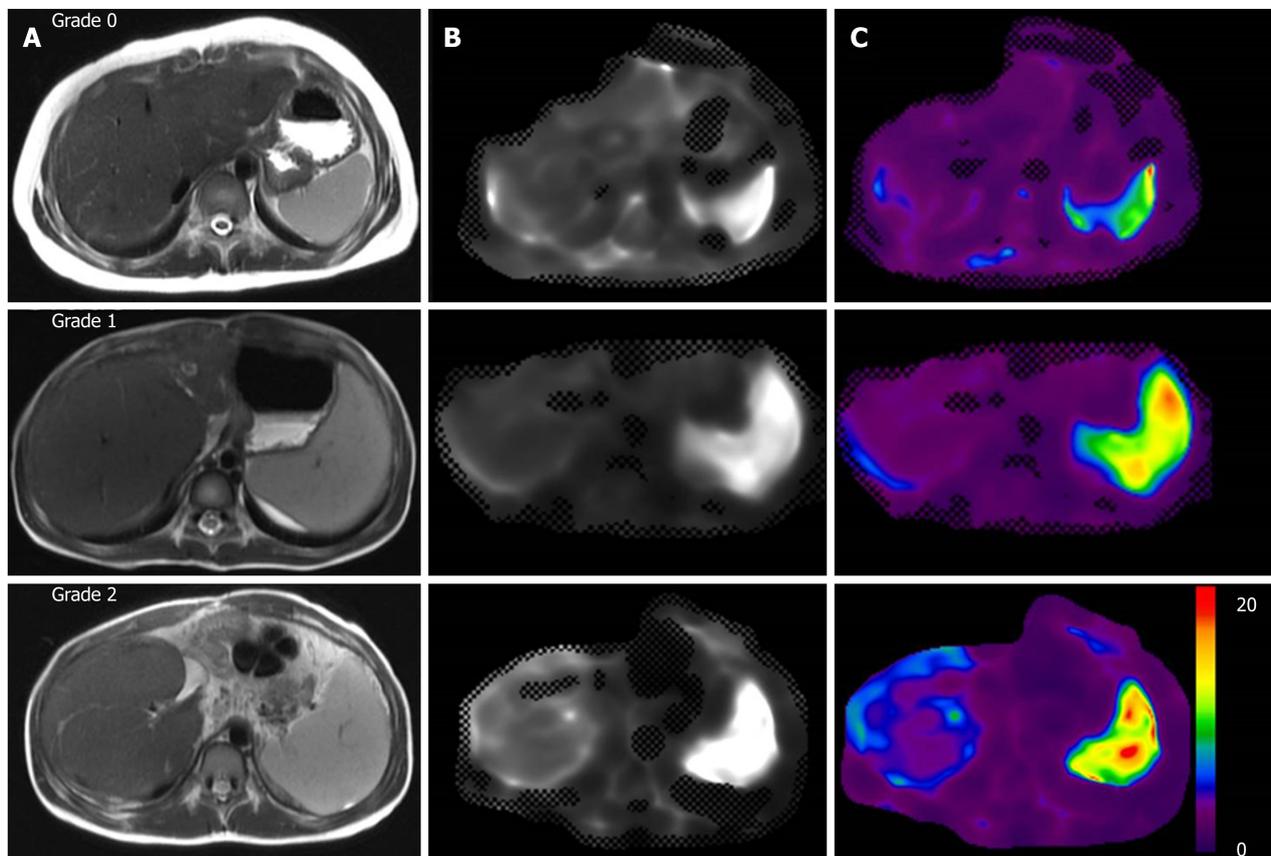

Figure 2 Liver magnetic resonance imaging of biliary atresia patients with different varices grades. Liver magnetic resonance imaging images are shown from three respective patients with grade 0 (first row), grade 1 (second row) and grade 2 (third row) gastroesophageal varices, including (A) axial single-shot fast spin-echo

T2-weighted images, (B) magnitude images and (C) post-processed shear stiffness maps with color-coded elastograms from 0 to 20 kPa. The elastograms display the progressively increasing splenic stiffness in these patients.
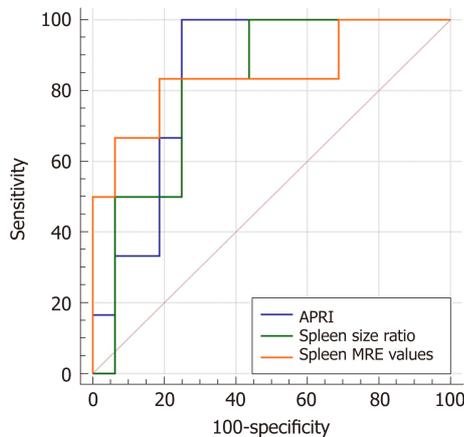

Figure 3 Comparison of area under the curve analyses for predicting varices. The area under the curve was 0.844 for the aspartate aminotransferase to platelet ratio index (cut-off, 0.65), 0.813 for the spleen size ratio (cut-off, 1.08) and 0.844 for the spleen magnetic resonance elastography values (cut-off, 9.9 kPa) for predicting gastroesophageal varices. The diagnostic performance did not differ among these three methods. APRI: Aspartate aminotransferase to platelet ratio index.

ARTICLE HIGHLIGHTS

Research background

Biliary atresia patients have high chance of disease progression to liver fibrosis even after Kasai operation. Therefore, regular long-term monitoring is required to early diagnose liver cirrhosis and portal hypertension. The primary aim of this study was to evaluate the utility of magnetic resonance elastography (MRE) for hepatic and splenic stiffness assessments to evaluate portal hypertension in pediatric patients with biliary atresia after the Kasai operation.

Research motivation

Hepatic fibrosis has been found to correlate with liver MRE values in adult and children. However, there is little discussion about the relationship between spleen stiffness measurement by MRE and portal hypertension in children.

Research objectives

This study analyzed the role of spleen MRE values in biliary atresia patients after Kasai operation with portal hypertension.

Research methods

We retrospectively reviewed abdominal MRE images in pediatric patients. Patients who had undergone Kasai operations for biliary atresia were selected for the Kasai group, and patients with normal livers and spleens were selected for the control group. Hepatic and splenic stiffness values were measured by MRE. Aspartate aminotransferase to platelet ratio index (APRI) from laboratory results and the normalized spleen size ratio were calculated. These parameters were compared between the Kasai group and the control group, and also among the Kasai group patients depending on the existence of portal hypertension or gastroesophageal varices.

Research results

The median spleen MRE value was 5.5 kPa in the control group and 8.6 kPa in the Kasai group. In the Kasai group, the APRI, spleen size ratio and spleen MRE values were higher in patients with portal hypertension and in patients with gastroesophageal varices, even though their liver MRE values were not different. The APRI, spleen size ratio and spleen MRE values also correlated with varices grades. The AUC in predicting gastroesophageal varices was 0.844 at a cut-off of 0.65 for the APRI, and 0.844 at a cut-off of 9.9 kPa for spleen MRE values.

Research conclusions

Spleen MRE values were useful for evaluating portal hypertension and gastroesophageal varices in biliary atresia patients after Kasai operation. At a cut-off of 9.9 kPa, spleen MRE values predicted gastroesophageal varices as well as the APRI and spleen size ratio. However, liver MRE values did not differ in patients with and without portal hypertension or gastroesophageal varices. Spleen MRE values may help screen out high-risk patients early and administer adequate interventions during follow up.

Research perspectives

For biliary atresia patients after Kasai operation, spleen MRE values can be used to evaluate portal hypertension and gastroesophageal varices without invasive monitoring. The results of this study, needs to be verified by a large sample size study with multiple institutions.

REFERENCES

1   **Serinet MO**, Wildhaber BE, Broué P, Lachaux A, Sarles J, Jacquemin E, Gauthier F, Chardot C. Impact of age at Kasai operation on its results in late childhood and adolescence: a rational basis for biliary atresia screening. *Pediatrics* 2009; **123**: 1280-1286 [PMID: 19403492 DOI: 10.1542/peds.2008-1949]

2   **Chardot C**, Buet C, Serinet MO, Golmard JL, Lachaux A, Roquelaure B, Gottrand F, Broué P, Dabadie A, Gauthier F, Jacquemin E. Improving outcomes of biliary atresia: French national series 1986-2009. *J Hepatol* 2013; **58**: 1209-1217 [PMID: 23402746 DOI: 10.1016/j.jhep.2013.01.040]

3   **Hartley JL**, Davenport M, Kelly DA. Biliary atresia. *Lancet* 2009; **374**: 1704-1713 [PMID: 19914515 DOI: 10.1016/S0140-6736(09)60946-6]

4   **Hadzić N**, Davenport M, Tizzard S, Singer J, Howard ER, Mieli-Vergani G. Long-term survival following Kasai portoenterostomy: is chronic liver disease inevitable? *J Pediatr Gastroenterol Nutr* 2003; **37**: 430-433 [PMID: 14508212]

5   **Piccinino F**, Sagnelli E, Pasquale G, Giusti G. Complications following percutaneous liver biopsy. A multicentre retrospective study on 68,276 biopsies. *J Hepatol* 1986; **2**: 165-173 [PMID: 3958472]

6   **Pariente D**, Franchi-Abella S. Paediatric chronic liver diseases: how to investigate and follow up? Role of imaging in the diagnosis of fibrosis. *Pediatr Radiol* 2010; **40**: 906-919 [PMID: 20432008 DOI: 10.1007/s00247-010-1600-3]

7   **Bedossa P**, Dargère D, Paradis V. Sampling variability of liver fibrosis in chronic hepatitis C. *Hepatology* 2003; **38**: 1449-1457 [PMID: 14647056 DOI: 10.1016/j.hep.2003.09.022]

8   **Regev A**, Berho M, Jeffers LJ, Milikowski C, Molina EG, Pyrsopoulos NT, Feng ZZ, Reddy KR, Schiff ER. Sampling error and intraobserver variation in liver biopsy in patients with chronic HCV infection. *Am J Gastroenterol* 2002; **97**: 2614-2618 [PMID: 12385448 DOI: 10.1111/j.1572-0241.2002.06038.x]

9   **Yin M**, Talwalkar JA, Glaser KJ, Manduca A, Grimm RC, Rossman PJ, Fidler JL, Ehman RL. Assessment of hepatic fibrosis with magnetic resonance elastography. *Clin Gastroenterol Hepatol* 2007; **5**: 1207-1213.e2 [PMID: 17916548 DOI: 10.1016/j.cgh.2007.06.012]

10   **Batheja M**, Vargas H, Silva AM, Walker F, Chang YH, De Petris G, Silva AC. Magnetic resonance elastography (MRE) in assessing hepatic fibrosis: performance in a cohort of patients with histological data. *Abdom Imaging* 2015; **40**: 760-765 [PMID: 25542217 DOI: 10.1007/s00261-014-0321-8]

11   **Yoshimitsu K**, Mitsufuji T, Shinagawa Y, Fujimitsu R, Morita A, Urakawa H, Hayashi H, Takano K. MR elastography of the liver at 3.0 T in diagnosing liver fibrosis grades; preliminary clinical experience. *Eur Radiol* 2016; **26**: 656-663 [PMID: 26060066 DOI: 10.1007/s00330-015-3863-4]

12   **Morisaka H**, Motosugi U, Ichikawa S, Sano K, Ichikawa T, Enomoto N. Association of splenic MR elastographic findings with gastroesophageal varices in patients with chronic liver disease. *J Magn Reson Imaging* 2015; **41**: 117-124 [PMID: 24243628 DOI: 10.1002/jmri.24505]

13   **Talwalkar JA**, Yin M, Venkatesh S, Rossman PJ, Grimm RC, Manduca A, Romano A, Kamath PS, Ehman RL. Feasibility of in vivo MR elastographic splenic stiffness measurements in the assessment of portal hypertension. *AJR Am J Roentgenol* 2009; **193**: 122-127 [PMID: 19542403 DOI: 10.2214/AJR.07.3504]

14   **Shin SU**, Lee JM, Yu MH, Yoon JH, Han JK, Choi BI, Glaser KJ, Ehman RL. Prediction of esophageal varices in patients with cirrhosis: usefulness of three-dimensional MR elastography with echo-planar imaging technique. *Radiology* 2014; **272**: 143-153 [PMID: 24620910 DOI: 10.1148/radiol.14130916]

15   **Nedredal GI**, Yin M, McKenzie T, Lillegard J, Luebke-Wheeler J, Talwalkar J, Ehman R, Nyberg SL. Portal hypertension correlates with splenic stiffness as measured with MR elastography. *J Magn Reson Imaging* 2011; **34**: 79-87 [PMID: 21608066 DOI: 10.1002/jmri.22610]

16   **Yin M**, Kolipaka A, Woodrum DA, Glaser KJ, Romano AJ, Manduca A, Talwalkar JA, Araoz PA, McGee KP, Anavekar NS, Ehman RL. Hepatic and splenic stiffness augmentation assessed with MR elastography in an in vivo porcine portal hypertension model. *J Magn Reson Imaging* 2013; **38**: 809-815 [PMID: 23418135 DOI: 10.1002/jmri.24049]

17   **Shin HJ**, Kim HG, Kim MJ, Koh H, Kim HY, Roh YH, Lee MJ. Normal range of hepatic fat fraction on dual- and triple-echo fat quantification MR in children. *PLoS One* 2015; **10**: e0117480 [PMID: 25659155 DOI: 10.1371/journal.pone.0117480]

18   **Binkovitz LA**, El-Youssef M, Glaser KJ, Yin M, Binkovitz AK, Ehman RL. Pediatric MR elastography of hepatic fibrosis: principles, technique and early clinical experience. *Pediatr Radiol* 2012; **42**: 402-409 [PMID: 22120578 DOI: 10.1007/s00247-011-2298-6]

19   **Xanthakos SA**, Podberesky DJ, Serai SD, Miles L, King EC, Balistreri WF, Kohli R. Use of magnetic resonance elastography to assess hepatic fibrosis in children with chronic liver disease. *J Pediatr* 2014; **164**: 186-188 [PMID: 24064151 DOI: 10.1016/j.jpeds.2013.07.050]

20   **Alústiza Echeverría JM**, Castiella A, Emparanza JI. Quantification of iron concentration in the liver by MRI. *Insights Imaging* 2012; **3**: 173-180 [PMID: 22696043 DOI: 10.1007/s13244-011-0132-1]

21   **Shneider BL**, Abel B, Haber B, Karpen SJ, Magee JC, Romero R, Schwarz K, Bass LM, Kerkar N, Miethke AG, Rosenthal P, Turmelle Y, Robuck PR, Sokol RJ; Childhood Liver Disease Research and Education Network. Portal hypertension in children and young adults with biliary atresia. *J Pediatr Gastroenterol Nutr* 2012; **55**: 567-573 [PMID: 22903006 DOI: 10.1097/MPG.0b013e31826eb0cf]

22   **Wai CT**, Greenson JK, Fontana RJ, Kalbfleisch JD, Marrero JA, Conjeevaram HS, Lok AS. A simple noninvasive index can predict both significant fibrosis and cirrhosis in patients with chronic hepatitis C. *Hepatology* 2003; **38**: 518-526 [PMID: 12883497 DOI: 10.1053/jhep.2003.50346]

23   **North Italian Endoscopic Club for the Study and Treatment of Esophageal Varices**. Prediction of the first variceal hemorrhage in patients with cirrhosis of the liver and esophageal varices. A

prospective multicenter study. *N Engl J Med* 1988; **319**: 983-989 [PMID: 3262200 DOI: 10.1056/nejm198810133191505]

24   **Megremis SD**, Vlachonikolis IG, Tsilimigaki AM. Spleen length in childhood with US: normal values based on age, sex, and somatometric parameters. *Radiology* 2004; **231**: 129-134 [PMID: 14990814 DOI: 10.1148/radiol.2311020963]

25   **Serai SD**, Towbin AJ, Podberesky DJ. Pediatric liver MR elastography. *Dig Dis Sci* 2012; **57**: 2713-2719 [PMID: 22569825 DOI: 10.1007/s10620-012-2196-2]

26   **Ma X**, Wang L, Wu H, Feng Y, Han X, Bu H, Zhu Q. Spleen Stiffness Is Superior to Liver Stiffness for Predicting Esophageal Varices in Chronic Liver Disease: A Meta-Analysis. *PLoS One* 2016; **11**: e0165786 [PMID: 27829057 DOI: 10.1371/journal.pone.0165786]

27   **Chongsrisawat V**, Vejapipat P, Siripon N, Poovorawan Y. Transient elastography for predicting esophageal/gastric varices in children with biliary atresia. *BMC Gastroenterol* 2011; **11**: 41 [PMID: 21501480 DOI: 10.1186/1471-230X-11-41]

28   **Shalaby A**, Makin E, Davenport M. Portal venous pressure in biliary atresia. *J Pediatr Surg* 2012; **47**: 363-366 [PMID: 22325391 DOI: 10.1016/j.jpedsurg.2011.11.031]

29   **Voutilainen S**, Kivisaari R, Lohi J, Jalanko H, Pakarinen MP. A Prospective Comparison of Noninvasive Methods in the Assessment of Liver Fibrosis and Esophageal Varices in Pediatric Chronic Liver Diseases. *J Clin Gastroenterol* 2016; **50**: 658-663 [PMID: 27105175 DOI: 10.1097/MCG.0000000000000532]

30   **Shin NY**, Kim MJ, Lee MJ, Han SJ, Koh H, Namgung R, Park YN. Transient elastography and sonography for prediction of liver fibrosis in infants with biliary atresia. *J Ultrasound Med* 2014; **33**: 853-864 [PMID: 24764341 DOI: 10.7863/ultra.33.5.853]

31   **Leschied JR**, Dillman JR, Bilhartz J, Heider A, Smith EA, Lopez MJ. Shear wave elastography helps differentiate biliary atresia from other neonatal/infantile liver diseases. *Pediatr Radiol* 2015; **45**: 366-375 [PMID: 25238807 DOI: 10.1007/s00247-014-3149-z]

32   **Shima H**, Igarashi G, Wakisaka M, Hamano S, Nagae H, Koyama M, Kitagawa H. Noninvasive acoustic radiation force impulse (ARFI) elastography for assessing the severity of fibrosis in the post-operative patients with biliary atresia. *Pediatr Surg Int* 2012; **28**: 869-872 [PMID: 22864589 DOI: 10.1007/s00383-012-3140-4]

33   **Goldschmidt I**, Streckenbach C, Dingemann C, Pfister ED, di Nanni A, Zapf A, Baumann U. Application and limitations of transient liver elastography in children. *J Pediatr Gastroenterol Nutr* 2013; **57**: 109-113 [PMID: 23539048 DOI: 10.1097/MPG.0b013e31829206a0]

34   **Yin M**, Glaser KJ, Talwalkar JA, Chen J, Manduca A, Ehman RL. Hepatic MR Elastography: Clinical Performance in a Series of 1377 Consecutive Examinations. *Radiology* 2016; **278**: 114-124 [PMID: 26162026 DOI: 10.1148/radiol.2015142141]

35   **Huwart L**, Sempoux C, Salameh N, Jamart J, Annet L, Sinkus R, Peeters F, ter Beek LC, Horsmans Y, Van Beers BE. Liver fibrosis: noninvasive assessment with MR elastography versus aspartate aminotransferase-to-platelet ratio index. *Radiology* 2007; **245**: 458-466 [PMID: 17940304 DOI: 10.1148/radiol.2452061673]

36   **Trout AT**, Sheridan RM, Serai SD, Xanthakos SA, Su W, Zhang B, Wallihan DB. Diagnostic Performance of MR Elastography for Liver Fibrosis in Children and Young Adults with a Spectrum of Liver Diseases. *Radiology* 2018; **287**: 824-832 [PMID: 29470938 DOI: 10.1148/radiol.2018172099]

37   **Lim JK**, Groszmann RJ. Transient elastography for diagnosis of portal hypertension in liver cirrhosis: is there still a role for hepatic venous pressure gradient measurement? *Hepatology* 2007; **45**: 1087-1090 [PMID: 17464984 DOI: 10.1002/hep.21731]

38   **Mannelli L**, Godfrey E, Joubert I, Patterson AJ, Graves MJ, Gallagher FA, Lomas DJ. MR elastography: Spleen stiffness measurements in healthy volunteers--preliminary experience. *AJR Am J Roentgenol* 2010; **195**: 387-392 [PMID: 20651194 DOI: 10.2214/AJR.09.3390]

Observational Study

Differential hepatic features presenting in Wilson disease-associated cirrhosis and hepatitis B-associated cirrhosis

Hao-Jie Zhong, Huan-Huan Sun, Lan-Feng Xue, Eileen M McGowan, Yu Chen

ORCID number: Hao-Jie Zhong (0000-0001-6586-756X); Huan-Huan Sun (0000-0002-7762-3260); Lan-Feng Xue (0000-0002-8175-6453); Eileen M McGowan (0000-0001-6371-3751); Yu Chen (0000-0003-0747-3479).

Author contributions: Zhong HJ, Sun HH, and Chen Y contributed to study conception and design; Zhong HJ, Sun HH, Xue LF, McGowan EM, and Chen Y contributed to data acquisition, data analysis and interpretation, and writing of the article; Zhong HJ, McGowan EM, and Chen Y contributed to editing, reviewing, and final approval of the article.

Hao-Jie Zhong, Lan-Feng Xue, Yu Chen, Department of Gastroenterology, The First Affiliated Hospital of Guangdong Pharmaceutical University, Guangzhou 510000, Guangdong Province, China

Hao-Jie Zhong, Department of Gastroenterology, Guangdong Medical University, Zhanjiang 524000, Guangdong Province, China

Huan-Huan Sun, Department of Gastroenterology, The First Affiliated Hospital of Xi'an Jiao Tong University, Xi'an 710000, Shaanxi Province, China

Eileen M McGowan, Faculty of Science, University of Technology Sydney, Sydney NSW 2007, Australia

Corresponding author: Yu Chen, MD, PhD, Doctor, Department of Gastroenterology, The First Affiliated Hospital of Guangdong Pharmaceutical University, No. 19, Nonglinxia Road, Guangzhou 510000, Guangdong Province, China. yuchen@gdpu.edu.cn
Telephone: 86-138-24462875
Fax: +86-020-61325957

Abstract

BACKGROUND
Cirrhosis is a chronic late stage liver disease associated with hepatitis viruses, alcoholism, and metabolic disorders, such as Wilson disease (WD). There are no clear markers or clinical features that define cirrhosis originating from these disparate origins. We hypothesized that cirrhosis is not one disease and cirrhosis of different etiology may have differential clinical hepatic features.

AIM
To delineate the liver features between WD-associated cirrhosis and hepatitis B-associated cirrhosis in the Chinese population.

METHODS
In this observational study, we reviewed the medical data of consecutive inpatients who had WD-associated cirrhosis or hepatitis B-associated cirrhosis from January 2010 to August 2018, and excluded patients who had carcinoma, severe heart or pulmonary diseases, or other liver diseases. According to the etiology of cirrhosis, patients were divided into two groups: WD-associated cirrhosis group (60 patients) and hepatitis B-associated cirrhosis group (56 patients). The liver fibrosis degree, liver function indices, and portal hypertension features of these patients were compared between the two groups.

RESULTS

No inter-group differences were observed in the diagnostic liver fibrosis markers, however, clinical features clearly defined the origin of cirrhosis. WD-associated cirrhosis patients (16-29 years) had lower levels of alanine transaminase, aspartate transaminase, and bilirubin, lower prothrombin time, lower incidence of hepatic encephalopathy, and lower portal vein diameter ($P < 0.05$), compared to cirrhosis resulting from hepatitis B in older patients (45-62 years). Importantly, they had decreased risks of progression from Child-Pugh grade A to B (odds ratio = 0.046, 95% confidence interval: 0.006-0.387, $P = 0.005$) and of ascites (odds ratio = 0.08, 95% confidence interval: 0.01-0.48, $P = 0.005$). Conversely, WD-associated cirrhosis patients had a higher risk of splenomegaly (odds ratio = 4.15, 95% confidence interval: 1.38-12.45, $P = 0.011$).

CONCLUSION

WD-associated cirrhosis presents a higher risk of splenomegaly associated with leukopenia and thrombocytopenia, although revealing milder liver dysfunction and portal hypertension symptoms, which recommends WD patients to be monitored for associated complications.

Key words: Chronic hepatitis B; Cirrhosis; Hepatic feature; Liver function; Portal hypertension; Wilson disease

Core tip: In Asia, especially China, the incidence of Wilson disease (WD) and its complications is much higher in the younger generation compared to Western societies. This article looks beyond the well-characterized, generalized definition of cirrhosis. It addresses an important but simple question: Can the origin of cirrhosis be classified by clinical features, especially in WD-associated cirrhosis? In this manuscript we define specific clinical characteristics of WD-associated cirrhosis in young patients which are very distinct to those of hepatitis-associated cirrhosis in older patients. These important findings may benefit the clinical diagnosis and ultimate treatment of these younger, vulnerable WD patients.

INTRODUCTION

Wilson disease (WD), also named hepatolenticular degeneration, is an autosomal recessive disease of copper metabolism caused by mutations in *ATP7B*, which encodes a copper transporting ATPase[1,2]. Dysfunction of this ATPase causes copper overload in the liver, brain, and other organs. Depending on the organs affected, WD has a wide spectrum of clinical symptoms, including hepatic, neurological, psychiatric, and ophthalmological manifestations[2]. As the liver is the primary organ for copper metabolism and has the highest expression level of copper transporting ATPase, hepatic changes are usually the earliest and most frequent manifestations in WD patients[2-4]. Although the prevalence of symptomatic WD is low worldwide (about 1/30000), the frequency of this disease is much higher in the Chinese population (about 5.87/100000)[2,5]. Cirrhosis is a common manifestation in WD patients compared to inpatients with other types of liver diseases[6,7].

Cirrhosis is the 11th most common cause of death globally, accounting for 3.5% of all-cause mortalities[8]. Therefore, it is important to understand the clinical features of cirrhosis for prevention and treatment of these manifestations and complications. A meta-analysis that investigated data from 12 studies estimated that the prevalence of cirrhosis was 34% in WD patients[9]. Clinical symptoms of WD, especially hepatic manifestations, often present in the first decade of life, and most occur between the

ages of 5–35[10]. As a result, WD frequently causes cirrhosis in children and young adults[9]. In some areas of Iran and India, WD was found to be the primary cause of cirrhosis in children[11,12]. Generally, cirrhosis is characterized by portal hypertension and hepatic dysfunction, leading to esophageal varices, splenomegaly, ascites, and liver injury[13]. However, cirrhosis caused by WD in children and young adults differs from non-alcoholic fatty liver disease and chronic hepatitis B. As the etiology and onset age of WD-associated cirrhosis are different from those of other kinds of liver cirrhosis, WD-associated cirrhosis may involve a different liver injury pathogenesis. Unfortunately, the hepatic features of cirrhosis in WD patients are less well reported.

Hepatitis B virus (HBV) infection, as the most common chronic viral infection, is the main cause of cirrhosis worldwide[6,13]. Globally, nearly 257 million people are living with HBV, and one third of them live in China[14,15]. About 10%–20% of Chinese patients with chronic hepatitis progress to cirrhosis within 5 years[16], making HBV the leading cause of cirrhosis in the Chinese population[17]. Therefore, we performed this study to delineate the liver features between WD-associated cirrhosis and hepatitis B-associated cirrhosis in the Chinese population.

MATERIALS AND METHODS

Study populations
In this observational study, we retrospectively reviewed the medical data of consecutive inpatients who were diagnosed with cirrhosis caused by either WD or HBV presenting from January 2010 to August 2018 at the First Affiliated Hospital of Guangdong Pharmaceutical University. The patients were excluded from the study if they met any of the following criteria: (1) Carcinoma; (2) severe heart or pulmonary diseases; (3) fatty liver disease, alcoholic liver disease, autoimmune liver disease, drug-induced liver injury, or hepatic parasitic infection; and (4) incomplete medical data. Patients who were hospitalized more than once were recorded only once. This study was performed with the approval of the Ethical Committee of the First Affiliated Hospital of Guangdong Pharmaceutical University. All patients in the study were de-identified.

Data collection
The following medical data were extracted from the subjects' electronic medical records: demographic characteristics, history of smoking and alcohol drinking, medical history (diabetes, hypertension, and liver disease), disease duration, manifestations of cirrhosis, imaging examinations, and laboratory test results including alanine transaminase (ALT), aspartate transaminase (AST), serum albumin (ALB), bilirubin, prothrombin time (PT), total cholesterol (TC), triglyceride, low-density lipoprotein (LDL), high-density lipoprotein, white blood cell (WBC) count, red blood cell (RBC) count, platelet count, procollagen type III N-terminal propeptide (PIIINP), type IV collagen, laminin, and hyaluronic acid.

In addition, disease duration was calculated based on the onset age of WD or HBV infection. Child-Pugh classification was assessed as previously described[18]. Leukopenia was defined as a WBC count $< 4.0 \times 10^9$/L. Erythropenia was defined as an RBC count $< 4.0 \times 10^{12}$/L for males or 3.5×10^{12}/L for females. Thrombocytopenia was defined as a platelet count $< 100 \times 10^9$/L. The indication for splenectomy was hypersplenism, characterized by splenomegaly, leukopenia, erythropenia, and thrombocytopenia[19]. Smokers were defined as patients who have smoked at some stages in their lifetime. Alcohol consumption was defined when patients drank more than 140g of alcohol per week.

In China, diagnosis of WD is based on the classic criteria: Age of onset; family history; low serum ceruloplasmin (< 200 mg/L); elevated urinary copper excretion (≥ 100 µg/24 h); elevated liver copper (> 250 µg/g dry weight); and elevated urinary copper excretion after challenge with 2 × 500 mg D-penicillamine (> 1600 µg/24 h)[20]. Chronic hepatitis B was diagnosed based on the clinical manifestations and serological and virological examinations[21].

Statistical analysis
The statistical analyses were performed using IBM SPSS statistics software, version 22 (IBM Corp., Armonk, NY, United States). Normally distributed continuous variables are presented as the mean ± standard deviation. Non-normally distributed continuous variables are presented as medians and interquartile ranges. Categorical variables are presented as frequencies and proportions. The statistical significance of the difference in means between the two groups was tested using the unpaired *t*-test. The statistical significance of the difference in medians between the two groups was tested using the

Mann-Whitney *U*-test. Categorical variables were tested using the Chi-square test or Fisher's exact test. To assess the association between cirrhosis etiology and portal vein diameter, and the association between cirrhosis etiology and liver fibrosis markers, multivariable linear regression analysis with a forward stepwise approach was used to adjust for confounders. To assess whether the risk of ascites, splenomegaly, and progression from Child-Pugh grade A to B or C differed between WD-associated cirrhosis patients and hepatitis B-associated cirrhosis patients, logistic regression analysis with a backward stepwise approach was used. Odds ratios (ORs) and 95% confidence intervals (CIs) were estimated. A *P*-value < 0.05 (two-tailed) was considered statistically significant.

RESULTS

Demographics and clinical characteristics
Based on the medical data, 56 inpatients with hepatitis B-associated cirrhosis and 60 with WD-associated cirrhosis were enrolled. The mean age and age range of these patients recorded in Table 1 clearly demonstrate that WD-associated cirrhosis was more prevalent in the younger age group, whereas, in general, hepatitis B occurred in older adults. The percentage of males, disease duration, LDL level, and prevalence of diabetes, hypertension, alcohol drinking, and smoking were significantly higher in hepatitis B-associated cirrhosis patients than in WD-associated cirrhosis patients (Table 1). In patients with hepatitis B-associated cirrhosis, 48.21% (27/56) were undergoing treatment with antiviral agents, and 47.06% (24/51) presented with low HBV DNA (≤ 2000 IU/mL).

Relationship between cirrhotic etiology and liver fibrosis markers
The levels of PIIINP, type IV collagen, and hyaluronic acid were lower in WD-associated cirrhosis patients than in hepatitis B-associated cirrhosis patients. However, the level of laminin was higher in WD-associated cirrhosis patients (Table 2). Despite presenting with distinct clinical variations, after adjustment for age, gender, disease duration, diabetes, hypertension, alcohol drinking, and smoking, the multivariable linear regression analysis showed no overt differences in any of the four liver fibrosis markers between the two groups of patients.

Relationship between cirrhotic etiology and liver function indices
The PT and the levels of ALT, AST, and bilirubin, but not the level of ALB, were lower in WD-associated cirrhosis patients compared with hepatitis B-associated cirrhosis patients. Additionally, the incidence of hepatic encephalopathy was lower in WD-associated cirrhosis patients. An important observation showed that the percentage of patients with Child-Pugh grades B and C was lower in WD-associated cirrhosis patients compared with hepatitis B-associated cirrhosis patients (Table 3). Logistic regression analysis showed that patients with WD-associated cirrhosis had a significantly decreased risk of progression from Child-Pugh A to B (OR = 0.046, 95% CI: 0.006-0.387, *P* = 0.005), and a non-significant decreased risk for progression to Child-Pugh C (OR = 0.164, 95% CI: 0.013-2.063, *P* = 0.162; Table 4), after adjustment for age, gender, disease duration, diabetes, hypertension, alcohol drinking, and smoking, as compared to patients with hepatitis B-associated cirrhosis.

Relationship between cirrhotic etiology and features of portal hypertension
Table 5 shows that the portal vein diameter and incidence of ascites were lower in WD-associated cirrhosis patients than in hepatitis B-associated cirrhosis. However, WD-associated cirrhosis patients had a statistical trend toward a higher incidence of splenomegaly (88.33% *vs* 75.00%, *P* = 0.062). Multivariable linear regression analysis showed that WD-associated cirrhosis was associated with a lower portal vein diameter. Moreover, after adjustment for age, gender, disease duration, diabetes, hypertension, alcohol drinking, smoking, and Child-Pugh classification, the logistic regression analysis showed that WD-associated cirrhosis patients had a significantly decreased risk of ascites compared with hepatitis B-associated cirrhosis patients (OR = 0.08, 95%CI: 0.01-0.48, *P* = 0.005). However, the logistic regression analysis showed that WD-associated cirrhosis patients had a significantly increased risk of splenomegaly compared with hepatitis B-associated cirrhosis patients (OR = 4.15, 95%CI: 1.38-12.45, *P* = 0.011).

Splenomegaly for hematocytopenia
Logistic regression analysis showed that splenomegaly was associated with a significantly increased risk of leukopenia (OR = 4.41, 95%CI: 1.29-15.12, *P* = 0.018) and thrombocytopenia (OR = 23.08, 95%CI: 2.86-186.11, *P* = 0.003; Table 6), but not

Table 1 Characteristics of patients with cirrhosis

	Wilson disease-associated cirrhosis (*n* = 60)	Hepatitis B-associated cirrhosis (*n* = 56)	*P* value
Age (yr)	22.00 (16.25-29.75)	52.00 (45.25-62.00)	< 0.001
Male gender	27 (45.00)	46 (82.14)	< 0.001
Disease duration (years)	3.00 (1.13-7.00)	17.50 (3.25-38.25)	< 0.001
Diabetes	1 (1.67)	11 (19.64)	0.001
Hypertension	0 (0)	13 (23.21)	< 0.001
Alcohol drinking	0 (0)	12 (21.42)	< 0.001
Smoking	2 (3.33)	13 (23.21)	0.001
TC (mmol/L)	4.22 (3.67-4.67) (*n* = 39)	4.10 (2.71-4.67) (*n* = 39)	0.327
TG (mmol/L)	0.94 (0.70-1.37) (*n* = 39)	0.99 (0.65-1.60) (*n* = 39)	0.853
HDL (mmol/L)	1.40 ± 0.30 (*n* = 39)	1.16 ± 0.32 (*n* = 39)	0.786
LDL (mmol/L)	2.17 ± 0.61 (*n* = 39)	2.28 ± 0.91 (*n* = 39)	0.014

Data are presented as medians (interquartile ranges) or *n* (%). HDL: High-density lipoprotein; LDL: Low-density lipoprotein; TC: Total cholesterol; TG: Triacylglycerol.

erythropenia. Eight patients with WD-associated cirrhosis and seven with hepatitis B-associated cirrhosis had undergone splenectomy. After splenectomy, 50.00% (4/8) of WD-associated cirrhosis patients and 28.57% (2/7) of hepatitis B-associated cirrhosis patients had a normal WBC count; 62.50% (5/8) and 28.57% (2/7) had a normal platelet count.

DISCUSSION

Liver disease is the most common clinical manifestation of WD, and cirrhosis is frequently presented in these patients[4]. WD is not a common disease, and its pathogenesis and early onset of age are quite different from those of other liver diseases[2]. The clinical manifestations of WD are diverse[4], and the clinical features of cirrhosis caused by WD are still unclear. To the best of our knowledge, this is the first study to analyze the liver features of WD-associated cirrhosis and present clear distinct features to distinguish WD-associated cirrhosis from hepatitis B-associated cirrhosis.

In this observational study, compared with patients with hepatitis B-associated cirrhosis, WD-associated cirrhosis presented in a younger age group, and patients developed milder liver dysfunction and portal hypertension manifestations. Consistent with our finding, a recent study involving 1357 WD patients showed that 39.5% of children and adolescents had cirrhosis at diagnosis[22]. As shown in a previous study, the prognosis of WD patients was excellent if the disease was treated appropriately[10]. Nonetheless, patients with WD-associated cirrhosis had a higher risk of splenomegaly, which was found to be a risk factor for leukopenia and thrombocytopenia. In contrast, due to long periods of immune tolerant phases and inactive residual phases, liver injury is more likely to occur at more advanced age in patients with HBV infection[23]. Thus, most patients with HBV infection who progress to cirrhosis do so after the age of 35 years[23].

The degree of liver fibrosis can be reflected by the levels of serum type III collagen, type IV collagen, laminin, and hyaluronic acid, which are components of the extracellular matrix during fibrosis[24,25]. Based on the multivariable linear regression analysis, no significant difference in any of these four markers was found between the two groups of patients. The results showed that the degree of liver fibrosis might be similar between WD-associated cirrhosis and hepatitis B-associated cirrhosis patients. However, these markers do not reflect liver fibrosis directly, and liver biopsy remains the gold standard method for fibrosis assessment. Thus, new diagnostic markers may be needed to assess liver damage and prognosis, and discern WD-associated cirrhosis and hepatitis B-associated cirrhosis treatments.

The liver performs many biochemical functions, such as the synthesis of protein and clotting factors and the metabolism of bilirubin and ammonia[26]. Thus, liver dysfunction, as a feature of cirrhosis, was assessed based on liver injury, synthesis function, metabolism function, and hepatic functional reserve. Compared with WD-associated cirrhosis patients, more severe liver injury was found in hepatitis B-associated cirrhosis patients, based on higher levels of ALT and AST. Moreover, the

Table 2 Relationship between cirrhotic etiology and liver fibrosis markers

	Wilson disease-associated cirrhosis (*n* = 60)	Hepatitis B-associated cirrhosis (*n* = 53)	*P* value
Type IV collagen (ng/mL)	61.55 (52.18-72.11)	79.48 (63.16-107.56)	< 0.001
PIIINP (μg/mL)	79.92(54.68-122.65)	109.16 (70.24-155.30)	0.019
Laminin (ng/mL)	104.09 (92.80-118.21)	96.27 (70.08-116.02)	0.013
Hyaluronic acid (ng/mL)	75.12 (39.27-131.98)	193.16 (74.77-625.90)	< 0.001

Data are presented as medians (interquartile ranges). PIIINP: Procollagen type III N-terminal propeptide.

lower ALB level and longer PT in hepatitis B-associated cirrhosis patients indicated a more serious impairment of synthesis function. It is well known that hepatic encephalopathy, associated with hyperammonemia, is caused by impairment of ammonia detoxification in the liver[27]. Thus, a higher incidence of hepatic encephalopathy and a higher level of bilirubin indicated a more severe impairment of metabolism function in hepatitis B-associated cirrhosis patients. Additionally, the Child-Pugh classification system, a comprehensive index, has been the most widely used model to evaluate liver functional reserve[28]. Our results showed that hepatitis B-associated cirrhosis was a risk factor for progressing from Child-Pugh grade A to B, which indicated that hepatitis B-associated cirrhosis could lead to a more serious impairment of liver functional reserve. Therefore, compared with WD-associated cirrhosis, hepatitis B-associated cirrhosis seemed to cause a more serious impairment of liver function.

Portal hypertension, as another feature of cirrhosis, was assessed based on the portal vein diameter, ascites, and splenomegaly[29,30]. We found that the portal vein diameter was higher in hepatitis B-associated cirrhosis patients than in WD-associated cirrhosis patients. However, a previous study involving 167 healthy children from 1 mo to 15 years old showed that portal vein diameter was correlated with age and height, which means that the wider portal vein diameter in hepatitis B-associated cirrhosis patients might also result from their more advanced age[31]. Thus, a more precise method, such as hepatic venous pressure gradient measurement, was needed to evaluate the portal vein pressure between the two groups of patients[32]. Hepatitis B-associated cirrhosis patients had a higher risk of ascites, which might result from the more serious portal hypertension and lower level of ALB caused by liver dysfunction[33].

Splenomegaly is the most common imaging finding of portal hypertension[30]. A previous study involving 910 cirrhosis patients showed that 50.5% of the patients presented with splenomegaly[34]. Interestingly, the present study showed that the incidence of splenomegaly (88.3%) was not only much higher than the incidence in the previous study, but also much higher than the incidence in hepatitis B-associated cirrhosis patients (75%). In WD, splenomegaly seems to occur frequently, and it can even be the earliest clinical manifestation, particularly in children[10]. Consistent with our finding, previous research estimated that the incidence of splenomegaly is 49.0% (25/51) in WD patients[35], which is higher than that in chronic hepatitis B patients (41.7%; 65/156)[36]. After adjustment for potential confounders, there was a 3.15-fold increased risk of splenomegaly in WD-associated cirrhosis patients compared to hepatitis B-associated cirrhosis patients. There are three possible explanations for these results. First, non-autoimmune hemolytic anemia, which can lead to splenomegaly, has been shown to be common and an onset symptom in 10%–15% of WD patients[37]. Second, high concentration of serum copper might also have toxic effects on the spleen. Third, with increasing age, the size and function of the spleen are easily affected[38], and the younger age among WD-associated cirrhosis patients might also lead to a higher sensitivity of the spleen to all kinds of stimulation.

Additionally, portal hypertension could bring about hypersplenism, which is characterized by splenomegaly and pancytopenia due to excessive portal flow[39]. In this study, we found that splenomegaly was associated with increased risks of leukopenia and thrombocytopenia. As risk factors for certain fatal infections and bleeding (such as spontaneous bacterial peritonitis, urinary tract infection, pneumonia, and esophageal variceal bleeding), leukopenia and thrombocytopenia in WD-associated cirrhosis patients should receive more attention[40]. Regarding hypersplenism treatment, a clinical study in China revealed that splenectomy was a safe and effective therapeutic method for hypersplenism in WD patients, and it demonstrated obvious improvements in WBC and platelet counts in all the patients after splenectomy[19]. Similarly, in our study, most of the WD-associated cirrhosis patients with hypersplenism had normal WBC and platelet counts after splenectomy.

Table 3 Relationship between cirrhotic etiology and liver function indices

	Wilson disease-associated cirrhosis (*n* = 60)	Hepatitis B-associated cirrhosis (*n* = 56)	*P* value
ALT (U/L)	23.00 (17.00-34.75)	33.50 (19.33-81.25)	0.002
AST (U/L)	25.00 (19.00-40.00)	41.50 (27.25-96.50)	< 0.001
Albumin (g/L)	40.00 (37.00-43.00)	33.00 (29.25-39.75)	< 0.001
PT (s)	14.05 (13.43-14.78)	15.50 (13.93-18.18)	0.003
Bilirubin (μmol/L)	12.40 (8.55-18.38)	21.70 (12.73-41.08)	< 0.001
Hepatic encephalopathy	0 (0)	3 (5.36)	0.109
Child-Pugh classification			< 0.001
A	54 (90.00)	24 (42.86)	
B	4 (6.67)	24 (42.86)	
C	2 (3.33)	8 (14.29)	

Data are presented as medians (interquartile ranges) or N (%). ALT: Alanine transferase; AST: Aspartate transaminase; PT: Prothrombin time.

The present study had several limitations. First, as gastroscopy was not performed regularly in the cirrhosis patients, esophageal varices, a typical feature of portal hypertension, could not be compared between the two groups of patients. Second, due to the low economic status of some of the patients and the poor medical services in some areas of China, the patients often received a delayed diagnosis, which might have biased the disease duration assessment. Third, some confounders (such as medication use and duration from onset to diagnosis of disease), which might have had an influence on the results, were not taken into consideration. Finally, the study was a single-center study with a limited sample size. Thus, the results regarding the comparison of hepatic features between WD-associated cirrhosis patients and hepatitis B-associated cirrhosis patients should be interpreted with caution, and large-scale, multi-center studies are needed to confirm these conclusions.

In conclusion, in this study, we provide evidence to show that cirrhosis is not one disease and there is a need for further classification for treatment options. Depending on the origin, cirrhosis presents different clinical features. Our findings, in concurrence with other studies in the literature, show that clinical features occur earlier in WD patients than in chronic hepatitis B patients. An important observation made in this study is that progression from Child-Pugh grade A to B or C differed between WD-associated cirrhosis patients and hepatitis B-associated cirrhosis patients. Notably, WD-associated cirrhosis patients had a higher risk of splenomegaly, which was found to be a risk factor for leukopenia and thrombocytopenia. Based on these findings, it is highly recommended that young Wilson's disease patients require regular monitoring for blood disorders and infections to alleviate further clinical complications. Additionally, splenectomy might be an effective therapy for hypersplenism in WD-associated cirrhosis patients.

Table 4 Logistic regression analysis of Child-Pugh classification in patients with Wilson disease-associated cirrhosis *vs* patients with hepatitis B-associated cirrhosis

	OR	95%CI	*P* value
Child-Pugh classification			
A	Ref.	-	-
B	0.046	0.006-0.387	0.005
C	0.164	0.013-2.063	0.162

Data were adjusted for age, gender, disease duration, diabetes, hypertension, alcohol drinking, and smoking. CI: Confidence interval; OR: Odds ratio; Ref: Reference.

Table 5 Relationship between cirrhotic etiology and features of portal hypertension

	Wilson disease-associated cirrhosis (*n* = 60)	Hepatitis B-associated cirrhosis (*n* = 56)	*P* value
Portal vein diameter (mm)	10.00 (8.00-10.00)	14.00 (12.00-16.00)	< 0.001
Ascites	2 (3.33)	24 (42.86)	< 0.001
Splenomegaly/splenectomy	53 (88.33)	42 (75.00)	0.062

Data are presented as medians (interquartile ranges) or *n* (%).

Table 6 Logistic regression analysis of risk of hematocytopenia due to splenomegaly

	OR	95%CI	*P* value
Leucopenia	4.41	1.29-15.12	0.018
Erythropenia	-	-	-
Thrombocytopenia	23.08	2.86-186.11	0.003

Data were adjusted for age, gender, disease duration, diabetes, hypertension, alcohol drinking, smoking, and Child-Pugh classification. CI: Confidence interval; OR: Odds ratio.

ARTICLE HIGHLIGHTS

Research background

Cirrhosis is a chronic late stage liver disease associated with hepatitis viruses, alcoholism, and metabolic disorders, such as Wilson disease (WD). As the etiology and onset age of WD-associated cirrhosis are different from those of other kinds of liver cirrhosis, WD-associated cirrhosis may involve a distinct liver injury pathogenesis.

Research motivation

We hypothesized that cirrhosis is not one disease and cirrhosis of different etiology may have differential clinical hepatic features.

Research objectives

To delineate the liver features between WD-associated cirrhosis and hepatitis B-associated cirrhosis in the Chinese population.

Research methods

We performed a cross-sectional study of 60 WD-associated cirrhosis and 56 hepatitis B-associated cirrhosis inpatients. We analyzed the liver fibrosis degree, liver function indices, and portal hypertension features between these two groups.

Research results

No inter-group differences were observed in the diagnostic liver fibrosis markers, however, clinical features clearly defined the origin of cirrhosis. Cirrhosis presenting in WD patients had worse liver function, lower incidence of hepatic encephalopathy, and lower portal vein diameter, compared to cirrhosis resulting from hepatitis B. They had decreased risks of progression from Child-Pugh grade A to B and of ascites. Conversely, WD-associated cirrhosis patients had a higher risk of splenomegaly, which was associated with a significantly increased risk of leukopenia and thrombocytopenia.

Research conclusions

WD-associated cirrhosis presents a higher risk of splenomegaly associated with leukopenia and thrombocytopenia, although revealing milder liver dysfunction and portal hypertension symptoms. These findings indicated that cirrhosis is not one disease and further classification for diagnosis and treatment options, dependent on origin, are needed.

Research perspectives

The higher risk of splenomegaly associated with leucopenia and thrombocytopenia in these younger, vulnerable WD patients with cirrhosis, suggests early and regular monitoring of associated blood disorders and infections to alleviate further clinical complications.

REFERENCES

1 **Bandmann O**, Weiss KH, Kaler SG. Wilson's disease and other neurological copper disorders. *Lancet Neurol* 2015; **14**: 103-113 [PMID: 25496901 DOI: 10.1016/S1474-4422(14)70190-5]

2 **Członkowska A**, Litwin T, Dusek P, Ferenci P, Lutsenko S, Medici V, Rybakowski JK, Weiss KH, Schilsky ML. Wilson disease. *Nat Rev Dis Primers* 2018; **4**: 21 [PMID: 30190489 DOI: 10.1038/s41572-018-0018-3]

3 **Asadi Pooya AA**, Eslami NS, Haghighat M. Wilson disease in southern Iran. *Turk J Gastroenterol* 2005; **16**: 71-74 [PMID: 16252195]

4 **Lin LJ**, Wang DX, Ding NN, Lin Y, Jin Y, Zheng CQ. Comprehensive analysis on clinical features of Wilson's disease: an experience over 28 years with 133 cases. *Neurol Res* 2014; **36**: 157-163 [PMID: 24107488 DOI: 10.1179/1743132813Y.0000000262]

5 **Xie JJ**, Wu ZY. Wilson's Disease in China. *Neurosci Bull* 2017; **33**: 323-330 [PMID: 28265897 DOI: 10.1007/s12264-017-0107-4]

6 **Trépo C**, Chan HL, Lok A. Hepatitis B virus infection. *Lancet* 2014; **384**: 2053-2063 [PMID: 24954675 DOI: 10.1016/S0140-6736(14)60220-8]

7 **Marengo A**, Rosso C, Bugianesi E. Liver Cancer: Connections with Obesity, Fatty Liver, and Cirrhosis. *Annu Rev Med* 2016; **67**: 103-117 [PMID: 26473416 DOI: 10.1146/annurev-med-090514-013832]

8 **Asrani SK**, Devarbhavi H, Eaton J, Kamath PS. Burden of liver diseases in the world. *J Hepatol* 2019; **70**: 151-171 [PMID: 30266282 DOI: 10.1016/j.jhep.2018.09.014]

9 **Roberts EA**, Socha P. Wilson disease in children. *Handb Clin Neurol* 2017; **142**: 141-156 [PMID: 28433098 DOI: 10.1016/B978-0-444-63625-6.00012-4]

10 **Boga S**, Ala A, Schilsky ML. Hepatic features of Wilson disease. *Handb Clin Neurol* 2017; **142**: 91-99 [PMID: 28433114 DOI: 10.1016/B978-0-444-63625-6.00009-4]

11 **Dehghani SM**, Imanieh MH, Haghighat M, Malekpour A, Falizkar Z. Etiology and complications of liver cirrhosis in children:report of a single center from southern Iran. *Middle East J Dig Dis* 2013; **5**: 41-46 [PMID: 24829669]

12 **Simon EG**, Joseph AJ, George B, Zachariah UG, Jeyamani R, Eapen CE, Chandy G, Ramakrishna BS, Kurian G, Chacko A. Aetiology of paediatric portal hypertension - experience of a tertiary care centre in South India. *Trop Doct* 2009; **39**: 42-44 [PMID: 19211426 DOI: 10.1258/td.2008.080050]

13 **Tsochatzis EA**, Bosch J, Burroughs AK. Liver cirrhosis. *Lancet* 2014; **383**: 1749-1761 [PMID: 24480518 DOI: 10.1016/S0140-6736(14)60121-5]

14 **Chen S**, Li J, Wang D, Fung H, Wong LY, Zhao L. The hepatitis B epidemic in China should receive more attention. *Lancet* 2018; **391**: 1572 [PMID: 29695339 DOI: 10.1016/S0140-6736(18)30499-9]

15 **Chen CJ**. Global elimination of viral hepatitis and hepatocellular carcinoma: opportunities and challenges. *Gut* 2018; **67**: 595-598 [PMID: 29367206 DOI: 10.1136/gutjnl-2017-315407]

16 **Liu J**, Fan D. Hepatitis B in China. *Lancet* 2007; **369**: 1582-1583 [PMID: 17499584 DOI: 10.1016/S0140-6736(07)60723-5]

17 **Zhang Y**, Zhang H, Elizabeth A, Liu XQ. Epidemiology of hepatitis B and associated liver diseases in china. *Chin Med Sci J* 2013; **27**: 243-248 [PMID: 23294591 DOI: 10.1016/S1001-9294(13)60009-7]

18 **Pugh RN**, Murray-Lyon IM, Dawson JL, Pietroni MC, Williams R. Transection of the oesophagus for bleeding oesophageal varices. *Br J Surg* 1973; **60**: 646-649 [PMID: 4541913 DOI: 10.1002/bjs.1800600817]

19 **Li LY**, Yang WM, Chen HZ, Wu YH, Fang X, Zhang J, Wang Z, Han YS, Wang Y. Successful Splenectomy for Hypersplenism in Wilson's Disease: A Single Center Experience from China. *PLoS One* 2015; **10**: e0124569 [PMID: 25910248 DOI: 10.1371/journal.pone.0124569]

20 **Chinese Society of Neurology**. Guideline of Wilson's disease diagnosis and treatment. *Zhonghua Shenjingke Zazhi* 2008; **41**: 566-569

21 **Chinese Society of Hepatology, Chinese Medical Association**. Chinese Society of Infectious Diseases, Chinese Medical Association, Hou JL, lai W. [The guideline of prevention and treatment for chronic hepatitis B: a 2015 update]. *Zhonghua Gan Zang Bing Za Zhi* 2015; **23**: 888-905 [PMID: 26739464 DOI: 10.3760/cma.j.issn.1007-3418.2015.12.002]

22 **Ferenci P**, Stremmel W, Członkowska A, Szalay F, Viveiros A, Stättermayer AF, Bruha R, Houwen R, Pop T, Stauber R, Gschwantler M, Pfeiffenberger J, Yurdaydin C, Aigner E, Steindl-Munda P, Dienes HP, Zoller H, Weiss KH. Age,sex, but not ATP7B genotype effectively influences the clinical phenotype of Wilson disease. *Hepatology* 2018 [PMID: 30232804 DOI: 10.1002/hep.30280]

23 **Liaw YF**, Chu CM. Hepatitis B virus infection. *Lancet* 2009; **373**: 582-592 [PMID: 19217993 DOI: 10.1016/S0140-6736(09)60207-5]

24 **El-Mezayen HA**, Habib S, Marzok HF, Saad MH. Diagnostic performance of collagen IV and laminin for the prediction of fibrosis and cirrhosis in chronic hepatitis C patients: a multicenter study. *Eur J Gastroenterol Hepatol* 2015; **27**: 378-385 [PMID: 25874509 DOI: 10.1097/MEG.0000000000000298]

25 **Plevris N**, Sinha R, Hay AW, McDonald N, Plevris JN, Hayes PC. Index serum hyaluronic acid independently and accurately predicts mortality in patients with liver disease. *Aliment Pharmacol Ther* 2018; **48**: 423-430 [PMID: 29971829 DOI: 10.1111/apt.14897]

26 **He GL**, Feng L, Cai L, Zhou CJ, Cheng Y, Jiang ZS, Pan MX, Gao Y. Artificial liver support in pigs with acetaminophen-induced acute liver failure. *World J Gastroenterol* 2017; **23**: 3262-3268 [PMID: 28566885 DOI: 10.3748/wjg.v23.i18.3262]

27 **Sidhu SS**, Sharma BC, Goyal O, Kishore H, Kaur N. L-ornithine L-aspartate in bouts of overt hepatic encephalopathy. *Hepatology* 2017 [PMID: 28749571 DOI: 10.1002/hep.29410]

28 **Peng Y**, Qi X, Guo X. Child-Pugh Versus MELD Score for the Assessment of Prognosis in Liver Cirrhosis: A Systematic Review and Meta-Analysis of Observational Studies. *Medicine (Baltimore)* 2016; **95**: e2877 [PMID: 26937922 DOI: 10.1097/MD.0000000000002877]

29 **Shung DL**, Garcia-Tsao G. Liver Capsule: Portal Hypertension and Varices: Pathogenesis, Stages, and Management. *Hepatology* 2017; **65**: 1038 [PMID: 28032650 DOI: 10.1002/hep.29026]

30 **Nuffer Z**, Marini T, Rupasov A, Kwak S, Bhatt S. The Best Single Measurement for Assessing Splenomegaly in Patients with Cirrhotic Liver Morphology. *Acad Radiol* 2017; **24**: 1510-1516 [PMID: 28800952 DOI: 10.1016/j.acra.2017.06.006]

31 **Soyupak S**, Gunesli A, Seydaoğlu G, Binokay F, Celiktas M, Inal M. Portal venous diameter in children: normal limits according to age, weight and height. *Eur J Radiol* 2010; **75**: 245-247 [PMID: 19409745 DOI: 10.1016/j.ejrad.2009.03.052]

32 **Tseng Y**, Li F, Wang J, Chen S, Jiang W, Shen X, Wu S. Spleen and liver stiffness for noninvasive assessment of portal hypertension in cirrhotic patients with large esophageal varices. *J Clin Ultrasound* 2018; **46**: 442-449 [PMID: 30132919 DOI: 10.1002/jcu.22635]

33 **Adebayo D**, Neong SF, Wong F. Refractory ascites in liver cirrhosis. *Am J Gastroenterol* 2018 [PMID: 29973706 DOI: 10.1038/s41395-018-0185-6]

34 **Orlando R**, Lirussi F, Basso SM, Lumachi F. Splenomegaly as risk factor of liver cirrhosis. A retrospective cohort study of 2,525 patients who underwent laparoscopy. *In Vivo* 2011; **25**: 1009-1012 [PMID: 22021698]

35 **Stremmel W**, Meyerrose KW, Niederau C, Hefter H, Kreuzpaintner G, Strohmeyer G. Wilson disease: clinical presentation, treatment, and survival. *Ann Intern Med* 1991; **115**: 720-726 [PMID: 1929042 DOI: 10.7326/0003-4819-115-9-720]

36 **Dou J**, Lou Y, Wu J, Lu Y, Jin Y. Thrombocytopenia in patients with hepatitis B virus-related chronic hepatitis: evaluation of the immature platelet fraction. *Platelets* 2014; **25**: 399-404 [PMID: 24047408 DOI: 10.3109/09537104.2013.832742]

37 **Dzieżyc K**, Litwin T, Członkowska A. Other organ involvement and clinical aspects of Wilson disease. *Handb Clin Neurol* 2017; **142**: 157-169 [PMID: 28433099 DOI: 10.1016/B978-0-444-63625-6.00013-6]

38 **Pelizzo G**, Guazzotti M, Klersy C, Nakib G, Costanzo F, Andreatta E, Bassotti G, Calcaterra V. Spleen size evaluation in children: Time to define splenomegaly for pediatric surgeons and pediatricians. *PLoS One* 2018; **13**: e0202741 [PMID: 30138410 DOI: 10.1371/journal.pone.0202741]

39 **Liu Y**, Li J, Jin Y, Zhao L, Zhao F, Feng J, Li A, Wei Y. Splenectomy Leads to Amelioration of Altered Gut Microbiota and Metabolome in Liver Cirrhosis Patients. *Front Microbiol* 2018; **9**: 963 [PMID: 29867867 DOI: 10.3389/fmicb.2018.00963]

40 **Chapin CA**, Bass LM. Cirrhosis and Portal Hypertension in the Pediatric Population. *Clin Liver Dis* 2018; **22**: 735-752 [PMID: 30266160 DOI: 10.1016/j.cld.2018.06.007]

Prospective Study

Do patients with gastroesophageal reflux disease and somatoform tendencies benefit from antireflux surgery?

Hans Friedrich Fuchs, Benjamin Babic, Karl-Hermann Fuchs, Wolfram Breithaupt, Gabor Varga, Frauke Musial

ORCID number: Hans Friedrich Fuchs (0000-0003-4764-8050); Benjamin Babic (0000-0003-0313-6862); Karl-Hermann Fuchs (0000-0002-3951-7133); Wolfram Breithaupt (0000-0002-5831-4411); Gabor Varga (0000-0002-0386-3659); Frauke Musial (0000-0003-0074-343X).

Hans Friedrich Fuchs, Department of General Surgery, University of Cologne, Cologne 50937, Germany

Benjamin Babic, Department of General Surgery, University of Mainz, Mainz D-55131, Germany

Karl-Hermann Fuchs, Department of Surgery, University of California San Diego, La Jolla, CA 92093, United States

Wolfram Breithaupt, Gabor Varga, Department of Surgery, Goethe University Frankfurt, Frankfurt am Main 60431, Germany

Frauke Musial, National Research Center in Complementary and Alternative Medicine, NAFKAM, Tromso N-9037, Norway

Frauke Musial, Department of Community Medicine, UiT, The Arctic University of Norway, Tromso N-9037, Norway

Corresponding author: Hans Friedrich Fuchs, MD, Assistant Professor, Department of General Surgery, University of Cologne, Kerpener Str. 62, Cologne 50937, Germany. hans.fuchs@uk-koeln.de
Telephone: +49-221-4784803
Fax: +49-221-4784843

Abstract

BACKGROUND
The clinical presentation of gastroesophageal reflux disease (GERD) shows a large symptom variation also in different intensities among patients. As several studies have shown, there is a large overlap in the symptomatic spectrum between proven GERD and other disorders such as dyspepsia, functional heartburn and/or somatoform disorders.

AIM
To prospectively evaluate the GERD patients with and without somatoform disorders before and after laparoscopic antireflux surgery.

METHODS
In a tertiary referral center for foregut surgery over a period of 3 years patients with GERD, qualifying for the indication of laparoscopic antireflux surgery, were investigated prospectively regarding their symptomatic spectrum in order to identify GERD and associated somatoform disorders. Assessment of symptoms was performed by an instrument for the evaluation of somatoform disorders

[Somatoform Symptom Index (SSI) > 17]. Quality of life was evaluated by Gastrointestinal Quality of Life Index (GIQLI).

RESULTS
In 123 patients an indication for laparoscopic antireflux surgery was established and in 43 patients further medical therapy was suggested. The portion of somatoform tendencies in the total patient population was 20.48% (34 patients). Patients with a positive SSI had a preoperative GIQLI of 77 (32-111). Patients with a normal SSI had a GIQLI of 105 (29-140) (*P* < 0.0001). In patients with GERD the quality of life could be normalized from preoperative reduced values of GIQLI 102 (47-140) to postoperative values of 117 (44-144). In patients with GERD and somatoform disorders, the GIQLI was improved from preoperative GIQLI 75 (47-111) to postoperative 95 (44-122) (*P* < 0.0043).

CONCLUSION
Patients with GERD and associated somatoform disorders have significantly worse levels of quality of life. The latter patients can also benefit from laparoscopic fundoplication, however they will not reach a normal level.

Key words: Gastroesophageal reflux disease; Antireflux surgery; Laparoscopic fundoplication; Somatization; Gastroesophageal reflux disease symptoms

Core tip: The current level of evidence performing antireflux surgery in patients with overlapping symptoms such as dyspepsia, functional heartburn and/or somatoform disorders is limited and debated in small case series. In a tertiary referral center for foregut surgery (the largest center for antireflux surgery in Germany), we studied patients with gastroesophageal reflux disease (GERD) regarding their symptomatic spectrum over a period of 3 years. It was found that patients with GERD and associated somatoform disorders have significantly worse levels of quality of life. The latter patients can also benefit from laparoscopic fundoplication, however they will not reach a normal level.

INTRODUCTION

The clinical presentation of gastroesophageal reflux disease (GERD) shows a large variety of symptoms also in different intensities among patients[1-3]. As several studies have shown, there is a large overlap in the symptomatic spectrum between proven GERD and other disorders such as dyspepsia, functional heartburn and/or somatoform disorders[4-10]. This makes a precise diagnosis, just based on symptoms quite unreliable for severe therapeutic decision making such as antireflux surgery[11]. GERD can be diagnosed rather easily in patients by the presence of esophagitis during upper gastrointestinal (GI) endoscopy and/or evidence of pathologic gastroesophageal reflux in 24h-impedance-pH-monitoring, favourably optimised by a positive symptom-reflux correlation as expressed by the symptom association probability (SAP > 95% significant)[3,12].

Symptom-overlapping disorders such as somatisation or a somatoform tendency can be detected in a patient, if a given person suffers from an excessive number of somatic complaints, which cannot be explained by pathophysiologic and/or measurable findings[13]. A symptomatic screening test by Rief *et al*[13-15] can be used to identify those patients with somatoform disorders among those with proven GERD. Recently we have shown that GERD patients do have an overlap with somatoform tendencies in about 20% of patients of an investigated population in a tertiary referral center[10]. A similar portion (20%) of patients with somatoform tendencies can be

detected in a population with foregut symptoms[16].

In GERD reliable decision making in long-term therapeutic strategies focuses on the reduction of troublesome symptoms and a dependable improvement of quality of life for the patients after treatment. The majority of GERD patients can be treated by conservative medical therapy such as protonpump inhibitors (PPI), while surgical therapy should be reserved for patients with severe and progressive disease, such as patients with anatomical and functional defects, substantial mucosal damage and/or increasingly reduced quality of life[12,17-20]. The results of antireflux surgery are well known and a good outcome ranges around 85%-90% in patients with proven GERD[12]. However, little is known about the success of antireflux surgery in patients with an overlapping problem of somatoform symptoms. The question emerges, whether it is justified to operate these patients with a combined problem of proven GERD and somatoform tendencies and if patients with a combination of GERD and somatoform problems would benefit from surgical therapy.

There are many reports on the outcome of laparoscopic antireflux surgery in GERD patients, but only few reports focusing on patients with associated and overlapping disorders such as depression or somatoform tendencies[12,17-20]. Especially data are lacking on pre- and postoperative quality of life in patients with GERD and combined somatoform disorders. As a consequence we performed a prospective evaluation of patients with GERD with and without a combination of somatoform disorders before and after laparoscopic antireflux surgery regarding their outcome.

MATERIALS AND METHODS

Methods
In a tertiary referral center for foregut surgery over a period of 3 years patients with GERD, qualifying for the indication of laparoscopic antireflux surgery, were investigated prospectively regarding their symptomatic spectrum in order to identify GERD and associated somatoform disorders. Patients, fulfilling the criteria for the indication for laparoscopic antireflux surgery, entered the protocol and were followed pre-, intra- and postoperatively. This allowed for the analysis of outcome parameters between patients with GERD with and without a combined problem of somatoform tendencies.

Patients
All patients with foregut symptoms such as heartburn who were suspicious for GERD and referred to our specialized referral center for GI functional disease over a time frame of 3 years were asked for their permission and registered in this present study after Institutional Review Board approval. This was followed by a prospective protocol of investigations, assessments and therapy as well as follow up assessments. Patients fulfilling the indication criteria based on the guidelines were informed and an indication for laparoscopic antireflux surgery was established. In patients with minor and /or non-progressive disease, a continuation of PPI-therapy was suggested.

Diagnostic work-up
Standardized questionnaires were used to assess all presenting symptoms, and all patients underwent a validated screening test to assess somatoform disorders and quality of life[10,15,21]. Medical history, physical exams, upper GI endoscopy, GI function testing (esophageal manometry and 24 h-pH-monitoring) were performed in order to determine the presence and severity of GERD. The severity of esophagitis was graded according to the classification of Savary-Miller or the Los Angeles Classification and the vertical extension of a hiatal hernia was recorded. Water perfusion esophageal manometry, later High Resolution Manometry was performed. Position, length, and pressure of the lower esophageal sphincter were determined with the pull-through manometry. pH-monitoring or later Impedance-pH-monitoring were performed using the DeMeester-reflux-score[1]. A a value of 14.7 was used as the borderline. Medication affecting motility and acid suppression was stopped one week prior to testing.

A symptom evaluation to identify somatoform disorders was performed according to Rief *et al*[13-15]. As a marker for the high probability for the presence of a somatoform tendency or disorder the somatoform symptom index (SSI) was used, as recently described[10]. The SSI is positive for the presence of a somatoform tendency, if a given patient has more than 17 different symptoms, of which no explanation or cause can be detected.

Quality of life was evaluated in this study population by the Gastrointestinal Quality of Life Index (GIQLI), which is a well established instrument and validated in

several languages[21]. The GIQLI carries 5 different components or dimensions of quality of life such as GI-symptoms, emotional factors, physical factors, social factors and influences by the administered therapy with a maximum index point of 144, evaluated by 36 questions.

Surgical procedure

Therapeutic decision making, especially the indication for laparoscopic antireflux surgery was based on the current guidelines[12]. Patients with progressive and advanced disease, usually with evidence of past or present esophagitis, hiatal hernia, incompetence of the lower esophageal sphincter, pathologic esophageal acid exposure and/or good PPI response, preferably a PPI dosage increase over the past years as well as a reduction in quality of Life were selected for surgical therapy. Patients with lacking positive criteria were suggested to continue their conservative medical therapy and change of life style.

Patients with indication for surgery had to sign an informed consent prior to surgery. Standard laparoscopic antireflux procedure was a short floppy Nissen fundoplication and a posterior hiatoplasty. In patients with severe esophageal motility disorder usually with less than 50% of effective esophageal peristalsis left, received a laparoscopic partial posterior Toupet hemifundoplication, also combined with a posterior hiatoplasty and gastropexy.

The standard procedure was started with the insertion of a Verres-needle to create a capnoperitoneum and after safety tests to access the abdominal cavity with a 10 mm camera port. Additional 4 trocars were placed and the procedure was started with a limited mobilisation of cranial gastric fundus especially the posterior part to create a floppy mobile fundus with a posterior and an anterior fundic flap. In addition the hiatus was dissected and subsequently the distal esophagus was mobilized in order to gain a tension free esophageal segment of about 3cm of lower esophageal sphincter within the abdominal cavity below the hiatal arch. Then the obligatory posterior hiatal narrowing with 1-3 "figure-of-8" stitches were performed to adapt the narrowing according to the diameter of the esophagus. Afterwards the Nissen fundoplication was shaped around the esophageal sphincter, calibrated by a 18 mm bougie, and sutured including the esophageal wall. Care was taken to shape the wrap symmetrically regarding the posterior and anterior fundic flap, fixing it to the right lateral wall of the distal esophagus. Care was also taken to identify both vagal truncs and avoid damage.

Postoperatively the patients followed some dietary restrictions starting with fluid postop day 1 and 2, and increasing to semisolid on day 3, followed by their dismissal with the suggestion of several small meal rather than one main meal for 4-8 wk and refrain from hard physical work for 8 wk. Postoperative follow-up consisted of questionaires after 12 mo and a suggestion for endoscopic and functional investigations. The same instruments were used as prior to surgery. Patients were separately followed and analysed depending on their choice of therapy. As a consequence, 2 groups were established: Group A post-surgical therapy; Group B: Surgery suggested, medical therapy performed.

Statistical analysis

All data were recorded and stored in an Excel file for later comparison. The results of the different groups were compared using the non-parametric test for paired samples with Wilcoxon matched pairs signed rank test and the *t*-test for paired samples. For comparison of quality-of-life data the Wilcoxon Two Sample test was used, since the samples had different sizes.

RESULTS

Patients

A total of 166 patients with foregut symptoms and heartburn were prospectively included in this study over 3 years. Mean age was 58 years (20-82) and there were 82 females. In 123 patients an indication for laparoscopic antireflux surgery was established and in 43 patients further medical therapy was suggested, based on the indication criteria of the EAES guidelines. Almost a third of the patients had some kind of concomitant disease and some risk factors. The duration since the onset of the symptoms was median 5 years (1-50). The most frequent chief complaint was heartburn (61%), followed by regurgitation (18%) and epigastric pain (15%). The previous response to medication was very limited in the recent months, which led to the referral of the patients to surgery. Esophagitis was visible on endoscopy in 51% of the patients. Hiatal hernia was documented in 78%. Esophageal manometry showed

in 86% an incompetent lower esophageal sphincter and in 16% an ineffective motility of the esophageal body. A pathologic esophageal acid exposure was documented in 88% of the patients.

After information about the disease and the operative procedure, finally 93 patients (Group A) agreed to undergo a laparoscopic antireflux procedure. Thirty patients decided to continue medical therapy despite the fact that an indication for laparoscopic antireflux surgery was suggested (Group B). The portion of somatoform tendencies in the total patient population was 20.48% (34 patients), when the SSI ≥ 17 symptoms was used as criterion for the presence of somatoform disorders. In Group A (patients with laparoscopic fundoplication) 22% (20 patients) showed a positive SSI for somatoform tendencies, while in Group B this portion was quite similar with 20% (6 patients) (Figure 1).

Figure 2 shows the preoperative level of the GIQLI in patients with and without a somatoform disorder as measured by the SSI (normal < 17 symptoms). Patients with a positive SSI (number of present symptoms ≥ 17) had a preoperative GIQLI of 77 (32-111). Patients with a normal SSI (< 17 symptoms) had a GIQLI of 105 (29-140). This difference was highly significant ($P < 0.0001$).

In all surgical cases the primary laparoscopic procedure could be performed without conversion. In four patients intraoperative opening of the pleural cavity on the left side occurred during mobilisation of the esophagus in the mediastinum, resulting in a compression of the lung by gas-insufflation. Two patients showed postoperative minor complications such as 1 patient with an extraordinary pain level, which needed 3 d of extra hospitalisation as well as 1 patient with abdominal distension and pain due to postoperative delayed intestinal motility recovery, which also needed prolonged hospital stay. All patients had dysphagia in the first 4 postoperative days during their hospitalisation and a stepwise increase in fluid, semisolid and finally solid food was given during this period in order to prevent excessive gagging and vomiting, which could cause early migration.

Follow-up

After minimum of 1 year follow-up time all patients were contacted and questionnaires were returned from 138 out of 166 patients, that were initially investigated. From the initially 93 patients with laparoscopic fundoplication, 77 patients responded and follow-up information could be obtained. Twenty-five out of 30 patients responded, who had been suggested for surgery, but decided to continue conservative treatment. Preoperative and postoperative quality of life as assessed by the GIQLI showed a significant difference ($P < 0.001$) for patients in Group A, operated upon with laparoscopic antireflux procedure (Figure 3).

The GIQLI of the operated patients, who responded to the follow-up, was elevated from a preoperative level of 99 (47-140) up to postoperative 117 (44-144) ($P < 0.001$). The normal level of GIQLI of healthy individuals is reported from 120 to 131. Patients with GERD, who decided to continue with conservative medical therapy despite the suggestion for laparoscopic surgery (group B), show after the follow-up time of at least 1 year a constant level of reduced quality of life with GIQLI of 98 (51-130; $P = 0.8279$; Figure 3). Within group B quality of life in those patients without somatoform tendency (SSI < 17) had an initial GIQLI of 102, which was documented at 1 year follow-up at 104 (not significant). Patients with a SSI > 17 had an initial GIQLI of 73, which was 1 year later at 72. Thus medical therapy did not change the level of Quality of life in this cohort.

Figure 4 demonstrates the main finding of the study, comparing the pre- and postoperative level of the GIQLI, related to the presence of a somatoform disorder. In both groups, patients with GERD alone and patients with GERD and combined somatoform disorder, the quality of life could be significantly increased by the laparoscopic antireflux procedure. In the operated patients with GERD alone, Quality of Life could be normalized from preoperative reduced values of GIQLI 102 (47-140) to postoperative values of 117 (44-144). In patients with GERD and combined somatoform disorders, the GIQLI was improved from preoperative GIQLI 75 (47-111) to postoperative 95 (44-122) ($P < 0.0043$).

In summary, quality of life in patients with GERD as selected for surgery using the criteria as published in the guidelines is severely reduced and can be elevated by laparoscopic fundoplication to normal levels. Patients with GERD and associated somatoform disorders have significantly worse levels of quality of life. The latter patients can also benefit from laparoscopic fundoplication, however they will not reach a normal level due to the large amount of present symptoms, which can not all be influenced by antireflux surgery.
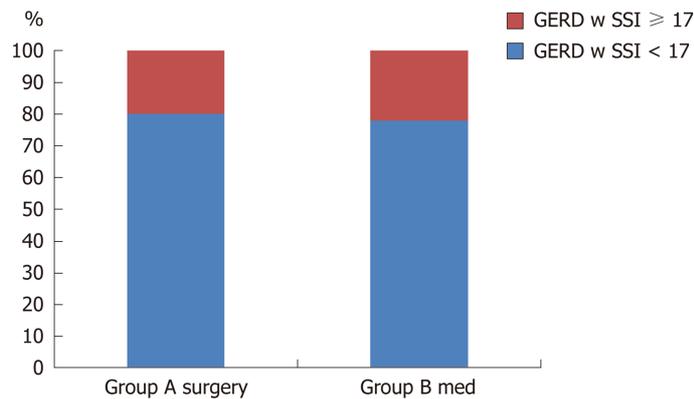
Figure 1 Incidence of somatoform symptoms in patients with gastroesophageal reflux disease. Group A: patients with indication for surgery, willing to undergo surgery. The percentage of SSI ≥ 17 was 22%; Group B: Patients with GERD and indication for surgery, who has refused antireflux surgery and have continued protonpump inhibitors therapy. The percentage of SSI ≥ 17 was 20%. GERD: Gastroesophageal reflux disease; SSI: Somatoform Symptom Index.

DISCUSSION

It has been shown that the classic clinical presentation of the GERD has a remarkable symptom overlap with other often functional disorders such as heartburn, somatization and/or hypertensive esophagus and others[3-10]. Several instruments have been used in the past to assess the presence of such conditions in order to verify the precise diagnosis and document the combination of GERD with somatoform tendencies[4-10,13-15]. Recently the relationship between GERD and somatoform disorders was published demonstrating a 20% incidence of combined somatoform tendencies in a population of GERD patients with more than 17 symptoms present[10]. This confirms early reports of similar involvement of patients with both conditions[16]. Two questions emerge whether a patient with somatoform disorder can be detected within a population of GERD-patients and secondly, if these patients should be selected for antireflux surgery.

Somatization represents a situation where somatic complaints cannot be explained by measurable findings[10,15]. Psychodiagnostic instruments are necessary to clarify the situation and establish an objective diagnosis. A variety of tests can be used to evaluate persons with the suspicion of a somatoform tendency[10,13,15,22-24]. Often these patients may have depression and anxiety, which can influence the clinical assessment of patients[23-25]. The basis for an optimal selection of patients with GERD for surgery is a comprehensive diagnostic work-up to generate evidence for an advanced, progressive disease with proven damage and functional defects.

Besides a good surgical technique, the optimal selection of the right patients for laparoscopic fundoplication is of utmost importance for the final result of surgical therapy. Laparoscopic fundoplication can produce an ideal solution for a patient with severe and progressive GERD, reducing most of the troublesome symptoms and enabling the patient to live a normal joyful life[12]. Having expressed this, it must be emphasized that performing a fundoplication on the wrong patient, who either does not need a fundoplication or who has other problems, which could be worsened by a fundoplication, can easily destroy the patient`s quality of life.

Patients with somatoform disorders usually have a large variety of symptoms, where typical reflux symptoms such as heartburn and acid regurgitation may play only a limited role or may be overrated by the patient due to the stress and heavy load of all symptoms. In these cases the question emerges, whether surgery is justified. Objective diagnostic testing is essential to verify pathologic gastroesophageal reflux, but still given the tests are positive, there is still a dilemma, whether patients would benefit from antireflux surgery. Some surgeons advise to see these patients as contraindications for antireflux surgery[17,18].

Little is known about the probability of success after surgical therapy in these patients with the combined problem. Therefore the present study shows very clearly that a precise diagnostic work-up is necessary to determine the presence of a somatoform tendency as well as the presence of severe GERD. The study is helpful in showing evidence that on one hand improvement of quality of life is possible, and on the other hand that quality of life can rather not be normalized, since too many other symptoms are involved with no connection the underlying reflux problem.

The problem is that patients with GERD and somatoform disorders start from a
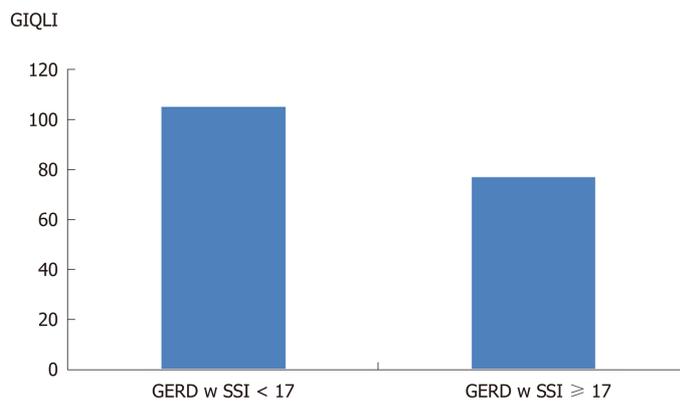
GIQLI

Figure 2 Preoperative quality of life, as measured by the Gastrointestinal Quality of Life Index in patients with gastroesophageal reflux disease alone (median GIQLI: 105) and patients with gastroesophageal reflux disease and associated somatoform tendencies (SSI ≥ 17) (median GIQLI: 77). This difference is significant ($P <$ 0.001). SSI: Somatoform Symptom Index; GIQLI: Gastrointestinal Quality of Life Index; GERD: Gastroesophageal reflux disease.

preoperative significantly lower level of quality of life than GERD patients without somatoform tendencies. Interesting enough laparoscopic antireflux surgery can elevate the GIQLI for about 20-25 points in patients. The latter causes in GERD-patients without associated problems a postoperative quality of life level of nearly normal levels while patients with both, GERD and somatisation will usually remain in a lower level, which can cause postoperative disappointment and frustration. This should be communicated to the patients prior to surgery to make sure that the preoperative expectations will not be unrealistic.

In conclusion, patients with GERD and overlapping symptoms due to somatoform disorders should not be withhold from laparoscopic antireflux surgery in general, if their GERD is proven by objective assessment. It must be however emphasized that these patients must be especially informed about their critical situation regarding their large number of often atypical symptoms, which cannot be cured completely. The latter causes continuing restrictions in their quality of life. As a consequence the indication for antireflux surgery must be discussed in detail with the patients and only those should be selected, in whom reflux-generated-symptoms are proven by reflux symptom-correlation[26]. These symptoms should be the major quality-of-life restricting factors.
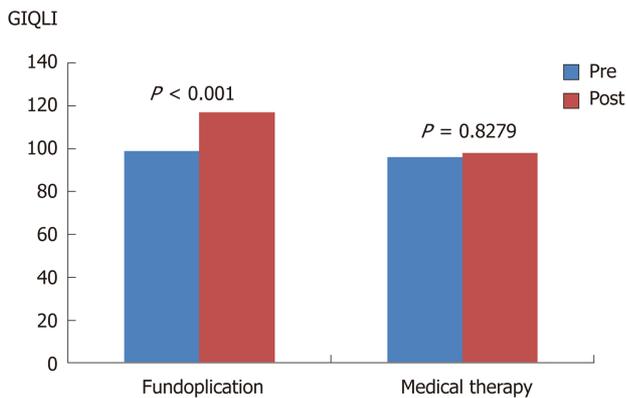
Figure 3 Pre-and post-therapeutic quality of life, as measured by the Gastrointestinal Quality of Life Index, for both groups. Group A after laparoscopic antireflux surgery (GIQLI preop: 91; postop 117; $P < 0{,}001$) and Group B after continued conservative treatment (GIQLI pre: 96; post: 98; $P = 0.8279$). In the surgical group, GIQLI could be significantly increased. GIQLI: Gastrointestinal Quality of Life Index.
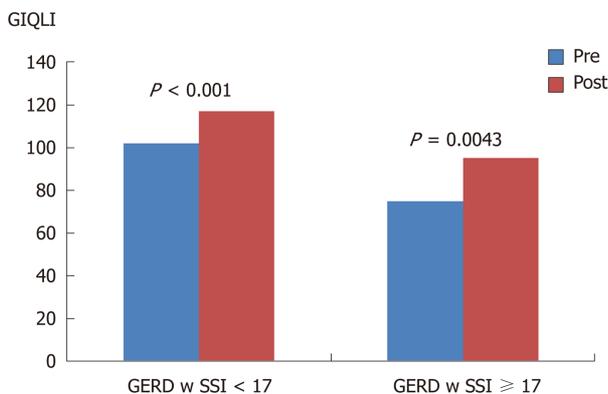

Figure 4 Comparison of pre- and postoperative levels of Gastrointestinal Quality of Life Index in relation to the presence of somatoform disorders. Patients with somatoform disorders will also improve their GIQLI postoperatively (GIQLI preop: 75; postop: 95; $P < 0.0043$), however it could not be increased to normal levels due to the large number of non-related symptoms. Patients with SSI < 17 could reach normal levels of GIQLI postoperatively (preop: 102; postop: 117; $P < 0.001$). GIQLI: Gastrointestinal Quality of Life Index; SSI: Somatoform Symptom Index; GERD: Gastroesophageal reflux disease.

ARTICLE HIGHLIGHTS

Research background

Gastroesophageal reflux disease (GERD) shows a large symptom variation also in different intensities among patients. Up-to-date, patients with somatoform tendencies were often per se excluded from surgery.

Research motivation

There is a large overlap in the symptomatic spectrum between GERD and other disorders such as dyspepsia, functional heartburn or somatoform disorders. We intended to be able to better differentiate between these different entities to provide optimal patient care. Before our study, it was still unclear if patients with somatoform tendencies should undergo surgery at all.

Research objectives

The purpose of this study is an evaluation of patients with GERD with and without somatoform disorders before and after laparoscopic antireflux surgery regarding their outcome.

Research methods

In the largest center for benign foregut surgery in Germany patients with GERD, qualifying for antireflux surgery were investigated prospectively regarding their symptomatic spectrum in order to identify GERD and associated somatoform disorders over a period of 3 years using an instrument for the evaluation of somatoform disorders. Quality of life was evaluated by Gastrointestinal Quality of Life Index (GIQLI). These parameters were compared depending on the group assignment of patients.

Research results

One fifth of all included patients suffered from somatoform tendencies (20.48%; 34 patients). Patients with this tendency had a preoperative GIQLI of 77 (32-111). Patients without this

tendency had a GIQLI of 105 (29-140; $P < 0.0001$). Quality of life could be normalized from preoperative reduced values of GIQLI 102 (47-140) to postoperative values of 117 (44-144) in patients with GERD. GIQLI of patients with GERD and somatoform tendency was improved from preoperative GIQLI 75 (47-111) to postoperative 95 (44-122; $P < 0.0043$).

Research conclusions

This is the first study to show that patients with a somatoform tendency should not be excluded from surgery, however they will not reach a normal level of quality of life. Patients with GERD and somatoform disorders have an impaired quality of life. The latter patients can also benefit from laparoscopic fundoplication, however they will not reach a normal level.

Research perspectives

The investigated instruments for assessment of quality of life and somatoform disorders can help to discriminate between the different symptom origins and should be used in all patients who undergo antireflux surgery.

REFERENCES

1   **DeMeester TR**. *Definition, detection and pathophysiology of gastroesophageal reflux disease*. In: DeMeester TR, Matthews HR (eds) Benign esophageal disease. International trends in general thoracic surgery. Mosby St. Louis; 1987; 99-127

2   **Klauser AG**, Schindlbeck NE, Müller-Lissner SA. Symptoms in gastro-oesophageal reflux disease. *Lancet* 1990; **335**: 205-208 [PMID: 1967675 DOI: 10.1016/0140-6736(90)90287-F]

3   **Vakil N**, van Zanten SV, Kahrilas P, Dent J, Jones R; Global Consensus Group. The Montreal definition and classification of gastroesophageal reflux disease: a global evidence-based consensus. *Am J Gastroenterol* 2006; **101**: 1900-1920; quiz 1943 [PMID: 16928254 DOI: 10.1111/j.1572-0241.2006.00630.x]

4   **Holtmann G**, Kutscher SU, Haag S, Langkafel M, Heuft G, Neufang-Hueber J, Goebell H, Senf W, Talley NJ. Clinical presentation and personality factors are predictors of the response to treatment in patients with functional dyspepsia; a randomized, double-blind placebo-controlled crossover study. *Dig Dis Sci* 2004; **49**: 672-679 [PMID: 15185877 DOI: 10.1023/B:DDAS.0000026317.00071.75]

5   **Clauwaert N**, Jones MP, Holvoet L, Vandenberghe J, Vos R, Tack J, Van Oudenhove L. Associations between gastric sensorimotor function, depression, somatization, and symptom-based subgroups in functional gastroduodenal disorders: Are all symptoms equal? *Neurogastroenterol Motil* 2012; **24**: 1088-e565 [PMID: 22816492 DOI: 10.1111/j.1365-2982.2012.01985.x]

6   **Bradley LA**, Richter JE, Pulliam TJ, Haile JM, Scarinci IC, Schan CA, Dalton CB, Salley AN. The relationship between stress and symptoms of gastroesophageal reflux: The influence of psychological factors. *Am J Gastroenterol* 1993; **88**: 11-19 [PMID: 8420248 DOI: 10.1097/00001610-199312000-00015]

7   **Johnston BT**, Lewis SA, Love AH. Stress, personality and social support in gastro-oesophageal reflux disease. *J Psychosom Res* 1995; **39**: 221-226 [PMID: 7595880 DOI: 10.1016/0022-3999(94)00102-B]

8   **Tack J**, Caenepeel P, Arts J, Lee KJ, Sifrim D, Janssens J. Prevalence of acid reflux in functional dyspepsia and its association with symptom profile. *Gut* 2005; **54**: 1370-1376 [PMID: 15972301 DOI: 10.1136/gut.2004.053355]

9   **Neumann H**, Monkemuller K, Kandulski A, Malfertheiner P. Dyspepsia and IBS symptoms in patients with NERD, ERD and Barrett's esophagus. *Dig Dis* 2008; **26**: 243-247 [PMID: 18463443 DOI: 10.1159/000121354]

10 **Fuchs KH**, Musial F, Ulbricht F, Breithaupt W, Reinisch A, Babic B, Fuchs H, Varga G. Foregut symptoms, somatoform tendencies, and the selection of patients for antireflux surgery. *Dis Esophagus* 2017; **30**: 1-10 [PMID: 28475727 DOI: 10.1093/dote/dox022]

11 **Costantini M**, Crookes PF, Bremner RM, Hoeft SF, Ehsan A, Peters JH, Bremner CG, DeMeester TR. Value of physiologic assessment of foregut symptoms in a surgical practice. *Surgery* 1993; **114**: 780-786; discussion 786-787 [PMID: 8211694 DOI: 10.1023/A:1016656812095]

12 **Fuchs KH**, Babic B, Breithaupt W, Dallemagne B, Fingerhut A, Furnee E, Granderath F, Horvath P, Kardos P, Pointner R, Savarino E, Van Herwaarden-Lindeboom M, Zaninotto G; European Association of Endoscopic Surgery (EAES). EAES recommendations for the management of gastroesophageal reflux disease. *Surg Endosc* 2014; **28**: 1753-1773 [PMID: 24789125 DOI: 10.1007/s00464-014-3431-z]

13 **Rief W**, Hiller W. Toward empirically based criteria for the classification of somatoform disorders. *J Psychosom Res* 1999; **46**: 507-518 [PMID: 10454165 DOI: 10.1016/S0022-3999(99)00023-9]

14 **Rief W**, Hessel A, Braehler E. Somatization symptoms and hypochondriacal features in the general population. *Psychosom Med* 2001; **63**: 595-602 [PMID: 11485113 DOI: 10.1097/00006842-200107000-00012]

15 **Rief W**, Hiller W. A new approach to the assessment of the treatment effects of somatoform disorders. *Psychosomatics* 2003; **44**: 492-498 [PMID: 14597684 DOI: 10.1176/appi.psy.44.6.492]

16 **Zaballa P**, Crega Y, Grandes G, Peralta C. The Othmer and DeSouza test for screening of somatisation disorder: Is it useful in general practice? *Br J Gen Pract* 2001; **51**: 182-186 [PMID: 11255898 DOI: 10.3109/07853890109002070]

17 **Kamolz T**, Granderath FA, Bammer T, Pasiut M, Pointner R. Psychological intervention influences the outcome of laparoscopic antireflux surgery in patients with stress-related symptoms of gastroesophageal reflux disease. *Scand J Gastroenterol* 2001; **36**: 800-805 [PMID: 11495073 DOI: 10.1080/003655201750313306]

18 **Velanovich V**, Karmy-Jones R. Psychiatric disorders affect outcomes of antireflux operations for

gastroesophageal reflux disease. *Surg Endosc* 2001; **15**: 171-175 [PMID: 11285962 DOI: 10.1007/s004640000318]

19   **Mearin F**, Ponce J, Ponce M, Balboa A, Gónzalez MA, Zapardiel J. Frequency and clinical implications of supraesophageal and dyspeptic symptoms in gastroesophageal reflux disease. *Eur J Gastroenterol Hepatol* 2012; **24**: 665-674 [PMID: 22330237 DOI: 10.1097/MEG.0b013e3283512139]

20   **Kamolz T**, Granderath F, Pointner R. Laparoscopic antireflux surgery: disease-related quality of life assessment before and after surgery in GERD patients with and without Barrett's esophagus. *Surg Endosc* 2003; **17**: 880-885 [PMID: 12618934 DOI: 10.1007/s00464-002-9158-2]

21   **Eypasch E**, Williams JI, Wood-Dauphinee S, Ure BM, Schmülling C, Neugebauer E, Troidl H. Gastrointestinal Quality of Life Index: Development, validation and application of a new instrument. *Br J Surg* 1995; **82**: 216-222 [PMID: 7749697 DOI: 10.1002/bjs.1800820229]

22   **Fink P**. Surgery and medical treatment in persistent somatizing patients. *J Psychosom Res* 1992; **36**: 439-447 [PMID: 1535658 DOI: 10.1016/0022-3999(92)90004-L]

23   **Mussell M**, Kroenke K, Spitzer RL, Williams JB, Herzog W, Löwe B. Gastrointestinal symptoms in primary care: Prevalence and association with depression and anxiety. *J Psychosom Res* 2008; **64**: 605-612 [PMID: 18501261 DOI: 10.1016/j.jpsychores.2008.02.019]

24   **Löwe B**, Spitzer RL, Williams JB, Mussell M, Schellberg D, Kroenke K. Depression, anxiety and somatization in primary care: Syndrome overlap and functional impairment. *Gen Hosp Psychiatry* 2008; **30**: 191-199 [PMID: 18433651 DOI: 10.1016/j.genhosppsych.2008.01.001]

25   **Cheville AL**, Basford JR, Dos Santos K, Kroenke K. Symptom burden and comorbidities impact the consistency of responses on patient-reported functional outcomes. *Arch Phys Med Rehabil* 2014; **95**: 79-86 [PMID: 23988394 DOI: 10.1016/j.apmr.2013.08.009]

26   **Savarino E**, Tutuian R, Zentilin P, Dulbecco P, Pohl D, Marabotto E, Parodi A, Sammito G, Gemignani L, Bodini G, Savarino V. Characteristics of reflux episodes and symptom association in patients with erosive esophagitis and nonerosive reflux disease: Study using combined impedance-pH off therapy. *Am J Gastroenterol* 2010; **105**: 1053-1061 [PMID: 19997095 DOI: 10.1038/ajg.2009.670]